

**ADVANCES IN BRØNSTED ACID CATALYSIS:
REACTIONS OF OXOCARBENIUM IONS**

by

Alina Borovika

A dissertation submitted in partial fulfillment
of the requirements for the degree of
Doctor of Philosophy
(Chemistry)
in the University of Michigan
2015

Doctoral Committee:

Assistant Professor Pavel Nagorny, Chair
Assistant Professor Jolanta E. Grembecka
Professor John Montgomery
Professor Melanie S. Sanford

To my mom and dad

Acknowledgements

First and foremost, I would like to thank Professor Pavel Nagorny for being a wonderful mentor. From the very beginning he inspired me to excel in my studies and research by involving with me in heated discussions and debates. In addition to that, Pavel also played a great role in my professional development, always pushing me to present at major conferences, apply to fellowships, and providing amazing support during the job application process. Finally, Pavel's commitment to research and education have, and will always continue to inspire me.

Special thanks go to Professor Edvīns Vedējs for his incredible support throughout my whole career in chemistry, and also for being an inspiration and a true friend. I would like to thank the members of my graduate committee, Professors John Montgomery, Melanie Sanford, and Jolanta Grembecka for helping me develop my thesis. I am also greatly thankful to Professor Vincent Pecoraro for being my adviser during my first rotation, and for continuous support throughout my time at Michigan. Additionally, Professor Adam Matzger and his research group are acknowledged for helping with numerous crystallography and azide sensitivity studies.

I have had a great pleasure working next to talented, smart, and hardworking people in Nagorny group. The Diels-Alder research would not have been possible without the help

from April Tang and Seth Klapman. Furthermore I am extremely grateful to all my lab friends, especially to Nathan, Seth, Danielle, Tay, and Bijay.

Finally, I would like to thank my family and my closest friends for continuous encouragement and tremendous support throughout these five years. Without them I would never be able to achieve this milestone. Most importantly, I am grateful to my mom and dad for believing in me and never letting me give up.

Table of Contents

Dedication	ii
Acknowledgements	iii
List of Figures	viii
List of Schemes	ix
List of Tables	xi
List of Appendices	xii
List of Abbreviations	xiii
Abstract	xv
Chapter 1. Hydrogen Bond-Catalyzed Reactions of Oxocarbenium Ions	1
1.1 Introduction into Chemistry of Oxocarbenium Ions	1
1.2 Hydrogen bond catalysis	3
1.3 Anion Activation	5
1.4 Protonation	10
References	22
Chapter 2. Thiophosphoramidate-Based Cooperative Catalysts for Brønsted Acid Promoted Ionic Diels-Alder Reaction.	25

2.1	Introduction	25
2.2	Gassman Cycloaddition.....	26
2.3	Thiophosphoramides as co-catalysts	28
2.4	Tosylate/thiophosphoramide complexation studies	38
2.5	Conclusions	42
2.6	Experimental	42
	References	53
Chapter 3. Chiral Brønsted Acid-Catalyzed Enantioselective Ionic [4+2] Cycloadditions		55
3.1	Introduction	55
3.2	Enantioselective Cycloaddition.....	57
3.3	Discussion	65
3.4	Conclusion.....	66
3.5	Experimental	67
	References	76
Chapter 4. Stereo- and Regioselective Synthesis of Aminoglycosides		78
4.1	Introduction to aminoglycosides	78
4.2	Strategy for regio- and stereoselective glycosylations of 2-deoxystreptamine..	82
4.3	Design of 2-deoxystreptamine derivatives for its desymmetrization.....	87
4.4	Design of glycosyl donor for glycosylation studies	98

4.5	Glycosylation studies	101
4.6	NMR analysis of diglycosides.....	107
4.7	Synthesis of neamine.....	110
4.8	Conclusions	111
4.9	Experimental	112
	References	126
	Appendices	129

List of Figures

Figure 1.1 Examples of hydrogen bond catalysts	10
Figure 1.2 Structure and acidities of chiral phosphoric acids and <i>N</i> -triflamides	12
Figure 2.1 Titration studies	39
Figure 2.2 X-ray structure of 2-10•2-31	40
Figure 2.3 Computed complex between 2-10 and mesylate	41
Figure 4.1 Structural diversity of natural aminoglycoside antibiotics	81
Figure 4.2 2-Deoxystreptamine and its synthons	83
Figure 4.3 Nitrogen protecting groups for 2-deoxystreptamine	88
Figure 4.4 Chiral Brønsted acids used in catalyst screening.....	103
Figure 4.5 Regioisomeric diglycosides	108

List of Schemes

Scheme 1.1 Generation of oxocarbenium ions.....	2
Scheme 1.2 Acetalization of carbonyls through stabilization of oxyanion	6
Scheme 1.3 Enantioselective addition to 1-chloroisochromans	7
Scheme 1.4 Cycloaddition reactions of oxocarbenium ions	9
Scheme 1.5 Aldol-type reaction of vinyl ethers by Terada	14
Scheme 1.6 Semipinacol rearrangement by Tu	15
Scheme 1.7 Asymmetric transacetalization by List	16
Scheme 1.8 Glycosylation catalyzed by CPAs.....	16
Scheme 1.9 Stereoselective spiroketalization.....	18
Scheme 1.10 Potential reaction mechanisms for spiroketalization reaction	19
Scheme 1.11 Enantioselective aza-Michael reactions.....	20
Scheme 2.1 Reactions of vinyl oxocarbenium ions.....	26
Scheme 2.2 [4+2] cycloaddition of vinyl oxocarbenium ions.....	27
Scheme 2.3 Proposed activation of dienophiles in Gassman cycloaddition	29
Scheme 2.4 Three-hydrogen bond donors.....	30
Scheme 2.5 Proposed mechanism for the ionic Diels-Alder reaction	41

Scheme 3.1 Stereoselective ionic Diels-Alder reactions	56
Scheme 3.2 Proposed reaction mechanism	66
Scheme 4.1 Proposed desymmetrization of 2-deoxystreptamine derivative.....	84
Scheme 4.2 CPA-controlled regioselective acetalization of chiral diols and enantioselective desymmetrization of <i>meso</i> -diols	85
Scheme 4.3 CPA mediated glycosylation with recognition of alcohol chirality.....	86
Scheme 4.4 Acidic degradation of neomycin.....	87
Scheme 4.5 Synthesis of 4-3 – 4-6	89
Scheme 4.6 Synthesis of 4-8 – 4-9	90
Scheme 4.7 Diazotransfer with trifluoromethanesulfonic anhydride.....	91
Scheme 4.8 Diazotransfer with imidazole-1-sulfonyl azide.....	92
Scheme 4.9 Desymmetrization of 4-7 via acetal formation	94
Scheme 4.10 Hydroxyl protection of 4-7	96
Scheme 4.11 Acetalization of 4-17	97
Scheme 4.12 Synthesis of allyl and benzyl protected 2-deoxystreptamines	98
Scheme 4.13 Synthesis of neamine by stereodifferentiation of 2-deoxystreptamine.....	99
Scheme 4.14 Synthesis of glycosyl donor	101
Scheme 4.15 Synthesis of perbenzyl-, perazidoneamine	110
Scheme 4.16 Semisynthesis of neamine and structural assignment.....	111

List of Tables

Table 1.1 Properties of hydrogen bonds and their examples	5
Table 2.1 Evaluation of hydrogen bond donors under Gassman cycloaddition reaction conditions	32
Table 2.2 Comparison of thiophosphoramidate with thiourea in presence of different Brønsted acids	34
Table 2.3 The scope of organocatalytic ionic [4+2] cycloaddition	36
Table 3.1 Preliminary catalyst and solvent screening	58
Table 3.2 Evaluation of various <i>N</i> -triflylphosphoramidates	60
Table 3.3 Evaluation of the solvent effect on ionic Diels-Alder stereoselectivity	62
Table 3.4 Substrate scope	64
Table 4.1 Preliminary catalyst screening	104
Table 4.2 Solvent screening	105
Table 4.3 Additional catalyst screening	107

List of Appendices

Appendix A.....	129
Appendix B.....	141
Appendix C.....	147

List of Abbreviations

Ac	Acetyl
Alloc	Allyloxycarbonyl
Ar	Aryl
Bn	Benzyl
Boc	tert-Butyloxycarbonyl
<i>t</i> -Bu	tert-Butyl
Bz	Benzoyl
Cat.	Catalyst
Cbz	Carboxybenzyl
CPA	Chiral phosphoric acid
CSA	Camphorsulphonic acid
DCM	Dichloromethane
DDQ	2,3-Dichloro-5,6-Dicyano-1,4-Benzoquinone
DMF	Dimethylformamide
Et	Ethyl
HBD	Hydrogen bond donor
MS	Molecular Sieves
NBS	<i>N</i> -Bromosuccinimide
Nu	Nucleophile

PG	Protecting Group
Ph	Phenyl
PMB	<i>para</i> -Methoxybenzyl
Pr	Propyl
<i>i</i> -Pr	iso-Propyl
TBAF	Tetrabutylammonium Fluoride
TBME	Methyl tert-butyl ether
TBS	tert-Butyldimethylsilyl
TES	Triethylsilyl
Tf	Trifluoromethanesulfonyl
THF	tetrahydrofuran
TMS	trimethylsilyl
Ts	<i>p</i> -Toluenesulfonyl

Abstract

Oxocarbenium ions are common intermediates or transition states for a variety of biological and synthetic transformations. Due to the fact that oxocarbenium ions are typically much more reactive than iminium ions, their reactivity is difficult to control. Especially challenging reactions of oxocarbeniums are stereoselective transformations. While there are several approaches to perform reactions of oxocarbeniums asymmetrically, the Nagorny group is particularly interested in using chiral hydrogen bond donors and Brønsted acids as catalysts for these reactions.

Chapter 1 of this thesis provides an introduction to chemistry of oxocarbenium ions, their generation and use in asymmetric reactions. Both anion activation and protonation of acetals and vinyl ethers with chiral hydrogen bond donors and chiral Brønsted acids are covered in this chapter.

Chapter 2 discusses ionic Diels-Alder reaction as well as the use of thiophosphoramidate as a co-catalyst for promoting this transformation. Thiophosphoramidate catalyst was found to bind sulfonate anions and was used to separate the vinyl oxocarbenium/sulfonate ion pair. This effect leads to acceleration of the Diels-Alder reaction of unsaturated acetals. Thiophosphoramidates are the most effective cocatalysts because of the stronger counterion activation effect resulting from three, rather than two, hydrogen bonds involved in anion binding.

Chapter 3 of this manuscript describes development of the first chiral catalyst-controlled enantioselective ionic Diels-Alder reaction of unsaturated acetals. Chiral BINOL-based *N*-triflylphosphoramides were used as catalysts for this transformation. This reaction proceeds through the intermediacy of a vinyl oxocarbenium/chiral anion pair, and the chiral *N*-triflylphosphoramide anion controls the stereoselectivity of the cycloaddition step. Moderate enantioselectivities (up to 80:20 e.r.) have been obtained when α,β -unsaturated dioxolanes were employed as the dienophiles. These reactions demonstrate strong dependence on the counterion coordinating properties and solvent polarity, a behavior characteristic of oxocarbenium ions.

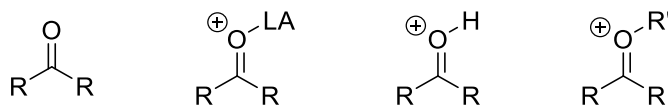
Finally, Chapter 4 describes attempts of stereo- and regioselective aminoglycosides via desymmetrization of *meso*-2-deoxystreptamine using chiral phosphoric acids as catalysts. We were able to show that chiral phosphoric acids facilitate desymmetrization of *meso*-diols via glycosylation reactions using mannose- α -trichloroacetimidate. Chiral phosphoric acid-promoted mannosylation of 2-deoxystreptamine produces a mixture of two α -mannosides. While (*R*)-enantiomer typically leads to glycosylation of 2-deoxystreptamine derivative with modest regioselectivities and a major regioisomer having glycosylation at *O*-4 (natural) of 2-deoxystreptamine, (*S*)-enantiomer favors glycosylation at *O*-6 with selectivities up to 1:5 (*O*-4 : *O*-6). This is the first report of desymmetrization of *meso*-diols via glycosylation using chiral phosphoric acids as catalysts. This method has a potential to be applied for glycodiversification of 2-deoxystreptamine and synthesis of new aminoglycoside antibiotics.

Chapter 1

Hydrogen Bond-Catalyzed Reactions of Oxocarbenium Ions

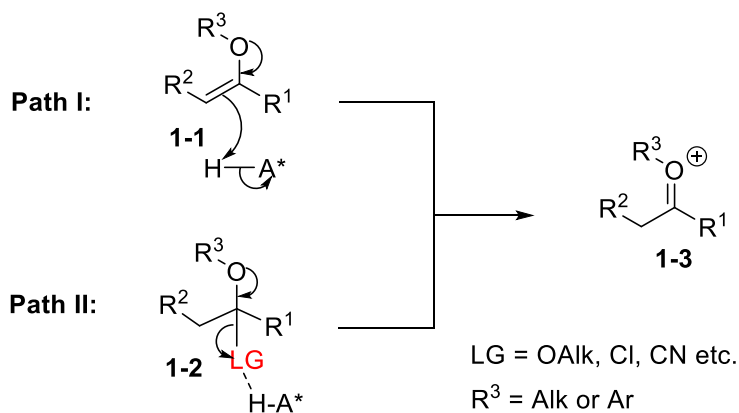
1.1 Introduction into Chemistry of Oxocarbenium Ions

An oxocarbenium ion is a carbocation, real or hypothetical, stabilized by electron pairs of neighboring oxygen atoms. Oxocarbeniums are common intermediates or transition states for many biological and synthetic processes (e.g. hydrolysis of glycosidic bonds, reduction of acetals, Diels-Alder reactions etc). The general structure of an oxocarbenium ion contains an oxygen-carbon double bond with the oxygen atom attached to another substituent. This structure has a formal positive charge that is placed on an oxygen atom. Being more highly polarized than typical carbonyls, they are far more reactive towards the addition of nucleophiles. A carbonyl can be activated with a Lewis acid coordination to oxygen, the smallest of which is a proton. The resulted structure can be considered an oxocarbenium ion if the full proton transfer occurs. An average dipole moment for a general ketone R_2CO is calculated to be $\delta = 0.51$, while a fully protonated ketone $[R_2COH]^+$ has a dipole moment of $\delta = 0.61$.



Lewis acid coordination to a carbonyl group can lead to formation of structures with a range of oxocarbenium ion character. The amount of positive charge on oxygen is determined by a number of factors but mainly by the strength of the bond between the Lewis acid and oxygen ranging from very weak electrostatic interactions to covalent bonds. That is why here we will focus only on oxocarbenium ions where oxygen is covalently bound to a carbon atom. Generation of oxocarbenium ions **1-3** can be achieved by either complete protonation of vinyl ethers **1-1** by strong Brønsted acids (Scheme 1.1, Path I) or by promoting leaving group dissociation from α -functionalized ethers **1-2** (Path II). Such dissociation can be promoted by both weakly acidic hydrogen bond donors and stronger Brønsted acids. Fully protonated carbonyls also have oxocarbenium ion character, however activation of carbonyls with chiral Brønsted acids has been recently reviewed¹ and will not be discussed here.

Scheme 1.1 Generation of oxocarbenium ions



Within the field of asymmetric catalysis, a variety of methods have been developed for highly enantio- and diastereoselective reactions of imines, as well as aldehydes and ketones. Many of these methods rely either on Lewis or Brønsted basicity of the

electrophilic substrates to bind chiral catalysts. Oxocarbenium ions are missing the Lewis basic site to bind the acidic catalyst, thus requiring other modes of controlling facial selectivity in such reactions. In addition to that, imines are far more basic than carbonyl compounds, making it easier to bind the acidic chiral catalyst. Finally, controlling reactions of oxocarbenium reactions is far more challenging² than of iminium ions due to high electrophilicity and reactivity of the former. It was our objective to study reactivity of oxocarbenium ions with the possibility to develop stereoselective reactions of oxocarbeniums.

1.2 Hydrogen bond catalysis

Over the past few decades enantioselective organocatalysis has emerged as an important paradigm for numerous stereoselective organic transformations. Hydrogen bond and Brønsted acid catalysis is one of the subfields of organocatalysis. Hydrogen bond donors possess the ability to coordinate to basic sites in substrate molecules, thus forming complexes with variable degrees of proton transfer.^{3,4,5} Organocatalysis, including hydrogen bond catalysis offers several advantages over Lewis acid catalysis. While many Lewis acid/base interactions are stronger and more directional, electrophilic activation by H-bond donors has also emerged as a powerful tool in asymmetric catalysis. H-bond catalysis typically does not use metals, making a contribution to green chemistry. Additionally, H-bond catalysts are typically non-toxic, shelf stable, as well as they offer promising advantages of immobilization on a solid phase.⁶

The relatively strong intramolecular interactions of molecules bearing X-H bonds, with proton acceptors A, were observed as early as the 19th century. Some of the examples

are Faraday's discovery of chlorine hydrate in 1823, while Nernst investigated the properties of molecules containing hydroxy groups. Huggins, Pauling, Bernal, Latimer, and Rodebush were among the first to recognize the generality of this phenomenon, and gave rise to the modern concept of H-bonding.⁷ The definition of the H-bond was recently provided by Steiner:

*“An X–H···A interaction is called a ‘hydrogen bond’, if 1) it constitutes a local bond, and 2) X–H acts as a proton donor to A.”*⁸

Hydrogen bond is a phenomenon that is very complex and chemically variable. Based on theoretical studies, hydrogen bond energies cover more than two orders of magnitude, about -0.2 to -40 kcal/mol. Hydrogen bonds have been subdivided to three categories: weak, moderate, and strong (Table 1.1). Since the maximum bond strength can be observed when X–H···A is 180° , this effect is mostly pronounced in strong hydrogen bonds, and is more relaxed in the case of moderate and weak H-bonds. The physical basis of hydrogen bonds also differs going from strong to weak interactions. While strong H-bonds are mostly considered to have covalent bonding character, moderate and weak hydrogen bonds are typically described as electrostatic interactions.⁹

Table 1.1 Properties of hydrogen bonds and their examples⁷

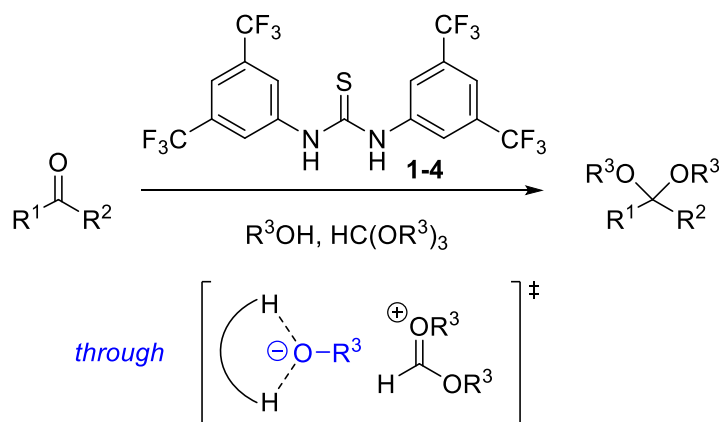
	Strong	Moderate	Weak
type of bonding	mostly covalent	mostly electrostatic	electrostatic
length of H-bond [Å]	1.2 - 1.5	1.5 - 2.2	2.2 - 3.2
bond angles[°]	175 - 180	130 - 180	90 - 150
bond energy [kcal/mol]	14 - 40	4 - 15	< 4
typical example	intramolecular NH...N bond in proton sponge	NH...O=C in peptide helices and sheets	bonds involving CH donors to N or O acceptors

Despite the long history of hydrogen bond and Brønsted acid catalysis, its asymmetric variations are relatively recent. The interest in Brønsted acid catalysis was reborn in the 1990's when weakly acidic hydrogen bond donors such as water and urea were shown to catalyze some organic transformations.¹⁰ This discovery roughly coincided with major progress in understanding the role of H-bonding in the function of different classes of enzymes.¹¹

1.3 Anion Activation

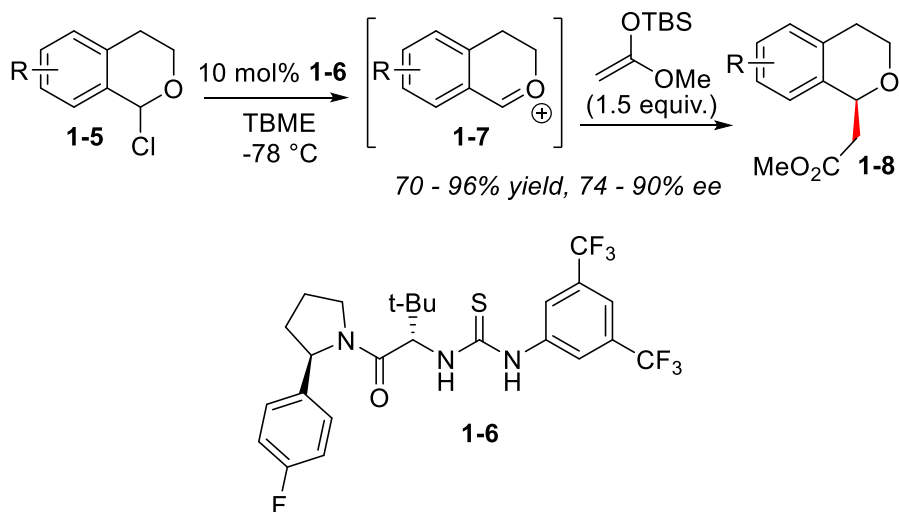
Studies of the mechanism of action of various enzymes identified hydrogen bonding as a key element for activation of various electrophiles, either through coordination to electrophiles, or through anion activation^{7,12} (Scheme 1.1, Path II). Independently, small molecule hydrogen bond donors were discovered to catalyze a variety of organic transformations through the same type of activation. The pioneering studies on this topic were published by Hine and co-workers. They identified biphenols and biphenylenediols as catalysts for nucleophilic addition of amines to epoxides.¹³ Soon a variety of different H-bond donors such as ureas, thioureas, squaramides, BINOLs, TADDOLs, etc. were developed and used for anion activation type of catalysis.

Scheme 1.2 Acetalization of carbonyls through stabilization of oxyanion



One of the first synthetic examples of anion activation using hydrogen bond donors was provided by Schreiner and Kotke. They reported an extremely efficient acetalization method of a variety of carbonyl compounds using thiourea **1-4** (Scheme 1.2). Their mechanistic studies showed that thiourea aids in the heterolysis of an orthoester stabilizing the oxyanion.¹⁴ Chiral variants of weakly acidic hydrogen bond donors were soon developed.¹⁵ Thus, pioneered by Prof. Eric Jacobsen, chiral ureas and thioureas were found to effectively promote dissociation of various leaving groups such as cyanides and chlorides,^{16b} resulting in cation/chiral anion pairs that subsequently undergo enantioselective nucleophilic attack. While successful in enantioselective reactions proceeding through iminium ions were developed,¹⁶ it was not immediately clear whether the same mode of activation would be applicable to more reactive oxocarbenium species. Unlike iminium ions, *O*-substituted oxocarbenium ions are typically more difficult to generate, are highly reactive, and can only be loosely coordinated to the chiral anion, impeding asymmetric induction. Development of stereoselective reactions of oxocarbenium ions thus presents a challenge.

Scheme 1.3 Enantioselective addition to 1-chloroisochromans



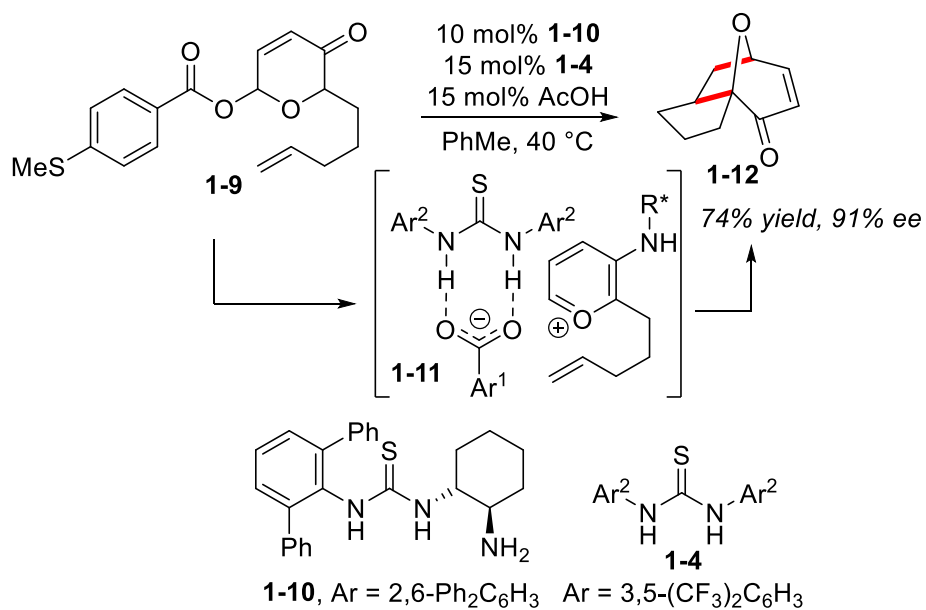
The first example of enantioselective oxocarbenium ion reaction catalyzed by H-bond donor was reported by the Jacobsen group (Scheme 1.3).¹⁷ Treating 1-chloroisochromans **1-5** with silyl ketene acetals and chiral thiourea **1-6** afforded alkylation products **1-8**. Methyl- and fluoro- substituents on the benzene ring of 1-chloro-isochroman were well tolerated, while addition of an electron-donating methoxy group at C-6 resulted in a moderate decrease in enantioselectivity, yet slightly increased yield (74% ee, 96% yield). Additionally, substitution on the silyl ketene acetal was well tolerated, providing α,α -disubstituted esters in high yields and enantioselectivities. Based on previous mechanistic studies on the addition of silyl ketene acetals to carbenium ions,¹⁸ as well as on the complete reaction inhibition with $n\text{Bu}_4\text{NCl}$, authors suggested a mechanism involving formation of oxocarbenium **1-7**/[**1-6**•Cl]⁻ ion pair.

While the aforementioned cases involve direct nucleophilic addition to the electrophilic carbon, hydrogen bond donors also promote oxocarbenium cycloaddition reactions (Scheme 1.4). In 2011 Jacobsen reported a protocol for enantioselective [5+2]

cycloaddition of pyrylium ions.¹⁹ To generate the pyrylium ion, *p*-thiomethylbenzoyl pyranones were treated with a mixture of Schreiner's thiourea **1-4** and chiral thiourea **1-10** (Scheme 1.4). High yields and enantioselectivities were achieved with substrates possessing olefin substitution on the terminal C atom (**1-9**), including allenes. Other modes of substitution were not tolerated well, providing low to no reactivity. Computational and experimental data support the intermediacy of aminopyrylium ion **1-11** forming via imine condensation between pyranone **1-9** and NH₂ group of **1-10**, followed by the loss of *p*-methylthiobenzoate. Although the substrate scope is rather limited by low reactivity, covalent binding of the chiral urea to the substrate explains high enantioselectivities achieved. It is possible that low reactivity is the consequence of the inherently low electrophilicity of the aromatic aminopyrylium ion. The covalent binding between the chiral catalyst and the substrate provides an exciting future opportunity for enhancing the electrophilicity of the intermediate.

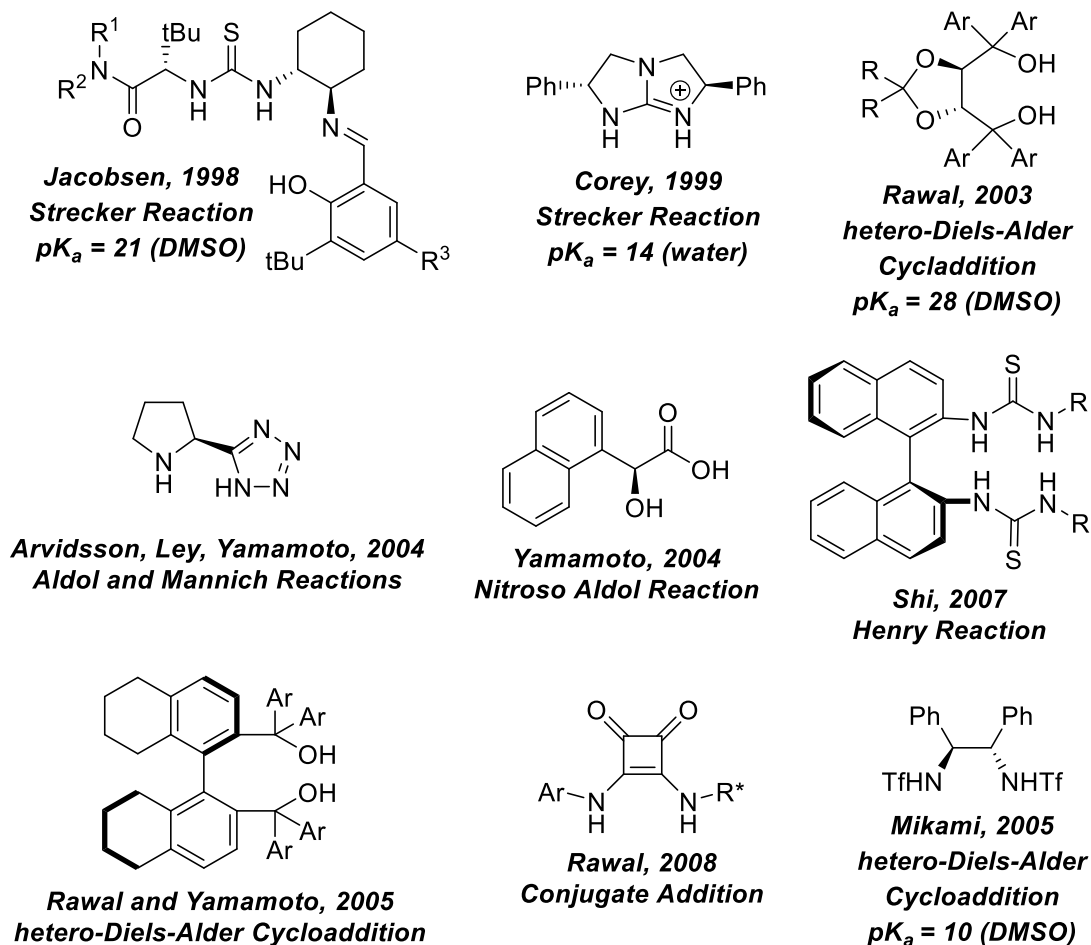
While H-bond donor ligands used for supramolecular purposes (such as anion recognition, anion transport, molecular cages etc.) typically provide the source for multiple hydrogen bonds, most of the hydrogen bond donors used in organocatalysis can simultaneously donate only up to two hydrogen bonds. Bifurcated H-bonding interactions benefit from increased strength and directionality relative to single hydrogen bond. Generally, any Lewis base is capable of engaging in bifurcated hydrogen bond. Electrophiles containing such groups as carbonyls, imine derivatives, N-acyliminium ions, and nitro compounds can all be activated by double-hydrogen bond donors.

Scheme 1.4 Cycloaddition reactions of oxocarbenium ions



Since the development of chiral thiourea by Jacobsen, there has been an explosion of research activity in the field of hydrogen bond catalysis. The H-bond donor catalysts now possess a wide range of structural and functional motifs (Figure 1.1). These catalysts differ widely in the mechanisms of electrophile activation and catalysis, as well as their acidities.

Figure 1.1 Examples of hydrogen bond catalysts²⁰



1.4 Protonation

As it was mentioned previously, electrophiles can be activated either through coordination to electrophiles, or through anion activation. Hence, coordination to electrophiles can be achieved with either Lewis or Brønsted acids. Since 1990s, chiral Brønsted acids have become popular catalysts for enantioselective synthesis due to the ubiquity of acid catalysis in organic transformations. Enantioselective Brønsted acid catalysis relies heavily on chiral inductions originating from chiral counter-anion or chiral counter-anion complexes. Therefore, the manipulation of chiral anions, by either structural

modification or strategic complexation, represents the most practical approach for the evolution of chiral Brønsted-acid catalysis.²¹

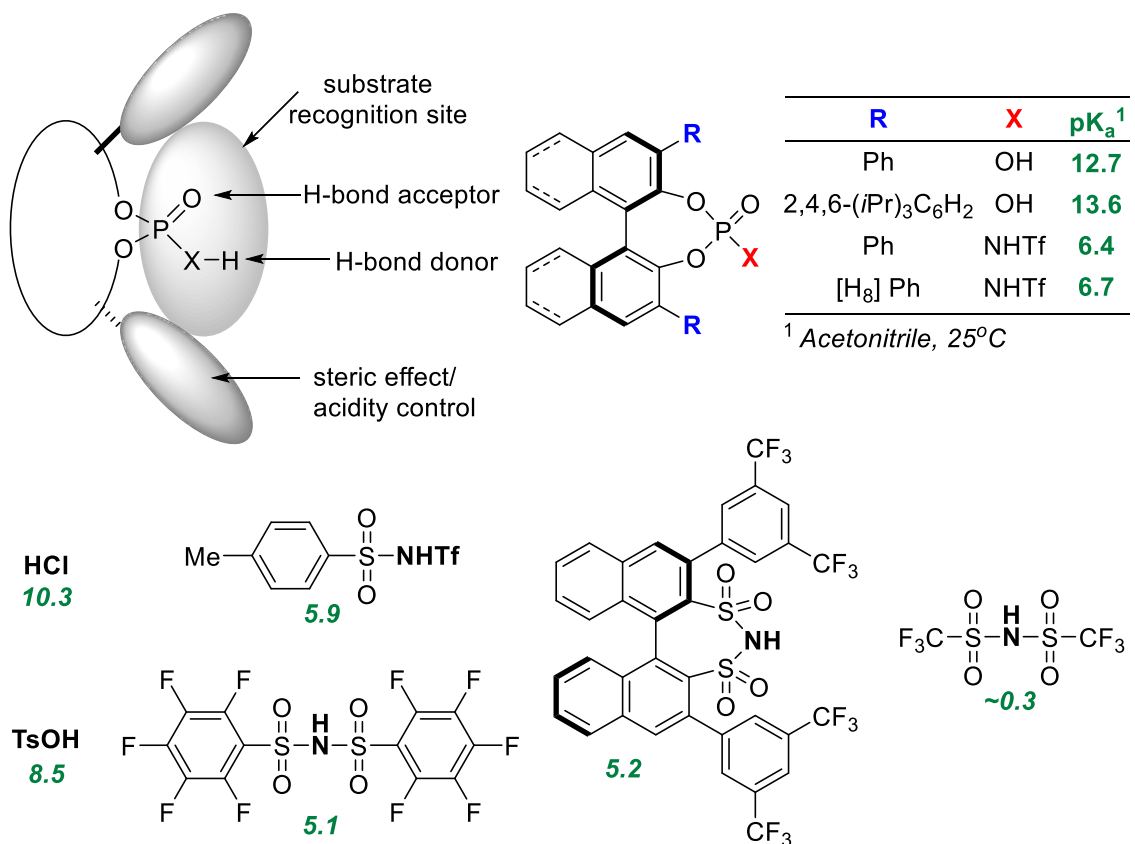
In 2004 a new group of chiral Brønsted acid organocatalysts was introduced by Akiyama and Terada. They independently reported synthesis of strong BINOL-derived chiral phosphoric acids (CPAs) and their application to Mannich-type reactions.^{22,23} Chiral phosphoric acids and their derivatives quickly became the most popular class of chiral Brønsted acids due to their high acidities and relative ease of structure modification.

The most widely used group of chiral phosphoric acids, is based upon a rigid C-2 symmetric BINOL scaffold (Figure 1.2). The binaphthyl moiety is most frequently modified by changing substituents at positions 3 and 3' which allows adjustment both of the steric properties around the substrate recognition site as well as pK_a of the phosphoric acid. In addition, the steric environment around the phosphate functionality may be attenuated by using H₈-BINOL rather than BINOL-based backbone. The OH group (Y = OH in Figure 1.2) on phosphorus acts as an acidic hydrogen-bond donor, and in some cases the phosphoryl oxygen (X = O in Figure 1.2) can also act as a hydrogen bond acceptor.

The pK_a of chiral phosphoric acids may range from 14 to 12.5 (in acetonitrile)²⁴, which is usually acidic enough to activate electrophiles such as imines or aziridines. However, chiral phosphoric acids are not as effective in coordinating to less basic functional groups. Ever since CPAs were introduced, there have been many attempts to increase their acidity in order to activate less reactive electrophiles. Because thioacids are known to be somewhat more acidic than the corresponding oxoacids, a diverse group of

thiophosphoric acids (Figure 1.2, X = S/O; Y = S) was synthesized and applied to enantioselective catalysis.²⁵

Figure 1.2 Structure and acidities of chiral phosphoric acids and *N*-triflamides



In 2006, Yamamoto and co-workers proposed a new group of highly acidic CPA derivatives.²⁶ The introduction of a strongly electron withdrawing *N*-triflamido group in place of the hydroxyl group furnished catalyst, which was sufficiently acidic to activate α,β -unsaturated ketones. This acid proved to be an excellent enantioselective catalyst for the Diels-Alder reactions between α,β -unsaturated ketones and reactive dienes and many other cases where a stronger Brønsted acid was desired. Further titration studies performed

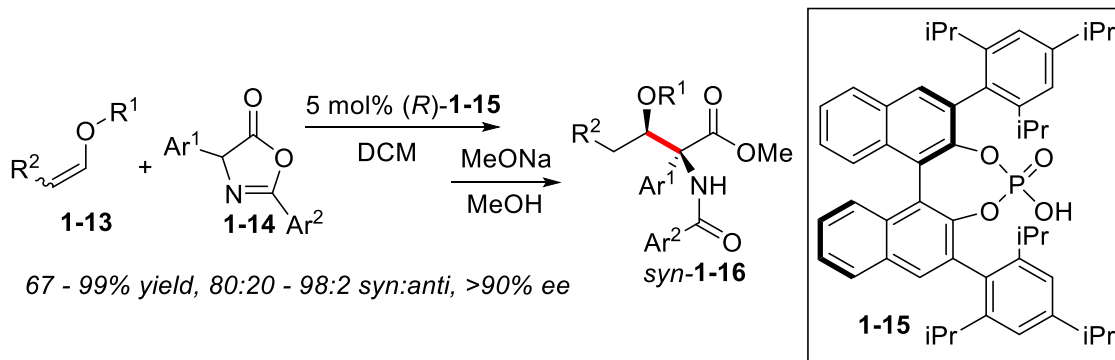
by Rueping and co-workers showed, that pK_a values of N-triflylphosphoramides range between 6 and 7.²⁴

Advances in chiral phosphoric acids and their derivatives allowed chemists to develop a variety of stereoselective reactions including reactions of oxocarbenium ions. In this case activation of an electrophile proceeds through complete protonation of a vinyl ether or an acetal. Thus, in 2009 Terada reported enantioselective addition of a carbon-nucleophile to an oxocarbenium ion catalyzed by chiral phosphoric acid (Scheme 1.5).²⁷ To form the oxocarbenium ion and promote direct aldol-type addition, vinyl ethers were treated with a chiral phosphoric acid **1-15** in the presence of azlactones **1-14**. Chiral phosphoric acids are much stronger hydrogen bond donors than thioureas, hence substantial protonation of the vinyl ether can be achieved. Enantio- and diastereoselectivities were determined after aldol adducts were treated with sodium methoxide in methanol to provide the corresponding methyl esters **1-16**.

In this reaction, Ar² substitution has a substantial effect on the reaction yield, as well as on both enantio- and diastereoselectivity. Thus, when electron-donating methoxy-substituents were present (Ar² = 3,5-(MeO)₂C₆H₃), the corresponding products were obtained in higher yields and stereoselectivities. Additionally, sterically demanding tert-butyl ether (R¹ = *t*Bu) was essential for selective formation of the *syn* stereoisomer. Substituent Ar¹, however, was shown to have almost no effect on enantio- and diastereoselectivity. While Terada showed that chiral phosphoric acids can indeed catalyze stereoselective nucleophilic addition to vinyl ethers, the effects of the substrate substitution on the product diastereoselectivity are rather substantial. It should be noted that the range of available chiral Brønsted acids has significantly expanded since the original report by

Terada, and the stereoselectivity issues may plausibly be resolved by newer catalysts. Additionally, a more convincing evidence for the intermediacy of oxocarbenium ions in this reaction is desirable.

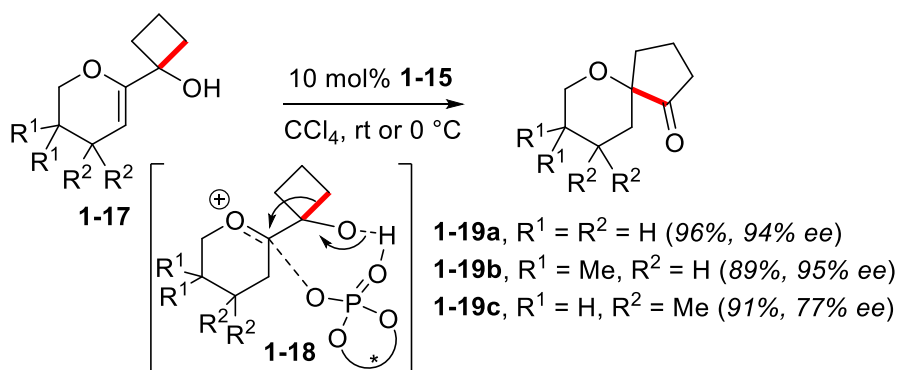
Scheme 1.5 Aldol-type reaction of vinyl ethers by Terada



Since Terada's report on the enantioselective nucleophilic addition to vinyl ethers (*vide supra*), chiral phosphoric acids and their derivatives became important catalysts for promoting stereoselective reactions of oxocarbenium ions. Tu and coworkers used the same chiral phosphoric acid **1-15** for a conceptually similar approach to enantioselective semipinacol rearrangement (Scheme 1.6).^{28a} This method allowed easy access to chiral spiroethers, a structural motif found in a selection of biologically significant drugs and natural products. To produce chiral spiroethers **1-19**, cyclic vinyl ethers **1-17** were treated with either chiral phosphoric acid (*R*)-**1-15** or its Ag salt. Here the chiral silver phosphate participates in Ag-proton exchange with the starting allyl alcohol, forming (*R*)-**1-15** in situ. Although geminal substitution at the C5 of dihydropyranyl (**1-19b**) ring was well tolerated, geminal substitution at the C4 (**1-19c**) or C6 resulted in decreased enantiocontrol (77-87% ee). The reaction was tentatively proposed to proceed through oxocarbenium ion **1-18**, however no detailed mechanistic data are available to support this hypothesis. Since the

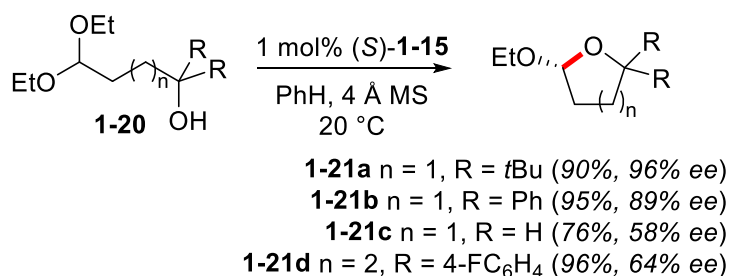
current study involved only substrates with *gem*-dialkyl or -diallyl substitution, additional studies would be necessary to fully define the substrate scope of this reaction. This methodology would have also benefited from applying it to the synthesis of spiroethers structurally similar to naturally occurring motifs.

Scheme 1.6 Semipinacol rearrangement by Tu



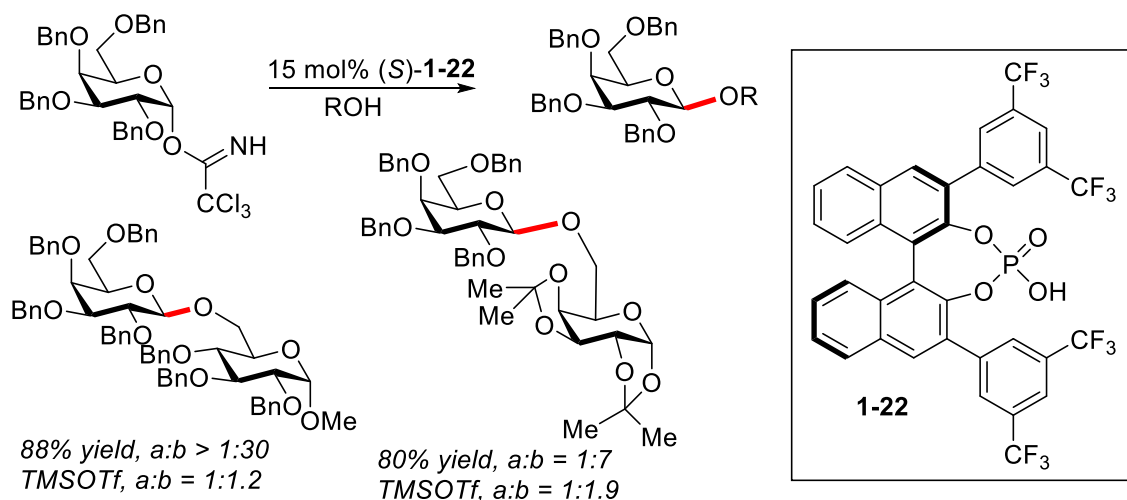
Addition of oxygen nucleophiles to oxocarbenium ions leads to formation of cyclic and acyclic *O,O*-acetals, including glycosides, saccharides, and spiroketals, which are ubiquitous among practically important natural and synthetic organic compounds. Asymmetric acetal synthesis presents a considerable challenge due to lability of the products under the reaction conditions, as well as due to weak interactions of the oxocarbenium with the chiral fragment. The propensity of product acetals to ionize to oxocarbenium ions can be partially moderated by limiting the Brønsted acidity of the catalyst.²⁹ It should be noted, however, that even relatively strongly acidic chiral phosphoric acids are known to be efficient catalysts for the stereoselective formation of *O,O*-acetals (*vide infra*).^{24,30}

Scheme 1.7 Asymmetric transacetalization by List



The first protocol for enantioselective formation of *O,O*-acetals by intramolecular transacetalization was reported by the List group (Scheme 1.7).³¹ Remarkably, TRIP-based phosphoric acid (*S*)-**1-15** was again found to be the most powerful catalyst, providing excellent enantioinduction. Aliphatic (**1-21a**) and aromatic (**1-21b**) geminal substituents are tolerated equally well, affording mixed acetals in high yields and enantioselectivities. Formation of unsubstituted acetal **1-21c** was less enantioselective (58% ee), apparently due to the smaller substrate size. Lower stereoselectivity was also observed for six-membered acetal formation (**1-21d**, 64% ee).

Scheme 1.8 Glycosylation catalyzed by CPAs



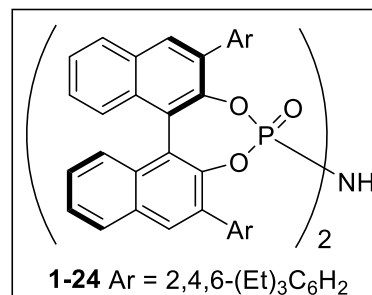
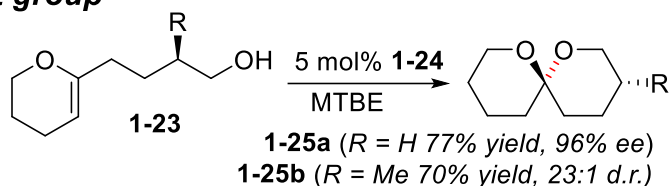
A contemporaneous report by the Fairbanks group demonstrated the first chiral phosphoric acid-controlled β -selective glycosylation (Scheme 1.8).³² While the reaction proceeded with good to excellent β -selectivity, it is not immediately clear whether this observation is entirely due to the effects of the chiral catalysts, since some stereocontrol by the chiral substrate might be anticipated. Later examples show that chiral phosphoric acids can also be utilized for regioselective acetylation and glycosylation of polyols, as well as for glycosylative chiral resolution of alcohols (see chapter 4).

Spiroketal motifs are important motifs that are often present in biologically active natural products. Racemic synthesis of thermodynamically more stable spiroketals is well developed. However, until recently, no direct chiral catalyst-controlled methods were available for stereoselective synthesis of thermodynamic and non-thermodynamic spiroketals.³³ Contemporaneously with the List group, our group identified that chiral phosphoric acids can be used as catalysts for enantioselective and diastereoselective non-thermodynamic synthesis of spiroketals without promoting significant epimerization at the anomeric position (Scheme 1.9).

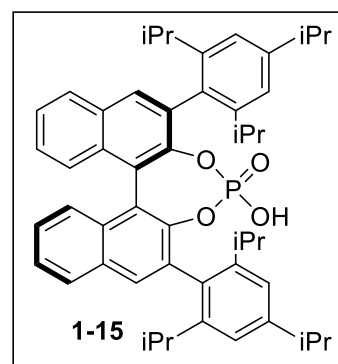
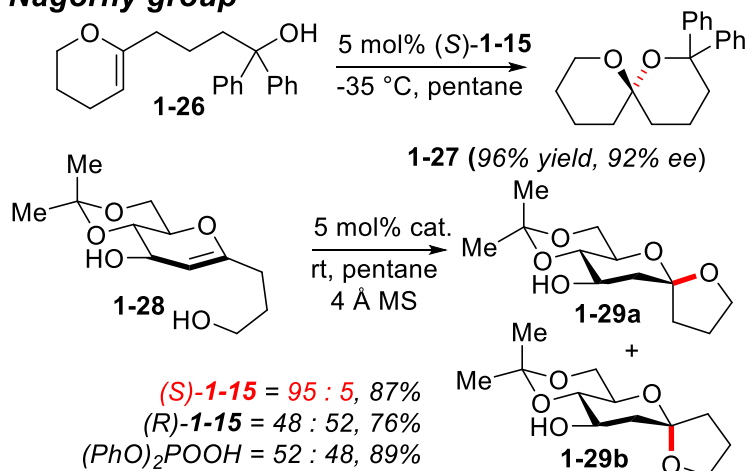
The List group aimed at stereoselective synthesis of unfunctionalized, sterically undemanding spiroketals.³⁴ Cycloisomerization of cyclic enol ethers possessing tethered alcohol moieties (**1-23**) was promoted by Brønsted acids. Since the most popular chiral phosphoric acids such as **1-15** provided unsatisfactory enantioselectivities for such small substrates, a variety of chiral BINOL-based diphosphorimides (i.e. **1-24**) were designed. By fine-tuning the catalyst structure, highly stereoselective and high yielding synthesis of both chiral and non-thermodynamic spiroketals were accomplished. Later, a similar strategy was applied to the synthesis of cyclic acetals.³⁵

Scheme 1.9 Stereoselective spiroketalization

List group



Nagorny group

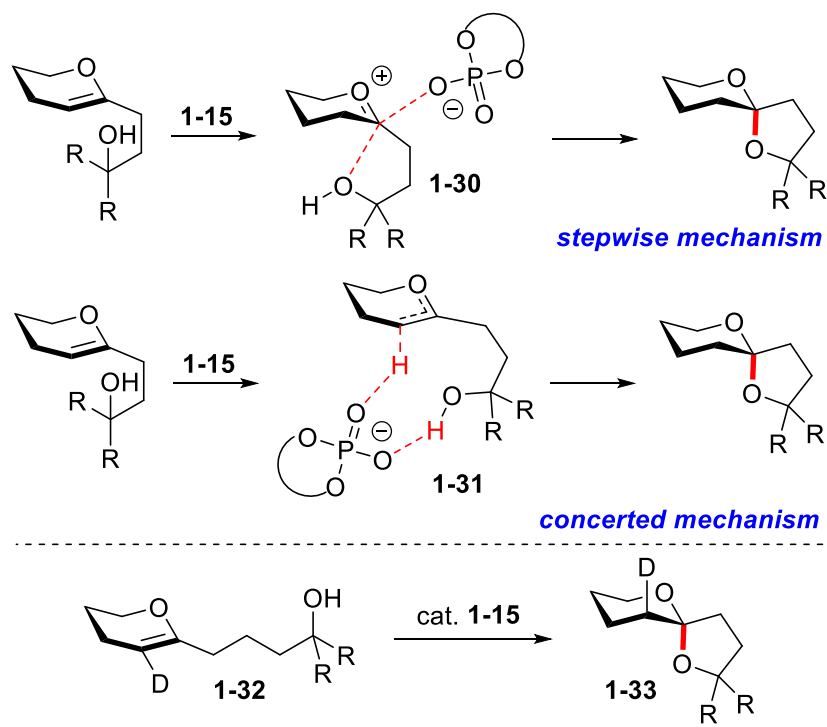


At the same time, our group used commercially available TRIP-phosphoric acid (*S*)-**1-15** for spiroketalization of sterically encumbered substrates.³⁶ Along with that, diastereoselective spirocyclizations of glycols (**1-28**) were investigated. Remarkably, a diastereodifferentiating reaction was observed, and while (*S*)-**1-15** catalyzed formation of non-thermodynamic spiroketals, the reactions promoted with (*R*)-**1-15** were completely unselective possibly due to matching/mismatching between the chiral catalyst and chiral glycols.

Although conventionally all of the discussed transformations can be generalized as oxocarbenium reactions, very few mechanistic studies are available to support the intermediacy of well-defined carbocationic species. For the majority of nucleophilic

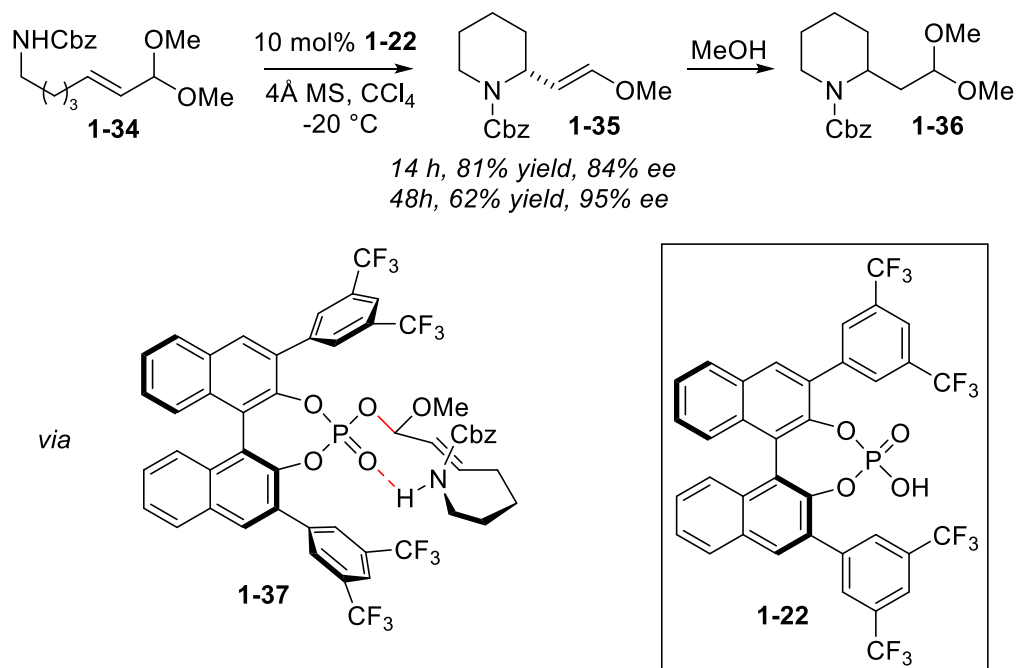
additions discussed in this chapter, more sophisticated concerted mechanisms have been proposed. Most importantly, the clear distinction between the mechanistic possibilities would potentially allow developing more efficient catalytic systems. Results from our group obtained by Grace A. Winshel show that in the case of spiroketalizations, reactions proceed through a concerted mechanism without forming an oxocarbenium ion intermediate (Scheme 1.10). In this case oxocarbenium species are present only in transition state. Additionally, protonation of cyclic deuterated enol ether **1-32** catalyzed by chiral phosphoric acid **1-15** results in stereospecific formation of spiroketal **1-33**. This supports the mechanism proceeding through transition state like **1-31** since such mechanisms suggests protonation of the double bond and nucleophilic attack from the same face of the molecule.

Scheme 1.10 Potential reaction mechanisms for spiroketalization reaction



Finally, our group recently developed a highly enantioselective heterocyclization of α,β -unsaturated acetals **1-34** catalyzed by chiral phosphoric acids (Scheme 1.11). The chiral vinyl ether products were shown to undergo enantioenrichment under the prolonged reaction conditions. Computational studies that were performed using the growing string method with exact transition state search (B3LYP, 6-31G**) showed that the reaction proceeds through the formation of mixed chiral phosphate acetal **1-37**, followed by S_N2'-like displacement.³⁷ These results oppose the generally accepted formation of vinyl oxocarbenium ion.

Scheme 1.11 Enantioselective aza-Michael reactions



The discussed examples indicate that hydrogen bond donors could serve as excellent catalysts for stereocontrolled reactions involving oxocarbenium ions. However, further developments in this area would serve to improve the scope of such transformations,

develop more efficient and stable catalysts, and gain a deeper understanding of the phenomena underlying hydrogen bond and Brønsted acid catalysis.

References

- ¹ Rueping, M.; Kuenkel, A.; Atodiresei, I. *Chem. Soc. Rev.* **2011**, *40*, 4539–4549.
- ² Watson, M.; Maity, P. *Synlett* **2012**, *23*, 1705–1708.
- ³ Cheon, C. H.; Yamamoto, H. *Chem. Commun.* **2011**, *47*, 3043.
- ⁴ Akiyama, T. *Chem. Rev.* **2007**, *107*, 5744–5758.
- ⁵ Rueping, M.; Kuenkel, A.; Atodiresei, I. *Chem. Soc. Rev.* **2011**, *40*, 4539.
- ⁶ Lee, J.-W.; Mayer-Gall, T.; Opwis, K.; Song, C. E.; Gutmann, J. S.; List, B. *Science* **2013**, *341*, 1225–1229.
- ⁷ Taylor, M. S.; Jacobsen, E. N. *Angew. Chem. Int. Ed.* **2006**, *45*, 1520–1543.
- ⁸ Steiner, T. *Angew. Chem. Int. Ed.* **2002**, *41*, 48–76.
- ⁹ Jeffery, G. A. *An Introduction to Hydrogen Bonding*; Oxford University Press: New York, NY, 1997.
- ¹⁰ (a) Blake, J. F.; Jorgensen, W. L. *J. Am. Chem. Soc.* **1991**, *113*, 7430–7432. (b) Blake, J. F.; Lim, D.; Jorgensen, W. L. *J. Am. Chem. Soc.* **1994**, *59*, 803–805. (c) Curran, D. P.; Kuo, L. H. *J. Org. Chem.* **1994**, *59*, 3259–3261.
- ¹¹ Silverman, R. B. *The Organic Chemistry of Enzyme-Catalyzed Reactions*; Academic Press: San Diego, CA, 2002.
- ¹² Zhang, Z.; Schreiner, P. R. *Chem. Soc. Rev.* **2009**, *38* (4), 1187.
- ¹³ (a) Hine, J.; Linden, S. M.; Kanagasabapathy, V. M. *J. Am. Chem. Soc.* **1985**, *107*, 1082–1083. (b) Hine, J.; Linden, S. M.; Kanagasabapathy, V. M. *J. Org. Chem.* **1985**, *50*, 5096–5099.
- ¹⁴ Kotke, M.; Schreiner, P. R. *Tetrahedron* **2006**, *62*, 434–439.
- ¹⁵ For reviews see: (a) Schreiner, P. R. *Chem. Soc. Rev.* **2003**, *32*, 289–296. (b) Pihko, P. M. *Angew. Chem. Int. Ed.* **2004**, *43*, 2062–2064. (c) Taylor, M. S.; Jacobsen, E. N. *Angew. Chem. Int. Ed.* **2006**, *45*, 1520–1543. (d) Doyle, A. G.; Jacobsen, E. N. *Chem. Rev.* **2007**, *107*, 5713–5743. (e) Rueping, M.; Nachtsheim, B. J.; Ieawsuwan, W.; Atodiresei, I. *Angew. Chem. Int. Ed.* **2011**, *50*, 6706–6720.

- ¹⁶ (a) Taylor, M. S.; Jacobsen, E. N. *J. Am. Chem. Soc.* **2004**, *126*, 10558–10559. (b) Raheem, I. T.; Thiara, P. S.; Peterson, E. A.; Jacobsen, E. N. *J. Am. Chem. Soc.* **2007**, *129*, 13404–13405.
- ¹⁷ Reisman, S. E.; Doyle, A. G.; Jacobsen, E. N. *J. Am. Chem. Soc.* **2008**, *130*, 7198–7199.
- ¹⁸ Burfeindt, J.; Patz, M.; Müller, M.; Mayr, H. *J. Am. Chem. Soc.* **1998**, *120*, 3629–3634.
- ¹⁹ Burns, N. Z.; Witten, M. R.; Jacobsen, E. N. *J. Am. Chem. Soc.* **2011**, *133*, 14578–14581.
- ²⁰ Akiyama, T. In *Hydrogen Bonding in Organic Synthesis*; Pihko, P. M., Ed.; Wiley-VCH Verlag GmbH & Co. KGaA: Weinheim, Germany; pp 5–14.
- ²¹ Lv, J.; Luo, S. *Chem. Commun.* **2013**, *49*, 847–858.
- ²² Akiyama, T.; Itoh, J.; Yokota, K.; Fuchibe, K. *Angew. Chem. Int. Ed.* **2004**, *43*, 1566–1568.
- ²³ Uraguchi, D.; Terada, M. *J. Am. Chem. Soc.* **2004**, *126*, 5356–5357.
- ²⁴ Kaupmees, K.; Tolstoluzhsky, N.; Raja, S.; Rueping, M.; Leito, I. *Angew. Chem. Int. Ed.* **2013**, *52*, 11569–11572.
- ²⁵ Shapiro, N. D.; Rauniyar, V.; Hamilton, G. L.; Wu, J.; Toste, F. D. *Nature* **2011**, *470*, 245–249.
- ²⁶ Nakashima, D.; Yamamoto, H. *J. Am. Chem. Soc.* **2006**, *128*, 9626–9627.
- ²⁷ Terada, M.; Tanaka, H.; Sorimachi, K. *J. Am. Chem. Soc.* **2009**, *131*, 3430–3431.
- ²⁸ (a) Zhang, Q.-W.; Fan, C.-A.; Zhang, H.-J.; Tu, Y.-Q.; Zhao, Y.-M.; Gu, P.; Chen, Z.-M. *Angew. Chem. Int. Ed.* **2009**, *48*, 8572–8574. For pinacol rearrangements catalyzed by chiral phosphoric acids see also: (b) Liang, T.; Zhang, Z.; Antilla, J. C. *Angew. Chem. Int. Ed.* **2010**, *49*, 9734–9736. (c) Snyder, S. A.; Thomas, S. B.; Mayer, A. C.; Breazzano, S. P. *Angew. Chem. Int. Ed.* **2012**, *51*, 4080–4084.
- ²⁹ Čorić, I.; Vellalath, S.; Müller, S.; Cheng, X.; List, B. In *Inventing Reactions*; Gooßen, L. J., Ed.; Springer Berlin Heidelberg: Berlin, Heidelberg, 2012; Vol. 44, pp. 165–193.
- ³⁰ Christ, P.; Lindsay, A. G.; Vormittag, S. S.; Neudörfl, J.-M.; Berkessel, A.; O'Donoghue, A. C. *Chem.-Eur.J.* **2011**, *17*, 8524–8528.
- ³¹ Čorić, I.; Vellalath, S.; List, B. *J. Am. Chem. Soc.* **2010**, *132*, 8536–8537.
- ³² Cox, D. J.; Smith, M. D.; Fairbanks, A. J. *Org. Lett.* **2010**, *12*, 1452–1455.

- ³³ Nagorny, P.; Sun, Z.; Winschel, G. *Synlett* **2013**, *24*, 661–665.
- ³⁴ Čorić, I.; List, B. *Nature* **2012**, *483*, 315–319.
- ³⁵ Kim, J. H.; Čorić, I.; Vellalath, S.; List, B. *Angew. Chem. Int. Ed.* **2013**, *52*, 4474–4477.
- ³⁶ Sun, Z.; Winschel, G. A.; Borovika, A.; Nagorny, P. *J. Am. Chem. Soc.* **2012**, *134*, 8074–8077.
- ³⁷ Sun, Z.; Winschel, G. A.; Zimmerman, P. M.; Nagorny, P. *Angew. Chem. Int. Ed.* **2014**, *53*, 11194–11198.

Chapter 2

Thiophosphoramidate-Based Cooperative Catalysts for Brønsted Acid Promoted Ionic Diels-Alder Reaction.

2.1 Introduction

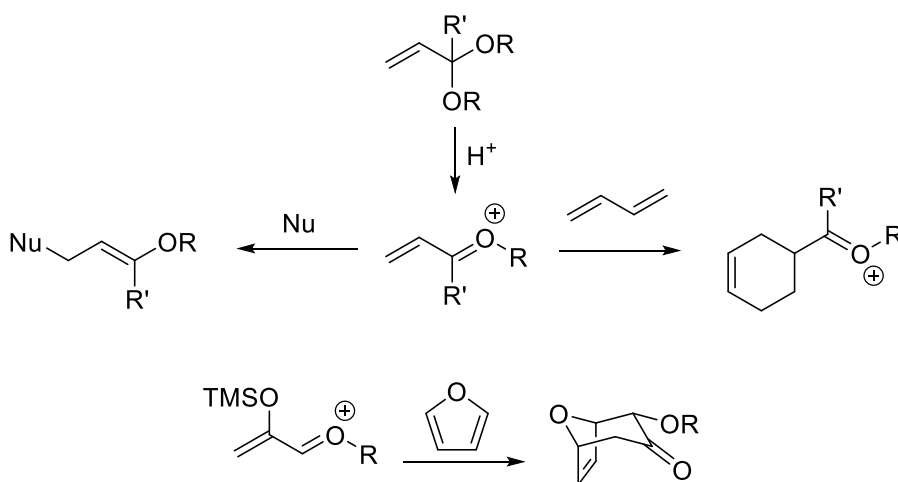
Over the past several decades, chemists have gathered significant evidence that enzymes could drastically accelerate nucleophilic addition reactions by establishing mutually reinforcing or cooperative hydrogen bonds within a receptor. These observations have inspired the development of various catalytic transformations, in which substrate activation is achieved by the formation of multiple hydrogen bonds with a synthetic hydrogen bond donor (HBD).¹

The majority of such transformations rely on HBD activation of neutral substrates by enhancing their electrophilicity. Recent studies, however, demonstrate that various ionic reactions proceeding through polar intermediates could also be catalyzed by HBDs.^{1b} In this case, HBD association with the counter anion of an *in situ*-generated ion pair results in enhanced reactivity of the cation (Chapter 1, Section 1.3). Pioneered by Jacobsen² and Schreiner³ groups, counterion activation has been utilized to enhance the reactivity of various iminium ions, as well as certain reactions proceeding through the stabilized oxocarbenium and carbenium-based ion pairs.⁴

2.2 Gassman Cycloaddition

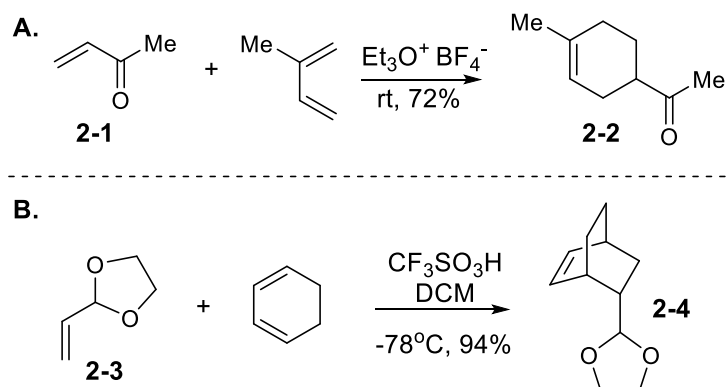
Our group is interested in developing organocatalytic transformations involving oxocarbenium ions. Particularly interesting to us are reaction of α,β -unsaturated or vinyl oxocarbenium ions. Vinyl oxocarbenium ions are allylic cations substituted by at least one oxygen atom at one of the terminal carbon atoms. Vinyl oxocarbeniums are typically more stable than saturated oxocarbeniums and hence have slightly different chemical behaviour compared to saturated oxocarbeniums.

Scheme 2.1 Reactions of vinyl oxocarbenium ions



The most common way to generate vinyl oxocarbenium ion intermediates or transition states is through protonation of α,β -unsaturated acetals. While vinyl oxocarbenium ions produced by activation of α,β -unsaturated acetals can be applied for Michael additions, Diels-Alder reactions, [3+4] cycloadditions, etc (Scheme 2.1), probably, one of the most known transformations of this type is the ionic [2+4] cycloaddition reaction (Gassman cycloaddition).

Scheme 2.2 [4+2] cycloaddition of vinyl oxocarbenium ions



Vinyl oxocarbenium ion participation in Diels-Alder reactions was first mentioned in 1982 when Sasaki *et. al.* reported a reaction between methyl vinyl ketone **2-1** and isoprene catalyzed by triethyloxonium tetrafluoroborate to afford Diels-Alder cycloadduct **2-2** in 72% yield (Scheme 2.2 A).^{5,6} However, no oxocarbenium ion intermediates were observed. Years later Gassman and co-workers showed that acrolein acetals (such as **2-3**) can be used as vinyl oxocarbenium dienophile precursors when activated by triflic acid (Scheme 2.2 B).⁷ Before this modification of Diels-Alder reaction was developed, α,β -unsaturated carbonyls were considered to be undesired dienophiles due to their participation in many unwanted side reactions such as oxidation and polymerization. α,β -Unsaturated acetals, on the other hand, are more stable under identical conditions. Thus, protection of carbonyl group with an acetal allowed chemists to utilize equivalents of α,β -unsaturated aldehydes and ketones as dienophiles in [4+2] cycloaddition reaction providing high yields for cycloadducts.

Despite these findings, there were still a number of dienes and dienophiles which would not undergo [4+2] cycloaddition or provide very low yields due to polymerization or low activity of the reagents. For example, hindered unsaturated acetals, ketals and

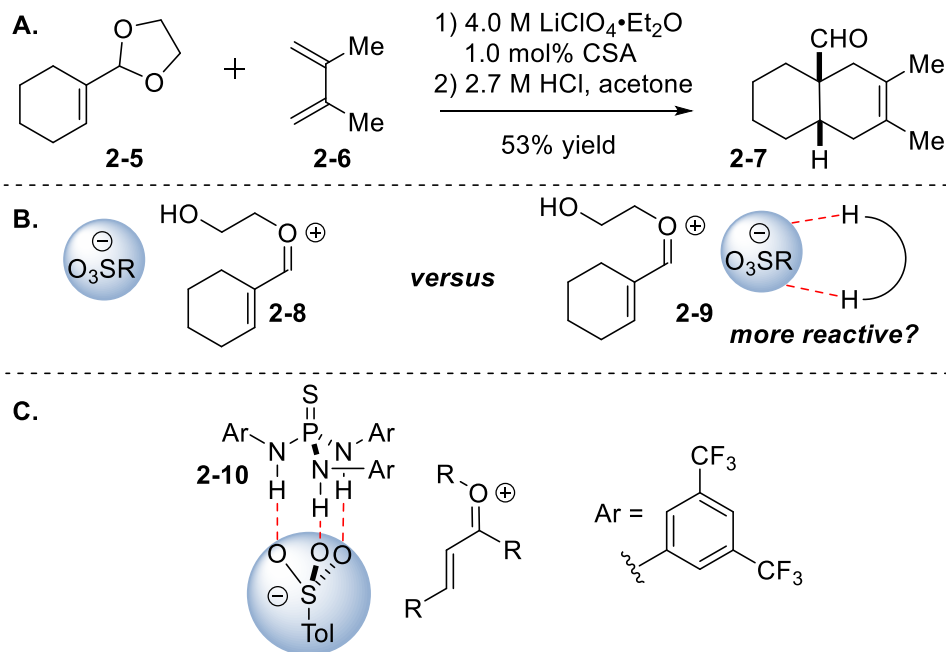
unreactive dienes typically cause such complications. The Gassman report was followed by a large number of publications based on application of vinyl oxocarbenium ions in Diels-Alder reactions which showed that both Lewis acids and Brønsted acids can be used as catalysts for generation of oxocarbenium ions. However, the only available protocol for rate acceleration of Gassman cycloaddition comes from the Grieco group.⁸ The procedure relies on the use of concentrated solution of lithium(I) perchlorate (4.0 M in diethyl ether) and catalytic amounts of sulfonic acids. Remarkably, challenging cycloaddition reactions could be achieved under these conditions. Thus, by employing Grieco protocol, the Danishefsky group has accomplished the formation of cycloadduct **2-7** (Scheme 2.3 A),⁹ which is notoriously difficult to obtain by Lewis acid activation of the carbonyl functionality-containing dienophiles equivalent to **2-5**. Both the presence of lithium(I) perchlorate and catalytic sulfonic acid are essential for the progression of this reaction, and no reaction occurs if one of these components is omitted. It has been proposed that highly ionic medium is essential for the separation of the counterions and the generation of a more reactive separated ion pair **2-8**.^{8,10} At the same time, a highly polar medium is important for the tighter association of **2-8** and diene **2-6** that results in a decreased transition state volume.

2.3 Thiophosphoramides as co-catalysts

Despite their synthetic utility, currently existing ionic [4+2] cycloaddition protocols have significant limitations since the use of Lewis acids in combination with low reaction temperatures or explosive additives such as lithium(I) perchlorate are necessary (Scheme 2.3 A). This chapter describes our development of a mild organocatalytic protocol that is based on the cooperative catalysis of Brønsted acids and HBD co-catalysts.¹¹ Driven by

the hypothesis that complexation to a hydrogen bond donor could significantly enhance the reactivity of **2-8** by the formation of a more separated ion pair **2-9** (Scheme 2.3 B), we have evaluated various HBDs and discovered that catalytic quantities of thiophosphoramidate **2-10** can significantly accelerate the rates of ionic Diels-Alder reactions catalyzed by the Brønsted acids. We are not aware of the prior use of the three-hydrogen bond donors such as **2-10** for anion-binding activation, and demonstrate that **2-10** is an excellent activator of sulfonate anions associated with vinyl oxocarbenium ions.

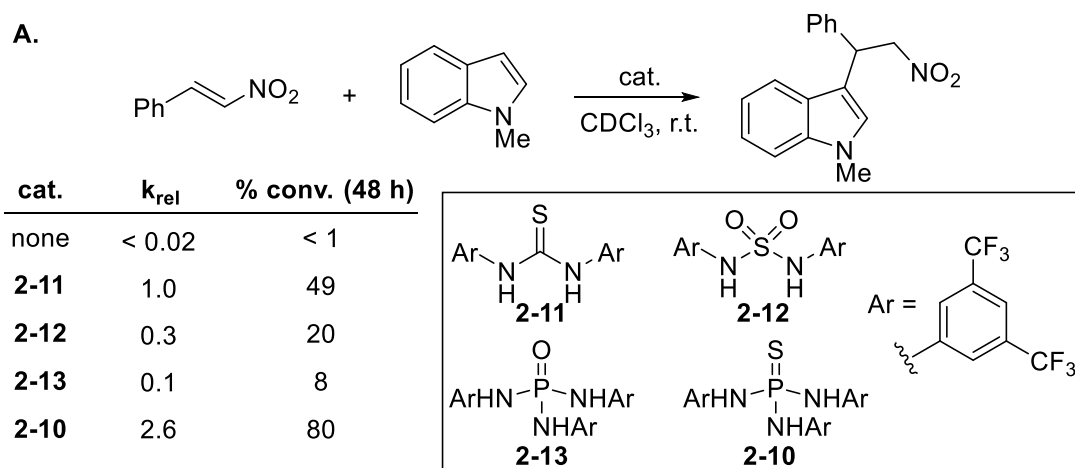
Scheme 2.3 Proposed activation of dienophiles in Gassman cycloaddition



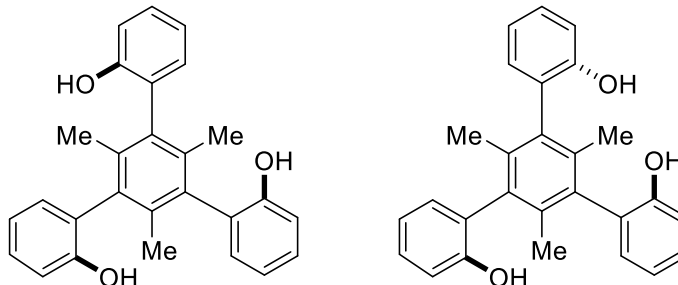
Since sulfonic acids are one of the most common class of Brønsted acids used for ionic [4+2] cycloadditions, we wanted to pursue HBDs that are able to accommodate the tridentate binding to the sulfonate anion. While most HBDs can provide only up to two hydrogen bonds at a time (*vide supra*), our attention turned to thiophosphortriamides (Scheme 2.3 C) which could potentially provide up to three hydrogen bonds at a time.

Previous results by the Shea group showed that thiophosphoramidate **2-10** is an excellent HBD, and can be used as catalysts in Baylis-Hillman and Friedel-Crafts reactions as activators of α,β -unsaturated esters and nitroalkenes (Scheme 2.4 A).¹² While both phosphoramidate **2-13** and thiophosphoramidate **2-10** showed excellent results, in all cases thiophosphoramidate **2-10** outperformed **2-13** in catalytic activity. Contemporaneously with our studies, Gale and coworkers published NMR titration studies comparing sulfinamide **2-21**, phosphoramidate **2-13**, and thiophosphoramidate **2-10** binding constants to a variety of anions.¹³ These results confirmed that **2-10** can be used as an excellent HBD for our purposes. While there have been a few other precedents of anion-binding to three-hydrogen-bond donors (Scheme 2.4 B),¹⁴ thiophosphoramidates have a potential of being used as chiral hydrogen bond donors for asymmetric reactions¹⁵ involving anion activation.

Scheme 2.4 Three hydrogen bond donors



B.



Our studies commenced with the evaluation of various HBD co-catalysts in the *p*-TSA-catalyzed ionic Diels-Alder reaction.¹⁶ Commercially available acrolein acetal **2-3** and cyclopentadiene were mixed together with catalytic amounts of *p*-TSA and HBD (Table 2.1) in toluene at -10 °C. When exposed to *p*-TSA (3 mol%) without a co-catalyst or in combination with thiourea **2-11** (6 mol%), no formation of cycloadduct **2-14** was detected after one hour under these conditions (entries 1 and 2). The NH hydrogens of squaramide **2-15** are further apart than in thiourea **2-11**, and consequently **2-15** is more geometrically suited for binding the oxygens of the sulfate anion.¹⁷ Indeed, when used as a co-catalyst under identical conditions, **2-15** promoted the formation of **2-14** (entry 3), albeit in 15% conversion. In the search of alternative HBDs, we turned our attention to thiophosphoramides **2-16**, **2-17**, and **2-10**.^{12,15} We surmised that known thiophosphoramide **2-10** is geometrically more suited for binding a sulfate anion and could potentially form up to three hydrogen bonds with the negatively charged oxygens of sulfate (*cf.* Scheme 2.3 C for an example of such complex).¹⁴ Gratifyingly, when used as a co-catalyst, **2-10** significantly accelerated the reaction of **2-3** and cyclopentadiene, and the quantitative formation of cycloadduct **2-14** was detected within one hour (entry 6). In order to test if all three NH bonds are essential for the anion activation, thiophosphoramides **2-16** and **2-17** were evaluated next (entries 4 and 5). Both catalysts were inferior to **2-10** in promoting the formation of **2-14** and only minor amounts of the product were observed in each case. A control experiment in the absence of *p*-TSA was conducted (entry 7); however, no formation of the product was detected.

Table 2.1 Evaluation of hydrogen bond donors under Gassman cycloaddition reaction conditions

2-11

2-15

2-16

2-17

2-10

Ar = -C₆H₃(CF₃)₂

entry	acid	catalyst	time, h	T, °C	endo/exo	conversion, (%) ^b
1	<i>p</i> -TSA	none	1	-10	n/a	0
2	<i>p</i> -TSA	2-11	1	-10	n/a	0
3	<i>p</i> -TSA	2-15	1	-10	1.5:1	15
4	<i>p</i> -TSA	2-16	1	-10	n/a	2
5	<i>p</i> -TSA	2-17	1	-10	2.5:1	7
6	<i>p</i> -TSA	2-10	1	-10	3:1	98
7	none	2-10	1	-10	n/a	0

[a] These experiments were performed on 0.5 - 0.7 mmol scale (0.3 M solution) using 3 equivalents of cyclopentadiene. [b] The reaction yields were determined by ¹H NMR analysis of the crude reaction mixtures using internal standard.

The geometry of **2-10** is optimal for forming three hydrogen bonds with polyoxygenated tetrahedral anions formed by group III elements (e.g. sulfonates, phosphates, perchlorates, etc.). However, even in the situation when there is no clear geometrical preference for the anion binding, **2-10** outperformed thiourea **2-11** as the co-catalyst (Table 2.2). While the acidity of HCl (pK_a = 1.8 in DMSO) is close to the acidity of sulfonic acids (pK_a of MsOH in DMSO is 1.6), a chloride anion could form a tighter ion pair with oxocarbenium than sulfonate anions, in which the negative charge is distributed among three oxygens. Consistent with this presumption, a significantly longer reaction

time (24 h) was required to observe the formation of the product **2-14**, and the reaction catalyzed by **2-10** proceeded to a higher extent (33%, Table 2.2, entry 3) than the corresponding reaction promoted by **2-11** (22%, entry 2). Similar trends were observed for the HBr-catalyzed formation of **2-14** (entries 4–6). HBr is stronger than both hydrochloric and *p*-toluenesulfonic acids ($\text{pK}_a = 0.9$ in DMSO), and bromide is a weaker coordinating anion than chloride. As expected, HBr alone promoted the reaction to a significantly higher extent than HCl (37% conversion, 10 h, entry 4). Similarly to the HCl case, the use of **2-10** as a co-catalyst resulted in an accelerated reaction (97% conversion, 10 h, entry 6). Importantly, these experiments indicate that weaker *p*-toluenesulfonic acid is a more effective catalyst than stronger HBr when combined with **2-10** in promoting formation of cycloadduct **2-14**. We attribute this effect to the higher affinity of **2-10** to the tetrahedral sulfate anion due to the geometric predisposition to form three hydrogen bonds with the sulfonate oxygens. Finally, to demonstrate that hydrogen bond donors could accelerate the reactions promoted by strong triflic acid, we conducted the experiments described in entries 7–9 (Table 2.2). Triflic acid alone promoted the formation of **2-14** at $-35\text{ }^\circ\text{C}$; however, this reaction was slow and only 20% of **2-14** was observed after 1.5 h. The addition of the thiourea co-catalyst **2-11** did not enhance the cycloaddition; however, 78% conversion was observed when **2-10** was employed as the catalyst (entry 9).

Table 2.2 Comparison of thiophosphoramidate with thiourea in presence of different Brønsted acids

Catalyst (6 mol%)^a
Acid (3 mol%),
toluene, T

2-11

2-10

entry	acid	catalyst	time, h	T, °C	endo/exo	conversion, (%) ^b
1	HCl	none	24	-10	n/a	0
2	HCl	2-11	24	-10	3:1	22
3	HCl	2-10	24	-10	2.9:1	33
4	HBr	none	10	-10	n/a	37
5	HBr	2-11	10	-10	3:1	46
6	HBr	2-10	10	-10	3:1	97
7	TfOH	none	1.5	-35	n/a	20
8	TfOH	2-11	1.5	-35	n/a	0
9	TfOH	2-10	1.5	-35	3:1	78

[a] These experiments were performed on 0.5 - 0.7 mmol scale (0.3 M solution) using 3 equivalents of cyclopentadiene. [b] The reaction yields were determined by ¹H NMR analysis of the crude reaction mixtures using internal standard.

With the optimal reaction conditions in hand, the scope of the ionic [4+2] cycloadditions was explored next (Table 2.3). In order to evaluate synthetic utility of this protocol, the scope of both dienes (entries 1–4) and dienophiles (entries 5–7) as well as the application of this method to the preparation of synthetically useful *cis*-decaline-based building blocks (entries 8–10) has been examined. The reaction of **2-3** with various dienes such as cyclopentadiene (entry 1), 2,3-dimethyl-1,3-butadiene (entry 2), 1,3-

cyclohexadiene (entry 3) and 1,4-diphenyl-1,3-butadiene (entry 4) resulted in the formation of cycloadducts in good to excellent isolated yields (57-92%) when *p*-TSA was used in combination with thiophosphoramidate **2-10**. However, neither *p*-TSA alone nor the combination of *p*-TSA and thiourea **2-11** could promote the formation of cycloadducts to a significant extent. Similarly, the reactions of 5,5-dimethyl-2-vinyl-1,3-dioxane **2-20** (entry 5), (*E*)-2-styryl-1,3-dioxolane **2-22** (entry 6) and (*E*)-2-(prop-1-en-1-yl)-1,3-dioxolane **2-24** (entry 7) resulted in synthetically useful yields (63–91%) when *p*-TSA/**2-10** were employed as the catalysts, but failed to result in significant amounts of cycloadducts when only *p*-TSA or the combination of *p*-TSA and thiourea **2-11** were used as catalysts.

The ionic [2+4] cycloadditions have found a widespread application in the synthesis of highly functionalized decalines (*vide supra*). To demonstrate that our protocol is amenable to the synthesis of these valuable building blocks, the reactions of 2-cyclohexenone and 2-methyl-2-cyclohexenone-derived dioxolanes (**2-26** and **2-28** respectively) were tested (entries 8 and 9). While the cycloadditions were found to be slow in toluene, the use of dichloromethane as the solvent and increased catalyst loadings (5 mol% of *p*-TSA, 10 mol% of **2-10**) lead to the formation of the corresponding cycloadducts in good yields (68% and 84% correspondingly).

Table 2.3 The scope of organocatalytic ionic [4+2] cycloaddition

entry	dienophile	diene	product	time, h	catalyst	yield, % ^b	dr
1				1	none	18	2.8:1
					2-11	< 5	–
				14	none	< 5	–
					2-10	< 5	–
				16	none	< 5	–
					2-10	85	20:1
4 ^{c,d}				6	none	< 5	–
					2-10	57	8.3:1
5				0.8	none	7	5.5:1
					2-11	17	4.6:1
				3	none	< 5	–
					2-10	63	4.8:1
7				2	none	9	2:1
					2-10	< 5	–
						81	2:1

[a] These experiments were performed on 0.5–0.9 mmol scale (0.3 M solution in toluene) using 5 equivalents of cyclopentadiene. [b] The isolated reaction yields are reported for the reactions catalyzed by *p*-TSA/**2-10**. The reaction yields for the reactions catalyzed by *p*-TSA or *p*-TSA/**2-11** were determined by ¹H NMR analysis of the crude reaction mixtures using internal standard. [c] These experiments were performed on 0.3–0.7 mmol scale (0.6 M solution in dichloromethane) using 5 equivalents of cyclopentadiene, 5 mol% of *p*-TSA and 10 mol% of **2-10** or **2-11**. [d] The reaction was conducted at room temperature.

Table 2.3 (continued) The scope of organocatalytic ionic [4+2] cycloaddition

entry	dienophile	diene	product	time, h	catalyst	yield, % ^b	dr
8 ^c	 2-26		 2-27	2	none	13	–
			 2-11		< 5	–	
			 2-10		68	–	
9 ^{c,d}	 2-28		 2-29	24	none	28	–
			 2-11		13	–	
			 2-10		84	–	
10 ^c	 2-5		 2-30	24	none 2-11 2-10	< 5 < 5 59	– – –

[a] These experiments were performed on 0.5-0.9 mmol scale (0.3 M solution in toluene) using 5 equivalents of cyclopentadiene. [b] The isolated reaction yields are reported for the reactions catalyzed by *p*-TSA/**2-10**. The reaction yields for the reactions catalyzed by *p*-TSA or *p*-TSA/**2-11** were determined by ¹H NMR analysis of the crude reaction mixtures using internal standard. [c] These experiments were performed on 0.3-0.7 mmol scale (0.6 M solution in dichloromethane) using 5 equivalents of cyclopentadiene, 5 mol% of *p*-TSA and 10 mol% of **2-10** or **2-11**. [d] The reaction was conducted at room temperature.

Finally, to test whether this method is applicable to the challenging cycloadditions the reaction of 2-(cyclohex-1-en-1-yl)-1,3-dioxolane **2-5** and 2,3-dimethyl-1,3-butadiene was executed (Table 2.3, entry 10). The Lewis acid-catalyzed reactions of cyclohex-1-enecarbaldehyde or cyclohex-1-enecarboxylates are notoriously difficult to execute with unactivated dienes (*vide infra*), while the Grieco protocol could be used to provide the analogous cycloadduct **2-7** in 53% yield (Scheme 2.3).⁹ Remarkably, co-catalyst **2-10** in combination with *p*-TSA was sufficient to promote the formation of the corresponding

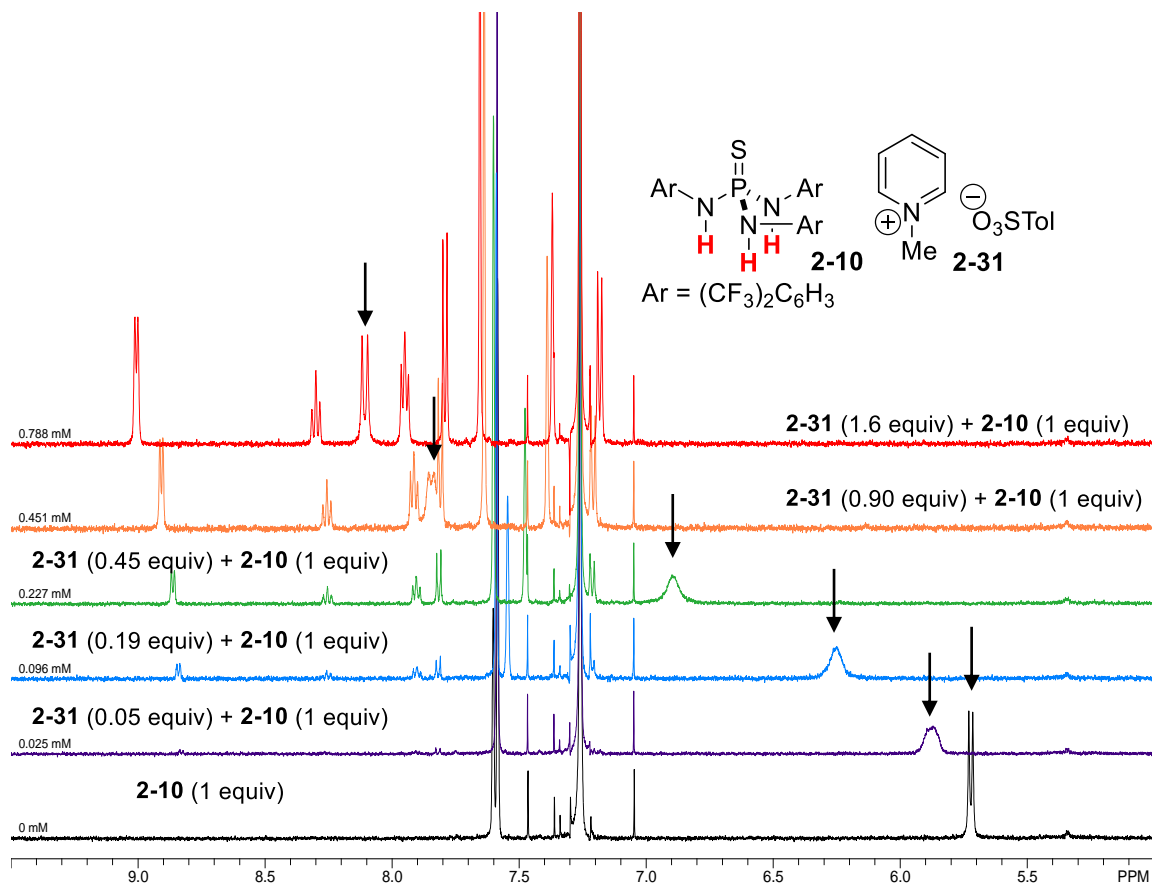
cycloadduct **2-30** in 59% yield (Table 2.3, entry 10) without resorting to the use of a highly ionic medium (4 M solution of lithium(I) perchlorate in diethyl ether).

2.4 Tosylate/thiophosphoramidate complexation studies

To confirm that **2-10** complexes anions and to gain a better understanding of the observed effect, binding and computational studies have been conducted. First, the association of **2-10** with sulfonate anions was confirmed by Pui-In Tang by combining **2-10** with known methylpyridinium tosylate (**2-31**) at different proportions and observing the resulting ^1H NMRs (Figure 2.1). Thus, the addition of **2-31** to solution of **2-10** resulted in a concentration-dependent shift of the phosphoramidate NH protons downfield, which is characteristic of hydrogen bonding to anion.¹⁸ WinEQNMR¹⁹ was used to establish the association constant of this complex ($K_a = 7.3 \cdot 10^4$ in CDCl_3). Based on the value of K_a , we conclude that **2-10** strongly binds tosylate anion of **2-31** in chloroform.

The stoichiometry of the resultant complex between **2-31** and **2-10** was determined by ^1H NMR titration using continuous variation method (Job plot, see Experimental Section).²⁰ The stoichiometry of binding is consistent with the formation of 1:1 complex between **2-31** and **2-10**. Our further attempts to compare the association constant value of **2-31** and **2-10** with the corresponding K_a 's of **2-11**/ Ts^- or **2-10**/ Cl^- did not result in conclusive results due to the more complex stoichiometries of the resultant supramolecular complexes.

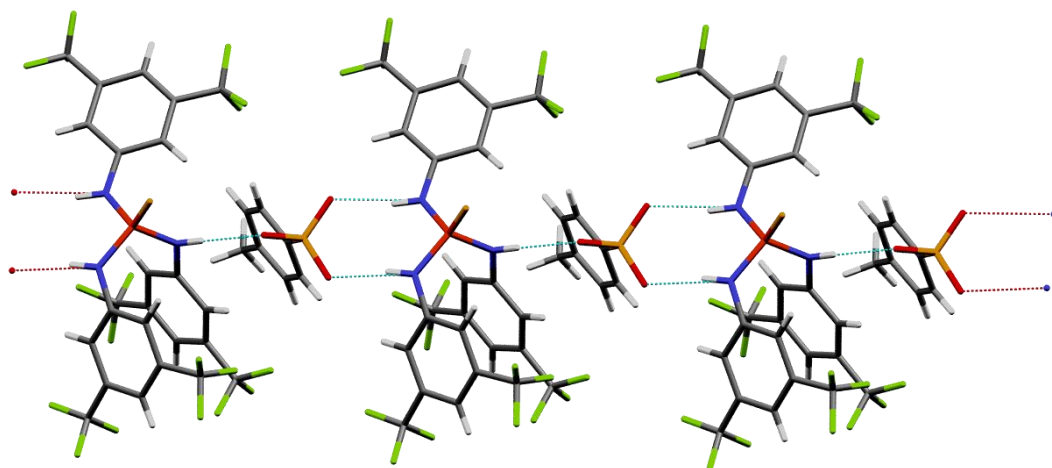
Figure 2.1 Titration studies



In addition to NMR studies, the complex between **2-10** and **2-31** was crystallized and the structure was analyzed using single crystal X-ray diffraction (Figure 2.2). Interestingly, **2-10** does form three hydrogen bonds with the tosylate anion, however the geometry of **2-10** in solid state precludes the formation of a tetrahedral structure (Scheme 2.3). In the solid state tosylate anion forms hydrogen bonds with two thiophosphoramidate molecules, while thiophosphoramidate provides three hydrogen bonds to two tosylates. Thus, the single crystal has a polymer-like structure based on hydrogen bonds. Bond distances were measured between nitrogens of **2-10** and oxygens of tosylate and were

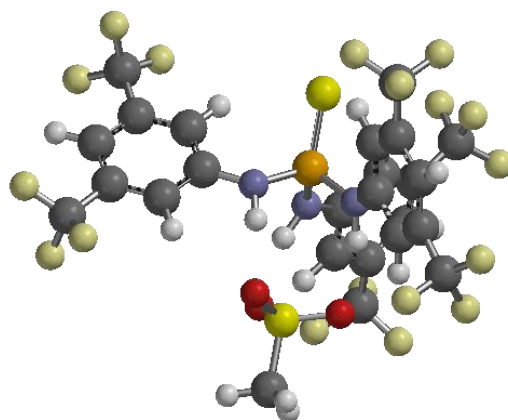
found to be 2.779 Å (single H-bond), 2.826 Å and 2.998 Å (two H-bonds). While the X-ray structure shows that one thiophosphoramidate molecule cannot form three hydrogen bonds with a tosylate, the possibility of forming such a complex in solution cannot be ruled out.

Figure 2.2 X-ray structure of **2-10**•**2-31**



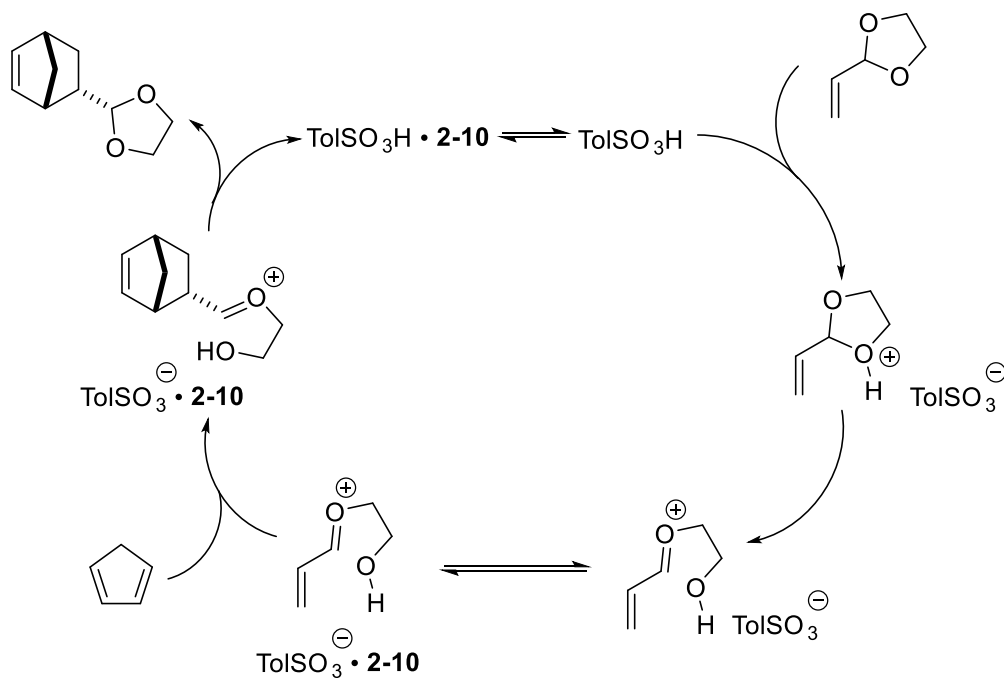
Finally, computational studies were initiated to model the interactions of the sulfonate and **2-10** (Figure 2.3). Thus, DFT-based geometry optimization of **2-10** and mesylate (B3LYP, 6-31+G*, toluene) resulted in a complex, in which three NH hydrogens of **2-10** are bound to all three oxygens of the mesylate anion. This complex was found to be by 3.7 kcal/mol more stable than the corresponding complex of thiourea **2-11**. While these results support the proposal that **2-10** is the most effective co-catalyst due to its stronger association with anions, which consequently result in more activated vinyl oxocarbenium ion, a more complex mechanistic scheme is likely to be operational.

Figure 2.3 Computed complex between **2-10** and mesylate



The proposed mechanism of the ionic Diels-Alder transformation catalyzed with *p*-toluenesulfonic acid and thiophosphoramidate **2-10** is depicted in Scheme 2.5. It is not clear however if the acidic species that participate in protonation of an acetal is pTSA or its complex with **2-10**.

Scheme 2.5 Proposed mechanism for the ionic Diels-Alder reaction



2.5 Conclusions

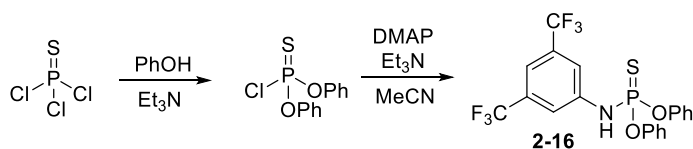
In conclusion, the combination of a Brønsted acid as the catalyst and a hydrogen bond donor as the co-catalyst can be used to catalyze a variety of ionic [2+4] cycloaddition reactions under mild conditions that do not require the use of a highly ionic medium (e.g. 4 M lithium(I) perchlorate in ether). Remarkably, thiophosphoramidate **2-10**, which has not been previously utilized for the anion binding was found to be superior to the standard two hydrogen bond donors such as thiourea **2-11** or squaramide **2-15**. Computational, X-ray, and NMR studies suggest that this could be attributed to the ability of **2-10** to form strong three hydrogen-bond-containing complexes with the anions. This effect was found to be especially strong for sulfonate anions, the geometry of which favors the formation of three hydrogen bonds with the sulfonate oxygens. Recent results from the Kozłowski group show that thiophosphoramidate **2-10** is one of the strongest neutral small molecule hydrogen bond donors available and used in organocatalysis.²¹

2.6 Experimental

Unless otherwise stated, all reagents were purchased from commercial suppliers and used without purification. Toluene (PhMe), dichloromethane (CH₂Cl₂) and diethyl ether (Et₂O) were filtered through a column (Innovative Technology PS-MD-5) of activated alumina under nitrogen atmosphere. All reactions were carried out under an atmosphere of nitrogen in flame- or oven-dried glassware with magnetic stirring. Reactions were cooled via external cooling baths: ice water (0 °C), Neslab Cryotrol CB-80 immersion cooler (0 to -60 °C) or Neslab Cryocool immersion cooler CC-100 II. Purification of the reactions mixtures was performed by flash chromatography using SiliCycleSiliaFlash P60 (230-400 mesh) silica gel. All spectra were recorded on Varian vnmrs 700 (700 MHz),

Varian vnmrs 500 (500 MHz), Varian MR400 (400 MHz), Varian Inova 500 (500 MHz) spectrometers and chemical shifts (δ) are reported in parts per million (ppm) and referenced to the ^1H signal of the internal tetramethylsilane according to IUPAC recommendations.²² Data are reported as (br = broad, s = singlet, d = doublet, t = triplet, q = quartet, qn = quintet, sext = sextet, m = multiplet; coupling constant(s) in Hz; integration). High resolution mass spectra (HRMS) were recorded on MicromassAutoSpecUltima or VG (Micromass) 70-250-S Magnetic sector mass spectrometers in the University of Michigan mass spectrometry laboratory. Infrared (IR) spectra were recorded as thin films on NaCl plates on a Perkin Elmer Spectrum BX FT-IR spectrometer. Absorption peaks were reported in wavenumbers (cm^{-1}). All commercially unavailable acetals and ketals were prepared following the procedure reported by Lu and coworkers.²³ Commercially unavailable hydrogen bond donors were synthesized by previously reported procedures.²⁴

Synthesis of thiophosphoramidate 2-16.

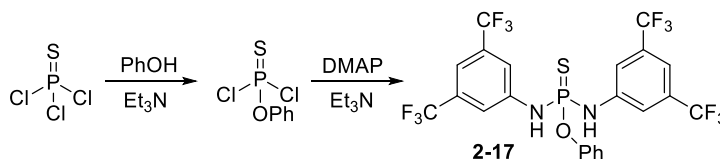


Phenol (1.11 g, 11.8 mmol) and triethylamine (1.81 mL, 18.9 mmol) were added to a flame-dried 200mL round bottom flask charged with 30 mL dry dichloromethane. Flask was cooled to 0 °C and thiophosphoryl chloride (0.60 mL, 5.9 mmol) was added dropwise. After two hours TLC indicated reaction went to completion. Solvent was evaporated and ^1H NMR confirmed desired diphenoxythiophosphoryl chloride. Compound was used

directly in the following reaction without purification. ^1H NMR (400 MHz, CDCl_3): $\delta = 7.44$ (t, $J = 7.6$ Hz, 2 H), 7.37-7.27 (m, 3 H).²⁵

Previously made diphenoxythiophosphoryl chloride (285 mg, 1 mmol) was dissolved in 3 mL of dry acetonitrile. 4-Dimethylaminopyridine (244.3 mg, 2 mmol) was then added followed by triethylamine (0.98 mL, 7 mmol), and 3,5-bis(trifluoromethyl)aniline (313 μL , 2 mmol) at room temperature. The mixture was refluxed for 48 hours. Reaction was then quenched with saturated NaHCO_3 . The product was extracted with diethyl ether, and then organic layer was dried over MgSO_4 , filtered and concentrated in vacuo. Crude product was purified by column chromatography (3:1 hexanes/ethyl acetate) and all fractions with product, including those with impurities were collected. Product was recrystallized from hexanes.

White solid, 62% yield (592 mg). IR (thin film, cm^{-1}): 3246, 1717, 1621, 1490, 1471, 1391, 1276, 1183, 1136, 986, 927, 794, 686. ^1H NMR (400 MHz, CDCl_3): δ 7.66 (s, 2H), 7.58 (s, 1H), 7.36 (t, $J = 7.7$ Hz, 4H), 7.24 (t, $J = 7.7$ Hz, 2H), 7.18 (d, $J = 7.7$ Hz, 4H), 6.01 (d, $J = 15.0$ Hz, 1H); ^{13}C NMR (175 MHz, CDCl_3): δ 150.1 (2C), 140.5, 133.0 (q, $J = 34$ Hz, 2C), 129.8, 126.0, 123.7, 122.2, 121.0 (2C), 117.9, 116.2, ^{31}P NMR (162 MHz, CDCl_3) δ 55.0 (s); ^{19}F NMR (376 MHz, CDCl_3) δ -63.1 (s); HRMS (ESI+) (m/z): $[\text{M}+\text{H}]^+$ calcd for $\text{C}_{20}\text{H}_{15}\text{F}_6\text{NO}_2\text{PS}$ 478.0453, found 478.0460.



Synthesis of thiophosphoramide 2-17.

Phenol (277.6 mg, 2.95 mmol) and triethylamine (0.50 mL, 3.54 mmol) were added to a flame-dried 200mL round bottom flask charged with 30 mL dry dichloromethane. The mixture was cooled to 0 °C and thiophosphoryl chloride (0.30 mL, 2.95 mmol) was added dropwise. After two hours TLC indicated reaction went to completion. Solvent was evaporated and ¹H NMR confirmed desired phenoxythiophosphoryl chloride. Compound used directly in following reaction without purification. ¹H NMR (400 MHz, CDCl₃): δ = 7.44 (t, J= 7.6 Hz, 2 H), 7.315 (m, 3 H).³

Phenoxythiophosphoryl chloride, together with 4-dimethylaminopyridine (1.194 g, 11.8 mmol) were added to a 200mL round bottom flask followed by triethylamine (15 mL, 88.5 mmol) and 3,5-bis(trifluoromethyl)aniline (2.7 g, 11.8 mmol). The mixture was refluxed for 48 hours. Reaction was then quenched saturated NaHCO₃. Products were extracted with diethyl ether. Organic layer was then dried over MgSO₄, filtered and concentrated. The product was purified by column chromatography using gradient from 5% to 20% dichloromethane in hexanes). All fractions with product, including those with impurities were collected. Product was then recrystallized from hexanes.

White solid, 40% yield (713 mg after 2 recrystallizations). IR (thin film, cm⁻¹): 3414, 3239, 1622, 1592, 1491, 1471, 1388, 1279, 1188, 1133, 1004, 979, 928, 896, 683. ¹H NMR (700 MHz, CDCl₃): δ= 7.56 (s, 4H), 7.55 (s, 2H), 7.39 (t, J = 7.8 Hz, 2H), 7.28 (t, J = 7.6 Hz, 1H), 7.16 (d, J = 7.9 Hz, 2H), 5.84 (d, J = 10.5 Hz, 2H); ¹³C NMR (175 MHz, CDCl₃) 149.1 (2C), 139.8, 133.0 (q, J = 33.7 Hz, 6C), 130.1, 126.4, 125.1, 123.6, 122.0, 121.2 (2C), 118.5, 116.8; ³¹P NMR (283 MHz, CDCl₃) δ 51.2 (s); ¹⁹F NMR (376

MHz, CDCl₃) δ -63.2 (s); HRMS (ESI+) (m/z): [M+H]⁺ calcd for C₂₂H₁₄F₁₂N₂OPS 613.0367, found 613.0361.

Synthetic procedures and characterization data for the cycloadducts from Table 2.

The cycloadducts **2-14**,²⁶ **2-18**,²⁷ **2-4**,²⁸ **2-21**,²⁹ **2-23**,²⁵ **2-25**³⁰ have been previously characterized. The characterization data for compounds **2-19**, **2-27**, **2-29**, and **2-30** is provided below.

General procedure for catalyst screening, Table 2.1.

Reactions were run on 0.5-0.7 mmol scale based on dienophile. An oven-dried 4-mL scintillation vial was charged with anthracene, 3 mol% pTSA and 6 mol% HBD. The vial was then flushed with nitrogen. Dry solvent (toluene or diethyl ether) was added to ensure 0.3 M concentration of 2-vinyl-1,3-dioxolane. The reaction mixture was brought to -78 °C and then 2-vinyl-1,3-dioxolane (1 equiv, 0.5 mmol) and cyclopentadiene (3 equiv, 1.5 mmol) were added via micro syringe. The resulting mixture was stirred at the temperature indicated in Table 1 for the indicated time. The reaction was quenched with approximately 6 mol% of triethylamine. The conversions were determined using the following formula: conversion (%) = 100% - (yield (starting material, %)). Yield of the starting material (%) = 100% • [ν (starting material) / ν (standard)] • n , where ν (product) / ν (standard) is the integral ratio of the corresponding ¹H NMR peaks and n is the ratio of the standard to the initial amount of starting material (in mol).

General procedure A for Diels-Alder reactions catalyzed by pTSA or pTSA/2-11, Table 2.3 (entries 1–3, 6, 7)

Reactions were run on 0.5-0.9 mmol scale based on dienophile. An oven-dried 4-mL scintillation vial was charged with anthracene, 3 mol% pTSA and 6 mol% catalyst **2-11**. The vial was then flushed with nitrogen. Dry toluene was added to ensure 0.3 M concentration of a dienophile. The reaction mixture was brought to 0 °C and then dienophile (1 equiv) and diene (5 equiv) were added via micro syringe. The resulting mixture was stirred at 0 °C for the time indicated in Table 2. The reaction was quenched with approximately 6 mol% of triethylamine. The ¹H NMR yields were calculated using the following formula: yield (%) = 100% • [v(product) / v(standard)] • n, where v(product) / v(standard) is the integral ratio of the corresponding ¹H NMR peaks and n is the ratio of the standard to starting material (in mol).

General procedure B for Diels-Alder reactions catalyzed by pTSA/2-10, Table 2.3 (entries 1–3, 6, 7)

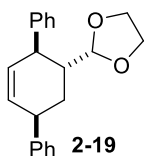
Reactions were run on 0.5-0.9 mmol scale based on dienophile. An oven-dried 4-mL scintillation vial was charged with 3 mol% pTSA and 6 mol% catalyst **2-10**. The vial was then flushed with nitrogen. Dry toluene was added to ensure 0.3 M concentration of a dienophile. The reaction mixture was brought to 0 °C and then dienophile (1 equiv) and diene (5 equiv) were added via micro syringe. The resulting mixture was stirred at 0 °C for the time indicated in Table 2. The reaction was quenched with approximately 6 mol% of triethylamine. The mixture was directly subjected to column chromatography. Elution with hexanes allowed removal of excess toluene and diene. Subsequent purification of the cycloadduct was performed using 20:1 hexanes/diethyl ether.

General procedure C for Diels-Alder reactions catalyzed by pTSA or pTSA/2-11, Table 2.3 (entries 5, 8–10)

Reactions were run on 0.3-0.7 mmol scale based on dienophile. An oven-dried 4-mL scintillation vial was charged with anthracene, 5 mol% pTSA and 10 mol% catalyst **2-11**. The vial was then flushed with nitrogen. Dry dichloromethane was added to ensure 0.6 M concentration of a dienophile. The reaction mixture was brought to 0 °C and then dienophile (1 equiv) and diene (5 equiv) were added via micro syringe. The resulting mixture was stirred at the temperature indicated in Table 2 for the indicated time. The reaction was quenched with approximately 10 mol% of triethylamine. The ¹H NMR yields were calculated using the following formula: yield (%) = 100% • [ν(product) / ν(standard)] • *n*, where ν(product) / ν(standard) is the integral ratio of the corresponding ¹H NMR peaks and *n* is the ratio of the standard to starting material (in mol).

General procedure D for Diels-Alder reactions catalyzed by pTSA/2-10, Table 2.3 (entries 5, 8–10)

Reactions were run on 0.3-0.7 mmol scale based on dienophile. An oven-dried 4-mL scintillation vial was charged with 5 mol% pTSA and 10 mol% catalyst **2-10**. The vial was then flushed with nitrogen. Dry dichloromethane was added to ensure 0.6 M concentration of dienophile. The reaction mixture was brought to 0 °C and then dienophile (1 equiv) and diene (5 equiv) were added via micro syringe. The resulting mixture was stirred at the temperature indicated in Table 2 for the indicated time. The reaction was quenched with approximately 10 mol% of triethylamine. Volatiles were evaporated in vacuo and then the mixture was subjected to column chromatography using 20:1 hexanes/diethyl ether.

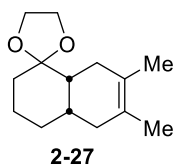


Synthesis of 2-(1',2',3',4'-tetrahydro-[1,1':4,1''-terphenyl]-2'-yl)-1,3-dioxolane (2-19, Entry 4)

An oven-dried 4-mL scintillation vial was charged with 5 mol% (3.6 mg, 0.0209 mmol) pTSA and 10 mol% (31.2 mg, 0.0418 mmol) catalyst **2-10**.

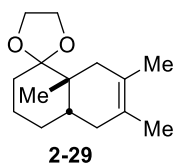
The vial was then flushed with nitrogen. In a separate vial a 0.9 M solution of 259 mg (1.25 mmol) (1*E*,3*E*)-1,4-diphenylbuta-1,3-diene (3 equiv) in dry dichloromethane was made and added to the mixture of catalysts. Then 41.8 μ L (0.418 mmol) of 2-vinyl-1,3-dioxolane (1 equiv) and was added via micro syringe. The resulting mixture was stirred at room temperature for 5 h. The reaction was quenched with approximately 10 mol% of triethylamine. Volatiles were evaporated in vacuo and then the mixture was subjected to column chromatography using 1:1 hexanes/toluene. Reactions catalyzed by pTSA or pTSA/**7a** were analyzed by crude ^1H NMR using anthracene as an internal standard.

Colorless oil, 62% yield, 8.3:1 endo/exo; IR (thin film, cm^{-1}) 3024, 2950, 2883, 1600, 1491, 1451, 1414, 1311, 1156, 1079, 1032, 957, 925, 857, 758, 701. *Endo product*: ^1H NMR (400 MHz, CDCl_3) δ 7.44 (d, $J = 7.6$ Hz, 2H), 7.39-7.33 (m, 4H), 7.33-7.28 (m, 2H), 7.27-7.19 (m, 2H), 6.02 (d, $J = 10.1$ Hz), 5.89 (ddd, $J = 10.1, 2.7, 2.4$ Hz, 1H), 4.07 (d, $J = 8.4$ Hz, 1H), 4.00-3.87 (m, 2H), 3.85-3.76 (m, 2H), 3.72-3.66 (m, 1H), 3.63-3.53 (m, 1H), 2.22 (dddd, $J = 13.2, 8.1, 5.5, 2.4$ Hz, 1H), 2.01 (dd, $J = 12.9, 5.5$ Hz, 1H), 1.56 (q, $J = 12.9$ Hz, 1H). *Distinct peaks for exo product*: ^1H NMR (400 MHz, CDCl_3) δ 4.81 (d, $J = 3.6$ Hz, 1H), 1.83 (dd, $J = 10.5, 6.6$ Hz, 1H); *Endo only*: ^{13}C NMR (101 MHz, CDCl_3) δ 145.3, 138.1, 135.4, 128.4, 128.1, 125.8, 106.8, 67.1, 51.5, 49.4, 47.0, 46.7, 44.3, 26.0; HRMS (ESI+) (m/z): $[\text{M}+\text{NH}_4]^+$ calcd for $\text{C}_{17}\text{H}_{24}\text{NO}_2$ 274.1802; found 274.1800.



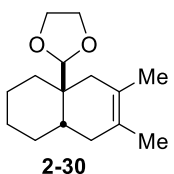
6,7-Dimethyl-3,4,4a,5,8,8a-hexahydro-2H-spiro[naphthalene-1,2'-[1,3]dioxolane] (2-27, Entry 8)

Colorless oil, 68% yield. IR (thin film, cm^{-1}) 2927, 2829, 1717, 1441, 1377, 1354, 1298, 1160, 1098, 1087, 1050, 940, 876, 771. ^1H NMR (400 MHz, CDCl_3) δ 3.98-3.87 (m, 4H), 2.25 (d, $J = 16.8$ Hz, 1H), 2.05-1.85 (m, 4H), 1.79-1.63 (m, 4H), 1.59 (br s, 6H), 1.54-1.47 (m, 1H), 1.37-1.17 (m, 2H). ^{13}C NMR (175 MHz, CDCl_3) δ 123.5, 122.6, 64.1, 40.9, 37.9, 32.9, 29.8, 29.6, 26.0, 23.2, 19.1, 18.9. HRMS (EI) (m/z): $[\text{M}]^+$ calcd for $\text{C}_{14}\text{H}_{22}\text{O}_2$ 222.1620, found 222.1621.



6',7',8a'-trimethyl-3',4',4a',5',8',8a'-hexahydro-2'H-spiro[[1,3]-dioxolane-2,1'-naphthalene] (2-29, Entry 9)

Pale yellow oil, 84% yield. IR (thin film, cm^{-1}) 2927, 1448, 1368, 1172, 1085, 950. ^1H NMR (700 MHz, CDCl_3) δ 3.98-3.92 (m, 4H), 2.27 (d, $J = 18.2$ Hz, 1H), 2.22 (d, $J = 18.2$ Hz, 1H), 1.73 (td, $J = 13.3, 4.6$ Hz, 1H), 1.68-1.60 (m, 3H), 1.59 (s, 6H), 1.57-1.52 (m, 3H), 1.49 (qt, $J = 13.3, 4.3$ Hz, 1H), 1.29 (qd, $J = 13.3, 3.8$ Hz, 1H), 1.27-1.22 (m, 1H), 0.97-0.87 (m, 1H), 0.85-0.76 (m, 1H); ^{13}C NMR (175 MHz, CDCl_3) δ 122.0, 121.9, 112.9, 65.0, 64.8, 41.3, 38.3, 36.2, 35.7, 30.3, 28.4, 22.8, 19.2, 19.0, 18.2. HRMS (ES+) (m/z): $[\text{M}+\text{H}]^+$ calcd for $\text{C}_{15}\text{H}_{24}\text{O}_2$ 237.1849, found 237.1841.



6,7-Dimethyl-1,3,4,5,8,8a-hexahydronaphthalen-4a(2H)-yl-1,3-dioxolane (2-30, Entry 10)

Colorless oil, 59% yield. IR (thin film, cm^{-1}) 2923, 2861, 1704, 1453, 1394, 1351, 1165, 1137, 1121, 1084, 1066, 955, 856. ^1H NMR (700 MHz, CDCl_3) δ 4.87 (s, 1H), 3.95-3.90 (m, 1H), 3.89-3.79 (m, 3H), 2.35 (d, $J = 18.3$ Hz, 1H), 2.19 (d, $J = 18.3$ Hz, 1H), 1.78-1.72 (m, 2H), 1.66-1.61 (m, 1H), 1.60 (s, 3H), 1.58 (s, 3H), 1.56-1.51 (m, 2H), 1.45-1.37 (m, 2H), 1.34-1.27 (m, 3H), 1.26-1.18 (m, 1H). ^{13}C NMR

(175 MHz, CDCl₃) δ 123.0, 121.8, 106.2, 65.3, 64.9, 39.2, 36.2, 34.9, 32.6, 29.2, 26.7, 25.8, 21.5, 19.0, 18.9. HRMS (EI) (m/z): [M]⁺ calcd for C₁₅H₂₄O₂ 236.1776, found 236.1776.

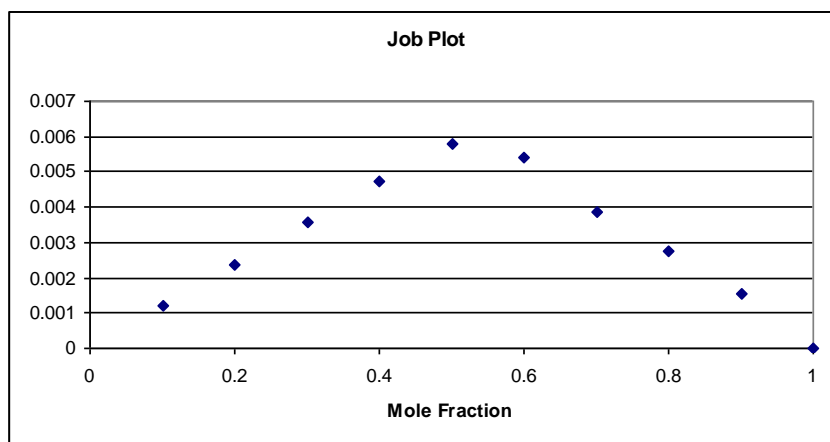
¹H NMR continuous variation method (Job plot)

Stock solutions of *N*-methylpyridinium tosylate and thiophosphoramidate in CDCl₃, both having a concentration of 5 mM, were prepared. Aliquots of each solution were mixed in several 5 mm NMR tubes such that the total volume in each tube was 1.0 mL and the mole fraction of catalyst was varied from 0.1 to 1.0 M across 10 samples. ¹H NMR spectra were collected on a 500 MHz instrument at 25°C. The chemical shift of the amide proton of the catalyst (δ_{obs}) was noted in each sample and a Job plot was created by plotting $(\delta_{\text{obs}} - \delta_{\text{free}}) \cdot [\text{catalyst}]_0$ against the mole fraction of the catalyst, where $[\text{catalyst}]_0$ is the initial concentration of catalyst measured into each sample. The plot thus obtained showed a maxima at a mole fraction of 0.5, suggesting a 1:1 binding stoichiometry in the tosylate-thiophosphoramidate complex.

N-H peak shift				
Mole fraction	δ_{obs}	$\delta_{\text{obs}} - \delta_{\text{free}}$	[Phosph] ₀	$(\delta_{\text{obs}} - \delta_{\text{free}}) \cdot [\text{Phosph}]_0$
0.1	8.1506	2.3925	0.0005	0.00119625
0.2	8.1448	2.3867	0.001	0.0023867
0.3	8.135	2.3769	0.0015	0.00356535
0.4	8.115	2.3569	0.002	0.0047138
0.5	8.0756	2.3175	0.0025	0.00579375

0.6	7.5603	1.8022	0.003	0.0054066
0.7	6.8571	1.099	0.0035	0.0038465
0.8	6.4503	0.6922	0.004	0.0027688
0.9	6.1046	0.3465	0.0045	0.00155925
1	5.7581	0	0.005	0

¹H NMR titrations



A 0.5 mM solution of thiophosphoramidate in CDCl₃ was prepared, of which 500 μL was placed in a 5 mm NMR tube. A 2.5 mM solution of *N*-methylpyridinium tosylate in CDCl₃ containing 0.5 mM thiophosphoramidate **2-10** was prepared as the titrant. Aliquots of 5 – 10 μL of the second solution were sequentially added to the NMR tube and the ¹H NMR spectrum was collected after each addition on a 500 MHz instrument at 25°C. The chemical shift of the amide proton of the catalyst was noted in each sample. The binding constant was then calculated using the WinEQNMR program.³¹ Three titrations were thus performed to furnish an averaged binding constant ($K_a = 7.3 \cdot 10^4$).

References

¹ Selected reviews: (a) Doyle, A. G.; Jacobsen, E. N. *Chem. Rev.* **2007**, *107* (12), 5713–5743. (b) Zhang, Z.; Schreiner, P. R. *Chem. Soc. Rev.* **2009**, *38* (4), 1187. (c) Brak, K.; Jacobsen, E. N. *Angew. Chem. Int. Ed.* **2013**, *52* (2), 534–561. (d) Beckendorf, S.; Asmus, S.; Mancheño, O. G. *ChemCatChem* **2012**, *4* (7), 926–936.

² Sigman, M. S.; Jacobsen, E. N. *J. Am. Chem. Soc.* **1998**, *120* (19), 4901–4902.1

³ (a) Kotke, M.; Schreiner, P. R. *Tetrahedron* **2006**, *62*, 434–439.

⁴ (a) Reisman, S. E.; Doyle, A. G.; Jacobsen, E. N. *J. Am. Chem. Soc.* **2008**, *130* (23), 7198–7199. (b) Burns, N. Z.; Witten, M. R.; Jacobsen, E. N. *J. Am. Chem. Soc.* **2011**, *133* (37), 14578–14581. (c) Brown, A. R.; Kuo, W.-H.; Jacobsen, E. N. *J. Am. Chem. Soc.* **2010**, *132* (27), 9286–9288.

⁵ Harmata, M. *Tetrahedron* **2003**, *59*, 2371–2395.

⁶ Sasaki, T.; Ishibashi, Y.; Ohno, M. *Tetrahedron Lett.* **1982**, *23*, 1693–1696.

⁷ Gassman, P. G.; Singleton, D. A.; Wilwerding, J. J.; Chavan, S. P. *J. Am. Chem. Soc.* **1987**, *109*, 2182–2184.

⁸ Grieco, P. A.; Collins, J. L.; Handy, S. T. *Synlett* **1995**, *1995* (11), 1155–1157.

⁹ Lee, J. H.; Kim, W. H.; Danishefsky, S. J. *Tetrahedron Lett.* **2010**, *51* (9), 1252–1253.

¹⁰ (a) Grieco, P. A.; Kaufman, M. D.; Daeuble, J. F.; Saito, N. *J. Am. Chem. Soc.* **1996**, *118* (8), 2095–2096. (b) Grieco, P. A.; Collins, J. L.; Henry, K. J. *Tetrahedron Lett.* **1992**, *33* (33), 4735–4738. (c) Grieco, P. A.; Nunes, J. J.; Gaul, M. D. *J. Am. Chem. Soc.* **1990**, *112* (11), 4595–4596.

¹¹ Thiourea-based HBDs have been previously used in combination with sulfonic acids to promote Povarov reactions: Xu, H.; Zuend, S. J.; Woll, M. G.; Tao, Y.; Jacobsen, E. N. *Science* **2010**, *327* (5968), 986–990. For selected examples of thiourea-catalyzed

¹² Rodriguez, A. A.; Yoo, H.; Ziller, J. W.; Shea, K. J. *Tetrahedron Lett.* **2009**, *50* (49), 6830–6833.

¹³ Cranwell, P. B.; Hiscock, J. R.; Haynes, C. J. E.; Light, M. E.; Wells, N. J.; Gale, P. A. *Chem. Commun.* **2013**, *49* (9), 874.

¹⁴ Beletskiy, E. V.; Schmidt, J.; Wang, X.-B.; Kass, S. R. *J. Am. Chem. Soc.* **2012**, *134* (45), 18534–18537.

- ¹⁵ Thiophosphoramides as one- and two-hydrogen bond donors: (a) Wu, R.; Chang, X.; Lu, A.; Wang, Y.; Wu, G.; Song, H.; Zhou, Z.; Tang, C. *Chem. Commun.* **2011**, 47 (17), 5034. (b) Lu, A.; Wu, R.; Wang, Y.; Zhou, Z.; Wu, G.; Fang, J.; Tang, C. *Eur. J. Org. Chem.* **2011**, 2011 (1), 122–127.
- ¹⁶ Borovika, A.; Tang, P.-I.; Klapman, S.; Nagorny, P. *Angew. Chem. Int. Ed.* **2013**, 52 (50), 13424–13428.
- ¹⁷ (a) Malerich, J. P.; Hagihara, K.; Rawal, V. H. *J. Am. Chem. Soc.* **2008**, 130 (44), 14416–14417. (b) Busschaert, N.; Kirby, I. L.; Young, S.; Coles, S. J.; Horton, P. N.; Light, M. E.; Gale, P. A. *Angew. Chem. Int. Ed.* **2012**, 51 (18), 4426–4430.
- ¹⁸ Pescatori, L.; Arduini, A.; Pochini, A.; Secchi, A.; Massera, C.; Ugozzoli, F. *Org. Biomol. Chem.* **2009**, 7 (18), 3698.
- ¹⁹ Hynes, M. J. *J. Chem. Soc., Dalton Trans.* **1993**, No. 2, 311.
- ²⁰ Olson, E. J.; Bühlmann, P. *J. Org. Chem.* **2011**, 76 (20), 8406–8412.
- ²¹ Walvoord, R. R.; Huynh, P. N. H.; Kozlowski, M. C. *J. Am. Chem. Soc.* **2014**, 136 (45), 16055–16065.
- ²² Harris, R. K.; Becker, E. D.; Cabral de Menezes, S. M.; Goodfellow, R.; Granger, P. *Pure Appl. Chem.* **2001**, 73, 1795.
- ²³ Lu, T.-J.; Yang, J.-F.; Sheu, L.-J. *J. Org. Chem.* **1995**, 60, 2931–2934.
- ²⁴ a) Kim, H. Y.; Oh, K. *Org. Lett.* **2011**, 13, 1306–1309; b) Liu, H.; Tomooka, C. S.; Moore, H. W. *Synth. Commun.* **1997**, 27, 2177–2180; c) Rodriguez, A. A.; Yoo, H.; Ziller, J. W.; Shea, K. J. *Tetrahedron Lett.* **2009**, 50, 6830–6833.
- ²⁵ Hoque, M. E. U.; Dey, S.; Guha, A. K.; Kim, C. K.; Lee, B.-S.; Lee, H. W. *J. Org. Chem.* **2007**, 72, 5493–5499.
- ²⁶ Chavan, S. P.; Sharma, A. K. *Synlett* **2001**, 2001, 0667–0669.
- ²⁷ Borovika, A.; Nagorny, P. *Tetrahedron* **2013**, 69, 5719–5725.
- ²⁸ Chavan, S. P.; Ethiraj, K. S.; Dantale, S. W. *Synthetic Commun* **2007**, 37, 2337–2343.
- ²⁹ Inokuchi, T.; Tanigawa, S.; Torii, S. *J. Org. Chem.* **1990**, 55, 3958–3961.
- ³⁰ Kumareswaran, R. *Tetrahedron* **1999**, 55, 1099–1110.
- ³¹ We thank Dr. Hynes for providing us permission to use WinEQNMR for calculating the K_a of **7e**: M. J. Hynes, *J. Chem. Soc., Dalton Trans.* **1993**, 311.

Chapter 3

Chiral Brønsted Acid-Catalyzed Enantioselective Ionic [4+2]

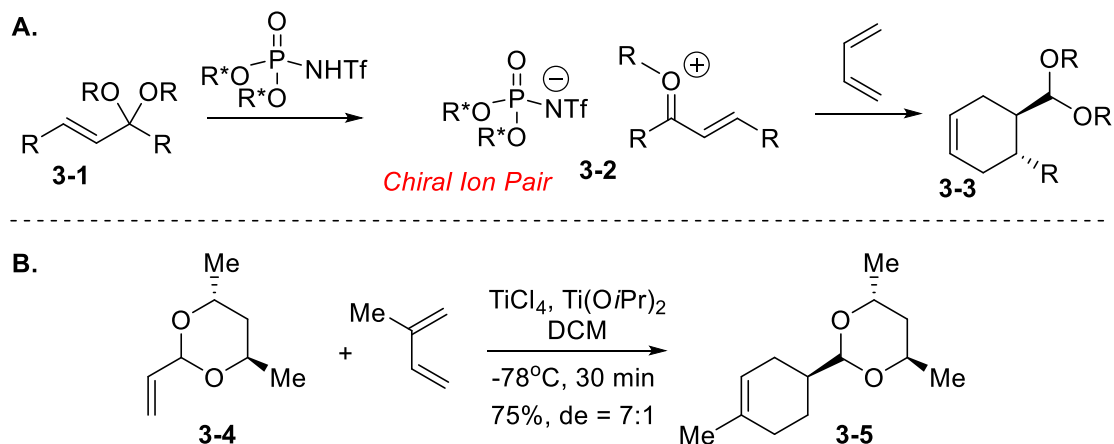
Cycloadditions

3.1 Introduction

While designing a catalyst capable of controlling the reactivity of an oxocarbenium ion still represents a formidable challenge, the use of chiral catalysts to control enantioselective reactions of oxocarbenium ions is well precedented.¹ In particular, several reports, describing chiral phosphoric acid-catalyzed reactions presumably proceeding through enantioselective nucleophilic addition to oxocarbenium ions, have appeared over the past three years.^{2,3} Although the precise nature of the catalytic mechanisms and intermediates in such transformations is yet to be clarified,³ the existence of oxocarbenium/chiral phosphate ion pair has been invoked. The chirality of a chiral counterion could, in theory, control not only the direct addition of nucleophiles to oxocarbenium ions, but also reactions at the remote sites. Thus, we surmised that the protonation of an α,β -unsaturated acetal with a chiral Brønsted acid or a combination of chiral HBD and achiral Brønsted acid would result in the formation of a vinyl oxocarbenium/chiral counterion pair **3-2** (Scheme 3.1 A), and that the olefinic portion of the resultant ion pair **3-2** could undergo various counterion-directed enantioselective reactions. Our group has obtained experimental evidence confirming the feasibility of such

counterion directed reactions. This chapter summarizes our studies in this vein and provides the first successful example of a catalytic enantioselective Gassman cycloaddition reaction of α,β -unsaturated acetals and dienes catalyzed by *N*-triflylphosphoramides.

Scheme 3.1 Stereoselective ionic Diels-Alder reactions

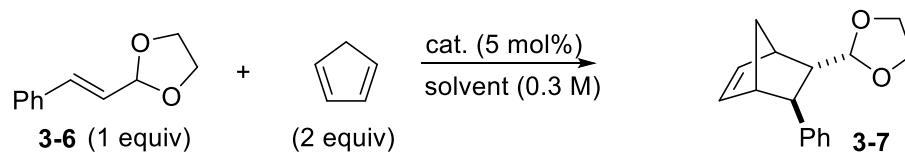


While Gassman cycloaddition is a popular protocol for ionic [4+2] cycloadditions and a variety of Lewis and Brønsted acids are used for activation of α,β -unsaturated acetals,⁴ no catalyst-controlled enantioselective Gassman cycloaddition was known. The only asymmetric cycloaddition was developed by the Sammakia group.⁵ The method is based on the use of chiral acetals derived from 2,4-pentandiol (**3-4**, Scheme 3.1 B). While diastereoselectivity of up to 15:1 was observed when the reaction was catalyzed by a TiCl_4 – $\text{Ti}(\text{O}i\text{Pr})_4$ mixture, the substrate scope was rather limited. Subsequent publications by other groups broadened the scope of the reaction and further optimized the reaction conditions.⁴

3.2 Enantioselective Cycloaddition

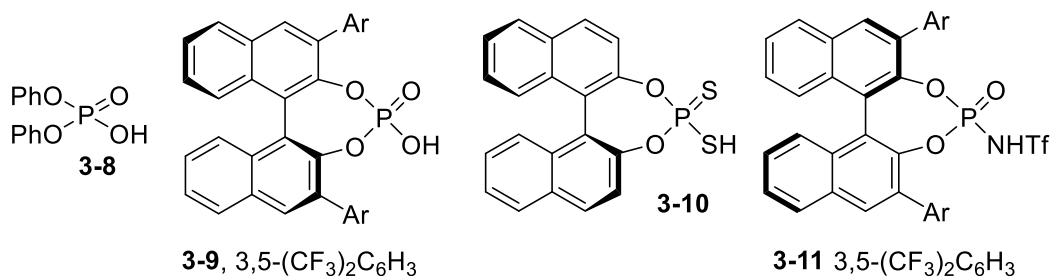
Our studies commenced with the attempts to identify an appropriate Brønsted acid catalyst that is capable of promoting a cycloaddition reaction between α,β -unsaturated acetal **3-6** and cyclopentadiene (Table 3.1). Representative Brønsted acids **3-8** – **3-11** were combined with dioxolane **3-6** and cyclopentadiene (2 equiv) in acetonitrile (entries 1–4) and toluene (entries 5–8), and the formation of **3-7** was monitored by GC-MS. While all of the catalysts promoted the formation of cycloadduct **3-7** in acetonitrile, only *N*-triflylphosphoramidate **3-11** catalyzed the cycloaddition in toluene (16 h, 65%, 44:56 e.r.). In addition, the reactions catalyzed by **3-9** and **3-11** were evaluated in dioxane (entries 9 and 10). While *N*-triflylphosphoramidate **3-11** catalyzed the formation of **3-7** (16 h, 80% yield), phosphoric acid **3-9** did not promote any cycloaddition.

The observed solvent effect could be attributed to the higher reactivity of the ion pair **3-2** in acetonitrile due to the better solvation of the intermediate oxocarbenium ion. Insignificant stereoselection is expected for the solvated ion pairs, which is consistent with the observation that the reactions catalyzed by **3-9** and **3-11** in acetonitrile produced racemic products (entries 2 and 4). The higher catalytic activity of **3-11** in toluene and dioxane could be attributed to a higher acidity of this compound relative to the other catalysts⁶ as well as to a lower coordinating ability of the resultant anion. A stronger Brønsted acid is expected to populate larger quantities of the oxocarbenium ion, while an ion pair (**3-2**) with a less coordinating anion will be more reactive due to the lower energy of the LUMO.

Table 3.1 Preliminary catalyst and solvent screening

entry ^a	catalyst	solvent	time, h	conversion, % ^b
1	3-8	MeCN	5	77
2	3-9	MeCN	5	80 (50 : 50 e.r.)
3	3-10	MeCN	16	89
4	3-11	MeCN	5	82 (50 : 50 e.r.)
5	3-8	PhMe	13	0
6	3-9	PhMe	13	0
7	3-10	PhMe	16	0
8	3-11	PhMe	16	65 (44 : 56 e.r.)
9	3-9	dioxane	16	0
10	3-11	dioxane	16	80 (43 : 57 e.r.)

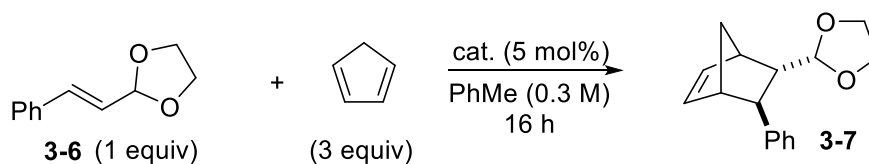
^aUp to 0.06 mmol scale. ^bDetermined by GC-MS.



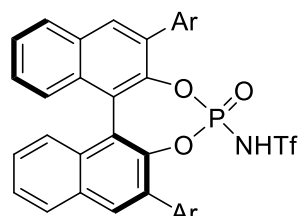
Based on the unique ability of **3-11** to catalyze the IDA of **3-6** and cyclopentadiene in various solvents, the evaluation of various *N*-sulfonylphosphoramides **3-12** – **3-19** in toluene was executed next (Table 3.2). The variation of the aromatic substituents (Ar) on the BINOL backbone of the catalyst (entries 2–4) helped to identify **3-14** (Ar = 2,4,6-*i*-Pr)₃C₆H₂) as the catalyst of choice (entry 4). Thus, the formation of **3-7** proceeded with

improved yield (75%) and selectivities (64:36 e.r., 5:1 d.r.) when compared to the catalysts **3-11** – **3-13**. To further improve the conversion for this reaction, more acidic *N*-triflylthiophosphoramidate **3-15** was utilized as a catalyst (entry 5). Although the enantioselectivity and d.r. for those reactions were similar to the corresponding selectivities observed for **3-14**, the product yield for the reaction catalyzed by catalyst **3-15** was found to be significantly lower (24%). Probably, the diminished activity of **3-15** results from the lower reactivity of the ion pair **3-2** due to the stronger coordination of the *N*-triflylthiophosphoramidate anion derived from **3-15** to the oxocarbenium ion. In an attempt to affect the coordinating properties of the *N*-sulfonylphosphoramidate counterion, we decided to evaluate the effect of the *N*-triflyl group on the cycloaddition rate and selectivity. Thus *N*-mesylphosphoramidate **3-16** (entry 6) and *N*-pentafluorophenylsulfonylphosphoramidate **3-17** (entry 7) were synthesized and screened. However, neither **3-16** nor **3-17** were found to promote the IDA reaction leading to **3-7**. This is likely to result from the significantly lower acidities of **3-16** and **3-17** in comparison with *N*-triflylphosphoramidates (for example, the pK_as of CH₃SO₂NH₂ and CF₃SO₂NH₂ in DMSO are 17.5, and 9.7, respectively).⁷ Finally, our attempts to evaluate H8-BINOL and VAPOL-based *N*-triflylphosphoramidates **3-18** and **3-19** did not result in improved reactivities or selectivities (entries 8 and 9). While both **3-18** and **3-19** could promote the formation of the cycloadduct **3-7**, the selectivities of these reactions were significantly lower than for the BINOL-derived *N*-sulfonylphosphoramidates **3-12** – **3-17**.

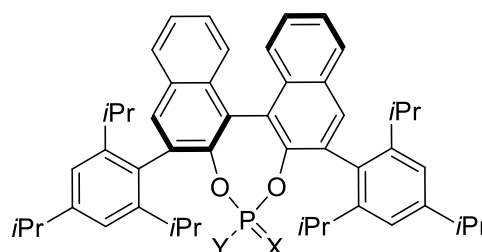
Table 3.2 Evaluation of various *N*-triflylphosphoramides



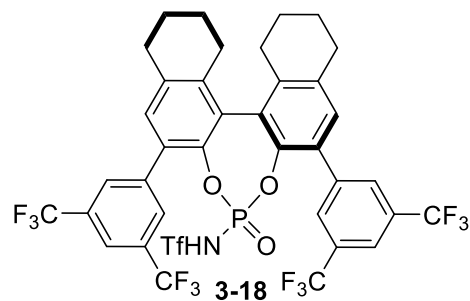
entry	catalyst	yield ^a	e.r. ^b	endo/exo
1	3-11	65	44 : 56	3 : 1
2	3-12	47	63 : 37	2 : 1
3	3-13	53 ^c	56 : 44	2 : 1
4	3-14	75	64 : 36	5 : 1
5	3-15	24	61 : 39	3 : 1
6	3-16	<5	n.d.	n.d.
7	3-17	<5	n.d.	n.d.
8	3-18	61	46 : 54	3 : 1
9	3-19	54 ^c	50 : 50	2 : 1



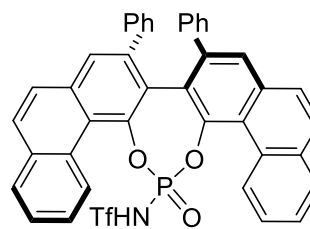
3-12 3,5-*t*Bu)₂C₆H₆
3-13 9-Anthr



3-14 X = O, Y = NHTf
3-15 X = S, Y = NHTf
3-16 X = O, Y = NHMs
3-17 X = O, Y = NHSO₂C₆F₅

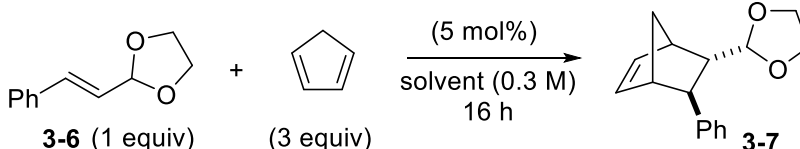


3-18



3-19

With the optimal catalyst (**3-14**) identified, the effect of the solvent on the formation of **3-7** was determined next to optimize the enantioselectivity of the cycloaddition (Table 3.3). Consistent, with the results obtained in acetonitrile, the formation of **3-7** in isopropanol was completely unselective (entry 1). Reducing the polarity of the solvents significantly improved the enantioselectivity and diastereoselectivity of the cycloaddition (entries 2–8). Remarkably, the reaction in weakly coordinating ethyl acetate (entry 8) was the most selective (73: 27 e.r., 7:1 d.r.). Employing other ester-containing solvents such as methyl pivalate (entry 9) and ethyl isobutyrate (entry 10) resulted in increased selectivities. Thus, the cycloaddition of **3-6** and cyclopentadiene in ethyl isobutyrate as the solvent resulted in enantio- and diastereoenriched **3-7** (80:20 e.r., 7:1 d.r.). It is noteworthy that the reactions utilizing other catalysts were also more selective when ethyl isobutyrate was employed as the solvent (entries 11–14). However, catalyst **3-14** was still found to be superior in terms of enantio- and diastereocontrol.

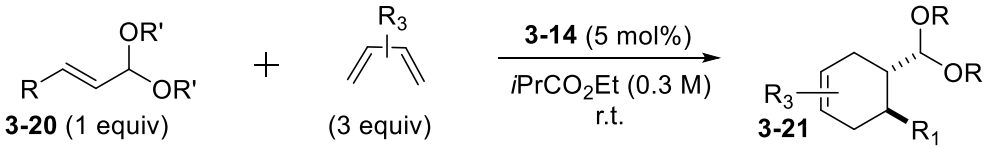
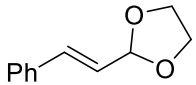

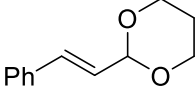

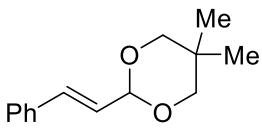
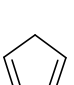
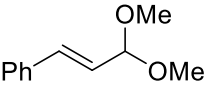
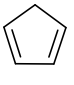
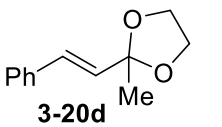

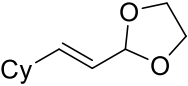

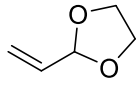

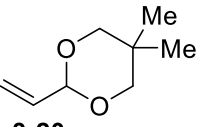
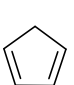
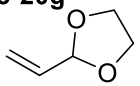
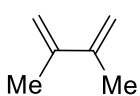
Table 3.3 Evaluation of the solvent effect on ionic Diels-Alder stereoselectivity

entry	catalyst	solvent	e.r. ^a	endo/exo
1	3-14	<i>i</i> -PrOH	50 : 50	3 : 1
2	3-14	CH ₂ Cl ₂	57 : 43	3 : 1
3	3-14	PhMe	64 : 36	5 : 1
4	3-14	hexanes	61 : 39	6 : 1
5	3-14	PhH	70 : 30	7 : 1
6	3-14	CCl ₄	69 : 31	3 : 1
7	3-14	Et ₂ O	70 : 30	4 : 1
8	3-14	EtOAc	73 : 27	7 : 1
9	3-14	<i>t</i> BuCO ₂ Me	76 : 24	7 : 1
10	3-14	<i>i</i>PrCO₂Et	80 : 20	7 : 1
11	3-11	<i>i</i> PrCO ₂ Et	41 : 59	4 : 1
12	3-12	<i>i</i> PrCO ₂ Et	68 : 32	2.5 : 1
13	3-15	<i>i</i> PrCO ₂ Et	64 : 36	3 : 1
14	3-18	<i>i</i> PrCO ₂ Et	43 : 57	4 : 1

The scope and limitation of the catalytic asymmetric ionic cycloaddition was evaluated next (Table 3.4). As the changes in the acetal portion of the dienophile could significantly affect the reaction rates and selectivities, substrates **3-20a** – **3-20c** were synthesized and subjected to cycloaddition with cyclopentadiene (entries 2–4). The hydrolysis of unsaturated 1,3-dioxanes such as **3-20a** is known to progress faster than the hydrolysis of the corresponding dioxolanes.⁸ However, the oxocarbenium ion resulting

from 1,3-dioxane **3-20a** was found to be a less reactive dienophile than **3-6** although both reactions proceeded with the similar levels of stereocontrol. The introduction of the additional *gem*-dimethyl substitution to the acetal backbone of 1,3-dioxane (**3-20b**, entry 3) resulted in significant reduction of the reactivity and no reaction was observed for **3-20b**. This observation is consistent with the experimental results obtained for the hydrolysis of *gem*-dimethyl substituted vinyl 1,3-dioxanes and could result from the both steric and stereoelectronic effects.⁸ Finally, the reaction of cinnamaldehyde dimethyl acetal (**3-20c**) with cyclopentadiene resulted in the formation of the corresponding product (68:32 e.r., 8:1 d.r.). Consistent with the observations made by Gassman, the cycloadduct yield for the reaction with **3-20c** was significantly lower than the corresponding yield with the cyclic acetal **3-6**. This could be ascribed to the higher reactivity of the intermediate oxocarbenium ion that undergoes competitive oligomerization. The possibility of utilizing ketone-derived dioxolane **3-20d** was examined next (entry 5). Although the ionization of **3-20d** should provide a significantly more stable oxocarbenium ion in comparison to the corresponding ionization of **3-6**, the reaction of **3-20d** was significantly slower albeit selective (29% yield, 70:30 e.r., endo isomer). In addition, significant amounts of the hydrolyzed starting material and products were also observed. To delineate the role of the C3 substitution, acetal **3-20e** was synthesized and evaluated (entry 6). Although the replacement of the phenyl substituent with the cyclohexyl should result in a less labile acetal, the reactivity of **3-20e** was not significantly different from **3-6** (60% yield, 4:1 d.r.).

Table 3.4 Substrate scope

						
entry	dienophile	diene	time	yield (conversion), % ^a	e.r. ^b	endo/exo
1	 3-6		16 h	64 (100)	80 : 20	7 : 1
2	 3-20a		16 h	32 (60)	81 : 19	12 : 1
3	 3-20b		16 h	0 (0)	n.d.	n.d.
4 ^c	 3-20c		20 h	33 (100)	68 : 32	8 : 1
5	 3-20d		16 h	29 (65) ^d	70 : 30 ^d	endo only
6 ^e	 3-20e		16 h	60 (100)	68 : 32 ^e	4 : 1
7 ^f	 3-20f		16 h	52 (88)	77 : 23	3 : 1
8	 3-20g		24 h	85 (95)	69 : 31	7 : 1
9	 3-20h		24 h	43 (89)	70 : 30	n.a

^aDetermined by ¹H NMR with Ph₃CH as an internal standard. ^bMeasured by chiral HPLC. ^cConducted at 0 °C. ^dThe yield, ee, and endo/exo ratio were determined after hydrolysis to a corresponding ketone. ^eDetermined after hydrolysis to the corresponding aldehyde. ^fConducted at -20 °C.

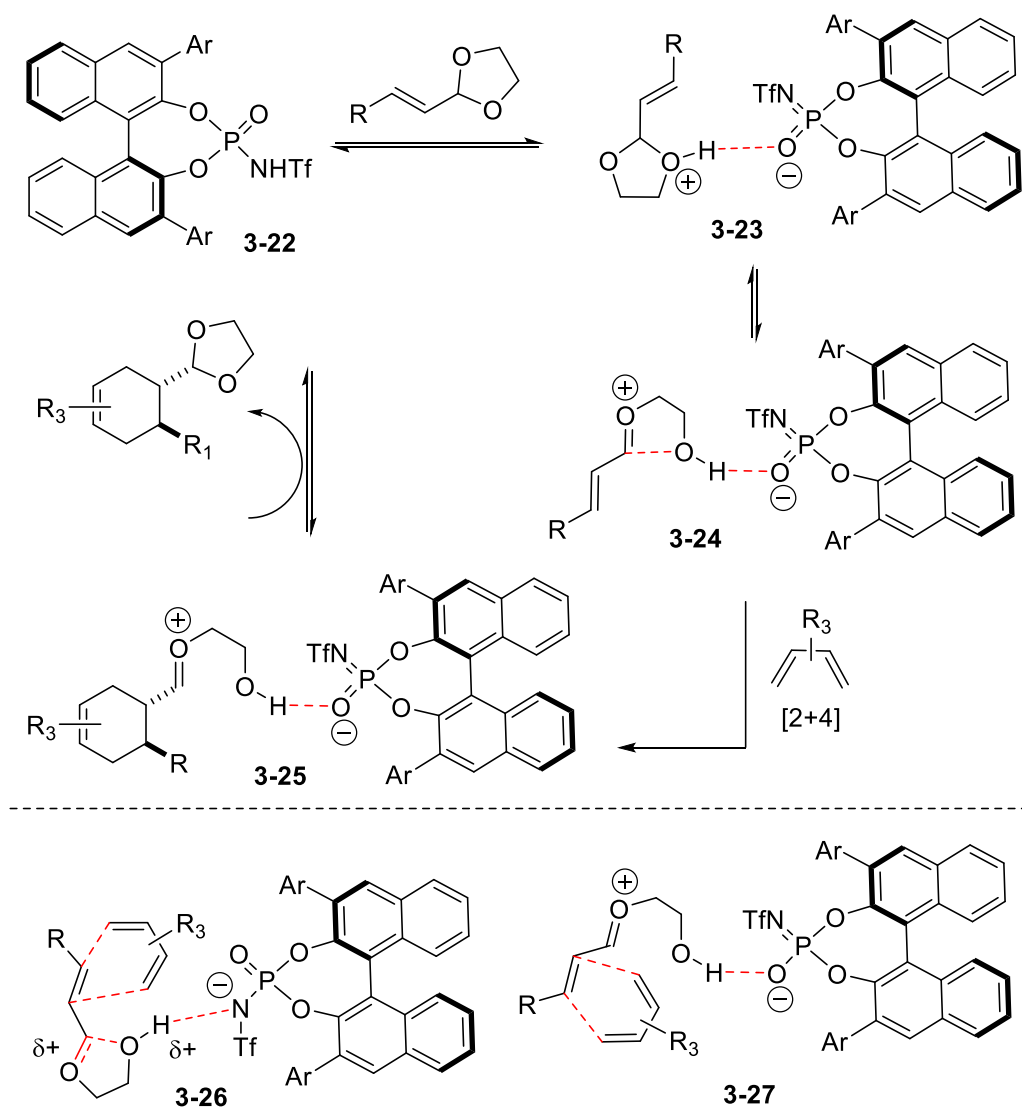
The acrolein-derived acetals **3-20f** – **3-20h** were significantly more reactive (entries 7–9). Thus, the reaction with vinyl dioxolane provided corresponding cycloadduct **3-21f** even at –20 °C (52% yield, 77:23 e.r., 3:1 d.r.). While the cinnamaldehyde-derived 5,5'-dimethyl-1,3-dioxane **3-20b** did not react with cyclopentadiene (*vide supra*), the reaction of acrolein-derived 5,5'-dimethyl-1,3-dioxane **3-20g** resulted in the formation of the corresponding cycloadduct **3-21g** (85% yield, 69:31 e.r., 7:1 d.r.). Finally, the reaction of vinyl dioxolane and 2,3-dimethyl-1,3-butadiene resulted in enantioselective formation of **3-21h** (43% yield, 70:30 e.r.) indicating that other dienes could also be employed for this reaction.

3.3 Discussion

While a conclusive mechanistic and computational investigation delineating the nature of the reaction intermediates is yet to be conducted, a tentative mechanism is summarized in Scheme 3.2. Thus, initial protonation of an unsaturated acetal with *N*-triflylphosphoramidate **3-22** results in the reversible formation of the contact ion pair **3-23**. The subsequent reversible ionization results in the unsaturated oxocarbenium ion **3-24** that undergoes a rate-limiting reaction with a diene. The cyclization of the resultant ionic cycloadduct **3-25** provides the product and regenerates the catalyst **3-22**. At the moment, it is not clear whether this reaction proceeds through a clearly defined oxocarbenium ion-like transition state **3-27** or through the transition state **3-26**, in which the breakage of the C–O bond is coupled with the cycloaddition event. It is clear that the acidity of the catalyst, coordinating ability of the counterion (see Chapter 2), and the reactivity of the dienophile play an important role in this reaction. Further mechanistic and computational studies will help to shed some light on the nature of the reaction intermediates and the transition states

(3-26 versus 3-27) and aid the design of superior catalysts for this and related transformations.

Scheme 3.2 Proposed reaction mechanism



3.4 Conclusion

In summary, this chapter describes the first example of an asymmetric chiral *N*-triflylphosphoramidate-catalyzed ionic DA reaction. This reaction presumably proceeds through the intermediacy of a vinyl oxocarbenium/chiral anion pair, and the chiral *N*-

triflylphosphoramidate anion controls the stereoselectivity of the cycloaddition step. Moderate enantioselectivities (up to 80:20 e.r.) have been obtained when α,β -unsaturated dioxolanes were employed as the dienophiles. These reactions demonstrate a strong dependence on the counterion coordinating properties and solvent polarity, a behavior characteristic of oxocarbenium ions. Demonstrated that chiral Brønsted acid-catalyzed activation of acetals could be more generally employed as an alternative to the Lewis or Brønsted acid-catalyzed LUMO activation of the α,β -unsaturated carbonyls. Other Brønsted acid-catalyzed transformations of α,β -unsaturated acetals as well as design of chiral thiophosphoramides as co-catalysts for ionic DA reaction reported herein are the subjects of the ongoing studies.

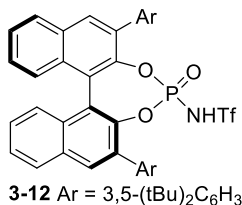
3.5 Experimental

Unless otherwise stated, all reagents were purchased from commercial suppliers and used without purification. Toluene (PhMe), tetrahydrofuran (THF), dichloromethane (CH_2Cl_2) and diethyl ether (Et_2O) were filtered through a column (Innovative Technology PS-MD-5) of activated alumina under nitrogen atmosphere. Ethyl isobutyrate ($i\text{PrCO}_2\text{Et}$) was dried with activated 4 Å molecular sieves according to the previously reported procedure by Smithers *et.al.* All reactions were carried out under an atmosphere of nitrogen in flame- or oven-dried glassware with magnetic stirring. Reactions were cooled via external cooling baths: ice water (0 °C), Neslab Cryotrol CB-80 immersion cooler (0 to -60 °C) or Neslab Cryocool immersion cooler CC-100 II. Purification of the reactions mixtures was performed by flash chromatography using SiliCycleSiliaFlash P60 (230-400 mesh) silica gel. The enantiomeric ratios (e.r.) were determined on Alliance Waters (separations module e2695, detector 2998) using CHIRALCEL OD-H column (4.6 mm x

250 mm, 5 μm) by comparing the samples with the appropriate racemic mixtures. ^1H NMR spectra were recorded on Varian vnmrs 700 (700 MHz), Varian vnmrs 500 (500 MHz), Varian MR400 (400 MHz), Varian Inova 500 (500 MHz) spectrometers and chemical shifts (δ) are reported in parts per million (ppm) with solvent resonance as the internal standard (CDCl_3 at δ 7.26). Data are reported as (br = broad, s = singlet, d = doublet, t = triplet, q = quartet, qn = quintet, sext = sextet, m = multiplet; coupling constant(s) in Hz; integration). Proton-decoupled ^{13}C NMR, as well as ^{19}F and ^{31}P spectra were recorded on Varian vnmrs 500 (500 MHz) or Varian vnmrs 700 (700 MHz) spectrometers and chemical shifts (δ) are reported in ppm with solvent resonance as the internal standard (CDCl_3 at δ 77.2). High resolution mass spectra (HRMS) were recorded on MicromassAutoSpecUltima or VG (Micromass) 70-250-S Magnetic sector mass spectrometers in the University of Michigan mass spectrometry laboratory. Infrared (IR) spectra were recorded as thin films on NaCl plates on a Perkin Elmer Spectrum BX FT-IR spectrometer. Absorption peaks were reported in wavenumbers (cm^{-1}). All previously reported phosphoramides were prepared according to published procedures.⁹ All commercially unavailable acetals and ketals were prepared following the procedure reported by Lu and coworkers.¹⁰ Racemic Diels-Alder reactions were performed according to the Chavan procedure.¹¹ Products were then purified by flash chromatography or preparatory HPLC (Waters Delta 600, column Agilent Zorbax RX-SIL, 21.2 x 250 mm, 7 μm) to ensure high purity standards for developing chiral HPLC assays.

Synthesis of catalysts 3-10 – 3-19.

Catalysts **3-10**,¹² **3-11**,^{9a} **3-13**,^{9b} **3-14**,^{9c} **3-18**,^{9c} **3-18**,^{9d} and **3-19**^{9e} have been synthesized according to the previously published procedures.

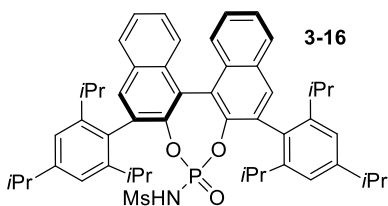


N-((11bS)-2,6-bis(3,5-di-tert-butylphenyl)-4-oxidodinaphtho[2,1-d:1',2'-f][1,3,2]dioxaphosphepin-4-yl)-1,1,1-trifluoromethanesulfonamide (3-12).

75.2 mg (0.104 mmol) of the corresponding chiral phosphoric acid was dissolved in 0.91 mL of dry 1,2 dichloroethane under nitrogen atmosphere. Then 1.0 μ L (0.0135 mmol) of DMF and 44.5 μ L (0.519 mmol) of oxalyl chloride were added. The resulting mixture was stirred at reflux for 20 h. After reaction completion volatiles were evaporated, the product was dried under high vacuum, and subjected to the next step without further purification. This product was isolated as a yellow solid, 77.1 mg, quantitative yield; IR (thin film, cm⁻¹) 2962, 2868, 1595, 1477, 1406, 1363, 1317, 1239, 1086, 922, 751. ¹H NMR (400 MHz, CDCl₃) δ 8.11 (d, *J* = 9.4 Hz, 2H), 8.02 (dd, *J* = 8.3, 4.8 Hz, 2H), 7.64 (d, *J* = 1.5 Hz, 2H), 7.58-7.51 (m, 2H), 7.47 (s, 4H), 7.44 (d, *J* = 8.6 Hz, 1H), 7.38-7.31 (m, 3H), 1.38 (s, 18H), 1.37 (s, 18H); ¹³C NMR (175 MHz, CDCl₃) 151.0, 150.8, 144.52, 144.46, 144.4, 135.7, 135.5, 134.9, 132.1, 132.0, 131.7, 128.8, 128.7, 127.4, 127.3, 126.94, 126.89, 126.64, 126.62, 124.7, 123.0, 122.7, 121.9, 35.3, 35.2, 31.7; ³¹P NMR (202 MHz, CDCl₃) δ 8.4 (s); HRMS (ESI+) (*m/z*): [M+Na] calcd for C₄₈H₅₂ClO₃PNa 765.3235; found 765.3216.

A solution of 16.3 mg (0.110 mmol) of trifluoromethanesulfonylamide in 0.5 mL of dry THF was treated with freshly prepared solution of LDA (made from 30.7 μ L (0.219 mmol) diisopropylamine, 0.14 mL 1.6 M (0.219 mmol) *n*-butyllithium and dry THF (0.5 mL) at -78 °C. The resulting solution was cannulated over a solution of phosphoryl chloride prepared above in dry THF (0.9 mL) again at -78 °C. The resulting reaction mixture was refluxed for 16 h. After that the reaction mixture was brought to room temperature and quenched with water. Organic products were extracted with DCM. Extract was then

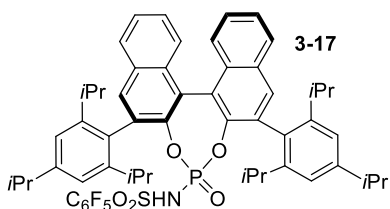
washed with 4N HCl and dried over anhydrous magnesium sulfate. The desired product was purified via preparatory TLC (10:1 DCM/Et₂O) and washed again with 4N HCl to provide a white solid, 42.2 mg, 49% yield; IR (thin film, cm⁻¹) 2961, 2922, 2869, 1595, 1432, 1364, 1203, 1151, 910, 733. ¹H NMR (700 MHz, CDCl₃) δ 8.15 (s, 1H), 8.06 (s, 1H), 8.02 (d, *J* = 8.3 Hz, 1H), 7.99 (d, *J* = 8.3 Hz, 1H), 7.58-7.51 (m, 5H), 7.51-7.42 (m, 4H), 7.38-7.30 (m, 3H), 1.37 (s, 18H), 1.34 (s, 18H); ¹³C NMR (175 MHz, CDCl₃) 151.5, 150.9, 144.0, 143.5, 135.7, 135.2, 134.9, 134.3, 132.3, 132.03, 131.99, 131.96, 128.8, 128.6, 127.4, 127.3, 127.0, 126.6, 124.6, 124.4, 122.9, 122.8, 122.5, 122.2, 35.21, 35.18, 31.6; ³¹P NMR (283 MHz, CDCl₃) δ -11.0 (s); ¹⁹F NMR (376 MHz, CDCl₃) δ -77.4; HRMS (ESI-) (*m/z*): [M-H] calcd for C₄₉H₅₂F₃NO₅PS 854.3259; found 854.3259.



N-((2s,11bS)-4-oxido-2,6-bis(2,4,6-triisopropylphenyl)dinaphtho[2,1-d:1',2'-f][1,3,2]dioxaphosphin-4-yl)methanesulfonamide (3-16).

Following the procedure described by Yamamoto and Nakashima,^{9a} the preparation of **3-16** was conducted on 0.28 mmol scale from the corresponding BINOL derivative and sulfonamide. The resultant product, was isolated as a white solid, 60 mg, 26% yield; IR (thin film, cm⁻¹) 2961, 2870, 1381, 1315, 1171, 912. ¹H NMR (700 MHz, CDCl₃) δ 8.00-7.94 (m, 4H), 7.58-7.53 (m, 2H), 7.39-7.33 (m, 3H), 7.29-7.26 (m, 1H), 7.15 (dd, *J* = 3.1, 1.9 Hz, 2H), 7.13 (d, *J* = 1.7 Hz, 1H), 7.02 (d, *J* = 1.7 Hz, 1H), 2.98-2.95 (m, 3H), 2.73-2.68 (m, 1H), 2.60-2.52 (m, 2H), 2.42 (s, 3H), 1.43 (s, 1H), 1.30 (d, *J* = 7.2 Hz, 6H), 1.26 (d, *J* = 6.9 Hz, 9H), 1.24 (dd, *J* = 10.0, 6.9 Hz, 6H), 1.21 (dd, *J* = 6.9, 1.9 Hz, 6H), 1.09 (d, *J* = 6.9 Hz, 3H), 1.00 (d, *J* = 6.9 Hz, 3H), 0.96 (d, *J* = 6.9 Hz, 3H); ¹³C NMR (175 MHz, CDCl₃) δ 149.9, 149.2, 148.7, 148.3, 147.2, 146.2, 146.0, 144.6, 133.0, 132.9, 132.6, 132.4, 132.3, 131.8, 131.3, 130.9, 130.7, 130.2, 128.6,

128.5, 127.5, 126.9, 126.5, 126.4, 122.1, 121.7, 121.6, 121.3, 120.3, 42.1, 34.6, 31.6, 31.4, 31.2, 30.8, 30.5, 29.9, 27.1, 27.0, 25.6, 25.2, 24.4, 24.2, 23.3, 23.2, 23.1; ^{31}P NMR (202 MHz, CDCl_3) δ -4.5 (s); HRMS (ESI+) (m/z): [M-H] calcd for $\text{C}_{51}\text{H}_{59}\text{NO}_5\text{PS}$ 828.3857; found 828.3854.



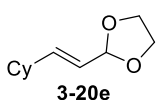
2,3,4,5,6-pentafluoro-N-(4-oxido-2,6-bis(2,4,6-triisopropylphenyl)di-naphtho[2,1-d:1',2'-f][1,3,2]-dioxaphosphepin-4-yl)benzenesulfonamide (3-17).

Following the procedure described by Yamamoto and Nakshima,^{19a} the preparation of **3-17** was conducted on

0.117 mmol scale from the corresponding BINOL derivative and sulfonamide. The resultant product, 11.6 mg was isolated as a white solid in 10% yield; IR (thin film, cm^{-1}) 2961, 2928, 2870, 1520, 1504, 1409, 1316, 1302, 1182, 1103, 996, 903, 733. ^1H NMR (700 MHz, CDCl_3) δ 8.02-7.91 (m, 4H), 7.60-7.51 (m, 2H), 7.42-7.29 (m, 4H), 7.22 (d, $J = 8.9$ Hz, 2H), 7.12 (d, $J = 1.4$ Hz, 1H), 7.06 (d, $J = 1.4$ Hz), 3.05-2.92 (m, 2H), 2.82-2.73 (m, 1H), 2.68-2.50 (m, 3H), 1.32 (d, $J = 6.8$ Hz, 12H), 1.26 (d, $J = 6.8$ Hz, 6H), 1.23-1.15 (m, 9H), 1.04 (d, $J = 6.8$ Hz, 3H), 0.98 (d, $J = 6.8$ Hz, 3H), 0.94 (d, $J = 6.8$ Hz); ^{13}C NMR (175 MHz, CDCl_3) δ 150.4, 148.9, 148.5, 147.7, 146.9, 146.3, 133.6, 133.2, 132.9, 132.4, 132.2, 131.8, 131.3, 130.3, 130.1, 129.8, 128.6, 127.7, 127.6, 126.9, 126.6, 126.5, 122.1, 122.0, 121.5, 121.4, 120.6, 34.6, 34.4, 31.8, 31.3, 31.2, 30.5, 29.9, 27.5, 26.9, 25.6, 25.4, 24.1, 24.0, 23.2, 23.1, 23.0, 22.7; ^{31}P NMR (202 MHz, CDCl_3) δ -6.0 (s); ^{19}F NMR (376 MHz, CDCl_3) δ -135.3 (d, $J = 21.9$ Hz, 2F), -144.9-(-145.2) (m, 1F), -159.6 (t, $J = 19.1$ Hz, 2F); HRMS (ESI-) (m/z): [M-H] calcd for $\text{C}_{56}\text{H}_{56}\text{F}_5\text{NO}_5\text{PS}$ 980.3542; found 980.3541.

Preparation of acetals 3-20 in Table 3.4. The unsaturated acetals **3-6**,¹⁰ **3-20a**,¹³ **3-20b**,¹³ **3-20c**,¹⁴ **3-20d**,^{13c} and **3-20g**,^{13f} have been synthesized according to previously published

procedures. Acetal **3-20e** was synthesized from the corresponding aldehyde following the protocol provided below. Acetal **3-20f** was purchased from Sigma-Aldrich and used as received.



(E)-2-(2-cyclohexylvinyl)-1,3-dioxolane (3-20e).

(*E*)-3-Cyclohexylacrylaldehyde (768.0 mg, 5.56 mmol) was dissolved in 6.8 mL of dry toluene, followed by addition of L-tartaric acid (10.2 mg, .0680 mmol) and anhydrous magnesium sulfate (869.4 mg, 7.22 mmol). The setup was flushed with nitrogen and then ethylene glycol was added (0.81 mL, 14.5 mmol). The reaction mixture was refluxed with a Dean-Stark column overnight. The reaction was quenched with 0.1 mL of triethylamine and then solids were quickly filtered off. The filtrate was then concentrated in vacuo and the desired product was purified by column chromatography. Light yellow oil, 60% yield; IR (thin film, cm^{-1}) 2924, 2852, 1674, 1449, 1400, 1139, 1064, 963. ^1H NMR (700 MHz, CDCl_3) δ 5.89 (dd, $J = 15.7, 6.5$ Hz, 1H), 5.42 (ddd, $J = 15.7, 6.7, 1.5$ Hz, 1H), 5.17 (d, $J = 6.7$ Hz, 1H), 4.03-3.97 (m, 2H), 3.92-3.86 (m, 2H), 2.04-1.97 (m, 1H), 1.78-1.68 (m, 4H), 1.67-1.61 (m, 1H), 1.30-1.22 (m, 2H), 1.15 (tt, $J = 12.7, 3.4$ Hz, 1H), 1.12-1.05 (m, 2H); ^{13}C NMR (175 MHz, CDCl_3) δ 143.8, 123.8, 104.8, 65.1, 40.2, 32.4, 26.3, 26.1; HRMS (EI) (m/z): [M-H] calcd for $\text{C}_{11}\text{H}_{17}\text{O}_2$ 181.1229; found 181.1224.

General procedure A for enantioselective Diels-Alder reactions.

An oven-dried 4-mL scintillation vial was charged with 1 eq of a dienophile and 5 mol% of a catalyst, capped with septum and flushed with nitrogen. Ethyl isobutyrate was then added to ensure 0.3 M concentration of dienophile. Cyclopentadiene (2 eq) was then added via micro syringe. The resulting reaction mixture was stirred at room temperature for 16

hours and then the reaction was quenched with about 2 eq of triethyl amine. Then triphenyl methane was added and volatiles were evaporated from the reaction vial. The crude mixture was analyzed by quantitative ^1H NMR and HPLC.

General procedure B for enantioselective Diels-Alder reactions.

An oven-dried 4-mL scintillation vial was charged with 5 mol% of a catalyst, capped with septum and flushed with nitrogen. Ethyl isobutyrate was then added to ensure 0.3 M concentration of dienophile. After that 1 eq of a dienophile and 2 eq of diene were added via micro syringe. The resulting reaction mixture was stirred at room temperature for 16-24 hours and then the reaction was quenched with about 2 eq of triethyl amine. Then, triphenyl methane was added and the crude mixture was analyzed by quantitative ^1H NMR and HPLC.

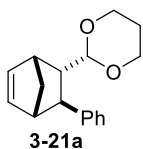
Characterization data for the cycloadducts 3-21 in Table 3.4.

The cycloadducts **3-7**,¹¹ **3-21c**,¹⁵ **3-21g**,¹¹ and **3-21h**,¹⁶ have been previously characterized. The characterization data for compounds **3-21a**, and **3-21e** is provided below. The crude product **3-21d** was hydrolyzed to the corresponding ketone that has been synthesized and characterized before.¹⁷ The hydrolysis procedure is provided below.

Hydrolysis of cycloadduct 3-21d.

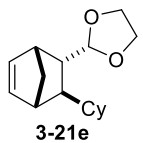
The crude reaction mixture was obtained following the **General Procedure A** described above. The reaction was quenched with ~10 mol% of triethylamine. Volatiles were evaporated from the reaction mixture, and then the resultant mixture was dissolved in dioxane (1.0 mL). To this, 4N HCl (0.5 mL) was added, the resultant mixture was stirred

at 40 °C for 2 h, then organics were extracted with diethyl ether. Organic layer was dried with MgSO₄ and filtered. The solvent was removed *in vacuo* and triphenylmethane was added. The resultant crude mixture was analyzed by ¹H NMR to establish the yield and d.r.¹⁷



2-(3-phenylbicyclo[2.2.1]hept-5-en-2-yl)-1,3-dioxane (3-21a).

Colorless oil, 32% yield (about 60% conversion) 12:1 endo/exo; IR (thin film, cm⁻¹) 3057, 2964, 2847, 1498, 1377, 1240, 1144, 1110, 1011, 720, 700. *Endo product*: ¹H NMR (400 MHz, CDCl₃) δ 7.39 (d, *J* = 7.6 Hz, 2H), 7.28 (t, *J* = 7.6 Hz, 2H), 7.16 (t, *J* = 7.3 Hz, 1H), 6.34 (dd, *J* = 5.6, 3.1 Hz, 1H), 6.15 (dd, *J* = 5.6, 2.8 Hz), 4.15-4.03 (m, 2H), 4.05 (d, *J* = 8.3 Hz, 1H), 3.75-3.62 (m, 2H), 3.02 (s, 1H), 2.93 (s, 1H), 2.49-2.45 (m, 1H), 2.45-2.39 (m, 1H), 2.13-1.99 (m, 1H), 1.66 (d, *J* = 8.6 Hz, 1H), 1.46 (dq, 8.6, 1.7 Hz, 1H), 1.32-1.26 (m, 1H). *Distinct peaks for exo product*: ¹H NMR (400 MHz, CDCl₃) δ 6.29 (dd, *J* = 5.5, 3.1 Hz, 1H), 5.92 (dd, *J* = 5.5, 2.9 Hz, 1H), 5.71-5.60 (m, 1H), 4.55 (d, *J* = 6.4 Hz, 1H), 3.21 (dd, *J* = 5.0, 3.5 Hz, 1H), 3.08 (br s, 1H), 2.98 (br s, 1H), 1.94-1.89 (m, 1H), 1.75 (d, *J* = 8.6 Hz, 1H), 1.34 (br s, 1H); *Endo only*: ¹³C NMR (175 MHz, CDCl₃) δ 145.3, 138.1, 135.4, 128.4, 128.1, 125.8, 106.8, 67.1, 51.5, 49.4, 47.0, 46.7, 44.3, 26.0; HRMS (ESI+) (*m/z*): [M+NH₄] calcd for C₁₇H₂₄NO₂ 274.1802; found 274.1800.



2-(3-cyclohexylbicyclo[2.2.1]hept-5-en-2-yl)-1,3-dioxolane (3-21e).

Light yellow oil, 60% yield, 3:1 endo/exo; IR (thin film, cm⁻¹) 2980, 2922, 2851, 1448, 1334, 1098, 1056, 990, 719. *Endo product*: ¹H NMR (400 MHz, CDCl₃) δ 6.18-6.13 (m, 1H, endo/exo), 6.09-6.04 (m, 1H, endo/exo), 4.26 (d, *J* = 7.6 Hz, 1H, endo), 4.03-3.88 (m, 2H, endo/exo), 3.88-3.73 (m, 2H, endo/exo), 2.88 (br s, 1H, endo/exo), 2.75

(br s, 1H, endo), 1.94-1.85 (2H, endo/exo), 1.80-1.70 (m, 2H, endo/exo), 1.68-1.53 (m, 2H, endo/exo), 1.41 (d, $J = 8.5$ Hz, 1H, endo), 1.31 (dd, $J = 8.5, 1.4$ Hz, 1H, endo/exo), 1.29-1.08 (m, 4 H, endo/exo), 1.06-0.86 (m, 3H, endo/exo) *Selected ^1H NMR peaks for exo product:* ^1H NMR (400 MHz, CDCl_3) δ 4.83 (d, $J = 5.0$ Hz, 1H), 2.80 (br s, 1H); *Endo only:* ^{13}C NMR (175 MHz, CDCl_3) δ 138.1, 134.6, 108.9, 65.0, 64.7, 48.2, 47.6, 46.7, 44.6 (2H), 42.3, 32.9, 32.3, 27.1, 26.9 (2H); MS (EI) (m/z): [M] calcd for $\text{C}_{16}\text{H}_{24}\text{O}_2$ 248.2; found 248.2.

References

¹ (a) Evans, D. A.; Thomson, R. J. *J. Am. Chem. Soc.* **2005**, *127* (30), 10506–10507. (b) Reisman, S. E.; Doyle, A. G.; Jacobsen, E. N. *J. Am. Chem. Soc.* **2008**, *130* (23), 7198–7199. (c) Terada, M.; Tanaka, H.; Sorimachi, K. *J. Am. Chem. Soc.* **2009**, *131* (10), 3430–3431. (d) Moquist, P. N.; Kodama, T.; Schaus, S. E. *Angew. Chem. Int. Ed.* **2010**, *49* (39), 7096–7100. (e) Maity, P.; Srinivas, H. D.; Watson, M. P. *J. Am. Chem. Soc.* **2011**, *133* (43), 17142–17145. (f) Kobayashi, S.; Arai, K.; Yamakawa, T.; Chen, Y.-J.; Salter, M. M.; Yamashita, Y. *Adv. Synth. Catal.* **2011**, *353* (11-12), 1927–1932. (g) Han, Z.-Y.; Guo, R.; Wang, P.-S.; Chen, D.-F.; Xiao, H.; Gong, L.-Z. *Tetrahedron Lett.* **2011**, *52* (45), 5963–5967. (h) Terada, M.; Toda, Y. *Angew. Chem. Int. Ed.* **2012**, *51* (9), 2093–2097. (i) Rueping, M.; Volla, C. M. R.; Atodiresei, I. *Org. Lett.* **2012**, *14* (17), 4642–4645.

² (a) Čorić, I.; Vellalath, S.; List, B. *J. Am. Chem. Soc.* **2010**, *132* (25), 8536–8537. (b) Cox, D. J.; Smith, M. D.; Fairbanks, A. J. *Org. Lett.* **2010**, *12*, 1452–1455. (c) Čorić, I.; Vellalath, S.; List, B. *J. Am. Chem. Soc.* **2010**, *132* (25), 8536–8537. (d) Čorić, I.; List, B. *Nature* **2012**, *483* (7389), 315–319. (e) Sun, Z.; Winschel, G. A.; Borovika, A.; Nagorny, P. *J. Am. Chem. Soc.* **2012**, *134* (19), 8074–8077. (f) Kimura, T.; Sekine, M.; Takahashi, D.; Toshima, K. *Angew. Chem. Int. Ed.* **2013**, *52* (46), 12131–12134. (g) Mensah, E.; Camasso, N.; Kaplan, W.; Nagorny, P. *Angew. Chem. Int. Ed.* **2013**, *52* (49), 12932–12936.

³ (a) Nagorny, P.; Sun, Z.; Winschel, G. *Synlett* **2013**, *24* (06), 661–665. (b) Sun, Z.; Winschel, G. A.; Zimmerman, P. M.; Nagorny, P. *Angew. Chem. Int. Ed.* **2014**, *53* (42), 11194–11198.

⁴ Harmata, M.; Rashatasakhon, P. *Tetrahedron* **2003**, *59* (14), 2371–2395.

⁵ Sammakia, T.; Berliner, M. A. *J. Org. Chem.* **1994**, *59* (23), 6890–6891.

⁶ (a) Schmidt, R. R.; Rücker, E. *Tetrahedron Lett.* **1980**, *21* (15), 1421–1424. (b) Schmidt, R. R.; Behrendt, M.; Toepfer, A. *Synlett* **1990**, *1990* (11), 694–696.

⁷ Christ, P.; Lindsay, A. G.; Vormittag, S. S.; Neudörfl, J.-M.; Berkessel, A.; O'Donoghue, A. C. *Chem.-Eur.J.* **2011**, *17*, 8524–8528.

⁸ Bordwell, F. G.; Algrim, D. *J. Org. Chem.* **1976**, *41* (14), 2507–2508.

⁹ (a) Nakashima, D.; Yamamoto, H. *J. Am. Chem. Soc.* **2006**, *128*, 9626–9627; (b) Rueping, M.; Antonchick, A. P.; Brinkmann, C. *Angew. Chem. Int. Ed.* **2007**, *46*, 6903–6906; (c) Cheon, C. H.; Yamamoto, H. *J. Am. Chem. Soc.* **2008**, *130*, 9246–9247; (d) Rueping, M.; Nachtsheim, B. J.; Koenigs, R. M.; Ieawsuwan, W. *Chem.-Eur.J.* **2010**, *16*, 13116–13126; (e) Desai, A.; Wulff, W. *Synthesis* **2010**, *2010*, 3670–3680.

¹⁰ Lu, T.-J.; Yang, J.-F.; Sheu, L.-J. *J. Org. Chem.* **1995**, *60*, 2931–2934.

- ¹¹ Chavan, S. P.; Sharma, A. K. *Synlett* **2001**, 2001, 0667–0669.
- ¹² Fabbri, D.; Delogu, G.; De Lucchi, O. *Tetrahedron: Asymmetry* **1993**, 4, 1591-1596.
- ¹³ Luminita, M.; Mirela, B.; Carmen, F.; Anamaria, T.; Grosu, I.; Mager, S.; Margineanu, D. *Studia Universitatis Babes-Bolyai, Chemia* **2002**, 47, 195-201.
- ¹⁴ Barbero, M.; Cadamuro, S.; Dughera, S.; Venturello, P. *Synthesis*, **2008**, 2008, 1379-1388; (c) McConville, M.; Saidi, O.; Blacker-J.; Xiao, J. *J. Org. Chem.* **2009**, 74, 2692-2698.
- ¹⁵ Bonini, B. F.; Capito, E.; Comes-Franchini, M.; Fochi, M.; Ricci, A.; Zwanenburg, B. *Tetrahedron: Asymmetry* **2006**, 17, 3135-3143
- ¹⁶ Inokuchi, T.; Tanigawa, S.; Torii, S. *J. Org. Chem.* **1990**, 55, 3958-3961.
- ¹⁷ Singh, R. S.; Adachi, S.; Tanaka, F.; Yamauchi, T.; Inui, C.; Harada, T. *J. Org. Chem.* **2008**, 73, 212-218.

Chapter 4

Stereo- and Regioselective Synthesis of Aminoglycosides

4.1 Introduction to aminoglycosides

Since the glucose structure elucidation by E. Fisher in 1891¹, the carbohydrate chemistry became a fascinating field for the organic synthesis community. Many methods were developed for the synthesis of complex carbohydrates. Carbohydrates are abundant as they are found in a plethora of natural products, and they have endless number of functions within the human body as well as all other organisms. Cellular and protein recognition is one of the major functions in biological processes that includes carbohydrates. For example, glycoproteins and glycolipids are overexpressed or modified on the cancer cell membranes.^{2,3}

As a part of carbohydrate family, aminoglycosides represent an important subclass of carbohydrate chemistry. Aminoglycosides are broad-spectrum antibiotics typically used for treatment of serious bacterial infections. These antibiotics target the prokaryotic ribosome by binding to the decoding A-site of the 16S rRNA fragment while interfering protein translation.⁴ Aminoglycoside antibiotics typically display bactericidal activity against Gram-negative aerobic bacteria and some anaerobic bacilli, and generally not against Gram-positive or anaerobic Gram-negative bacteria. The first isolation of a known

naturally available aminoglycoside streptomycin from *Streptomyces griseus* by Schatz and Waksman in 1944⁵, multiple naturally available aminoglycoside antibiotic agents were discovered (Figure 4.1). Aminoglycosides are composed of several aminocarbohydrate units that are glycosidically bound to an aminocyclitol ring (either streptamine or 2-deoxystreptamine).⁶

The substitution pattern on aminocyclitol rings vary substantially depending on the aminoglycoside. Thus, 2-deoxystreptamine, the central core in most popular aminoglycosides can be substituted at positions 4 and 5 (neomycin, paromomycin, and ribostamycin), or at positions 4 and 6 (amikacin, kanamycin A and B, tobramycin, gentamycin etc.), while streptidine core is found in streptomycin (Figure 4.1).

Naturally occurring aminoglycosides are produced by *Streptomyces* and *Micromonospora* soil bacteria, which proactively methylate their ribosomes to survive the bactericidal action of their secondary metabolites.⁷ There are three major pathways that lead to bacterial resistance to aminoglycosides: enzymatic modification by aminoglycoside-modifying enzymes, reduction of the drug-target activity by modification of 30S fragment of the A-site of rRNA, or active removal of aminoglycoside from the bacterial cell through efflux pumps. Along with some developed resistance, aminoglycosides also sometimes cause nephro- and oto-toxic, as well as neuromuscular side effects. Molecular mechanisms that lead to the side effects are not yet completely understood and are the subject of several medicinal studies.⁶ Overall, aminoglycosides show a strong synergistic effect when coadministered with penicillin, a particularly useful combination for treatment of infections of unknown origin.⁸ Some semisynthetic derivatives such as amikacin, netilmicin, arbekacin etc. are also on the market due to

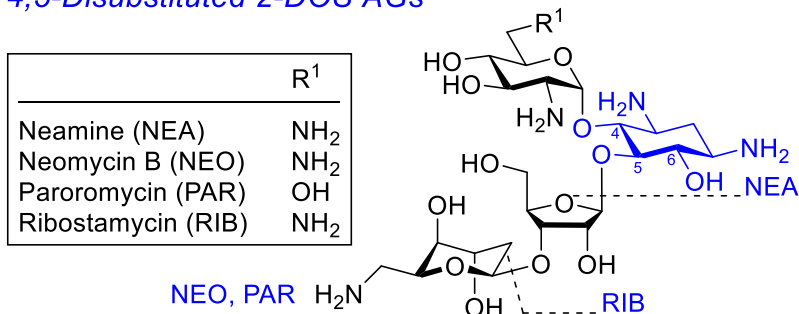
particular activity against bacteria that developed resistance against early aminoglycosides.⁹ However, in recent years it became obvious that the battle against bacterial resistance is not over. On the contrary, resistance of bacterial strains is reported with increasing frequency, with the associated severe consequences such as untreatable patients or temporary closure of hospital intensive cares.⁸

Aside from antibiotic activity, aminoglycosides are gaining popularity in the field of potentially broader application, that is, regulation of protein production at RNA level. Since aminoglycosides are rather unselective ligands for all sorts of RNA, often in low micromolar concentration, their characteristics have been extensively studied in the field of “RNA as a drug target”: the understanding that RNA plays a central role in protein production from DNA provides wide opportunities for pharmaceutical development.

Drug resistance, high levels of toxicity, and the variety of biological activities of aminoglycosides and their synthetic analogs have encouraged chemists to develop chemical strategies and methodologies for the design and preparation of novel aminoglycosides. It was our objective to develop a regio- and stereoselective method for synthesis of aminoglycoside derivatives using chiral Brønsted acids as catalysts.

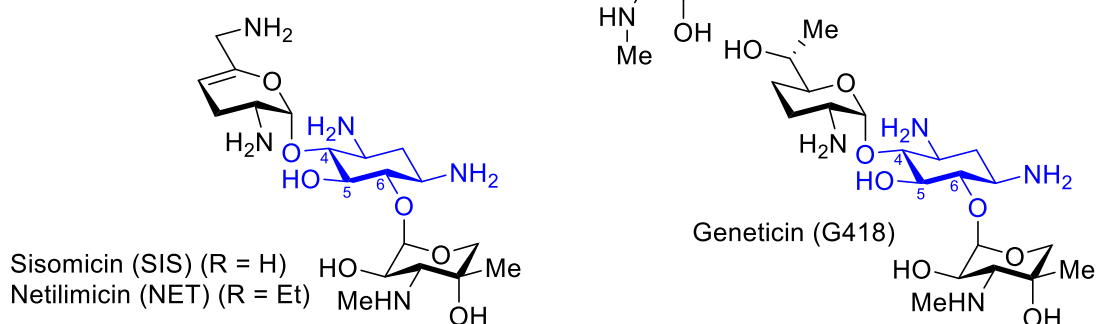
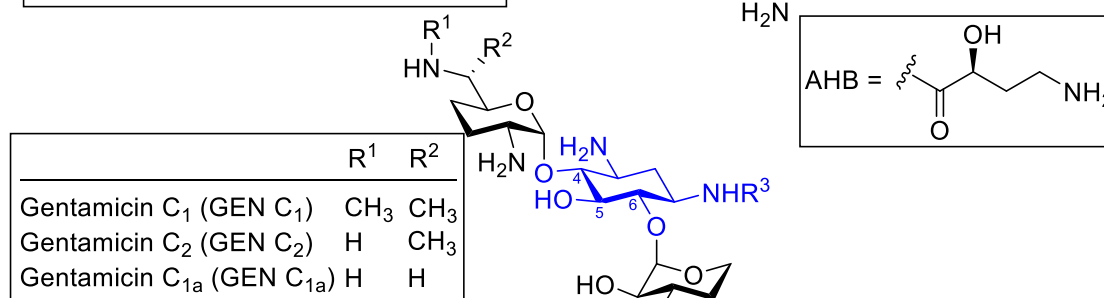
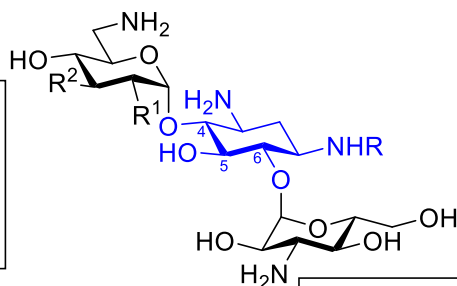
Figure 4.1 Structural diversity of natural aminoglycoside antibiotics

4,5-Disubstituted 2-DOS AGs

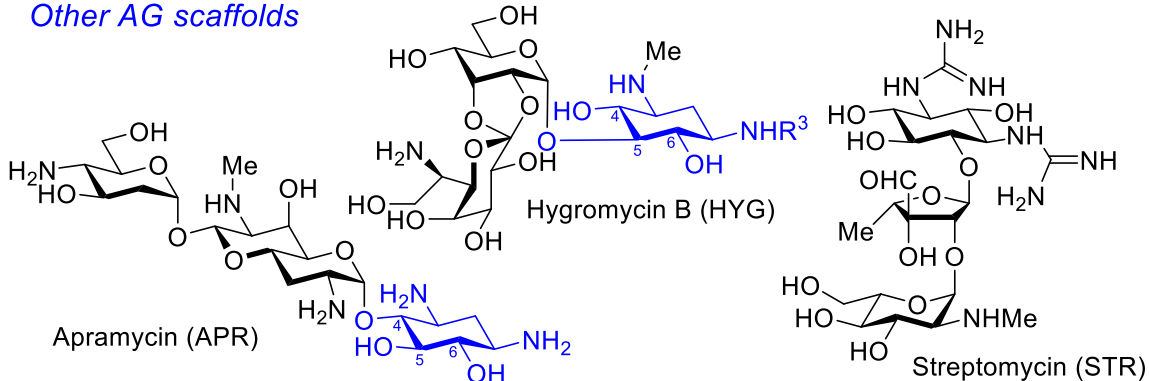


4,6-Disubstituted 2-DOS AGs

	R ¹	R ²	R ³
Amikacin (AMK)	OH	OH	AHB
Kanamycin A (KAN A)	OH	OH	H
Kanamycin B (KAN B)	NH ₂	OH	H
Tobramycin (TOB)	NH ₂	H	H



Other AG scaffolds

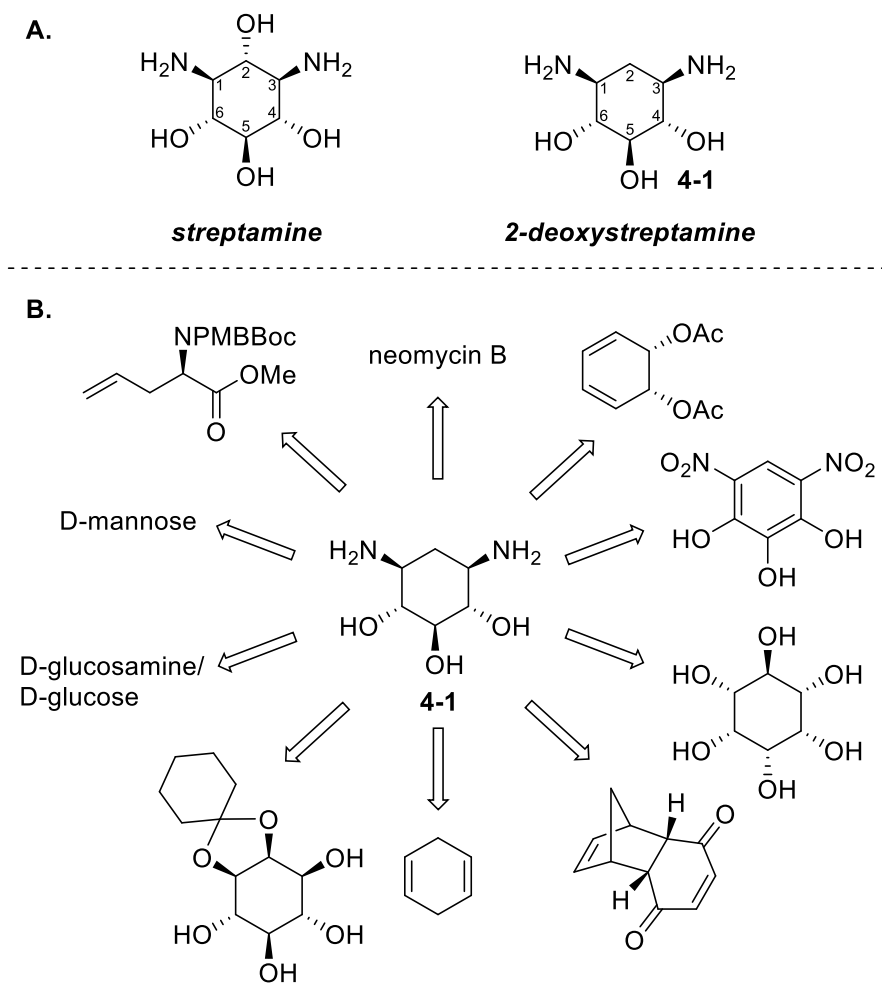


4.2 Strategy for regio- and stereoselective glycosylations of 2-deoxystreptamine

As seen from Figure 4.1, members of aminoglycoside family are predominantly built up by a variety of aminosugars. These aminosugars, often 6-amino or 2,6-diamino type can be additionally decorated or functionalized. Some additional rings or rare carbohydrates can be present in some aminoglycosides, however of higher significance is the aminocyclitol that is present in each of the structures. 2-deoxystreptamine is a central core in most aminoglycosides. Due to the presence of many amino functionalities, aminoglycosides are heavily protonated under physiological conditions, thus providing a rationale for the strong affinity for nucleotides in RNA.¹⁰

The omnipresence and central location of 2-deoxystreptamine (or in some cases other aminocyclitols) suggests a crucial role for biological activity. X-Ray structures of several aminoglycosides complexed to the 30S ribosomal particle^{11,12,13} or to an A-site oligonucleotide sequence^{14,15,16} without exception show a similar binding pattern to 2-deoxystreptamine regardless its 4,5- or 4,6-substitution. Additional evidence of the crucial role of 2-deoxystreptamine in biological activity of aminoglycosides comes from the observation that the presence of bivalent structure of 2-deoxystreptamine alone, without aminosugar substitution, already shows low micromolar binding to RNA hairpin loops.¹⁷

Figure 4.2 2-Deoxystreptamine and its synthons

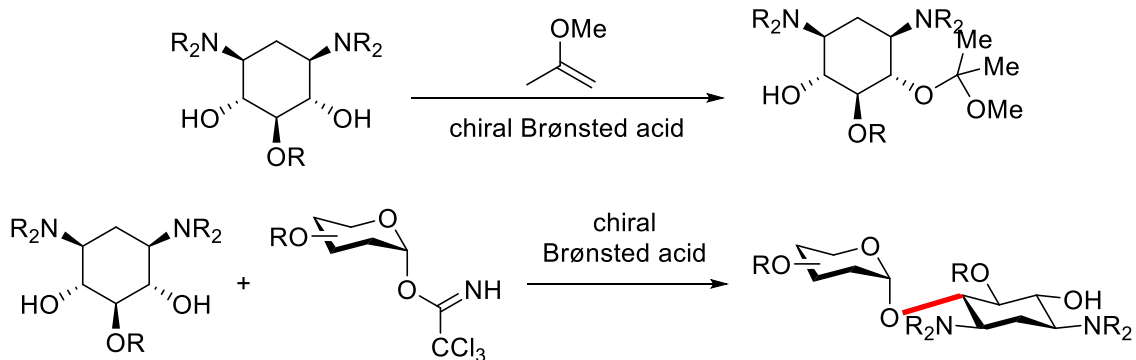


High activity of 2-deoxystreptamine and diversity of carbohydrate residues that 2-deoxystreptamine is bound with suggests that glycodiversification of 2-deoxystreptamine **4-1** could potentially be a valid strategy for design and synthesis of novel aminoglycosides. 2-Deoxystreptamine is an all-trans substituted *meso* molecule that has two amino and three hydroxyl groups (Figure 4.2A). Numerous synthetic strategies have been developed in order to access 2-deoxystreptamine, many of which begin with chiral starting materials (Figure 4.2B). Considering the fact that 2-deoxystreptamine is a symmetric molecule, the choice of an enantiomerically pure starting material might seem awkward at first, however

that provides access to useful enantiomerically pure intermediates that can be applied for the synthesis of novel aminoglycosides.

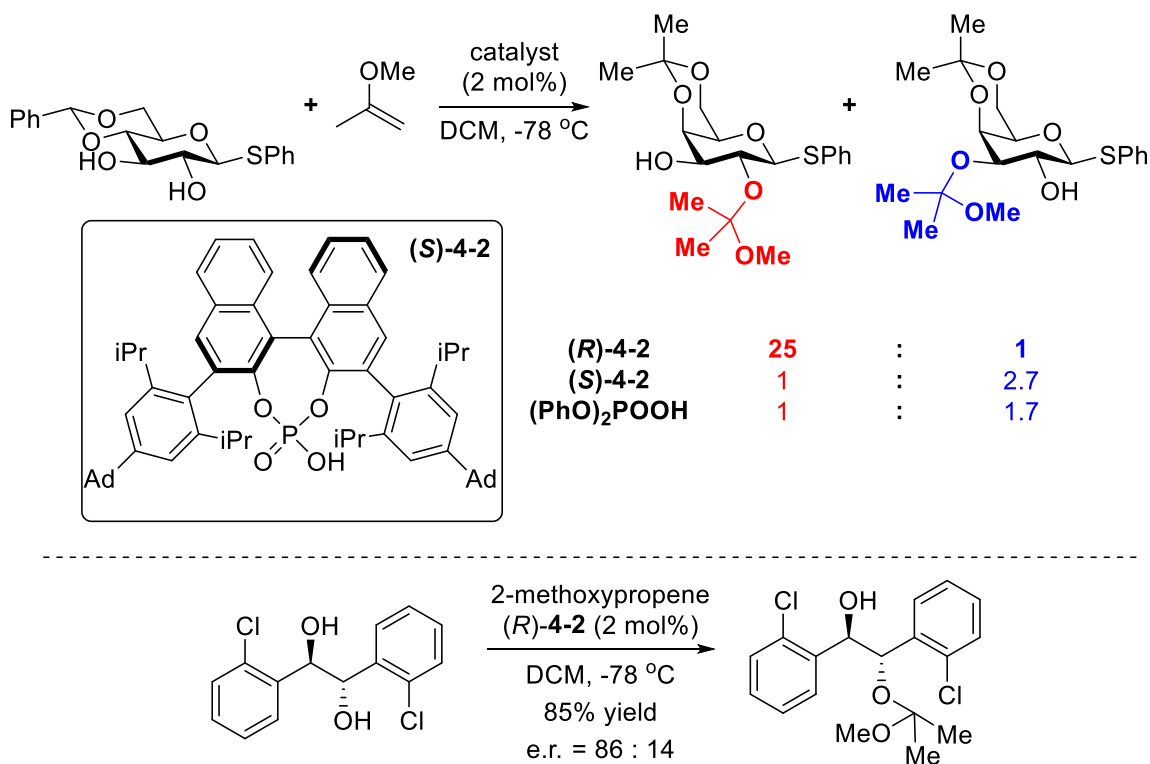
Our approach, however, implies the use of *meso* starting material that will be desymmetrized using chiral Brønsted acids. Such desymmetrization would proceed through either stereoselective protection of alcohol groups or their direct glycosylation when catalyzed by chiral phosphoric acids or their derivatives (Scheme 4.1).

Scheme 4.1 Proposed desymmetrization of 2-deoxystreptamine derivative



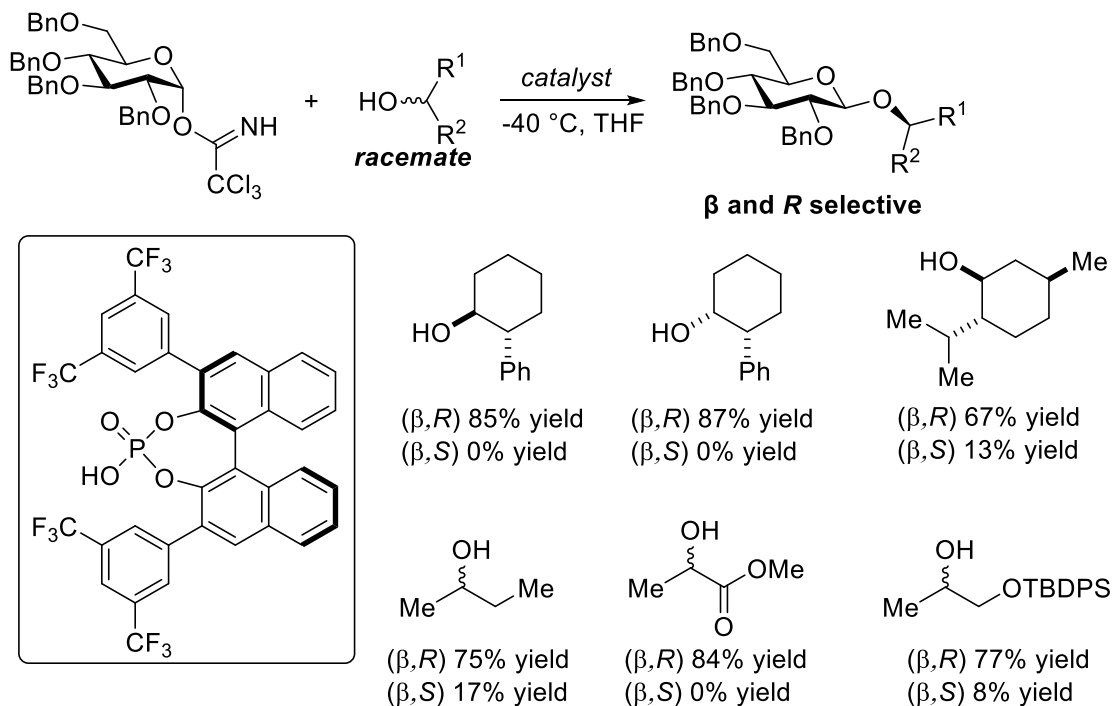
The enantioselective desymmetrization of *meso*-diols is one of the most popular methods to access the corresponding monoprotected derivatives in their enantiopure form. The nonenzymatic desymmetrization of *meso*-diols has been achieved through asymmetric monoacylation,¹⁸ silylation,¹⁹ hydrolysis of acetals,²⁰ hydrolysis of *meso*-diesters, oxidation of diols, etc.²¹ While those approaches commonly include use of chiral amines or chiral Lewis acids as catalysts, up until 2015 no methods for desymmetrization of *meso*-diols catalyzed by chiral Brønsted acids were available.^{19d}

Scheme 4.2 CPA-controlled regioselective acetalization of chiral diols and enantioselective desymmetrization of *meso*-diols



In 2013 our group published a method for chiral phosphoric acid-directed regioselective acetalization of carbohydrate-derived 1,2-diols (Scheme 4.2).²² This method combines the approach of CPA-catalyzed nucleophilic addition to oxocarbenium ions as well as differentiation of two alcohol groups that are present in the same molecule. This was the first study that presented catalyst-controlled (rather than substrate- or reagent-controlled) regioselective acetalization reaction. In addition to that, preliminary studies in desymmetrization of *meso*-diols via acetalization using chiral phosphoric acids was reported as well. This approach was later used in attempt to desymmetrize 2-deoxystreptamine derivatives (*vide infra*).

Scheme 4.3 CPA mediated glycosylation with recognition of alcohol chirality

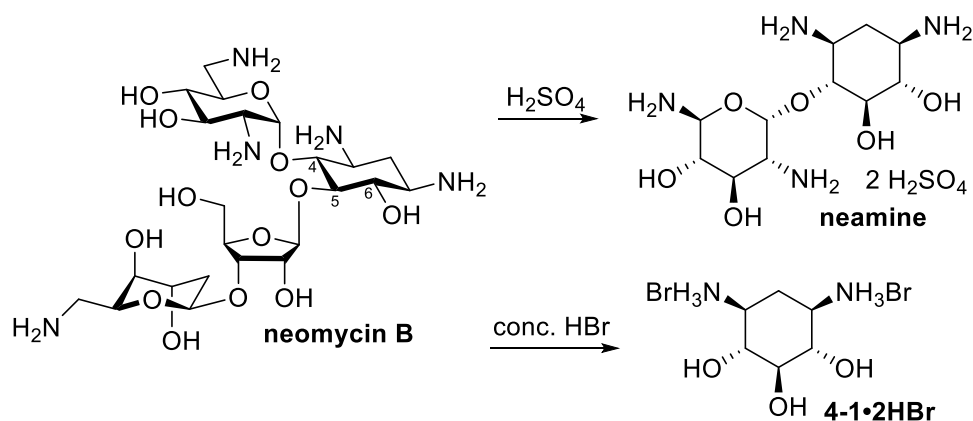


Another way to desymmetrize 2-deoxystreptamine is to do a glycosylation reaction without prior enantioselective protection of *meso*-2-deoxystreptamine. Chiral phosphoric acids have shown that they can promote glycosylation reaction between trichloroacetimidate glycosyl donors and acceptors, often enhancing the α/β selectivities.^{23,24,25} In addition to α/β selectivity, chiral phosphoric acids proved to perform chiral recognition of racemic alcohols during the glycosylation reaction with sufficiently high selectivity (Scheme 4.3).²⁴ The aforementioned reports by our group²² and Toshima suggest that chiral phosphoric acids can potentially be used as catalysts for regio- and stereoselective glycosylation of 2-deoxystreptamine derivative.

4.3 Design of 2-deoxystreptamine derivatives for its desymmetrization

While many synthetic pathways exist that allow to access enantiomerically pure chiral 2-deoxystreptamine derivatives, the most practical way to obtain 2-deoxystreptamine is by straightforward acidic degradation of neomycin B (Scheme 4.4). This is the approach we are also using to access 2-deoxystreptamine.

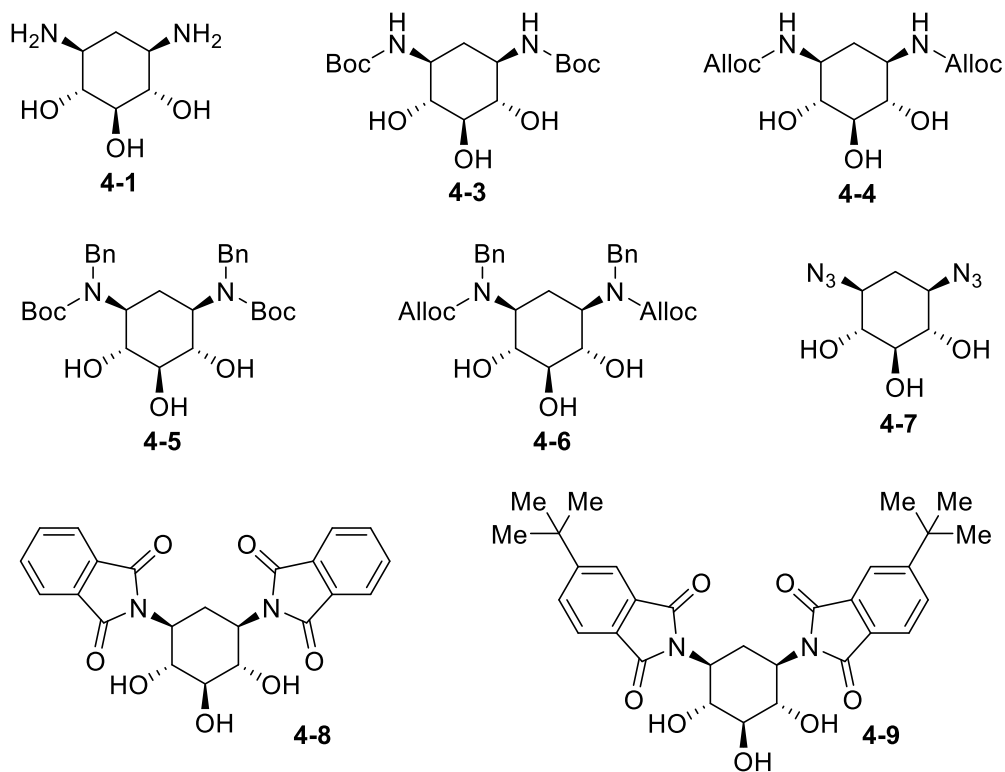
Scheme 4.4 Acidic degradation of neomycin



As it was mentioned before, 2-deoxystreptamine is a polar molecule that has two amino and three hydroxyl groups. These five polar functionalities make 2-deoxystreptamine extremely hydrophilic making it soluble only in water. Presence of water in the reaction catalyzed with a chiral Brønsted acid will lead to specific acid catalysis which will result in low stereoselectivities due to solvent association of the chiral acid anion. Hence, in order to perform enantio- or diastereoselective reactions using chiral Brønsted acids as catalysts, it is extremely important to eliminate all the water from the reaction mixture. In addition to that, it is also necessary to protect basic nitrogens since amines react with Brønsted acids. Thus, a variety of nitrogen (and oxygen) protecting

groups had to be considered in order to make the *meso*-triol more lipophilic and less basic (Figure 4.3).

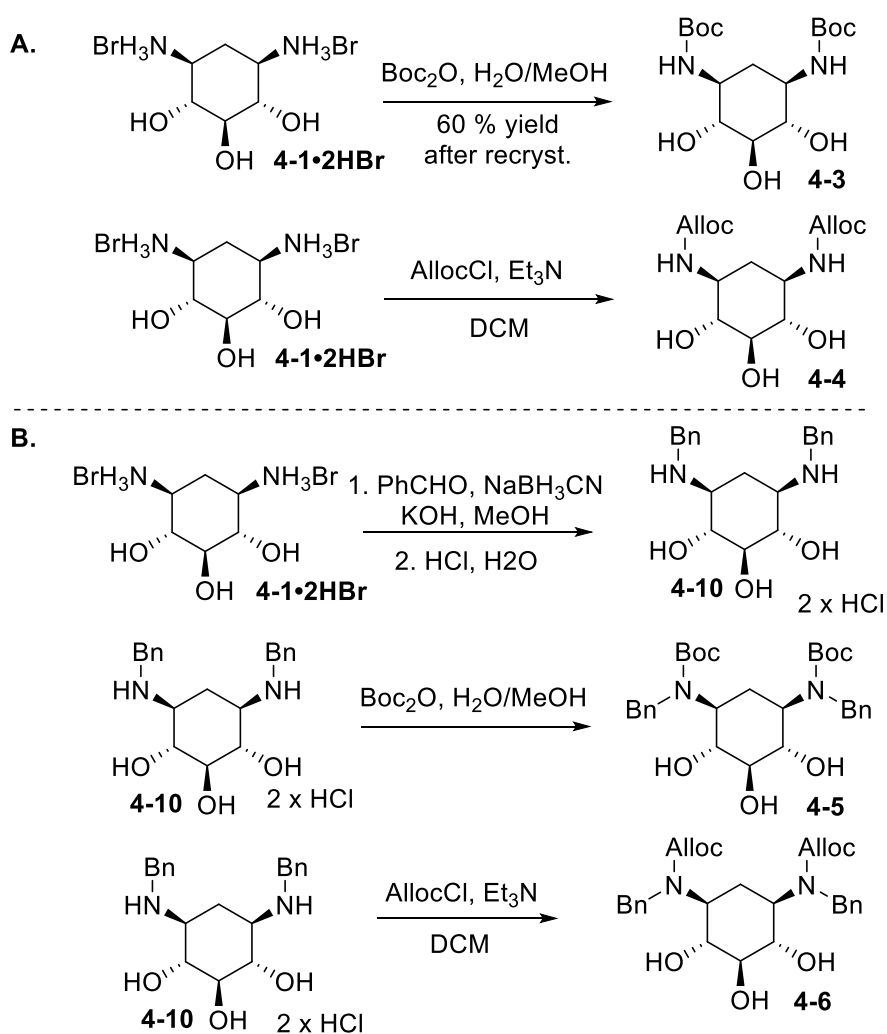
Figure 4.3 Nitrogen protecting groups for 2-deoxystreptamine



First carbamate-based protective groups were selected in order to test their effects on the solubility of 2-deoxystreptamine. Thus, Boc and Alloc groups were installed. The lipophilic character of those groups suggested that the product could potentially be far more soluble in non-polar organic solvents than the unprotected diamine. While both Boc and Alloc groups made the substrate more soluble in methanol, **4-3** and **4-4** were still rather poorly soluble in other organic solvents such as chloroform or benzene (Scheme 4.5 A). Hence, to increase the solubility even more, a benzyl protecting group was introduced as well. While benzyl protecting group in combination with Alloc or Boc protection gave

greater increase in solubility; however, complicated the detection and analysis of **4-5** and **4-6** by NMR spectroscopy due to the formation of the C-N bond rotamers (Scheme 4.5 B). Since we anticipated that the NMR techniques would be key in analyzing and interpreting the acetalization or glycosylation of 2-deoxystreptamine results, compounds **4** and **5** were abandoned as potential substrates for the study.

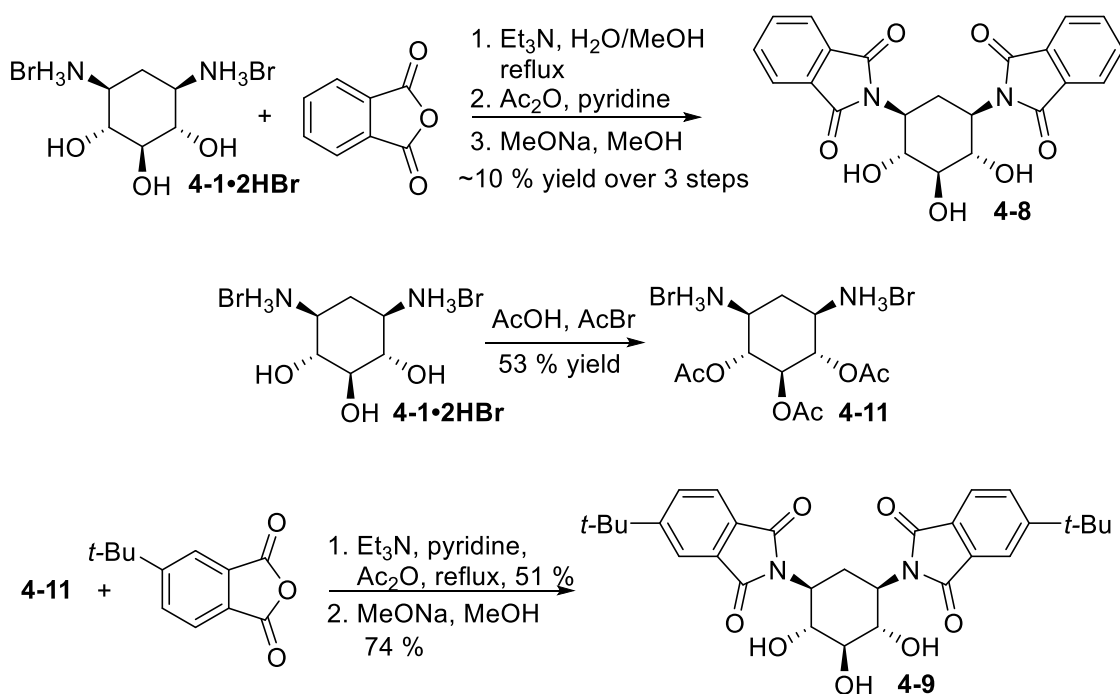
Scheme 4.5 Synthesis of **4-3** – **4-6**



Phtalimide is another common protective group for nitrogen. The substitution of primary amine with a phtalimide protective group allows to block both hydrogens on

nitrogen to avoid secondary hydrogen bond interaction with the chiral catalyst or the glycosyl donor. The synthesis of phtalimides proceeds through dehydrative condensation of phtalic anhydride at high temperatures with primary amines. Thus, two phtalimide groups were introduced to 2-deoxystreptamine that resulted in formation of methanol soluble **4-8**. While **4-8** was proved to be insoluble in nonpolar solvents, *tert*-butylphtalimide-derived 2-deoxystreptamine **4-9** was rather soluble in dichloromethane and ethyl acetate (Scheme 4.6).

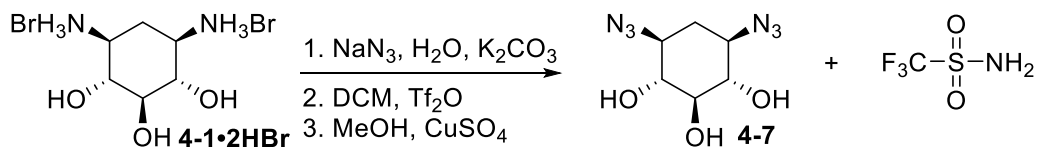
Scheme 4.6 Synthesis of **4-8** – **4-9**



Finally, azides were also explored as a protecting group of nitrogen. Small steric size of azides would be beneficial for reasonably bulky chiral phosphoric acids. Thus, diazotransfer reaction was performed with trifluoromethanesulfonic anhydride and sodium azide (Scheme 4.7). While original procedure²⁶ reported 69% yield for the double diazo

transfer on 2-deoxystreptamine, the observed yield in our case was nearly quantitative. This alarming observation was carefully studied. Although ^1H NMR showed no impurities present in the crystalline product, ^{19}F NMR suggested strong presence of some fluorine containing impurity, probably trifluoromethanesulfonylamide (TfNH_2), a byproduct in diazotransfer reactions where both sodium azide and Tf_2O are used. The evaluation of the product mixture revealed that most of the material consisted of TfNH_2 with only minor amounts of the desired diazide **4-7**. Unfortunately, the properties of both the diazide and TfNH_2 made the separation of two impossible by column chromatography. Hence, another diazotransfer reaction strategy had to be employed.

Scheme 4.7 Diazotransfer with trifluoromethanesulfonic anhydride

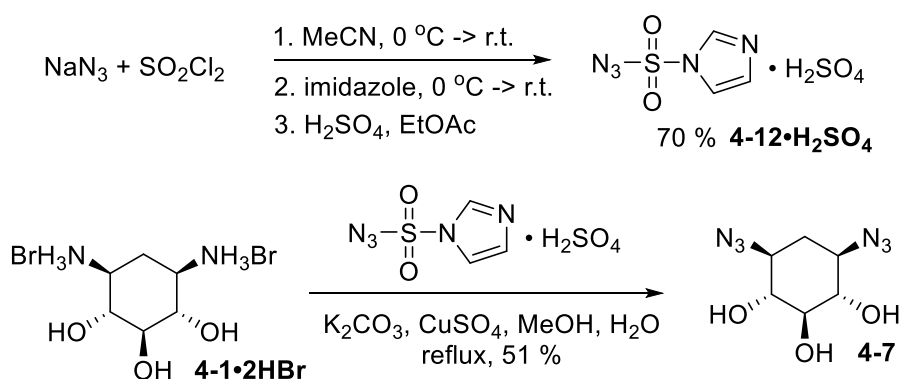


In 2007 Goddard-Borger reported preparation and application of a novel imidazole-1-sulfonyl azide hydrochloride (Scheme 4.8). This diazotransfer reagent allows to circumvent formation of TfNH_2 .²⁷ However, shock sensitivity and heat stability of low-molecular weight azides has always been a cause for concern. While the original paper reported that **4-12·HCl** is neither shock nor heat sensitive, there was an actual explosion during the synthesis of **4-12·HCl**. Thus, Goddard-Borger in collaboration with Klapotke studied the sensitivities of imidazole-1-sulfonyl azide salts.²⁸ All salts investigated proved to be equally good diazo donors, however their safety profile varied substantially. All things considered, **4-12·HBF₄** and **4-12·H₂SO₄** are the safest-to-handle materials. Since hydrogen sulfate is easier and less expensive to prepare, it became the diazotransfer reagent

of our choice. It is important to note that imidazole-1-sulfonyl azide and its salts are energetic materials and should be handled with caution. Plastic filters and suction funnels should be used for the isolation of crystalline materials. Mother liquors and any other waste should be treated with excess sodium nitrite and acidified to neutralize any azide-containing species.

2-Deoxystreptamine diazide **4-7** was synthesized using Goddard-Borger method (Scheme 4.8), and was sufficiently soluble in solvents such as dichloromethane and chloroform. Due to its rather sterically unencumbered structure, as well as simplicity of its synthesis (1 step, 51% yield vs 3 steps, 20% yield for **4-9**), azide was selected as protecting group of choice. In general, the introduction of an azido group into a molecule typically increases its energy content by 69–85 cal/mol. Organic azides are considered as explosives whenever the nitrogen content in the molecule is abnormally high. As a rule of thumb, violent decomposition reactions can be expected for azido compounds having (C + O)/N ratio of < 3.²⁹ Thus, **4-7** having two azido groups brings this ratio to 1.5. Since **4-7** might be potentially explosive, it was important to study its stability.

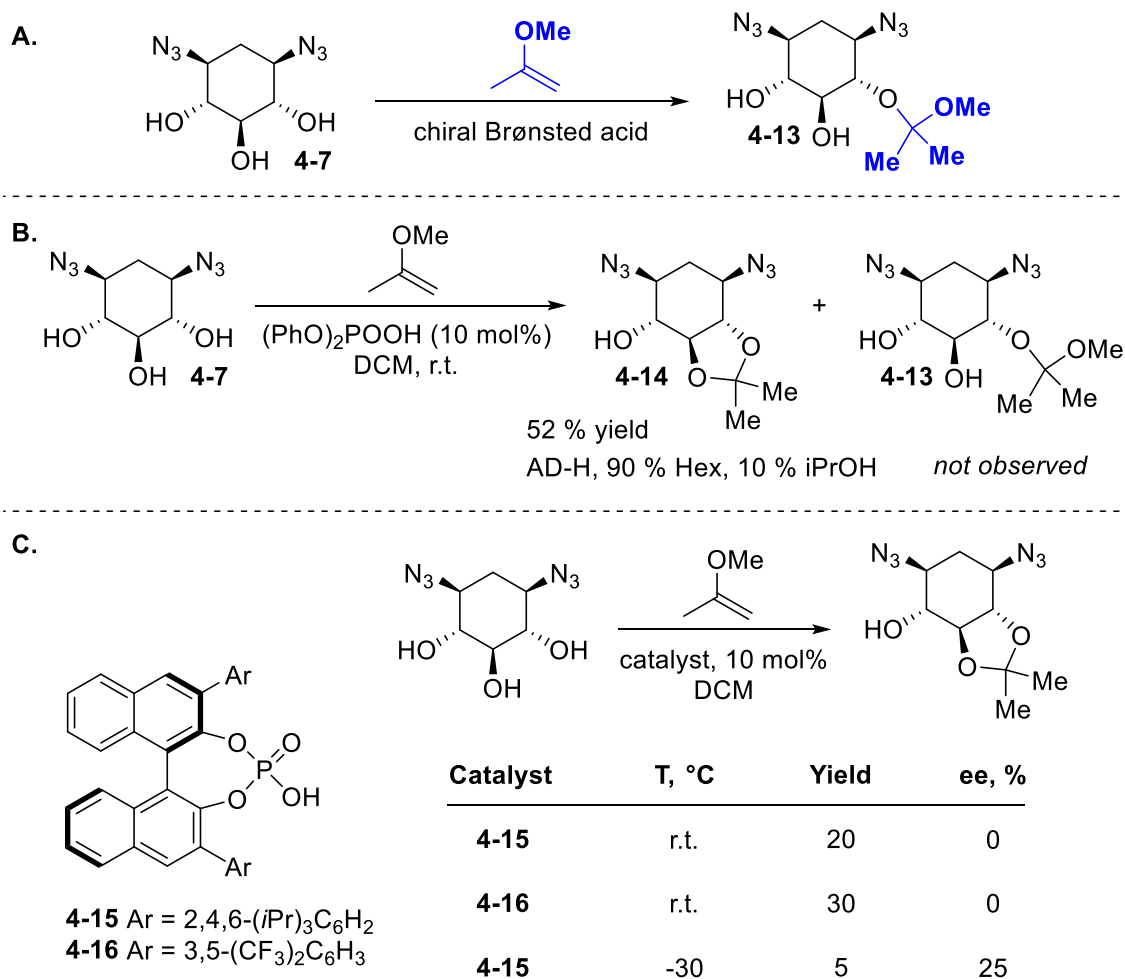
Scheme 4.8 Diazotransfer with imidazole-1-sulfonyl azide



There are several tests available to evaluate the stability of organic azides. The impact sensitivity of energetic compounds is tested with a so-called fall hammer equipment. Samples are exposed to the impact of a falling weight from variable heights and the measured sensitivity parameter is the height at which the samples explode or decompose. The drop test was performed on diazo-2-deoxystreptamine **4-7** and it showed some mild shock sensitivity. Thus, 10 mg of the sample went off when 1 lbs weight was dropped from 145 cm height; however, it did not explode or decompose when the same weight was dropped from 125 cm height. While this test gave us only preliminary data, it became clear that **4-7** has to be treated with caution. Hence, the azide **4-7** has always been stored in desiccated area, in small, up to 200 mg quantities. Differential Scanning Calorimetry (DSC) was also performed. It showed that **6** was not thermally sensitive and had a melting point of 136 °C.

As it was mentioned before, chiral phosphoric acids are able to control regioselective acetalization of chiral diols and enantioselective desymmetrization of *meso*-diols by forming mixed acetals. We decided that chiral phosphoric acids could potentially catalyze formation of mixed acetals (Scheme 4.9 A).

Scheme 4.9 Desymmetrization of **4-7** via acetal formation



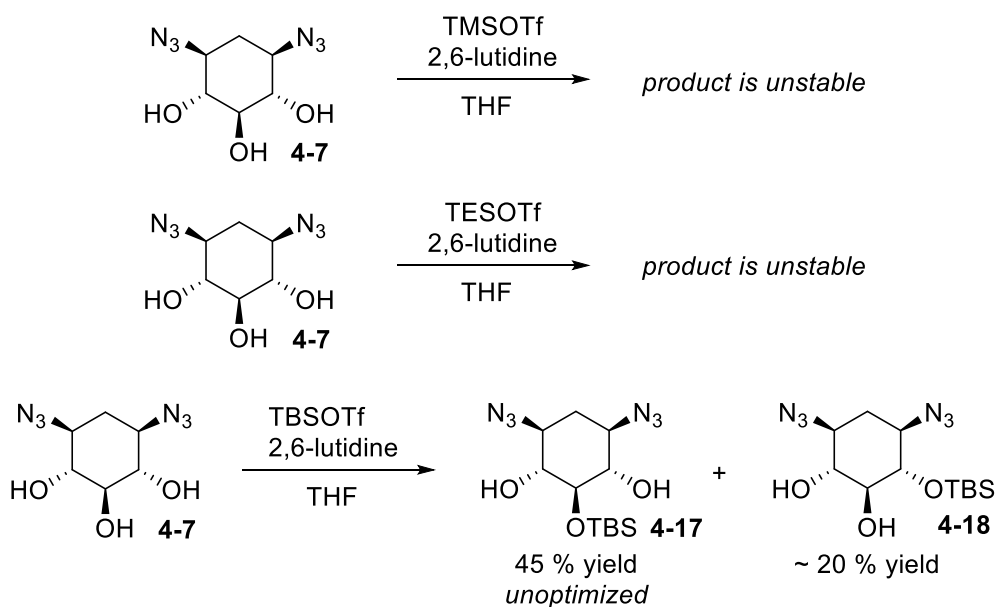
Thus, the studies commenced with evaluation of phosphoric acids in the presence of diazide-2-deoxystreptamine **4-7** and 2-methoxypropene. First, achiral diphenylphosphate was used in order to prepare a racemic standard for the chiral HPLC assay (Scheme 4.9 B). To our surprise, instead of forming a mixed acetal **4-13**, an acetonide **4-14** was formed instead with no traces of acetal **4-13** present in the mixture. Since the reaction produced asymmetric product, we proceeded with evaluation of chiral phosphoric acids under the same reaction conditions. The most common chiral phosphoric acids **4-15** and **4-16** were evaluated. These preliminary results showed that under these conditions

asymmetric acetal **4-13** was still not observed, even at very low conversions. Reactions at room temperature led to formation of racemic acetone **4-14** at reasonably low conversions after stirring the reaction mixture overnight. When the reaction was performed at -30 °C in the presence of 10 mol% of **4-15**, the yield dropped substantially, while enantioselectivity increased only to 25% ee (Scheme 4.9 C). Slow reaction rates were attributed to poor solubility of **4-7**, especially at lower temperatures. Thus, poor conversion and low enantioselectivities suggested that a protecting group on *O*-4 could potentially improve the enantioselectivity of asymmetric acetalization. In addition to that, direct glycosylation reaction studies would benefit from having protection at this position because it would lead to formation of fewer regioisomeric glycosides which would simplify the reaction analysis substantially. Finally, the protection would increase the molecular weight of the bis-azide and thus decrease its shock sensitivity.

Several oxygen protecting groups were considered. The protecting group had to be reasonably non-labile under acidic conditions, as well as it should be possible to put just one protecting group on the middle oxygen, avoiding having a statistical mixture of mono- and bis-protected 2-deoxystreptamine derivatives. Therefore, several silyl protecting groups were evaluated such as TMS, TES and TBS (Scheme 4.10). TMS and TES protection resulted in statistical mixture of *O*-4 and *O*-3 protected positions, as well as some amount of double-protected products. Attempt to isolate either one of those products via column chromatography failed due to decomposition and/or rearrangement of the products. This suggested sufficient acidic instability and both TMS and TES groups were abandoned. On the other hand, TBS protection was rather successful providing *O*-4 protection with 45% yield (unoptimized). Since this diol still had reasonably low carbon

and oxygen to azide ratio, shock and heat sensitivity tests were also performed on it. As before, **4-17** was not heat sensitive based on DSC analysis (m.p. = 110.6 °C). As expected, the TBS protection contributed to increased stability of the compound. The drop test showed that the sample went off only in 30% of the cases when 1 lbs weight was dropped off 145 cm height. Thus, while TBS-protected 2-deoxystreptamine **4-17** is more stable than **4-7**, it still should be handled with great care.

Scheme 4.10 Hydroxyl protection of **4-7**

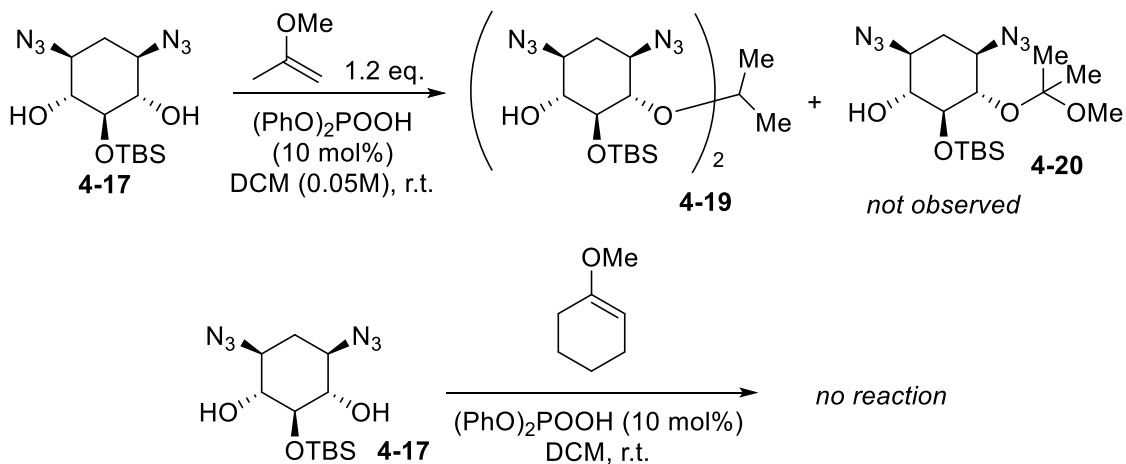


Finally, the acetylation reaction provided full statistical mixture of mono-, bis- and trisprotected 2-deoxystreptamine derivatives that was too complicated to analyze and purify. Attempts to improve the yield for *O*-4 acetylated product were also unsuccessful.

With the TBS-protected diol **4-17** in hand, we resumed our acetalization studies with a hope to develop a faster desymmetrization of a *meso*-2-deoxystreptamine derivative. Since *O*-4 was already protected, we assumed that formation of a mixed acetal **4-20** will

take place in presence of 2-methoxypropene and diphenylphosphate (Scheme 4.11). To our surprise, however, we observed formation of acetonide **4-19** (~10% conversion) resulting from condensation of two diol molecules with one 2-methoxypropene. No formation of mixed acetal **4-20** was observed even at lower concentration or with excess of 2-methoxypropene. An attempt to perform acetalization reaction with 2-methoxycyclohexene was not successful – only starting material was recovered. Since enantioselective desymmetrization of 2-deoxystreptamine did not provide positive preliminary studies, it was decided to attempt desymmetrization via glycosylation of *meso*-2-deoxystreptamine derivatives.

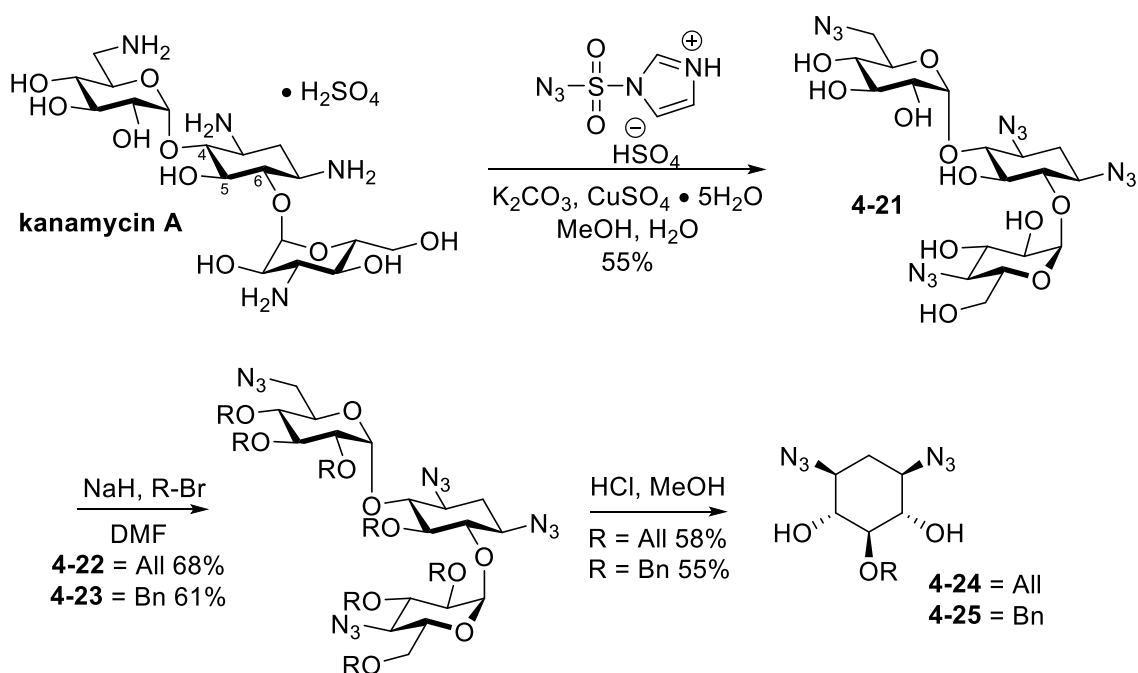
Scheme 4.11 Acetalization of **4-17**



To increase the chances of successful glycosylation studies, we synthesized two additional glycosyl acceptors **4-24** and **4-25** with allyl and benzyl protection at *O*-5 position. To perform regioselective allylation or benzylation of diazido-2-deoxystreptamine, kanamycin A was subjected to diazotransfer, followed by treatment with allyl- or benzylbromide (Scheme 4.12). The resulted modified **4-22** and **4-23** was then hydrolyzed under acidic conditions to produce glycosyl acceptors **4-24** and **4-25**.³⁰ Since

this synthetic pathway proceeds through formation of intermediates and products rich in azide groups, stability tests were also performed. Thus, azidated kanamycin A **4-21**, as well as both allyl and benzyl protected 2-deoxystreptamine **4-24** and **4-25** proved to be both shock and heat insensitive.

Scheme 4.12 Synthesis of allyl and benzyl protected 2-deoxystreptamines



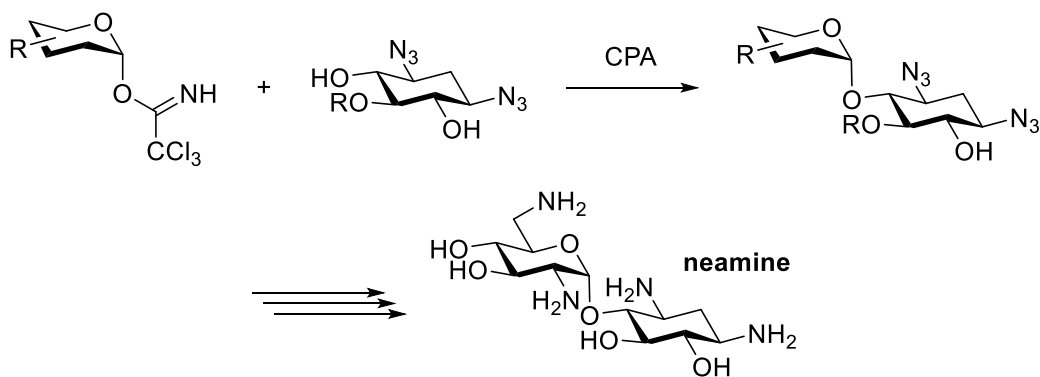
4.4 Design of glycosyl donor for glycosylation studies

Analysis of glycosylation reactions can be rather difficult at times, especially if a glycosyl acceptor molecule contains several free hydroxyl groups. Thus, if a glycosyl acceptor contains three hydroxyl groups, one can expect to produce at least six isomeric disaccharides: three α and three β products plus possibly some amount of trisaccharides resulting from double glycosylation of glycosyl acceptor. If, however, a glycosyl acceptor contains only two hydroxyl groups, the number of possible outcomes reduces down to four

disaccharides with possible addition of trisaccharides. Consequently, it was decided to use *meso*-2-deoxystreptamine-based acceptors with protection at *O*-5 position.

The desymmetrizing glycosylation of *meso*-diols will produce an additional anomeric stereocenter and result in desymmetrization of deoxystreptamine subunit (for clarity we will refer to the latter as “regioselection” in the following discussions). As the determination of the site of glycosylation (i.e. “regioselectivity”) can potentially be challenging, it was decided to first design a glycosyl donor, that upon coupling with 2-deoxystreptamine, would produce a disaccharide that after some protecting group manipulations would produce a natural aminoglycoside or its known derivative. This would allow us to compare the spectroscopic data and unambiguously assign the stereocenters of the glycosylation products. One of the most common glycosyl residues that 2-deoxystreptamine bound to is 2,6-diamino-2,6-dideoxyglucose (Figure 4.1, NEA, Scheme 4.13) with neamine being the simplest aminoglycoside available.

Scheme 4.13 Synthesis of neamine by stereodifferentiation of 2-deoxystreptamine

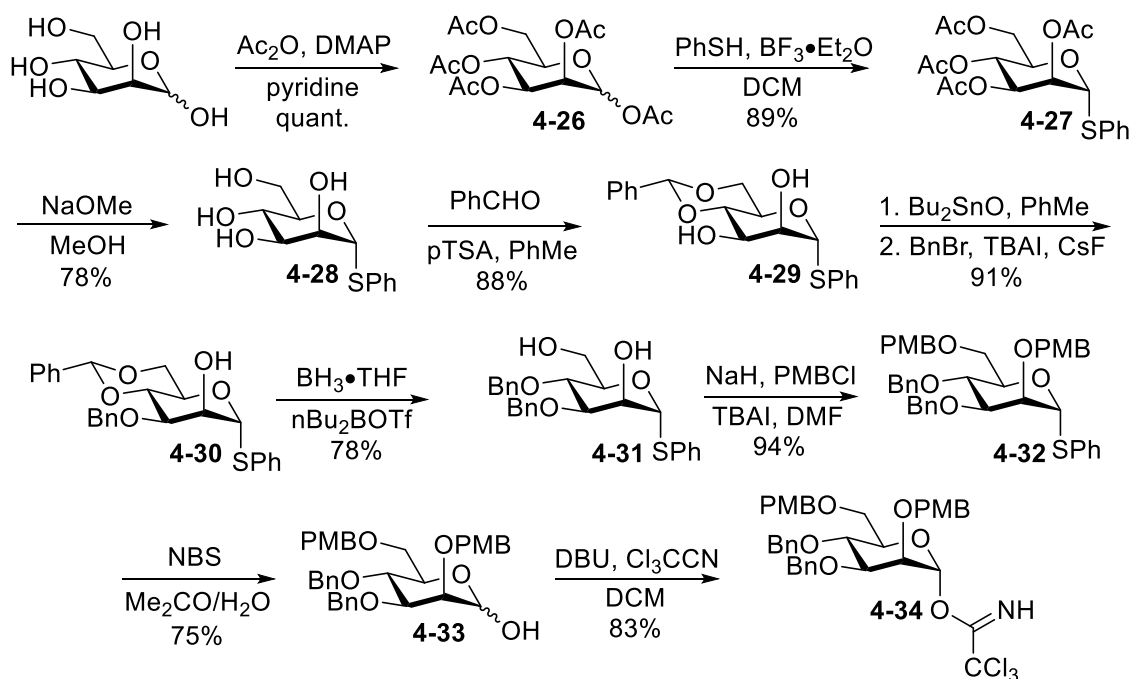


Hence, by looking at the structure of neamine, one can notice several prerequisites for the glycosyl donor. The carbohydrate residue of neamine has amino groups at positions

C-2 and C-6 that should be protected if chiral phosphoric acids will be used as catalysts for glycosylation reaction. In addition, in this case as well as in case of most aminoglycosides, the glycosidic linkage is α . Since 2-azido-2-deoxyglycopyranose donors rarely lead to clean formation of α -glycosides,³¹ we decided against having azides as protecting groups of amines. Mannose trichloroacetimidates, on the other hand, often times lead to rather stereoselective formation of α -disaccharides.^{32,33} Therefore, to accommodate all of the requirements for the glycosyl donor, we decided to design a mannose-based trichloroacetimidate with protecting groups at *O*-2 and *O*-6 orthogonal to protecting groups at *O*-3 and *O*-4. Since previous results showed that electron-withdrawing protecting groups on glycosyl trichloroacetimidates tend to slow down the glycosylation reactions,³⁴ it was decided to use benzyl ethers as protecting groups on alcohols. In this case, *p*-methoxybenzyl and benzyl ethers can be installed on mannose and removed under orthogonal to each other conditions.³⁵

The synthesis of trichloroacetimidate **4-34** commenced with full acetyl protection of mannose, followed by anomeric substitution with thiophenol in the presence of boron trifluoride, and deprotection of acetates with sodium methoxide. The resulting tetraol **4-28** was protected with benzylidene acetal. The resulting acetal **4-29** was regioselectively benzylated through the formation of tin acetal.³⁶ Next, 4,6-benzylidene functionality of **4-30** could be reduced by borane/THF complex in the presence of dibutylboron triflate.³⁷ Resulting diol **4-31** was then protected with PMB groups. Finally, hydrolysis of the anomeric sulfide **4-32** in the presence of *N*-bromosuccinimide, followed by treatment with trichloroacetonitrile and catalytic amounts of DBU resulted in desired α -trichloroacetimidate **4-34** with small amount of β anomer present ($\alpha/\beta = 10:1$).

Scheme 4.14 Synthesis of glycosyl donor



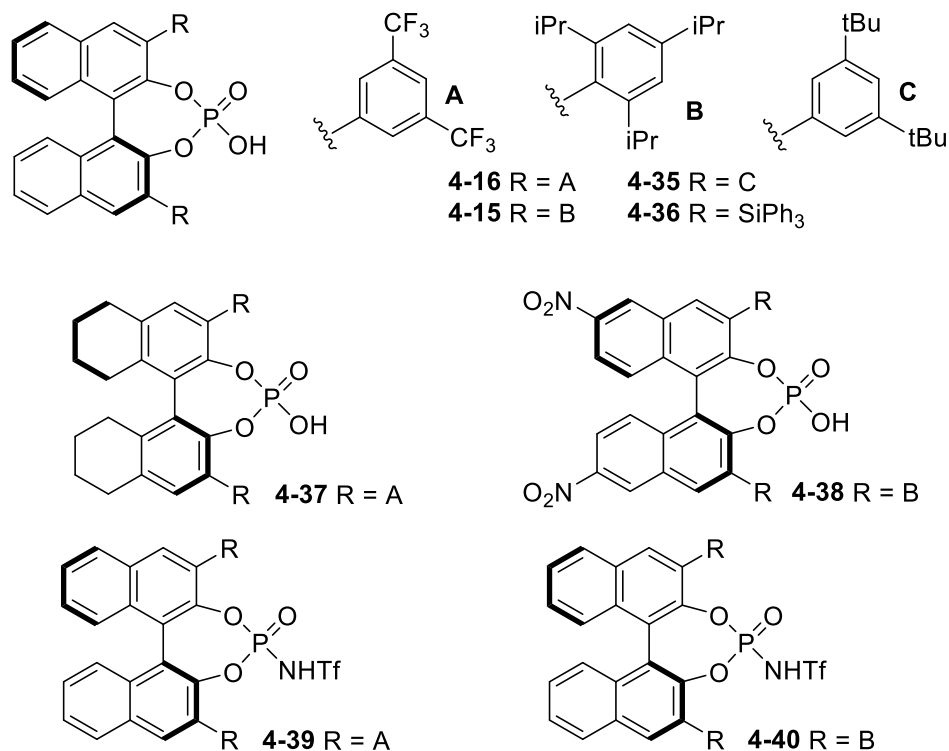
4.5 Glycosylation studies

The investigation of glycosylative coupling between mannose trichloroacetimidate **4-34** and diazido-2-deoxystreptamine **4-17** began with evaluation of chiral phosphoric acids and their derivatives (Figure 4.4).

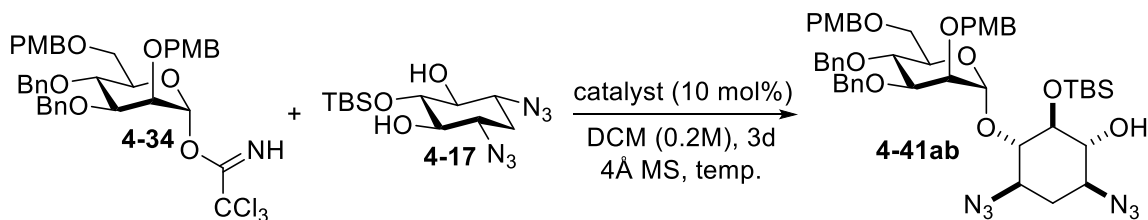
The glycosyl donor **4-34** (1.2 – 2 eq.) was combined with a glycosyl acceptor **16**, activated 4 Å MS, and 10 mol% of a catalyst, and the formation of glycosides was monitored by NMR. The studies commenced with evaluation of CF_3 -based chiral phosphoric acids (*S*)-**4-16** and (*R*)-**4-16**. In both cases two glycosylated products were produced (Table 4.1, entries 1–4) that upon careful NMR analysis were determined to be both α anomers.³⁸ This result suggested formation of two regioisomeric products. Interestingly, 1:2 regioselectivity was observed when reaction was catalyzed with (*S*)-**4-16**

and it was reversed when the enantiomer of the catalyst was used. Unfortunately, the phosphoric acids with lacking the electron-withdrawing groups on their backbones failed to produce any glycosylated product by either promoting decomposition of the glycosyl donor to glycal (Table 4.1, entry 3), or by not catalyzing the reaction at all, (entries 6 – 8). Additionally, hydrogenation of the BINOL residue was found to negatively affect the regioselectivity (entry 9). While it became obvious that we were rather limited in the use of BINOL scaffolds, CPAs (*S*)-**4-16** and (*R*)-**4-16** provided two regioisomeric products with reverse selectivities when enantiomers of the CF₃-based catalyst were used. This prompted us to investigate other strong chiral Brønsted acids such as nitrated CPA (*S*)-**4-38** (entry 10) or *N*-triflylphosphoramides **4-39** and **4-40** (entries 11 and 12). While nitration of a chiral phosphoric acid did not result in dramatic increase in the catalyst activity, use of chiral *N*-triflylphosphoramides resulted in formation of glycosylated products. Unfortunately, in the case of TRIP-based *N*-triflylphosphoramide **4-40** (entry 12), we observed unselective formation of all four products (α - and β - regioisomers). In the case of CF₃-based *N*-triflylphosphoramide **4-39** though, the glycosylation resulted in slightly reduced regioselectivity. It is important to note that all glycosylation reactions were always accompanied by some formation of glycal, usually in the amount of 30% relative to glycosylated products. In addition, reaction with TMSOTf in DCM at -30 °C resulted in unselective formation of all four glycosylation products. These results prompted us to reinvestigate other chiral phosphoric acids before advancing to more complex and difficult to synthesize *N*-triflylphosphoramides.

Figure 4.4 Chiral Brønsted acids used in catalyst screening



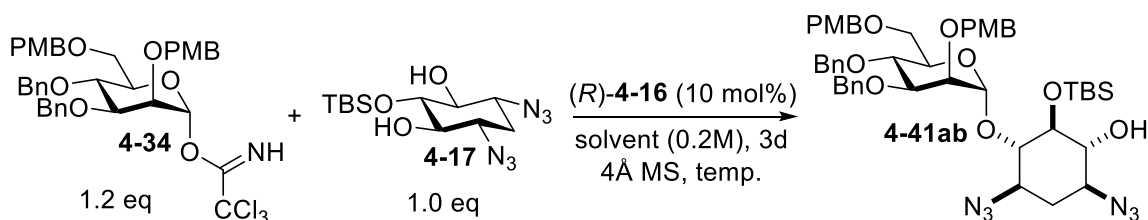
To improve the yield and regioselectivity, we performed evaluation of different parameters of the reaction conditions. Thus, glycosylation yields could be improved if 2 equivalents of the glycosyl donor are used instead of 1.2. In addition, the use of the higher reaction temperature did not reduce the regioselectivity significantly, but resulted in a better conversion. The reaction conversions can be further improved if the reaction is refluxed for a prolonged period of time (2 equivalents of donor, 5 days at reflux in DCM give 50% conversion).

Table 4.1 Preliminary catalyst screening

Entry	Catalyst	<i>T</i> , °C	Conversion, % ^b	Regioselectivity
1	(<i>S</i>)- 4-16	r.t.	< 15	1 : 2
2	(<i>R</i>)- 4-16	r.t.	< 15	2 : 1
3	(PhO) ₂ POOH	r.t.	Decomposition	
4	(<i>S</i>)- 4-16	40	22	1 : 2.4
5	(<i>R</i>)- 4-16	40	22	1.8 : 1
6	(<i>R</i>)- 4-15	40	No rxn	
7	(<i>R</i>)- 4-35	40	No rxn	
8	(<i>R</i>)- 4-36	40	No rxn	
9	(<i>S</i>)- 4-37	40	18	1 : 1.25
10	(<i>S</i>)- 4-38	40	No rxn	
11	(<i>S</i>)- 4-39	40	60	1 : 1.8
12 ^a	(<i>S</i>)- 4-40	40	30	1 : 1

^a The reaction produced equal amounts of β anomer. ^b Conversions are based on NMR peak integrations of the product to the glycosyl acceptor

In addition to that, we also performed a preliminary solvent screening. The screening was executed with 1.2 equivalents of glycosyl donor, 10 mol% (*R*)-**4-16**, at 40°C. While glycosylation in toluene, CCl₄ and hexanes was somewhat faster, regioselectivity dropped significantly either producing two α -regioisomers with 1:1 ratio (Table 4.2, entry 2) or producing all α - and β -regioisomers (entries 4, 5). Reaction in THF was unacceptably slow, however surprisingly enough it produced a mixture of two α -regioisomers with reverse selectivity to what was expected. This phenomenon should be further investigated.

Table 4.2 Solvent screening

Entry	Solvent	Conversion, %	Regioselectivity
1	DCM	22	1.8 : 1
2	PhMe	40	1.03 : 1
3	THF	4	1 : 1.63
4 ^a	CCl ₄	40	unselective
5 ^a	hexanes	24	unselective

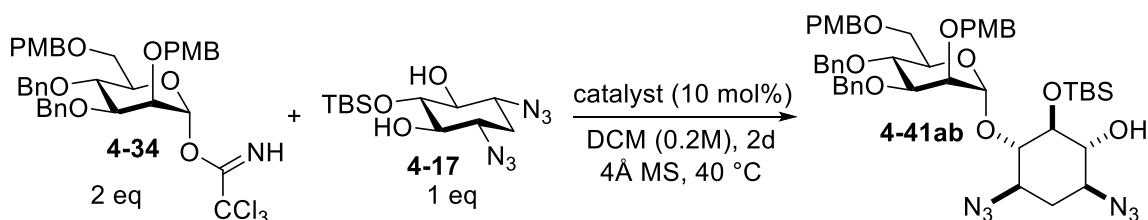
^a The reaction produced equal amounts of β anomer. ^b Conversions are based on NMR peak integrations of the product to the glycosyl acceptor

Typical glycosylation reactions of trichloroacetimidate donors catalyzed with chiral phosphoric acids have rather fast reaction rates with reaction times ranging from 10 hours to 48 hours at temperatures below zero with 15 mol% catalyst loading.^{23,24} Reaction rates in case of 2-deoxystreptamine are surprisingly low. Hypothesizing that the glycosyl acceptor might be too sterically hindered, allyl and benzyl protected 2-deoxystreptamines (**4-24** and **4-25** respectively) were tested under standard glycosylation conditions. Benzyl protected acceptor **4-24** was poorly soluble in DCM, leading to even slower glycosylation rates. Surprisingly, smaller in size allyl protected acceptor **4-25** was approximately as reactive as **4-17**. Unfortunately, analysis of the mixture of glycosylation products was complicated by the overlapped anomeric ¹H NMR peaks. While we could not interpret the outcomes of glycosylations with **4-24** and **4-25**, we concluded that poor reactivity of glycosyl acceptor was not due to steric hindrance. We hypothesize that intramolecular hydrogen bonding in 2-deoxystreptamine donors is responsible for the low nucleophilicity

the of oxygen atoms. This hypothesis also explains poor reactivity observed in stereoselective acetalization reactions of 2-deoxystreptamine (*vide supra*).

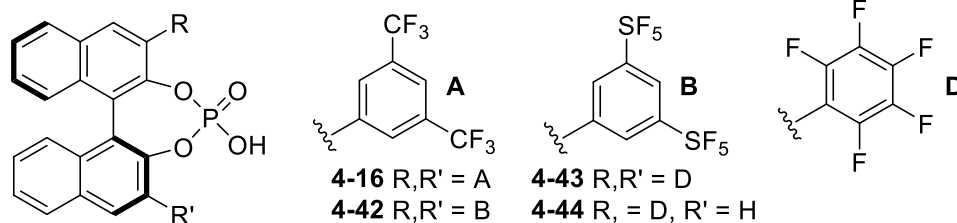
At this point more chiral phosphoric acids with electron-withdrawing became available. Thus, catalysts **4-42** – **4-44** were evaluated. As expected, SF₅-based chiral phosphoric acid was more reactive and provided much higher conversion after two days than its CF₃ analog. Additionally, the (*S*) enantiomer of **4-42** also provided higher selectivity, while (*R*) enantiomer on the contrary led to reduction of regioselectivity. This result suggests that in fact it is a matching/mismatching case between the chiral catalyst and chiral glycosyl donor. C₆F₅-Based chiral phosphoric acids **4-43** and **4-44** confirmed this hypothesis providing higher regioselectivities when (*S*) enantiomer of CPA was used and lower when the reaction was catalyzed with (*R*) CPA.

Based on these data SF₅-based CPA (*S*)-**4-42** was chosen as the most selective and reactive catalyst and further optimization studies were done with it. The reaction can be run for 5 days providing the mixture of two glycosides with 1:5 selectivity and 88% conversion. Purification by column chromatography results in 78% yield of a glycosidic mixture of 1:4 – 1:3 with some amount of major regioisomer being lost along the way. A great care should be taken to purify the diglycosides from the glycal byproduct due to their extremely similar R_f values. Additionally, 4Å molecular sieves seem not to have any great effect on either selectivity of yield of the diglycosides.

Table 4.3 Additional catalyst screening

Entry	Catalyst	Conversion, % ^a	Regioselectivity
1	(<i>S</i>)- 4-16	25	1 : 2.2
2	(<i>R</i>)- 4-16	25	1.8 : 1
3	(<i>S</i>)- 4-42	67	1 : 5
4	(<i>R</i>)- 4-42	61	1.3 : 1
5	(<i>S</i>)- 4-43	22	1 : 2.9
6	(<i>R</i>)- 4-43	22	1.4 : 1
9	(<i>S</i>)- 4-44	17	1 : 2.8
10	(<i>R</i>)- 4-44	12	1 : 1
11 ^b	(<i>S</i>)- 4-42	88 (78) ^c	1 : 5

^aConversions are based on NMR peak integrations of the product to the glycosyl acceptor; ^b5 days; ^cIsolated yield

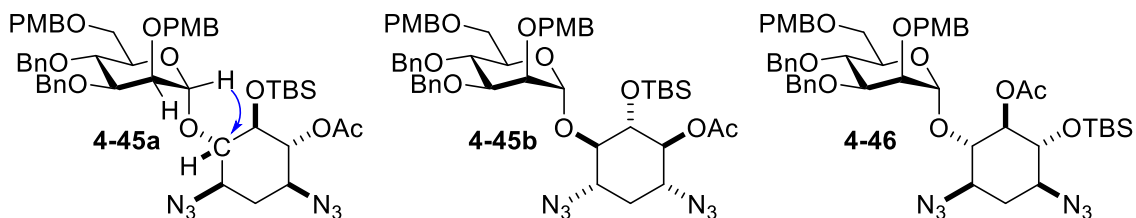


4.6 NMR analysis of diglycosides

In order to optimize the glycosylation reaction conditions, several additional experiments with higher concentration and catalyst loading were performed. Interestingly, when the reaction was performed in 0.5 M DCM, no previously observed glycosylation products **4-41ab** were observed. Instead, another glycosylated product was isolated that had the same molecular weight and very similar ¹H NMR pattern.

The anomeric configuration of the new diglycoside was determined by observing $^1J_{C-H}$ coupling constant between the anomeric hydrogen and carbon. Typical coupling constants for α -mannosides are around 170 Hz, while coupling constants for β -mannosides are usually 160 Hz. All three isomeric diglycosides showed coupling constants above 170 Hz (174.3 and 170.6 for typical products). This suggested formation of a third glycoside with α configuration at the anomeric position. Since glycosyl acceptor **4-17** contains only two free hydroxyl groups, we suspected that a rearrangement of either product or the starting material happened. Because 1H , COSY, HSQC and HMBC – based analysis of the three glycosides was inconclusive, acetylation of the residual hydroxyl group was performed. Using the HMBC and HSQC NMR techniques we were able to establish the connectivity between the mannose residue and 2-deoxystreptamine, while COSY 2D NMR analysis was used to determine connectivity of all groups on 2-deoxystreptamine residue. Thus, it was determined that the regularly observed glycosylation products have expected substitution pattern (**4-45a** and **4-45b**). However, the new disaccharide **4-46** had a TBS group shifted from *O*-5 to the neighboring oxygen atom.

Figure 4.5 Regioisomeric diglycosides



This rearranged product (**4-46**) has been occasionally observed in up to 5% in reactions under normal reaction conditions. However, the attempts to optimize the TBS rearrangement unfortunately were unsuccessful. Additionally, refluxing glycosyl acceptor

4-17 or the mixture of **4-41a** and **4-41b** in the presence of 10 mol% of SF₅-CPA (**4-42**) did not facilitate TBS shift nor change in regioisomeric ratio.

In addition to $^1J_{(C,H)}$ coupling constants, $^3J_{(C,H)}$ coupling constants can also be observed. Anomeric hydrogen of a conformationally rigid mannoside forms a dihedral angle with C-3 which corresponds to 180° in case of α -mannoside, and about 60° for β -mannoside. Hence, Karplus relationship can be used for stereochemical assignment of the resulting disaccharide system³⁹ (~8 Hz and 3 Hz $^3J_{(C,H)}$ coupling constants respectively).⁴⁰ Direct measurement of $^3J_{(C,H)}$ using ¹³C NMR is difficult due to low method sensitivity which is further complicated with low signal/noise ratio due to coupling of the signal. Analysis of carbohydrate molecules using such method is practically impossible due to the overlap or close arrangement of the ¹³C signals.

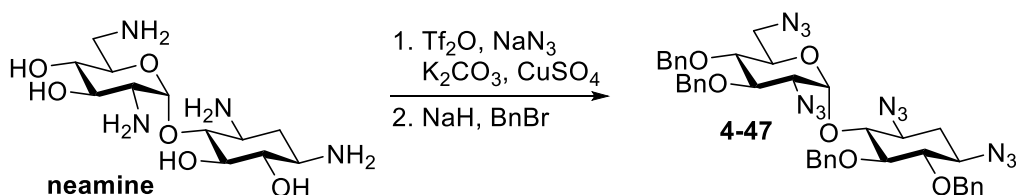
HMBC experiment can be used for indirect observation of $^3J_{(C,H)}$ coupling constants. Modification of the pulse sequences in the HMBC experiment allows selective discrimination of the signals based on their (C,H) coupling constants. Since HMBC is measured in the magnitude mode, signal intensity directly correlates to the conformity between the indirect spin-spin coupling constants and the filter value. Standard HMBC pulse sequence includes two low pass filters which are responsible for filtration of signals that correspond to $^1J_{(C,H)}$ coupling constants (default setting 135 – 170 Hz) and inclusion of signals with $^{2-4}J_{(C,H)}$ coupling constants (default setting 8 Hz).⁴¹ Thus, changing the pulse delay time, and analyzing the intensity of the cross peaks in HMBC spectrum one can obtain necessary information about stereochemical configuration of a molecule or its fragment.

The HMBC experiments were performed with the help of Dr. Iaroslav Khomutnyk. Gradient selected multiple bond correlation with adiabatic pulses (*g*HMBCAD) pulse sequence was used. The necessary sensitivity was achieved by using non-uniform sampling method (NUS). The experiments were run using two *J*_{HNx} filter values which correspond to 8 Hz (default) and 3 Hz (custom) coupling constants. The filter values were calculated using simplified formula $J_{HNx} \text{ (ms)} = \frac{1}{2} * J$, and were equal to 62.5 and 166.7 ms correspondingly. Thus, when both **4-48a** and **4-52** (perbenzylated **4-48b**) were analyzed using *g*HMBCAD (62.5 ms) the crosspeaks between anomeric hydrogen and C-3 were observed, while the same experiment with 166.7 ms delay time showed no crosspeaks in that region (See Appendix C). This confirms the previously made assignment of **4-45a** and **4-45b** both being α -mannosides.

4.7 Synthesis of neamine

In order to unambiguously assign the regio- and stereoselectivity of the resulting glycosides, we attempted the synthesis of synthetically modified neamine (Scheme 4.15) that has been previously reported, from glycosidic mixture of **4-41a** and **4-41b**.

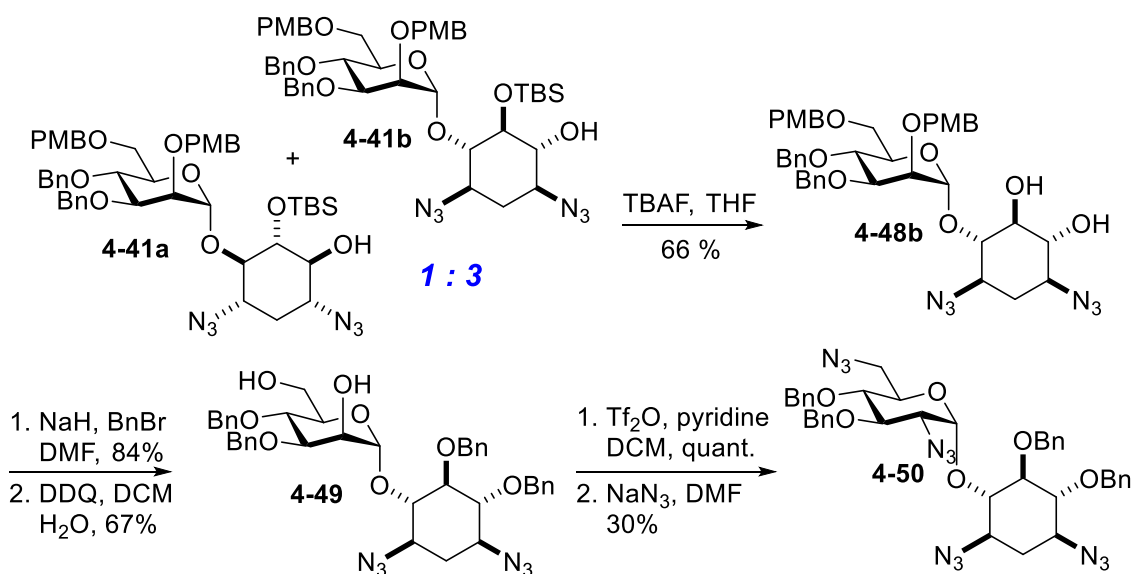
Scheme 4.15 Synthesis of perbenzyl-, perazidoneamine



To access neamine **4-47**, the 1:3 glycosidic mixture was subjected to TBAF in order to deprotect TBS group (Scheme 4.16). The resulting mixture of regioisomeric diols was separated and the major regioisomer was benzylated, followed by deprotection of PMB

groups with DDQ. Diol **4-49** was then tosylated and tosyl groups were inverted with sodium azide to yield **4-50**. While having the desired molecular weight, ^1H NMR of glycoside **4-50** did not match previously published spectra⁴² for natural neamine **4-47**. The resulting NMR data suggests that (*S*)-**4-42** leads to formation of two regioisomeric glycosides **4-41a** and **4-41b** with the ratio of 1:5 respectively.

Scheme 4.16 Semisynthesis of neamine and structural assignment



4.8 Conclusions

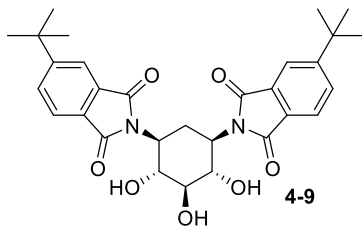
In conclusion, we were able to show that chiral phosphoric acids facilitate desymmetrization of *meso*-diols via glycosylation reactions using mannose- α -trichloroacetimidate **4-34**. Chiral phosphoric acids typically produce a mixture of two α -glycosides. While (*R*)-enantiomer typically leads to glycosylation of 2-deoxystreptamine derivative **4-17** with modest regioselectivities and a major regioisomer having glycosylation at *O*-4 (natural) of 2-deoxystreptamine, (*S*)-enantiomer favors glycosylation at *O*-6 with selectivities up to 1:5 (*O*-4 : *O*-6). This is the first report of desymmetrization

of *meso*-diols via glycosylation using chiral phosphoric acids as catalysts. This method has a potential to be applied for glycodiversification of 2-deoxystreptamine and synthesis of new aminoglycoside antibiotics.

4.9 Experimental

Unless otherwise stated, all reagents were purchased from commercial suppliers and used without purification. Toluene (PhMe), dichloromethane (CH₂Cl₂) and diethyl ether (Et₂O) were filtered through a column (Innovative Technology PS-MD-5) of activated alumina under nitrogen atmosphere. All reactions were carried out under an atmosphere of nitrogen in flame- or oven-dried glassware with magnetic stirring. Reactions were cooled via external cooling baths: ice water (0 °C), Neslab Cryotrol CB-80 immersion cooler (0 to -60 °C) or Neslab Cryocool immersion cooler CC-100 II. Purification of the reactions mixtures was performed by flash chromatography using SiliCycleSiliaFlash P60 (230-400 mesh) silica gel. All spectra were recorded on Varian vnmrs 700 (700 MHz), Varian vnmrs 500 (500 MHz), Varian MR400 (400 MHz), Varian Inova 500 (500 MHz) spectrometers and chemical shifts (δ) are reported in parts per million (ppm) and referenced to the ¹H signal of the internal tetramethylsilane according to IUPAC recommendations.⁴³ Data are reported as (br = broad, s = singlet, d = doublet, t = triplet, q = quartet, qn = quintet, sext = sextet, m = multiplet; coupling constant(s) in Hz; integration). High resolution mass spectra (HRMS) were recorded on MicromassAutoSpecUltima or VG (Micromass) 70-250-S Magnetic sector mass spectrometers in the University of Michigan mass spectrometry laboratory. Infrared (IR) spectra were recorded as thin films on NaCl plates on a Perkin Elmer Spectrum BX FT-IR spectrometer. Absorption peaks were reported in wavenumbers (cm⁻¹).

Preparation of 2-deoxystreptamine derivatives



2,2'-((1R,3S,4R,5r,6S)-4,5,6-trihydroxycyclohexane-1,3-diyl)bis(5-(tert-butyl)isoindoline-1,3-dione) (4-9)

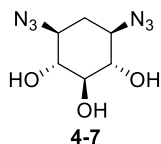
100 mg (0.22 mmol) of 2-deoxystreptamine dihydrogenbromide⁴⁴ was mixed with 100 mg (4.49 mmol)

of 5-(tert-butyl)isobenzofuran-1,3-dione, followed by addition of pyridine (0.74 mL) and trimethylamine (0.14 mL). The resulting mixture was stirred at 100 °C overnight. The reaction mixture was cooled down, diluted with ethyl acetate and 1M solution of copper(II) sulfate. The product was extracted with ethyl acetate. The extracts were washed with copper(II) sulfate until light blue color of organic layer. Organic layer was dried with magnesium sulfate. The crude mixture was separated by column chromatography (3:2 hexanes/ethyl acetate) (75.1 mg, 51% yield).

The desired product was then suspended in methanol and to that ~1 mg of sodium hydride was added. The resulting suspension was stirred for 1 hour at room temperature. The mixture was then quenched with a drop of 1M HCl, and volatiles were removed in vacuo. Column chromatography (4:1 hexanes/ethyl acetate) resulted in 44.9 mg (74%) of white solid.

IR (thin film, cm^{-1}): 3472 (br), 2964, 2254, 1770, 1714, 1622, 1431, 1365, 1222, 1110, 919, 734. ^1H NMR (500 MHz, CDCl_3) δ 7.88 (s, 2H), 7.78-7.70 (m, 4H), 4.51 (t, $J = 9.6$ Hz, 2H), 4.31 (m, 2H), 3.52 (t, $J = 9.6$ Hz, 1H), 3.18 (q, $J = 12.8$ Hz, 1H), 2.96 (s, 1H), 2.54 (s, 2H), 1.90 (td, $J = 4.2, 12.8$ Hz, 1H), 1.37 (s, 18H). ^{13}C NMR (175 MHz, CDCl_3) δ 168.9,

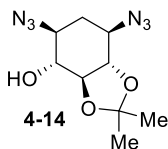
168.5, 158.9, 132.0, 131.2, 129.2, 123.4, 120.8, 78.0, 71.3, 51.3, 35.9, 31.3, 28.8; HRMS (ESI+) (m/z): $[M+H]^+$ calcd for $C_{30}H_{35}N_2O_7$ 535.2439, found 535.2439.



(1R,2r,3S,4R,6S)-4,6-diazidocyclohexane-1,2,3-triol (4-7)

2-Deoxystreptamine • 2HBr (324 mg, 1.0 mmol) was mixed together with potassium carbonate (650.9 mg, 2.4 mmol) and copper (II) sulfate pentahydrate (677.2 mg, 4.9 mmol). The resulting mixture was suspended in 1:1 mixture of methanol and water (10 mL) followed by careful addition of 1H-imidazole-1-sulfonyl azide • H_2SO_4 (650.9 mg, 2.4 mmol). The resulting crude mixture was refluxed overnight, then solvents were evaporated in vacuo. Resulting crude product was suspended in methanol/dichloromethane mixture and solids were filtered off, when washed with methanol/dichloromethane and acetone. Resulting filtrate was concentrated, and the product was purified by column chromatography (1:1 dichloromethane/acetone). The procedure resulted in white crystalline solid (110 mg, 52% yield). The 1H NMR data coincide with the previous report.⁴⁵

1H NMR (400 MHz, CD_3OD) δ 3.42-3.33 (m, 2H), 3.25-3.20 (m, 3H), 2.09 (dt, $J = 13.0$ Hz, 4.5 Hz, 1H), 1.24 (q, $J = 13.0$ Hz, 1H).

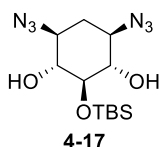


***rac*-(3aS,4R,5S,7R,7aS)-5,7-diazido-2,2-dimethylhexahydrobenzo[d][1,3]dioxol-4-ol**

(1R,2r,3S,4R,6S)-4,6-diazidocyclohexane-1,2,3-triol (**4-7**) (50.0 mg, 0.233 mmol) and diphenylphosphate (5.8 mg, 0.0233 mmol) were mixed in an oven-dried 10 mL flask, and flushed with N_2 , to which DCM (5.8 mL) was added, followed by 2-methoxypropene (26.8 μ L, 0.280 mmol). The reaction was left overnight, then quenched

with trimethylamine, and volatiles were evaporated. Column chromatography (4:1 to 1:1 hexanes/ethyl acetate) resulted in 41.5 mg of white solid. The ^1H NMR data coincide with the previous report.⁴⁶ Chiral assay: AD-H column, 90% hexanes, 10% isopropanol, 7.4 and 9.2 min retention times.

^1H NMR (400 MHz, CDCl_3) δ 3.79-3.61 (m, 2H), 3.45-3.36 (m, 3H), 2.55 (s, 1H), 2.34 (dt, $J = 13.8, 5.1$ Hz, 1H), 1.50 (q, $J = 13.8$ Hz, 1H), 1.47 (s, 6H).



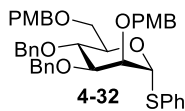
(1R,2r,3S,4R,6S)-4,6-diazido-2-((tert-butyldimethylsilyl)oxy)-cyclohexane-1,3-diol (4-17)

(1R,2r,3S,4R,6S)-4,6-diazidocyclohexane-1,2,3-triol (**4-7**) (0.770 mg, 3.27 mmol) was dissolved in 33 mL of dry THF under nitrogen, and cooled

down to 0 °C. To that solution 2,6-lutidine (1.51 mL, 13.1 mmol) and TBSOTf (1.66 mL, 7.2 mmol) were added dropwise. The reaction mixture was warmed up to room temperature and quenched with methanol after 3 hours. Column chromatography (10:1 hexanes/ethyl acetate) resulted in 964 mg of white crystalline material. The ^1H NMR data coincide with the previous report.

^1H NMR (400 MHz, C_6D_6) δ 2.97 (t, $J = 9.7$ Hz, 1H), 2.75 (td, $J = 9.7, 3.6$ Hz, 2H), 2.52 (ddd, $J = 12.5, 9.7, 4.5$ Hz, 2H), 1.42 (td, $J = 12.5, 4.5$ Hz, 1H), 0.93 (s, 9H), 0.81 (q, $J = 12.5$ Hz, 1H), 0.11 (s, 6H).

Preparation of mannose trichloroacetimidate

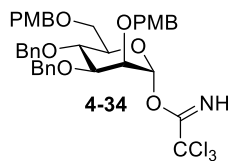


(2R,3R,4S,5S,6R)-3,4-bis(benzyloxy)-5-((4-methoxybenzyl)oxy)-2-(((4-methoxybenzyl)oxy)methyl)-6-(phenylthio)tetrahydro-2H-pyran (4-32)

An oven dried and N₂ flushed 250 mL round bottom flask was charged with 783 mg (1.73 mmol) of (2R,3S,4R,5R,6R)-4,5-bis(benzyloxy)-6-(hydroxymethyl)-2-(phenylthio)tetrahydro-2H-pyran-3-ol (**4-31**) and anhydrous DMF (15 mL). This mixture was cooled to 0 °C and sodium hydride (60%, 280 mg, 6.921 mmol) was added portion wise over 20 min period. When the evolution of H₂ has stopped, *p*-methoxybenzyl chloride (0.82 mL, 6.055 mmol) was added dropwise followed by TBAI (64 mg, 0.173 mmol). The reaction was stirred at room temperature overnight. Then the reaction was cooled to 0 °C and 3 mL of methanol was added dropwise, followed by addition of 50 mL of water. Organics were extracted with diethyl ether. Organic layer was washed with water, and then dried with magnesium sulfate. The product was purified by column chromatography (5:1 to 3:1 hexanes/ethyl acetate) resulting in 1.04 g (87%) of colorless oil.

IR (thin film, cm⁻¹): 3061, 3001, 293, 2865, 2059, 1884, 1756, 1612, 1585, 1248, 1097, 1034, 820, 698. ¹H NMR (700 MHz, CDCl₃) δ 7.45-7.42 (m, 2H), 7.35-7.33 (m, 2H), 7.30-7.23 (m, 13H), 7.18 (d, *J* = 7.1 Hz, 2H), 6.81 (t, *J* = 8.2 Hz, 4H), 5.58 (d, *J* = 1.5 Hz, 1H), 4.89 (d, *J* = 10.7 Hz, 1H), 4.67 (d, *J* = 11.7 Hz, 1H), 4.6-4.54 (m, 4H), 4.50 (d, *J* = 10.7 Hz, 1H), 4.41 (d, *J* = 11.7 Hz, 1H), 4.25 (ddd, *J* = 9.7, 5.0, 1.6, 1H), 4.04 (t, *J* = 9.7 Hz, 1H), 3.99-3.97 (m, 1H), 3.85-3.80 (m, 2H), 3.78 (s, 3H), 3.77 (s, 3H), 3.70 (dd, *J* = 11.0, 1.6 Hz, 1H). ¹³C NMR (175 MHz, CDCl₃) δ 159.4, 159.2, 138.6, 138.4, 134.6, 131.7, 130.6, 130.0, 129.7, 129.6, 129.1, 128.5, 128.4, 128.1, 127.9, 127.8, 127.7, 127.4, 113.9,

113.8, 85.9, 80.2, 75.7, 75.3, 75.1, 73.0, 72.9, 72.1, 71.6, 68.8, 55.4, 55.3, 31.7. HRMS (ESI+) (m/z): $[M+Na]^+$ calcd for $C_{26}H_{28}O_5SNa$ 710.3146, found 710.3122.



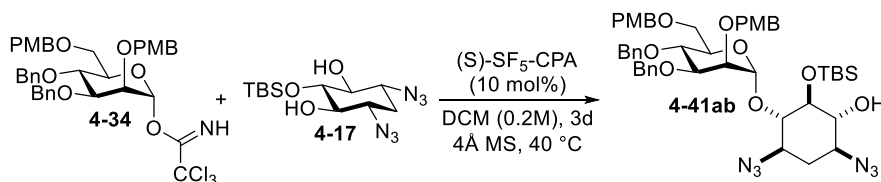
(2R,3S,4S,5R,6R)-4,5-bis(benzyloxy)-3-(((4-methoxybenzyl)oxy)-6-(((4-methoxybenzyl)oxy)methyl)tetrahydro-2H-pyran-2-yl 2,2,2-trichloroacetimidate (4-34)

A 250 mL round bottom flask was charged with (2R,3R,4S,5S,6R)-3,4-bis(benzyloxy)-5-(((4-methoxybenzyl)oxy)-2-(((4-methoxybenzyl)oxy)methyl)-6-(phenylthio)tetrahydro-2H-pyran (**4-32**) and dissolved in a 9:1 mixture of acetone and water. This mixture was cooled to 0 °C and NBS (540 mg, 3.01 mmol) was added. The reaction mixture was monitored by TLC and upon reaction completion it was quenched with solid sodium carbonate. Volatiles were removed in vacuo and organics were extracted with ethyl acetate. The combined organic layer was washed with saturated sodium bicarbonate, then brine, then dried with magnesium sulfate. The crude product was purified by column chromatography (2:1 to 1:1 hexanes/ethyl acetate) resulting in 700 mg (81%) of colorless oil ($\alpha/\beta = 2:1$).

An oven dried and nitrogen flushed 250 mL round bottom flask was charged with mannose from the previous step (**4-33**) (700 mg, 1.165 mmol) and dry DCM (7.8 mL). This mixture was cooled to 0 °C and trichloroacetonitrile (0.35 mL, 3.49 mmol) was added, followed by DBU (87 μ L, 0.583 mmol). The resulting reaction mixture was warmed to room temperature and stirred for 6 hours. The crude product was purified by column chromatography (5:1 to 3:1 hexanes/ethyl acetate) resulting in the pure product as pale-yellow oil (0.529 mg, 61%, $\alpha/\beta = 20:1$).

IR (thin film, cm^{-1}): 3473, 2928, 1723, 1612, 1514, 1454, 1363, 1249, 1108, 1035, 836, 698. ^1H NMR (700 MHz, C_6D_6 , α only) δ 8.47 (s, 1H), 7.33-7.28 (m, 4H), 7.26 (d, $J = 7.4$ Hz, 2H), 7.22 (d, $J = 8.9$ Hz, 2H), 7.16-7.11 (m, 4H), 7.08 (d, 7.0 Hz, 2H), 6.79-6.72 (m, 5H), 5.00 (d, $J = 11.0$ Hz, 1H), 4.65 (d, $J = 11.0$ Hz, 1H), 4.61-4.57 (m, 3H), 4.57-4.51 (m, 3H), 4.39 (d, $J = 11.7$ Hz, 1H), 4.27 (dd, $J = 9.6, 3.4$ Hz, 1H), 4.16 (dd, $J = 9.6, 3.1$), 4.03 (t, $J = 2.5$ Hz, 1H), 3.89 (dd, $J = 11.4, 4.3$ Hz, 1H), 3.73 (d, $J = 11.4$ Hz, 1H), 3.30 (s, 3H), 3.29 (s, 3H). ^{13}C NMR (175 MHz, C_6D_6 , α only) δ 160.6, 159.8, 159.6, 139.3, 139.0, 131.1, 130.6, 129.8, 129.7, 128.5, 128.4, 128.3, 128.2, 128.0, 127.7, 127.6, 114.1, 114.0, 96.9, 79.7, 76.0, 75.4, 74.8, 73.9, 73.3, 72.7, 72.3, 68.8, 54.7. (ESI+) (m/z): $[\text{M}+\text{NH}_4]^+$ calcd for $\text{C}_{38}\text{H}_{44}\text{Cl}_3\text{N}_2\text{O}_8$ 761.2158, found 761.2152.

Glycosylation studies

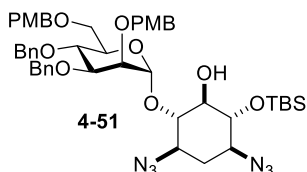


A flame-dried 4 mL vial was charged with mannose trichloroacetimidate **4-34** (175.6 mg, 0.236 mmol), 2-deoxystreptamine **4-17** (38.7 mg, 0.118 mmol), 4 Å MS (~100 mg), and (S)-SF₅-CPA catalyst (11.8 mg, 0.0236 mmol). The resulting mixture was flushed with nitrogen, then dry dichloromethane (0.59 mL) was added. The resulting mixture was refluxed for 5 days, then quenched with triethylamine. Crude ^1H NMR showed 88% conversion with 1:5 selectivity. The mixture was purified by column chromatography (9:1 hexanes/ethyl acetate). Purification resulted in some mixed fractions of glycal with glycosylated product and fractions of pure glycosylation products (1:4 regioselectivity).

All fractions containing glycal and glycosylation products were combined and used in the next deprotection step. 78% yield (colorless oil).

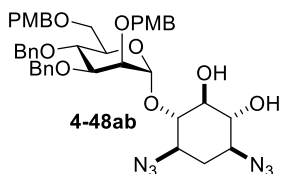
IR (thin film, cm^{-1}): 3478, 3031, 2933, 2857, 1612, 1514, 1248, 1095, 1037, 837. ^1H NMR (700 MHz, C_6D_6 , **4-41a** only) δ 7.44 (d, $J = 8.5$ Hz, 2H), 7.39 (d, $J = 8.5$ Hz, 2H), 7.30 (d, $J = 7.5$ Hz, 2H), 7.25 (d, $J = 8.5$ Hz, 2H), 7.21-7.17 (m, 3H), 7.14-7.05 (m, 3H), 6.82 (d, $J = 8.5$ Hz, 2H), 6.76 (d, $J = 8.5$ Hz, 2H), 5.70 (d, $J = 1.6$ Hz, 1H), 5.16 (d, $J = 11.0$ Hz, 1H), 5.01 (d, $J = 11.7$ Hz, 2H), 4.85 (d, $J = 11.9$ Hz, 1H), 4.79 (d, $J = 11.0$ Hz, 1H), 4.76 (d, $J = 11.9$ Hz, 1H), 4.67 (d, $J = 11.4$ Hz, 1H), 4.62 (d, $J = 11.4$ Hz, 1H), 4.55 (dd, $J = 9.5, 5.0$), 4.45 (d, $J = 11.7$ Hz, 1H), 4.34 (dd, $J = 9.5, 2.4$ Hz, 1H), 4.22 (t, $J = 2.4$ Hz, 1H), 3.96 (dd, $J = 11.0, 4.8$, 1H), 3.89 (dd, $J = 11.0, 1.4$ Hz, 1H), 3.50 (t, $J = 9.5$ Hz, 1H), 3.32 (s, 3H), 3.315 (s, 3H), 3.23 (t, $J = 8.9$ Hz, 1H), 2.68 (dd, $J = 9.5, 4.0$ Hz, 1H), 2.47 (ddd, $J = 12.3, 9.7, 4.6$ Hz, 1H), 1.81 (d, $J = 3.9$ Hz, 1H), 1.49 (dt, $J = 12.3, 4.6$, 1H), 1.0 (s, 9H), 0.19 (s, 3H), 0.18 (s, 3H). ^1H NMR (700 MHz, C_6D_6 , **4-41b** only) δ 7.40 (t, $J = 8.0$ Hz, 4H), 7.34 (d, $J = 7.3$ Hz, 2H), 7.30-7.25 (m, 3H), 7.25-7.18 (m, 2H), 7.12-7.07 (m, 3H), 6.82 (d, $J = 8.3$ Hz, 2H), 6.78 (d, $J = 8.3$ Hz, 2H), 5.64 (d, $J = 1.7$ Hz, 1H), 5.02 (d, $J = 10.9$ Hz, 1H), 4.85 (d, $J = 12.5$ Hz, 1H), 4.78 (d, $J = 10.9$ Hz, 1H), 4.75 (d, $J = 5.5$ Hz, 1H), 4.68 (d, $J = 11.7$ Hz, 1H), 4.62 (d, $J = 10.9$ Hz, 1H), 4.60 (d, $J = 10.9$ Hz, 1H), 4.46-4.38 (m, 3H), 4.29-4.26 (m, 2H), 3.92 (dd, $J = 10.1, 4.7$, 1H), 3.84 (d, $J = 10.9$ Hz, 1H), 3.33 (s, 3H), 3.31 (s, 3H), 3.17 (dd, $J = 12.5, 8.1$ Hz, 2H), 2.79 (dt, $J = 12.2, 9.5, 4.2$, 1H), 2.49 (ddd, $J = 12.5, 9.8, 4.8$ Hz, 1H), 1.90 (d, $J = 3.6$ Hz, 1H), 1.45 (dt, $J = 12.5, 4.5$ Hz, 1H), 1.02 (s, 9H), 0.88 (q, $J = 12.7$ Hz, 1H), 0.33 (s, 3H), 0.21 (s, 3H). ^{13}C NMR (175 MHz, C_6D_6) δ 159.9, 159.8, 159.7, 159.6, 139.7, 139.6, 139.5, 139.4, 131.4, 131.3, 131.1, 131.0, 130.1, 129.7 (3C), 128.7, 128.6, 128.5, 128.4, 128.0, 127.8, 127.7 (4C), 127.5 (2C), 114.2, 114.1 (2C), 114.0,

99.8 ($J = 174.3$ Hz), 99.0 ($J = 170.6$ Hz), 81.5, 80.0, 77.9, 77.8, 77.1, 76.8, 76.6, 75.9, 75.7, 75.4, 75.1, 74.9, 74.8, 74.1, 73.9, 73.4, 73.3, 73.2, 73.1, 72.4, 69.9, 69.6, 60.8, 60.7, 60.4, 60.0, 54.8, 54.7, 32.1, 31.8, 26.5, 26.4, 18.7, 18.6, -2.5, -3.1, -3.2, -3.3. (ESI+) (m/z): $[M+NH_4]^+$ calcd for $C_{48}H_{62}N_6O_{10}SiNH_4$ 928.4635, found 928.4631.



Characterization data for 4-51

IR (thin film, cm^{-1}): 3475, 3036, 1620, 1565, 1265, 1084, 1047, 831. 1H NMR (500 MHz, C_6D_6) δ 7.41 (d, $J = 7.2$ Hz, 2H), 7.34 (d, $J = 8.3$ Hz, 2H), 7.23-7.14 (m, 5H), 7.15-7.06 (m, 5H), 6.81 (d, $J = 8.7$ Hz, 2H), 6.77 (d, $J = 8.3$ Hz, 2H), 5.05 (d, $J = 1.6$ Hz, 1H), 4.94 (d, $J = 11.4$ Hz, 1H), 4.73-4.60 (m, 5H), 4.51-4.38 (m, 3H), 3.74 (dd, $J = 10.0, 1.6$ Hz, 1H), 3.56 (dd, $J = 9.7, 8.1$ Hz, 1H), 3.30 (d, $J = 2.1$ Hz, 6H), 3.23-3.14 (m, 2H), 2.86 (t, $J = 8.5$ Hz, 1H), 2.73 (ddd, $J = 12.9, 8.8, 4.4$ Hz, 1H), 2.59 (ddd, $J = 12.9, 9.7, 4.4$ Hz, 1H), 1.50 (dt, $J = 13.2, 4.4$ Hz, 1H), 0.87 (q, $J = 12.7$ Hz, 1H). ^{13}C NMR (500 MHz, C_6D_6) δ 160.0, 159.9, 139.1 (2C), 130.6, 130.4, 130.0, 128.7, 128.5, 128.3, 127.7, 114.2, 101.1 ($J = 170.6$ Hz), 89.1, 80.3, 77.1, 75.6, 75.2, 75.0, 73.5, 73.1 (2C), 72.0, 69.0, 62.3, 59.7, 54.8, 54.7, 32.1, 27.2, 26.3, 18.8, -3.4, -4.5. (ESI+) (m/z): $[M+NH_4]^+$ calcd for $C_{48}H_{62}N_6O_{10}SiNH_4$ 928.4635, found 928.4635.



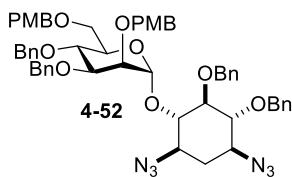
The resulting mixture **4-41ab** isolated from the previous reaction was mixed with ~50 mg of 4Å MS, flushed with nitrogen, and then dissolved in 3.0 mL dry THF. The reaction was cooled down to 0 °C, and 0.11 mL (0.111 mL) of TBAF (1.0 M) was added. The reaction was warmed up to room temperature and was stirred overnight. Then the reaction was quenched with

NaHCO₃ (sat.) and extracted with ethyl acetate. Organics were washed with brine/water (1:1) x2, then brine. Extracts were dried with magnesium sulfate, filtered and evaporated. The mixture was purified by column chromatography (3:1 to 2:1 hexanes/ethyl acetate). The procedure yielded of 36.5 mg (66%) of major isomer (**4-48b**) and 10.9 mg (59%) of minor isomer (**4-48a**). The major isomer was then used in the next steps.

4-48a IR (thin film, cm⁻¹): 3428, 2926, 1720, 1612, 1586, 1514, 1454, 1364, 1250, 1104, 1033, 818, 699. ¹H NMR (500 MHz, C₆D₆) δ 7.39 (d, *J* = 7.5 Hz, 2H), 7.35 (d, *J* = 7.5, 2H), 7.27-7.12 (m, 8H), 7.12-7.06(m, 2H), 6.79 (d, *J* = 8.3 Hz, 2H), 5.48 (d, *J* = 1.3 Hz, 1H), 4.95, (d, *J* = 11.7 Hz, 1H), 4.82 (d, *J* = 11.7 Hz, 1H), 4.70 (d, *J* = 11.7 Hz, 1H), 4.56 (s, 2H), 4.54-4.46 (m, 2H), 4.40 (d, *J* = 11.0 Hz, 1H), 4.27 (d, *J* = 11.0 Hz, 1H), 4.20-4.12 (m, 3H), 3.88 (dd, *J* = 10.0, 1.3 Hz, 1H), 3.71 (dd, *J* = 10.0, 7.3 Hz, 1H), 3.42 (t, *J* = 10.0 Hz, 1H), 3.32 (s, 3H), 3.31-3.26 (m, 1H), 3.29 (s, 3H), 2.98 (t, *J* = 9.4 Hz, 1H), 2.70-2.58 (m, 2H), 1.51 (dt, *J* = 12.8, 4.7 Hz, 1H), 0.91 (q, *J* = 12.8 Hz, 1H). ¹³C NMR (125 MHz, C₆D₆) δ 160.0 (2C), 139.3, 139.2, 130.9, 130.2, 130.1, 128.6, 128.5, 128.0, 127.9, 127.8, 127.7, 114.2 (2C), 96.4 (*J* = 170.6 Hz), 80.9, 80.3, 76.6, 75.8, 75.7, 74.8, 73.4, 73.2, 72.9, 72.4, 70.1, 59.9, 58.0, 54.8, 32.4. (ESI+) (*m/z*): [M+NH₄]⁺ calcd for C₄₂H₅₂N₇O₁₀ 814.3770, found 814.3769.

4-48b IR (thin film, cm⁻¹): 3469, 2654, 1702, 1613, 1586, 1369, 1256, 1109, 1033, 816, 689, 658. ¹H NMR (500 MHz, C₆D₆) δ 7.42 (d, *J* = 7.4 Hz, 2H), 7.34 (d, *J* = 8.5 Hz, 2H), 7.25 (d, *J* = 7.4 Hz, 2H), 7.23-7.17 (5H), 7.15-7.07 (m, 3H), 6.82 (dd, *J* = 8.5, 6.6 Hz, 4H), 5.04 (d, *J* = 1.6 Hz, 1H), 4.99 (d, *J* = 11.1 Hz, 1H), 4.95 (d, *J* = 3.1 Hz, 1H), 4.71 (d, *J* = 11.8 Hz, 1H), 4.68 (d, *J* = 11.5 Hz, 1H), 4.63 (d, *J* = 8.1 Hz, 1H), 4.61 (d, *J* = 8.1 Hz, 1H), 4.45 (d, *J* = 11.5 Hz, 1H), 4.27-4.19 (m, 3H), 4.15 (t, *J* = 2.0 Hz, 1H), 4.09 (dd, *J* = 9.3, 3.3

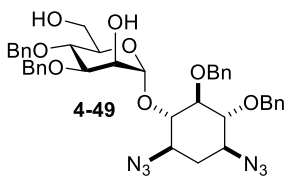
Hz, 1H), 4.01 (t, $J = 9.3$ Hz, 1H), 3.81 (dd, $J = 9.7, 1.6$ Hz, 1H), 3.3 (t, $J = 9.0$ Hz, 1H), 3.35 (s, 3H), 3.33-3.27 (m, 1H), 3.30 (s, 3H), 3.18 (t, $J = 9.7$ Hz, 1H), 3.06 (td, $J = 8.8, 2.8$ Hz, 1H), 2.95-2.83 (m, 3H), 2.56 (ddd, $J = 12.7, 9.5, 4.6$, 1H), 1.50 (dt, $J = 13.2, 4.6$, 1H), 0.89 (q, $J = 13.2$ Hz, 1H). ^{13}C NMR (125 MHz, C_6D_6) δ 160.1, 160.0, 139.1, 139.0, 130.6, 130.1, 130.0, 129.9, 128.7, 128.6, 128.0, 127.9, 127.8, 114.2, 114.1, 100.4 ($J = 169.4$ Hz), 88.1, 80.5, 76.4, 75.6, 75.2, 75.1 (2C), 73.4, 73.3, 73.0, 71.9, 70.0, 59.6, 54.9, 54.8, 32.2. (ESI+) (m/z): $[\text{M}+\text{NH}_4]^+$ calcd for $\text{C}_{42}\text{H}_{52}\text{N}_7\text{O}_{10}$ 814.3770, found 814.3767.



The major diol (30.6 mg, 0.0384 mmol) isolated from the previous reaction (**4-48b**) was dissolved in dry DMF (0.38 mL). To that 6.1 mg of sodium hydride was added (60%, 0.154 mmol), and the reaction mixture was flushed with nitrogen. To that 22.8 μL (0.192 mmol) of benzyl bromide was added. The resulting mixture was stirred at 40 $^\circ\text{C}$ overnight. Reaction was then diluted with DCM, and aqueous ammonia chloride was added. Organics were extracted with DCM, and then washed with brine and dried with magnesium sulfate. Column chromatography (9:1 to 4:1 hexanes/ethyl acetate) resulted in 30.6 mg of colorless oil.

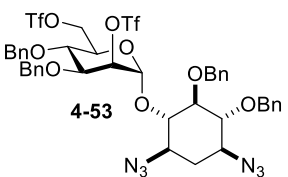
^1H NMR (400 MHz, C_6D_6) δ 7.45 (d, $J = 7.2$ Hz, 2H), 7.41-7.33 (m, 6H), 7.26-7.17 (m, 10H), 7.14-7.04 (m, 6H), 6.81 (d, $J = 8.3$ Hz, 2H), 6.75 (d, $J = 8.3$ Hz, 2H), 5.68 (s, 1H), 5.01 (d, $J = 11.3$ Hz, 1H), 4.84 (d, $J = 5.7$ Hz, 2H), 4.80 (d, $J = 3.4$ Hz, 2H), 4.75 (d, $J = 10.8$ Hz, 1H), 4.70 (d, $J = 10.8$ Hz, 1H), 4.66 (s, 2H), 4.63 (d, $J = 8.6$ Hz, 1H), 4.60 (d, $J = 8.6$ Hz, 1H), 4.48 (t, $J = 9.5$ Hz, 1H), 4.38 (d, $J = 11.7$ Hz, 1H), 4.34-4.27 (m, 1H), 4.18-4.12 (m, 2H), 3.71-3.63 (m, 2H), 3.39 (t, $J = 9.4$ Hz, 1H), 3.33 (s, 3H), 3.30 (s, 3H), 3.04

(t, $J = 9.4$ Hz, 1H), 2.95 (t, $J = 9.4$ Hz, 1H), 2.72-2.59 (m, 2H), 1.44(dt, $J = 13.1, 4.3$ Hz, 1H), 0.84 (q, $J = 13.1$ Hz, 1H).



Compound **4-52** (45.8 mg, 0.0469 mmol) was mixed together with DDQ (21.3 mg, 0.0937 mmol), then 0.32 mL of DCM was added along with 1 drop of water. The mixture was stirred at room temperature for 1.5 hours. Then the reaction was quenched with saturated sodium bicarbonate, and extracted with DCM. Organics were washed with saturated sodium bicarbonate, brine, dried with magnesium sulfate. Column chromatography (4:1 to 3:2 hexanes/ethyl acetate) resulted in 23.1 mg (67%) of colorless oil.

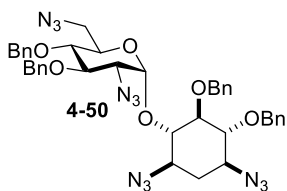
^1H NMR (400 MHz, C_6D_6) δ 7.36 (d, $J = 7.5$ Hz, 2H), 7.33 (d, $J = 7.5$ Hz, 2H), 7.26-7.21 (m, 4H), 7.20-7.04 (m, 12H), 5.65 (s, 1H), 4.88 (d, $J = 11.3$ Hz, 1H), 4.84 (d, $J = 11.0$ Hz, 1H), 4.72 (d, $J = 11.3$ Hz, 1H), 4.69 (s, 2H), 4.65 (d, $J = 11.3$ Hz, 1H), 4.53 (s, 2H), 4.29 (s, 1H), 4.16-4.05 (m, 2H), 4.97 (dd, $J = 8.6, 3.2$ Hz, 1H), 3.73 (d, $J = 12.2$ Hz, 1H), 3.66-3.57 (m, 1H), 3.28 (t, $J = 9.5$ Hz, 1H), 2.99 (t, $J = 9.3$ Hz, 1H), 2.93 (d, $J = 9.3$ Hz, 1H), 2.72-2.55 (m, 3H), 1.44 (dt, $J = 12.9, 4.1$ Hz, 1H), 0.85 (q, $J = 12.9$ Hz, 1H).



Compound **4-49** (23.1 mg, 0.0314 mmol) was dissolved in 0.17 mL of dry DCM, and cooled down to -15 °C under nitrogen. To this mixture 12.6 μL of pyridine (0.157 mmol) was added, followed by 21.1 μL of trifluoromethanesulfonic anhydride (0.125 mmol). The resulting mixture was stirred at the same temperature for 10 minutes. Then the mixture was diluted with DCM and water. Organics were extracted with DCM. Extracts were washed with

saturated sodium bicarbonate and water, dried with magnesium sulfate. The crude material was used in the next step without purification. (30.1 mg, 96 % yield).

^1H NMR (500 MHz, C_6D_6) δ 7.38 (t, $J = 7.0$ Hz, 3H), 7.24 (d, $J = 7.5$ Hz, 2H), 7.15-7.07 (m, 10H), 7.07-7.03 (m 5H), 5.67 (d, $J = 1.7$ Hz, 1H), 5.39 (t, $J = 2.2$ Hz, 1H), 4.92 (d, $J = 11.2$ Hz, 1H), 4.77-4.66 (m, 4H), 4.62 (d, $J = 11.5$ Hz, 1H), 4.39 (dd, $J = 11.2, 3.9$ Hz, 2H), 4.19 (dd, $J = 10.9, 1.7$, 1H), 4.16 (d, $J = 11.2$ Hz, 1H), 4.11 (ddd, $J = 10.2, 4.6, 1.7$ Hz, 1H), 3.93 (dd, $J = 9.3, 2.8$ Hz, 1H), 3.79 (dd, $J = 11.2, 4.6$ Hz, 1H), 7.37 (t, $J = 9.7$ Hz, 1H), 3.07 (t, $J = 9.7$ Hz, 1H), 3.0-2.87 (m, 3H), 2.66-2.54 (m, 2H), 1.39 (dt, $J = 12.9, 4.8$ Hz, 1H), 0.76 (q, $J = 12.9$ Hz, 1H).



The resulting triflate **4-53** (30.1 mg, 0.0301 mmol) was dissolved in dry DMF, flushed with nitrogen. To that sodium azide (7.8 mg, 0.120 mmol). The mixture was stirred at 40 °C for 4 hours.

Then in was diluted with DCM and water. The organics were extracted with DCM, then washed with brine/water (1:1), and then brine. Organic layer was dried with magnesium sulfate. The product was purified by column chromatography (4:1 hexanes/ethyl acetate). The procedure yielded 3 mg of the desired product.

4-50 IR (thin film, cm^{-1}): 2924, 2103, 1722, 1454, 1361, 1260, 1124, 739, 697. ^1H NMR (700 MHz, CDCl_3) δ 7.37-7.31 (m, 7H), 7.31-7.27 (m, 8H), 7.20 (d, $J = 7.3$ Hz, 1H), 7.17-7.13 (m, 4H), 5.56 (d, $J = 3.7$ Hz, 1H), 5.30 (s, 1H), 5.02 (d, $J = 11.0$ Hz, 1H), 4.90-4.86 (m, 3H), 4.84 (d, $J = 10.6$ Hz, 1H), 4.79 (d, $J = 11.5$ Hz, 1H), 4.68 (d, $J = 11.5$ Hz, 1H), 4.47 (d, $J = 11.5$ Hz, 1H), 4.00-3.97 (m, 1H), 3.87 (t, $J = 9.7$ Hz, 1H), 3.60-3.55 (m, 1H), 3.55-3.47 (m, 4H), 3.46-3.43 (m, 2H), 3.40 (dd, $J = 10.3, 3.7$ Hz, 1H), 3.05 (dd, $J = 13.4,$

2.1 Hz, 1H), 2.68 (dd, $J = 13.4, 3.4$ Hz, 1H), 2.31 (dt, $J = 13.2, 4.5$ Hz, 1H), 1.50 (q, $J = 13.2$ Hz, 1H). ^{13}C NMR (175 MHz, CDCl_3) δ 138.1, 137.8, 137.6, 137.3, 128.6, 128.5 (2C), 128.4, 128.2 (2C), 128.1, 127.9, 127.8, 127.7, 127.4, 97.6, 84.8, 81.9, 80.1, 78.6 (2C), 76.2, 76.0, 75.6, 75.1, 70.5, 63.6, 61.6, 60.5, 50.4, 32.8, 29.8. (ESI+) (m/z): $[\text{M}+\text{Na}]^+$ calcd for $\text{C}_{40}\text{H}_{42}\text{N}_{12}\text{O}_6\text{Na}$ 809.3242, found 809.3232.

References

- ¹ Fischer, E. *Ber. Dtsch. Chem. Ges.* **1891**, *24*, 1836–1845.
- ² Feizi, T. *Nature* **1985**, *314* (6006), 53–57.
- ³ Livingston, P. O. *Immunol. Rev.* **1995**, *145* (1), 147–166.
- ⁴ Magnet, S.; Blanchard, J. S. *Chem. Rev.* **2005**, *105* (2), 477–498.
- ⁵ Schatz, A.; Bugie, E.; Waksman, S. A. *Proc. Soc. Exp. Biol. Med.*, **1944**, *55*, 66–69.
- ⁶ Berkov-Zrihen, Y.; Fridman, M. In *Modern Synthetic Methods in Carbohydrate Chemistry*; Werz, D. B., Vidal, S., Eds.; Wiley-VCH Verlag GmbH & Co. KGaA: Weinheim, Germany, 2013; pp 161–190.
- ⁷ Fosso, M. Y.; Li, Y.; Garneau-Tsodikova, S. *Med. Chem. Commun.* **2014**, *5* (8), 1075.
- ⁸ Busscher, G. F.; Rutjes, F. P. J. T.; van Delft, F. L. *Chem. Rev.* **2005**, *105* (3), 775–792.
- ⁹ Mingeot-Leclercq, M.-P.; Glupczynski, Y.; Tulkens, P. M. *Antimicrob. Agents Chemother.* **1999**, *43*, 727–737.
- ¹⁰ Hermann, T.; Westhof, E. *J. Mol. Biol.* **1998**, *276* (5), 903–912.
- ¹¹ Carter, A. P.; Clemons, W. M.; Brodersen, D. E.; Morgan-Warren, R. J.; Wimberly, B. T.; Ramakrishnan, V. *Nature* **2000**, *407*, 340–348.
- ¹² Ogle, J. M.; Brodersen, D. E.; Clemons, W. M. Jr.; Tarry, M. J.; Carter, A. P.; Ramakrishnan, V. *Science* **2001**, *292* (5518), 897–902.
- ¹³ Ogle, J. M.; Murphy IV, F. V.; Tarry, M. J.; Ramakrishnan, V. *Cell* **2002**, *111* (5), 721–732.
- ¹⁴ Vicens, Q.; Westhof, E. *Structure* **2001**, *9*, 647–658.
- ¹⁵ Vicens, Q.; Westhof, E. *Chem. Biol.* **2002**, *9*, 747–755.
- ¹⁶ Vicens, Q.; Westhof, E. *J. Mol. Biol.* **2003**, *326*, 1175–1188.
- ¹⁷ Liu, X.; Thomas, J. R.; Hergenrother, P. J. *J. Am. Chem. Soc.* **2004**, *126* (30), 9196–9197.
- ¹⁸ Enríquez-García, Á.; Kündig, E. P. *Chem. Soc. Rev.* **2012**, *41* (23), 7803.

- ¹⁹ (a) Zhao, Y.; Rodrigo, J.; Hoveyda, A. H.; Snapper, M. L. *Nature* **2006**, *443* (7107), 67–70. (b) Zhao, Y.; Mitra, A. W.; Hoveyda, A. H.; Snapper, M. L. *Angew. Chem. Int. Ed.* **2007**, *46* (44), 8471–8474. (c) Manville, N.; Alite, H.; Haeffner, F.; Hoveyda, A. H.; Snapper, M. L. *Nat. Chem.* **2013**, *5* (9), 768–774. (d) Hyodo, K.; Gandhi, S.; van Gemmeren, M.; List, B. *Synlett* **2015**.
- ²⁰ Kinugasa, M.; Harada, T.; Oku, A. *J. Am. Chem. Soc.* **1997**, *119* (38), 9067–9068.
- ²¹ Suzuki, T. In *Comprehensive Chirality*; Elsevier, 2012; pp 502–533.
- ²² Mensah, E.; Camasso, N.; Kaplan, W.; Nagorny, P. *Angew. Chem. Int. Ed.* **2013**, *52* (49), 12932–12936.
- ²³ Cox, D. J.; Smith, M. D.; Fairbanks, A. J. *Org. Lett.* **2010**, *12*, 1452–1455.
- ²⁴ Kimura, T.; Sekine, M.; Takahashi, D.; Toshima, K. *Angew. Chem. Int. Ed.* **2013**, *52* (46), 12131–12134.
- ²⁵ Liu, D.; Sarrafpour, S.; Guo, W.; Goulart, B.; Bennett, C. S. *J. Carbohydr. Chem.* **2014**, *33* (7-8), 423–434.
- ²⁶ Alper, P. B.; Hung, S.-C.; Wong, C.-H. *Tetrahedron Lett.* **1996**, *37* (34), 6029–6032.
- ²⁷ Goddard-Borger, E. D.; Stick, R. V. *Org. Lett.* **2007**, *9* (19), 3797–3800.
- ²⁸ Fischer, N.; Goddard-Borger, E. D.; Greiner, R.; Klapötke, T. M.; Skelton, B. W.; Stierstorfer, J. *J. Org. Chem.* **2012**, *77* (4), 1760–1764.
- ²⁹ Keicher, T.; Lbbecke, S. In *Organic Azides*; Brse, S., Banert, K., Eds.; John Wiley & Sons, Ltd: Chichester, UK, 2009; pp 1–27.
- ³⁰ Aslam, M. W.; Busscher, G. F.; Weiner, D. P.; Gelder, R. de; Rutjes, F. P. J. T.; Delft, F. L. van. *J. Org. Chem.* **2008**, *73* (13), 5131–5134.
- ³¹ Paulsen, H.; Stenzel, W. *Eur. J. Inorg. Chem.* **1978**, *111* (6), 2334–2347.
- ³² Aoyama, N.; Kobayashi, S. *Chem. Lett.* **2006**, *35* (2), 238–239.
- ³³ Sun, S.; Li, Z.-J. *J. Chin. Pharm. Sci.* **2011**, *20* (6), 549–556.
- ³⁴ Borovika, A., Nagorny, P. *Unpublished*.
- ³⁵ Wright, J. A.; Yu, J.; Spencer, J. B. *Tetrahedron Lett.* **2001**, *42* (24), 4033–4036.
- ³⁶ Nicolaou, K. C.; Mitchell, H. J.; Suzuki, H.; Rodríguez, R. M.; Baudoin, O.; Fylaktakidou, K. C. *Angew. Chem. Int. Ed.* **1999**, *38* (22), 3334–3339.

- ³⁷ Dudkin, V. Y.; Miller, J. S.; Dudkina, A. S.; Antczak, C.; Scheinberg, D. A.; Danishefsky, S. J. *J. Am. Chem. Soc.* **2008**, *130* (41), 13598–13607.
- ³⁸ (a) Bock, K.; Pedersen, C. *Carbohydr. Res.* **1985**, *145* (1), 135–140. (b) Uhrínova, S.; Uhrían, D.; Liptaj, T.; Bella, J.; Hirsch, J. *Magn. Reson. Chem.* **1991**, *29* (9), 912–922.
- ³⁹ Matheson, N. K. In *Studies in Natural Products Chemistry*; Elsevier, 2002; Vol. 26, pp 1113–1173.
- ⁴⁰ Chertkov, V. A.; Sergeyev, N. M. *J. Am. Chem. Soc.* **1977**, *99* (20), 6750–6752.
- ⁴¹ Furrer, J. *Concepts Magn. Reson., Part A* **2012**, *40A* (3), 101–127.
- ⁴² Pang, L.-J.; Wang, D.; Zhou, J.; Zhang, L.-H.; Ye, X.-S. *Org. Biomol. Chem.* **2009**, *7* (20), 4252.
- ⁴³ Harris, R. K.; Becker, E. D.; Cabral de Menezes, S. M.; Goodfellow, R.; Granger, P. *Pure Appl. Chem.* **2001**, *73*, 1795.
- ⁴⁴ Chen, Y.-L.; Pyplo-Schnieders, J.; Redlich, H.; Luftmann, H.; Fröhlich, R. *Tetrahedron Lett.* **2007**, *48* (46), 8145–8148.
- ⁴⁵ Alper, P. B.; Hung, S.-C.; Wong, C.-H. *Tetrahedron Lett.* **1996**, *37* (34), 6029–6032.
- ⁴⁶ Ding, Y.; Hofstadler, S. A.; Swayze, E. E.; Griffey, R. H. *Chem. Lett.* **2003**, *32* (10), 908–909.

Appendix A

Thiophosphoramidate Catalyst 2-10

Energy (kcal/mol): -2273472.26

Job type: Single point.

Method: RB3LYP

Basis set: 6-31+G*

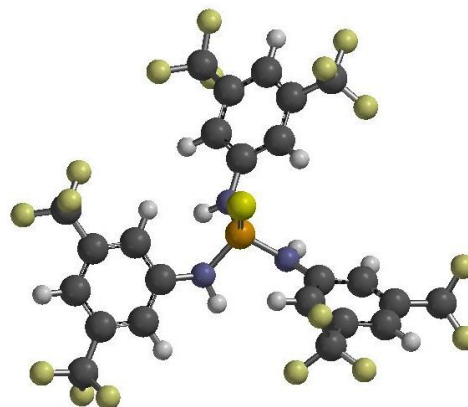
Number of shells: 261

Number of basis functions: 925

Multiplicity: 1

Coordinates (XYZ):

	X	Y	Z
P	-0.054160	0.009696	-0.189104
C	2.359336	-4.915996	0.058476
C	1.447459	-2.332969	-0.603251
C	3.146376	-4.059166	-0.714679
C	1.113154	-4.464877	0.491034
C	0.648562	-3.187890	0.165880
C	2.704656	-2.778032	-1.038428
H	-0.327224	-2.868146	0.514556
H	3.335131	-2.123795	-1.634109
C	-4.468079	1.312396	0.546018
C	-3.874591	-0.889114	-1.041591
C	-3.141999	1.046840	0.209496
C	-5.510446	0.497843	0.094649
C	-5.198292	-0.599878	-0.704581



C	-2.836358	-0.064459	-0.592187
H	-2.355444	1.697811	0.571914
H	-6.538528	0.719248	0.353674
H	-3.652505	-1.755958	-1.658715
C	3.352900	3.100822	0.540394
C	1.134808	3.771585	-0.992777
C	3.199705	4.418648	0.110055
C	2.420406	2.115252	0.210647
C	1.299119	2.447375	-0.561318
C	2.081254	4.740038	-0.661557
H	3.929937	5.175760	0.367739
H	2.566823	1.101499	0.565327
H	0.265380	4.046286	-1.584084
H	2.705760	-5.911041	0.308212
N	1.010518	-1.050273	-0.997629
H	1.611907	-0.583006	-1.668944
N	-1.515469	-0.348888	-0.997127
H	-1.426644	-1.108211	-1.665144
N	0.348374	1.482031	-0.952097
H	-0.358220	1.810150	-1.602496
C	0.223802	-5.354353	1.327080
C	4.523171	-4.495713	-1.154227
C	-6.285685	-1.504636	-1.231319
C	-4.789312	2.480919	1.447515
C	1.901285	6.142009	-1.190830

C	4.529729	2.711399	1.403730
F	-5.964778	3.064932	1.111939
F	-4.900023	2.094824	2.743620
F	-3.835993	3.441918	1.402666
F	-7.515251	-1.128024	-0.821119
F	-6.103386	-2.790321	-0.836088
F	-6.302597	-1.520320	-2.590920
F	0.701802	-6.614420	1.426227
F	0.081138	-4.879336	2.588899
F	-1.027117	-5.438976	0.802281
F	4.859821	-3.973518	-2.360292
F	4.624470	-5.840531	-1.253918
F	5.476562	-4.091913	-0.275394
F	0.604128	6.535116	-1.150711
F	2.293480	6.237039	-2.490231
F	2.620248	7.050389	-0.496100
F	5.500960	3.651330	1.403453
F	5.093426	1.549644	0.983239
F	4.159927	2.518729	2.694189
S	-0.064692	-0.034590	1.746971

Thiophosphoramidate Catalyst **2-10** + Mesylate

Energy (kcal/mol): -2690086.83

Job type: Single point.

Method: RB3LYP

Basis set: 6-31+G*

Number of shells: 293

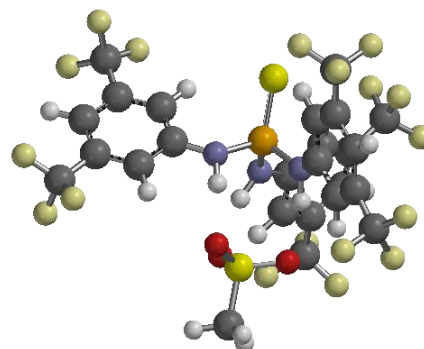
Number of basis functions: 1030

Charge : -1

Multiplicity: 1

Coordinates (XYZ):

	X	Y	Z
P	-0.010625	0.013533	-0.740398
C	1.677731	-5.232520	-0.468896
C	0.420573	-2.712024	-0.206436
C	0.806370	-4.974540	0.592557
C	1.913017	-4.210784	-1.389866
C	1.298570	-2.962082	-1.274564
C	0.187630	-3.734832	0.733005
H	1.495461	-2.192254	-2.010312
H	-0.468465	-3.538845	1.575176
C	2.786153	3.745765	-1.280467
C	3.073421	2.035209	0.890391
C	1.995327	2.596226	-1.205134



C	3.724828	4.054411	-0.296411
C	3.855216	3.181874	0.788373
C	2.135044	1.723613	-0.114087
H	1.280144	2.376130	-1.987910
H	4.333707	4.948522	-0.367604
H	3.164586	1.379268	1.749923
C	-4.618481	0.660922	-1.445585
C	-3.359870	1.558378	0.862481
C	-5.393704	1.210925	-0.423859
C	-3.229448	0.559428	-1.339243
C	-2.583332	1.009287	-0.176112
C	-4.742726	1.659017	0.728551
H	-6.469888	1.286392	-0.520410
H	-2.649395	0.140951	-2.152858
H	-2.866699	1.885653	1.772846
H	2.159705	-6.197610	-0.572395
N	-0.257761	-1.500165	-0.016362
H	-0.698434	-1.431682	0.914235
N	1.404256	0.537191	0.035752
H	1.522747	0.107367	0.967375
N	-1.193258	0.969859	0.011178
H	-0.910978	1.256915	0.961997
C	2.812096	-4.488895	-2.565982
C	0.581688	-6.036600	1.635599
C	4.835770	3.529598	1.876476

C	2.672611	4.646328	-2.482375
C	-5.554033	2.195305	1.878042
C	-5.286490	0.218866	-2.721277
F	1.462470	4.576438	-3.083078
F	2.882651	5.953112	-2.166103
F	3.597109	4.338434	-3.437400
F	6.037047	3.925541	1.368585
F	5.084411	2.498192	2.715332
F	4.399001	4.564903	2.648686
F	2.147795	-5.118716	-3.577446
F	3.347936	-3.366190	-3.097779
F	3.849425	-5.306064	-2.235067
F	-0.616051	-5.914702	2.256893
F	1.528813	-6.002717	2.615025
F	0.628560	-7.291061	1.110961
F	-5.869203	1.223072	2.779200
F	-6.735885	2.731270	1.471575
F	-4.902773	3.161625	2.570394
F	-6.584443	-0.136570	-2.526907
F	-4.669218	-0.842586	-3.292648
F	-5.302070	1.207049	-3.661294
S	0.009403	0.034169	-2.696421
S	-0.043295	-0.079759	3.241550
O	-0.932373	-1.204407	2.799335
O	1.385606	-0.277328	2.827404

O	-0.576322	1.264187	2.837836
C	-0.054451	-0.109925	5.044604
H	0.589994	0.695028	5.404064
H	0.322743	-1.081951	5.369082
H	-1.082750	0.037785	5.381037

Thiourea Catalyst **2-11**

Energy (kcal/mol):-1480032.09

Job type: Single point.

Method: RB3LYP

Basis set: 6-31+G*

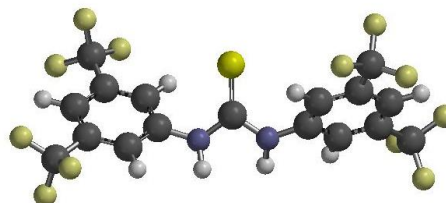
Number of shells: 177

Number of basis functions: 628

Multiplicity: 1

Coordinates (XYZ):

	X	Y	Z
C	0.000000	0.000000	0.247169
C	4.270519	1.094513	-0.600500
C	3.395253	-0.901622	1.125949
C	2.923564	1.032493	-0.251415
C	5.194294	0.174071	-0.093396
C	4.746340	-0.817699	0.776016
C	2.481704	0.021899	0.612949
H	2.224230	1.761286	-0.639156
H	6.240779	0.235222	-0.369543



H	3.055148	-1.695174	1.785260
C	-4.270519	-1.094513	-0.600500
C	-3.395253	0.901622	1.125949
C	-5.194294	-0.174071	-0.093396
C	-2.923564	-1.032493	-0.251415
C	-2.481704	-0.021899	0.612949
C	-4.746340	0.817699	0.776016
H	-6.240779	-0.235222	-0.369543
H	-2.224230	-1.761286	-0.639156
H	-3.055148	1.695174	1.785260
N	1.134252	-0.047417	1.041215
H	1.006729	-0.439253	1.968273
N	-1.134252	0.047417	1.041215
H	-1.006729	0.439253	1.968273
C	5.723410	-1.791359	1.386512
C	4.749230	2.152849	-1.565536
C	-5.723410	1.791359	1.386512
C	-4.749230	-2.152849	-1.565536
F	3.892747	3.196651	-1.649269
F	5.957957	2.650916	-1.204358
F	4.892101	1.655307	-2.820511
F	6.834392	-1.946038	0.633637
F	5.173678	-3.019878	1.555506
F	6.134298	-1.379822	2.616597
F	-6.134298	1.379822	2.616597

F	-6.834392	1.946038	0.633637
F	-5.173678	3.019878	1.555506
F	-5.957957	-2.650916	-1.204358
F	-3.892747	-3.196651	-1.649269
F	-4.892101	-1.655307	-2.820511
S	0.000000	0.000000	-1.412840

Thiourea Catalyst **2-11** + Mesylate

Energy (kcal/mol): -1896642.93

Job type: Single point.

Method: RB3LYP

Basis set: 6-31+G*

Number of shells: 209

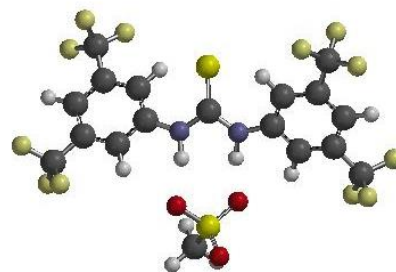
Number of basis functions: 733

Charge : -1

Multiplicity: 1

Coordinates (XYZ):

	X	Y	Z
C	0.007778	-0.728897	-0.084693
C	-4.343415	-1.617060	0.692652
C	-3.375901	0.593532	-0.686417
C	-2.966388	-1.390787	0.642416
C	-5.249046	-0.765620	0.057173



C	-4.746195	0.343879	-0.626421
C	-2.467334	-0.281610	-0.061024
H	-2.285575	-2.060342	1.147351
H	-6.315109	-0.956757	0.098572
H	-2.995089	1.468765	-1.203274
C	4.411972	-1.655478	-0.606802
C	3.386635	0.691371	0.468922
C	5.294270	-0.706340	-0.095310
C	3.027096	-1.462245	-0.584139
C	2.497675	-0.284967	-0.031865
C	4.760001	0.471508	0.437775
H	6.364908	-0.873379	-0.112332
H	2.365025	-2.214818	-0.986315
H	2.983181	1.618719	0.864718
N	-1.113337	0.069294	-0.123433
H	-0.971052	1.076239	-0.329541
N	1.137548	0.043229	0.028108
H	0.982183	1.037723	0.278592
C	-5.708810	1.307299	-1.267259
C	-4.867844	-2.827352	1.418215
C	5.706225	1.527049	0.944547
C	4.952852	-2.954644	-1.141817
F	-4.031997	-3.256092	2.394212
F	-6.072683	-2.590795	2.007989
F	-5.062314	-3.887095	0.582572

F	-6.809364	0.677847	-1.765317
F	-5.156400	1.999786	-2.288896
F	-6.176509	2.231152	-0.379006
F	6.246878	2.260348	-0.069627
F	6.763223	0.981012	1.611862
F	5.119934	2.403881	1.788568
F	6.229040	-2.839036	-1.599501
F	4.213466	-3.448186	-2.164828
F	4.982307	-3.927048	-0.186176
S	-0.025474	-2.412307	-0.170634
S	0.002866	3.645398	0.031812
O	0.683763	4.646309	-0.814114
O	-1.044412	2.827253	-0.681626
O	0.929243	2.738776	0.806460
C	-0.900061	4.571612	1.298294
H	-1.421069	3.861758	1.944682
H	-1.612919	5.229511	0.795716
H	-0.178264	5.157310	1.872345

Appendix B

See figure 2.2 for X-ray of **2-10•2-31**. A careful layering of cyclohexane on top of the solution of **2-10•2-31** produced X-ray quality crystals of colorless needles.

A crystal dimensions 0.29x0.24x0.12 was mounted on a Bruker APEX-I CCD X-ray diffractometer equipped with a low temperature device and fine focus Mo-target X-ray tube ($\lambda = 0.71073 \text{ \AA}$) operated at 1500 W power (50 kV, 30 mA). The X-ray intensities were measured at 85(1) K; the detector was placed at a distance 5.081 cm from the crystal. A total of 4905 frames were collected with a scan width of 0.5° in ω and 0.45° in ϕ with an exposure time of 15 s/frame. The integration of the data yielded a total of 101188 reflections to a maximum 2θ value of 34.37° of which 16951 were independent and 13092 were greater than $2\sigma(I)$. The final unit cell constants of **2-10•2-31** (triclinic with space group symmetry $P1$) were $a = 9.7859(2) \text{ \AA}$, $b = 12.3058(3) \text{ \AA}$, $c = 18.1842(4) \text{ \AA}$; $\alpha = 70.4237(7)^\circ$, $\beta = 85.3597(7)^\circ$, $\gamma = 79.4903(7)^\circ$, $V = 2028.15(8) \text{ \AA}^3$, $Z = 2$ for the formula $C_{37}H_{27}F_{18}N_4O_3PS_2$. All non-hydrogen atoms were refined anisotropically with the hydrogen atoms placed in the idealized positions. Refinement was performed using SHELXL-97 by full-matrix least squares on F^2 . Full matrix least-squares refinement based on F^2 converged at $R1 = 0.0474$ and $wR2 = 0.1196$ [based on $I > 2\sigma(I)$], $R1 = 0.0664$, $wR2 = 0.1338$ for all data, GOF = 1.023.

Chemical formula weight	1012.72
Symmetry cell setting	Triclinic
Symmetry space group name H-M	$P-1$
Cell length a	9.7859(2)
Cell length b	12.3058(3)
Cell length c	18.1842(4)
Cell angle alpha	70.4237(7)

Cell angle beta	85.3597(7)
Cell angle gamma	79.4903(7)
Cell volume	2028.15(8)
Cell formula units Z	2
Cell measurement temperature	85(2)
Cell measurement reflns_used	9849
Cell measurement theta_min	2.38
Cell measurement theta_max	34.26
Exptl crystal description	plate
Exptl crystal colour	colorless
Exptl crystal size_max	0.29
Exptl crystal size_mid	0.24
Exptl crystal size_min	0.12
Exptl crystal density_diffn	1.658
Exptl crystal density_method	'not measured'
Exptl crystal _F_000	1020
Exptl absorpt coefficient_mu	0.298
Exptl absorpt correction type	multi-scan
Exptl absorpt correction T min	0.9186
Exptl absorpt correction T max	0.9651
Exptl absorpt process details	

Blessing, R. Acta Cryst. (1995) A51 33-38. Sheldrick, G. SADABS (Version 2008/1)

Bruker AXS area detector absorption and other corrections, University of Gottingen, Germany
2008.

Exptl specialdetails 4905 frames x 15 sec @ 5.081 cm; 0.5 deg omega scans; 0.45 deg phi scans;

Diffn ambient temperature	85(2)
Diffn radiation wavelength	0.71073
Diffn radiation type	MoK α
Diffn radiation source	'fine-focus sealed tube'
Diffn radiation monochromator	graphite
Diffn measurement device type	'Bruker APEX-I CCD'
Diffn measurement method	' ϕ and ω scans'
Diffn reflns number	101188
Diffn reflns av R equivalents	0.0534
Diffn reflns limit h min	-15
Diffn reflns limit h max	15
Diffn reflns limit k min	-19
Diffn reflns limit k max	19
Diffn reflns limit l min	-28
Diffn reflns limit l max	28
Diffn reflns theta min	1.78
Diffn reflns theta max	34.37
Reflns number total	16951
Reflns number gt	13092
Reflns threshold expression	>2sigma(I)
Computing data collection	'Bruker SMART'
Computing cell refinement	'Bruker SAINT'

Computing data reduction	'Bruker SAINT'
Computing structure solution	'SHELXS-97 (Sheldrick, 2008)'
Computing structure refinement	'SHELXL-97 (Sheldrick, 2008)'
Computing molecular graphics	'Bruker SHELXTL'
Computing publication material	'Bruker SHELXTL'

Refine special details:

Two -CF₃ groups are rotationally disordered. Partial occupancy fluorine atoms were placed in two orientations. SADI/SIMU/DELU restraints were employed to maintain chemical sensibility. For C31/F16/F17/F18, the disorder was adequately described by a 50/50 occupancy of the two orientations. For C23/F10/F11/F12, a free variable was refined for the site occupancy at values 0.703(5)/0.297(5).

Refinement of F^2 against ALL reflections. The weighted R-factor wR and goodness of fit S are based on F^2 , conventional R-factors R are based on F, with F set to zero for negative F^2 . The threshold expression of $F^2 > 2\sigma(F^2)$ is used only for calculating R-factors(gt) etc. and is not relevant to the choice of reflections for refinement. R-factors based on F^2 are statistically about twice as large as those based on F, and R- factors based on ALL data will be even larger.

Refine ls structure factor coef	Fsqd
---------------------------------	------

Refine ls matrix type	full
-----------------------	------

Refine ls weighting scheme	calc
----------------------------	------

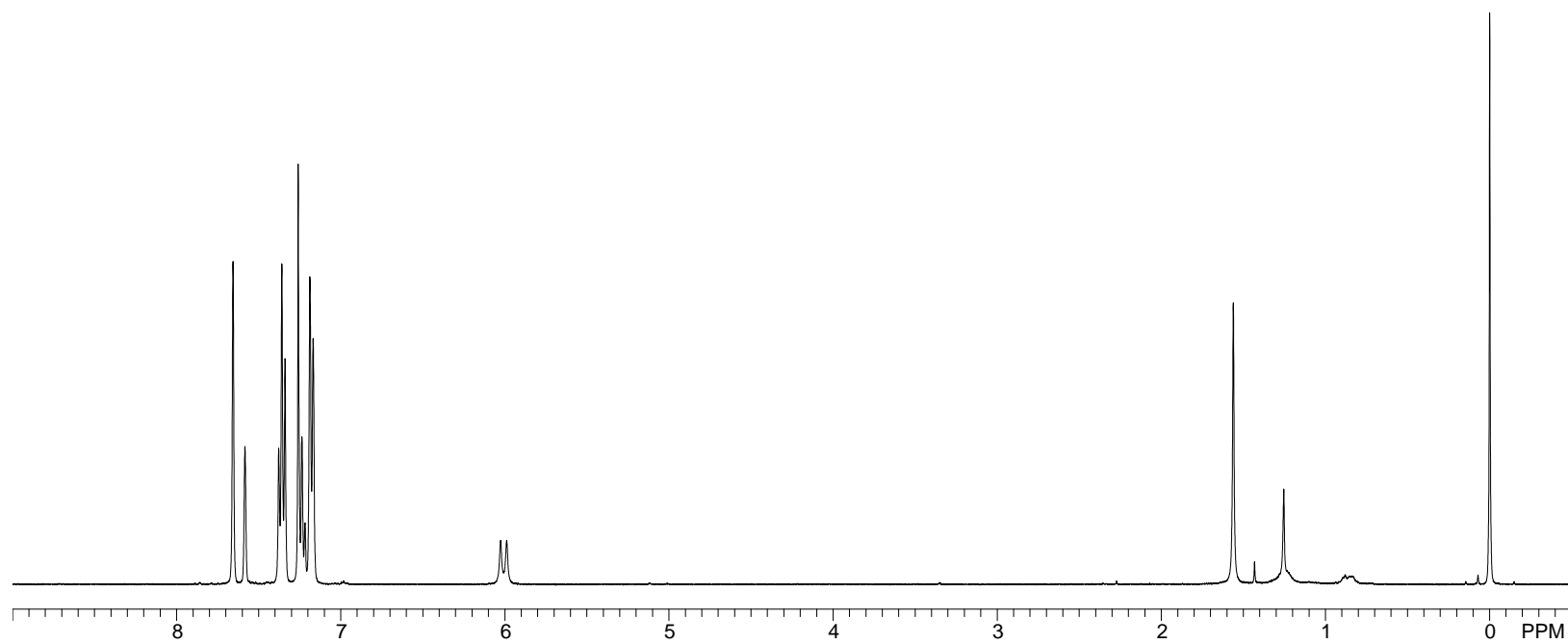
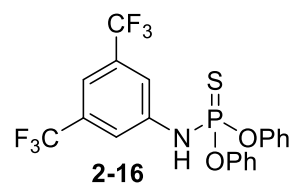
Refine ls weighting details: 'calc $w=1/[\sigma^2(F_o^2)+(0.0689P)^2+0.9239P]$ where $P=(F_o^2+2F_c^2)/3$ '

Atom sites solution primary	direct
-----------------------------	--------

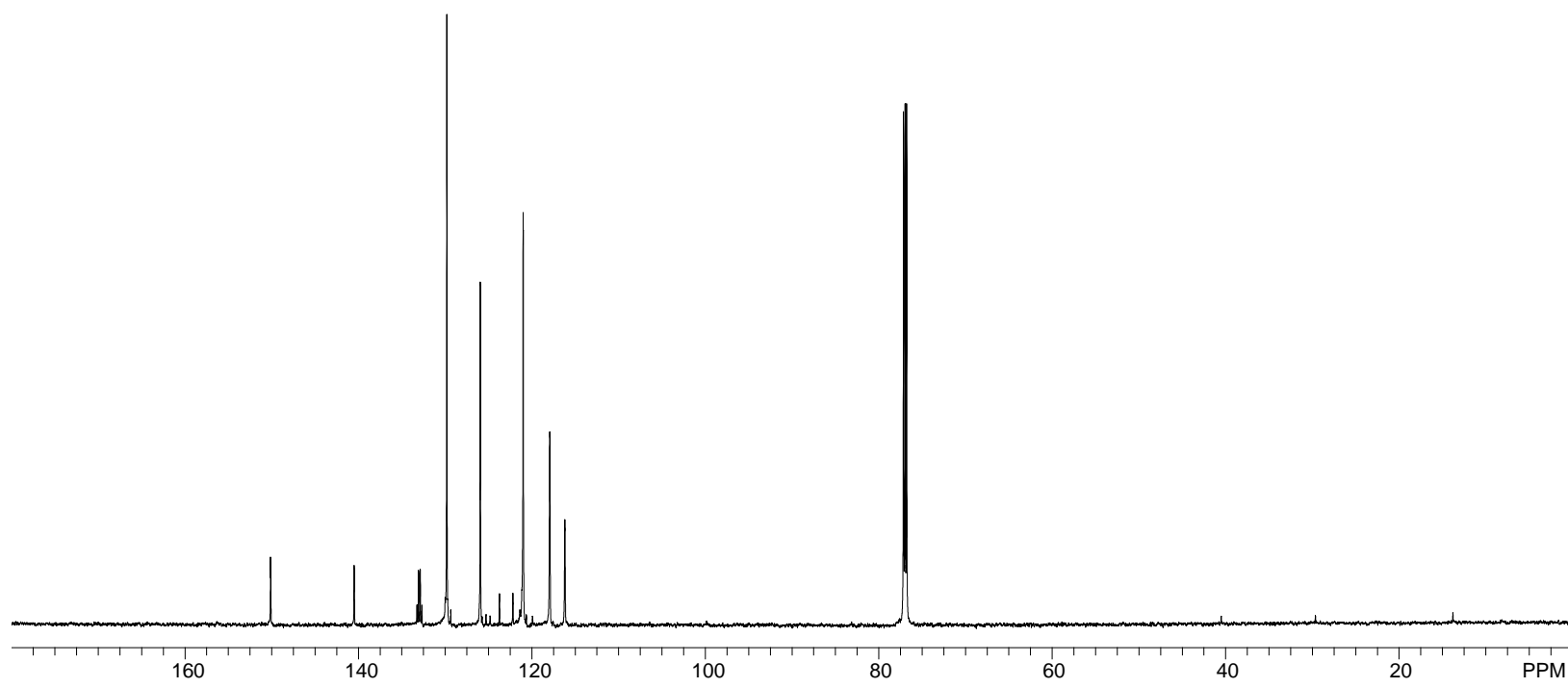
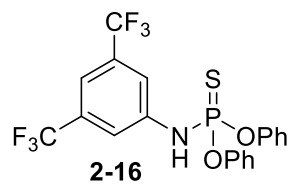
Atom sites solution secondary	difmap
Atom sites solution hydrogens	geom
Refine ls hydrogen treatment	mixed
Refine ls extinction method	none
Refine ls extinction coef	?
Refine ls number reflns	16951
Refine ls number parameters	655
Refine ls number restraints	30
Refine ls R factor all	0.0664
Refine ls R factor gt	0.0474
Refine ls wR factor ref	0.1338
Refine ls wR factor gt	0.1196
Refine ls goodness of fit ref	1.023
Refine ls restrained S all	1.026
Refine ls shift/su max	0.001
Refine ls shift/su mean	0.000

Appendix C

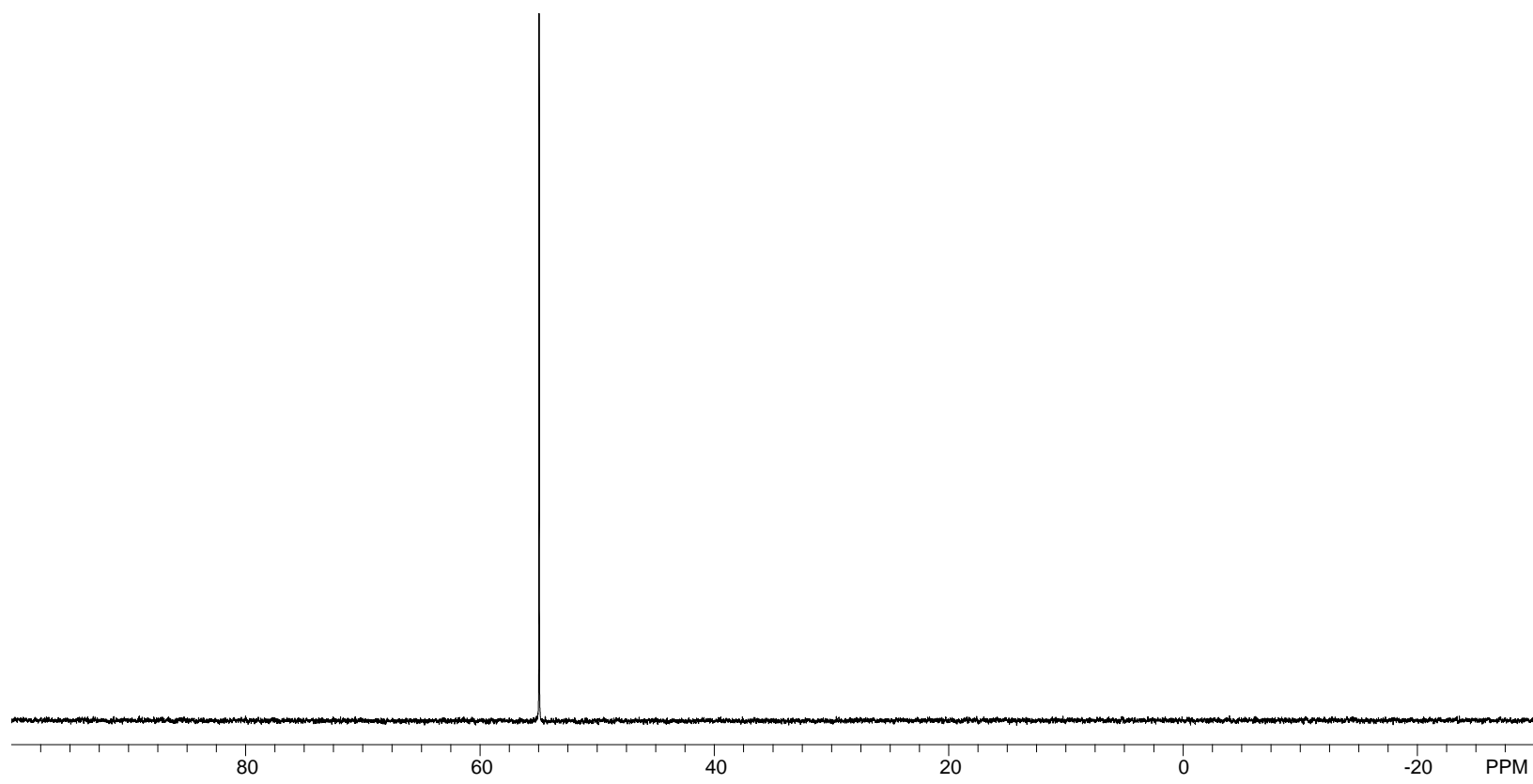
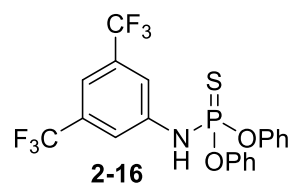
^1H NMR 400 Hz



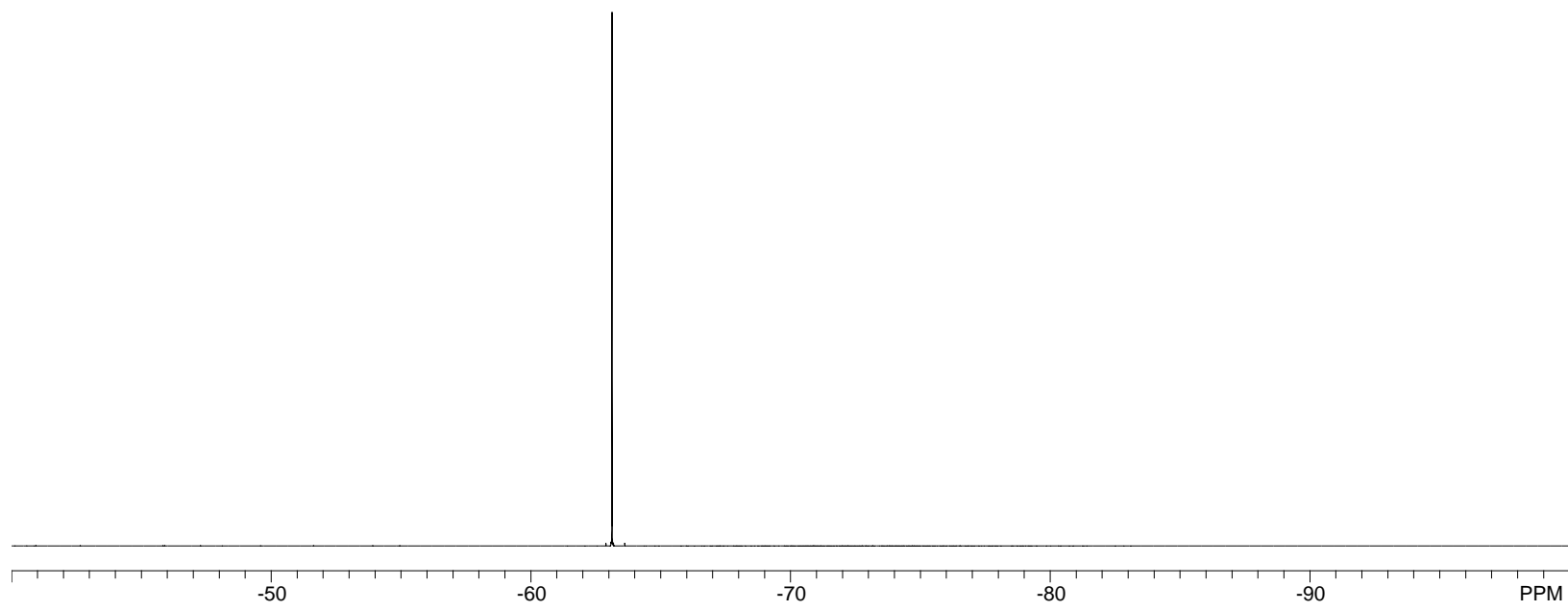
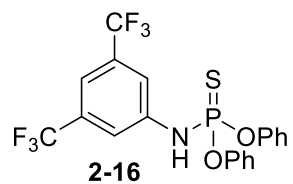
^{13}C NMR, 175 MHz



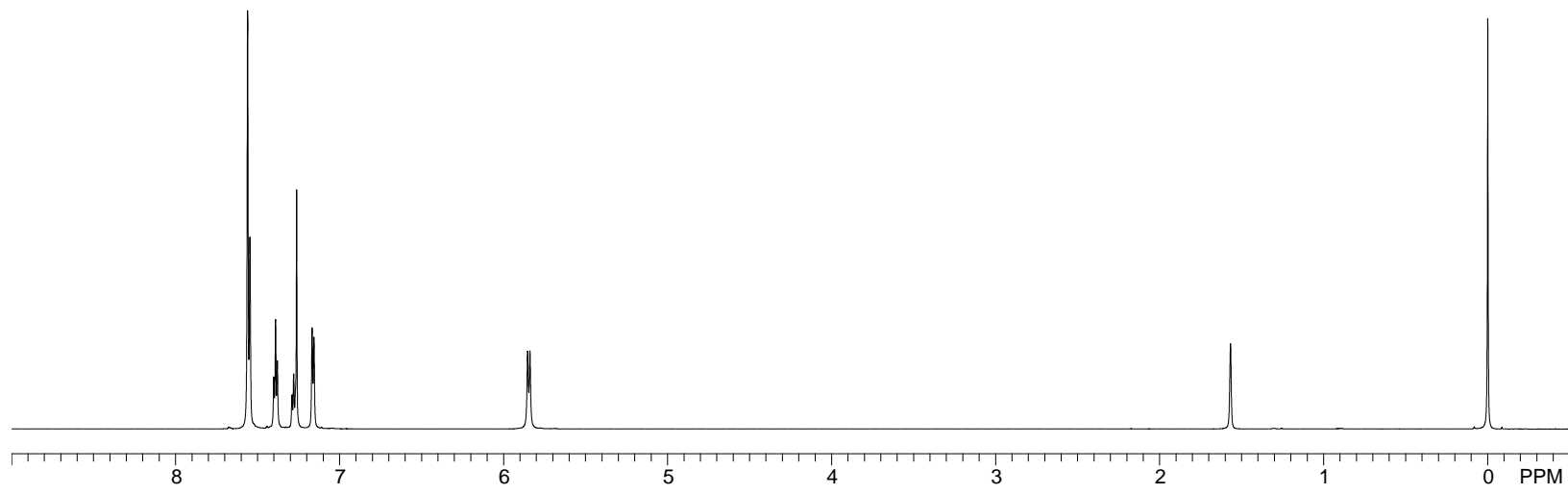
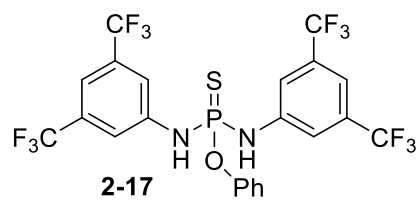
^{31}P NMR, 162 MHz



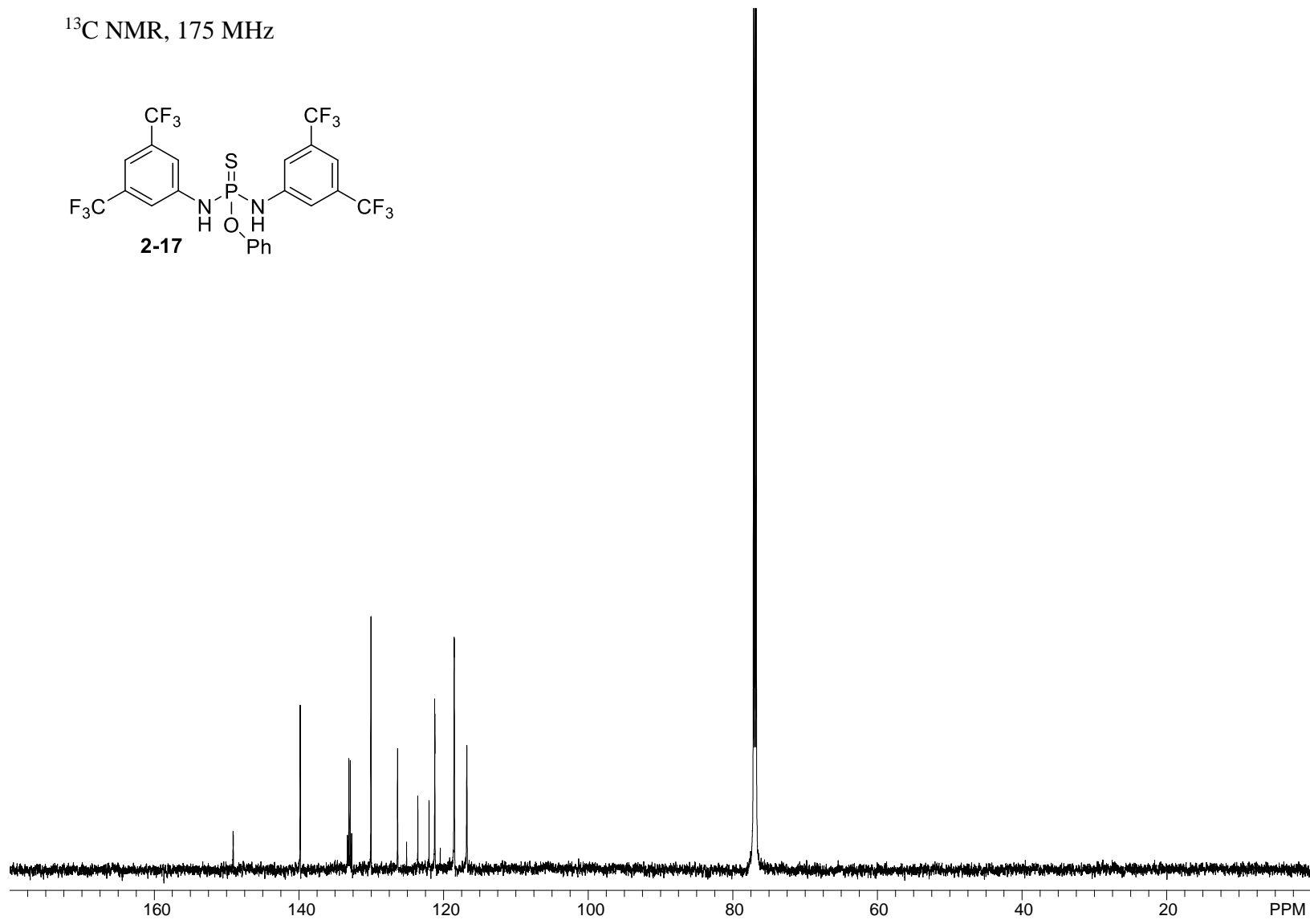
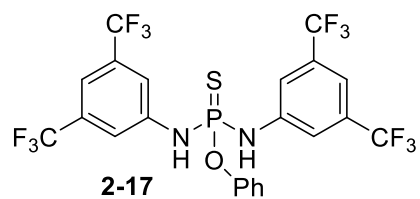
^{19}F NMR, 376 MHz



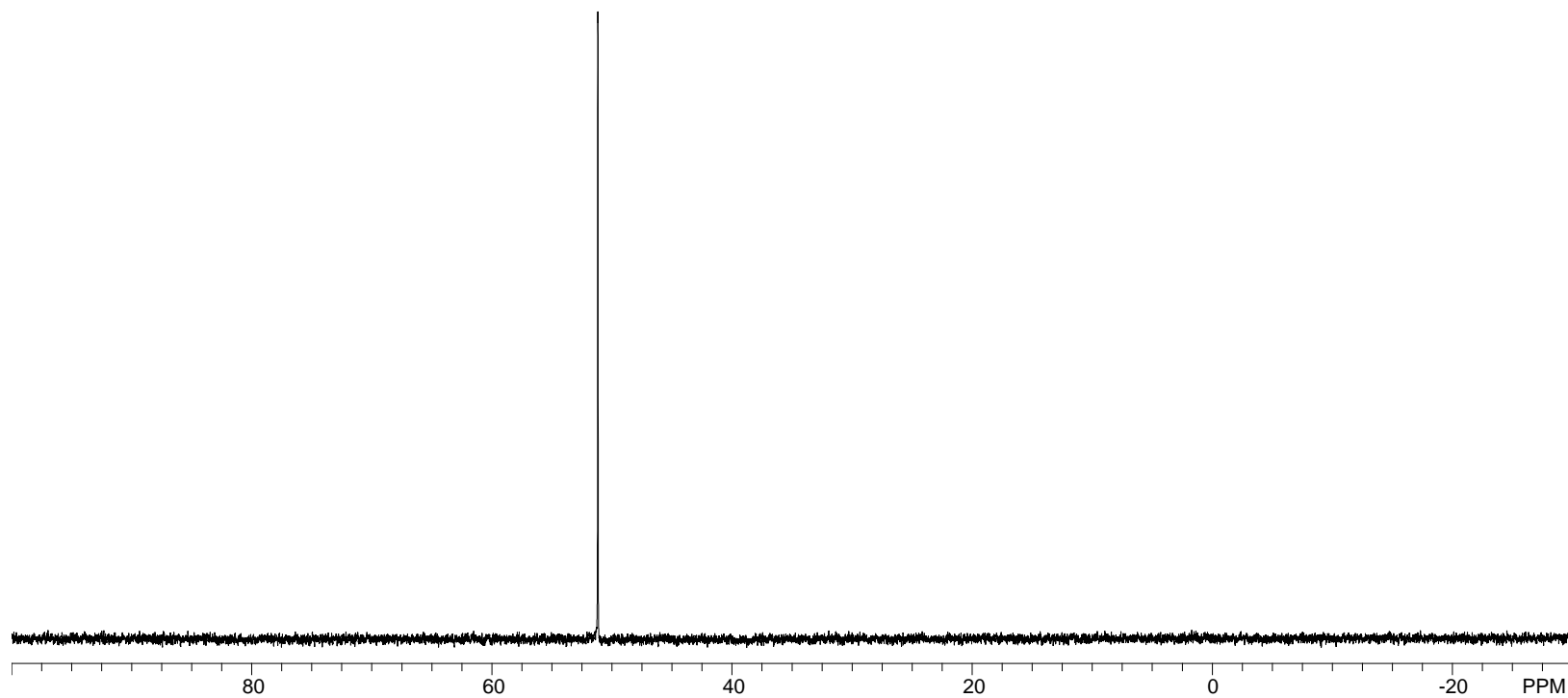
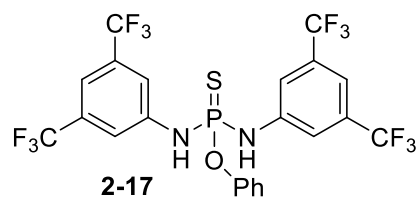
^1H NMR, 700 MHz



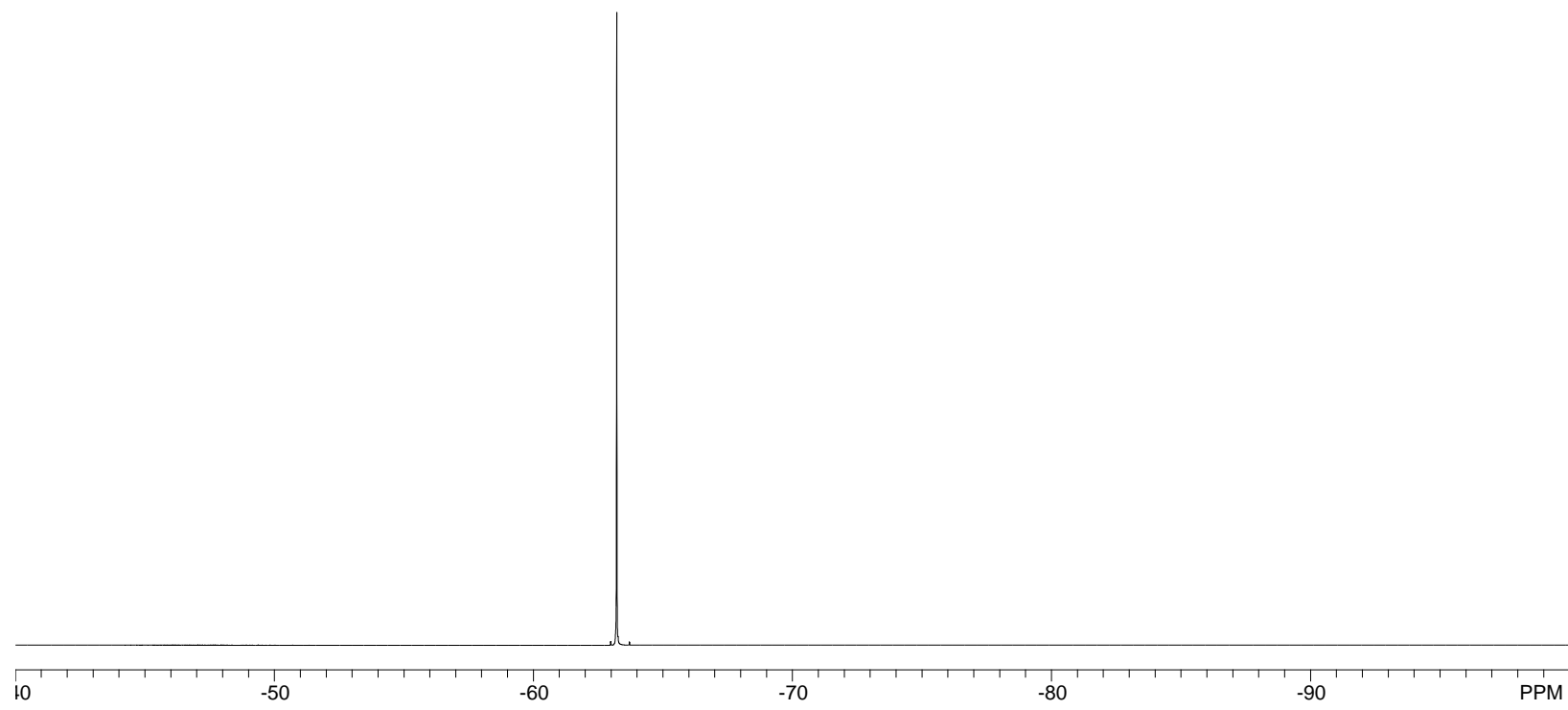
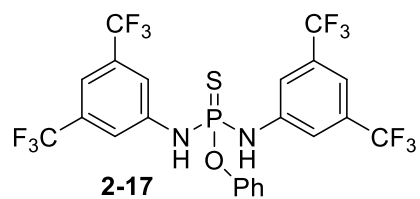
^{13}C NMR, 175 MHz



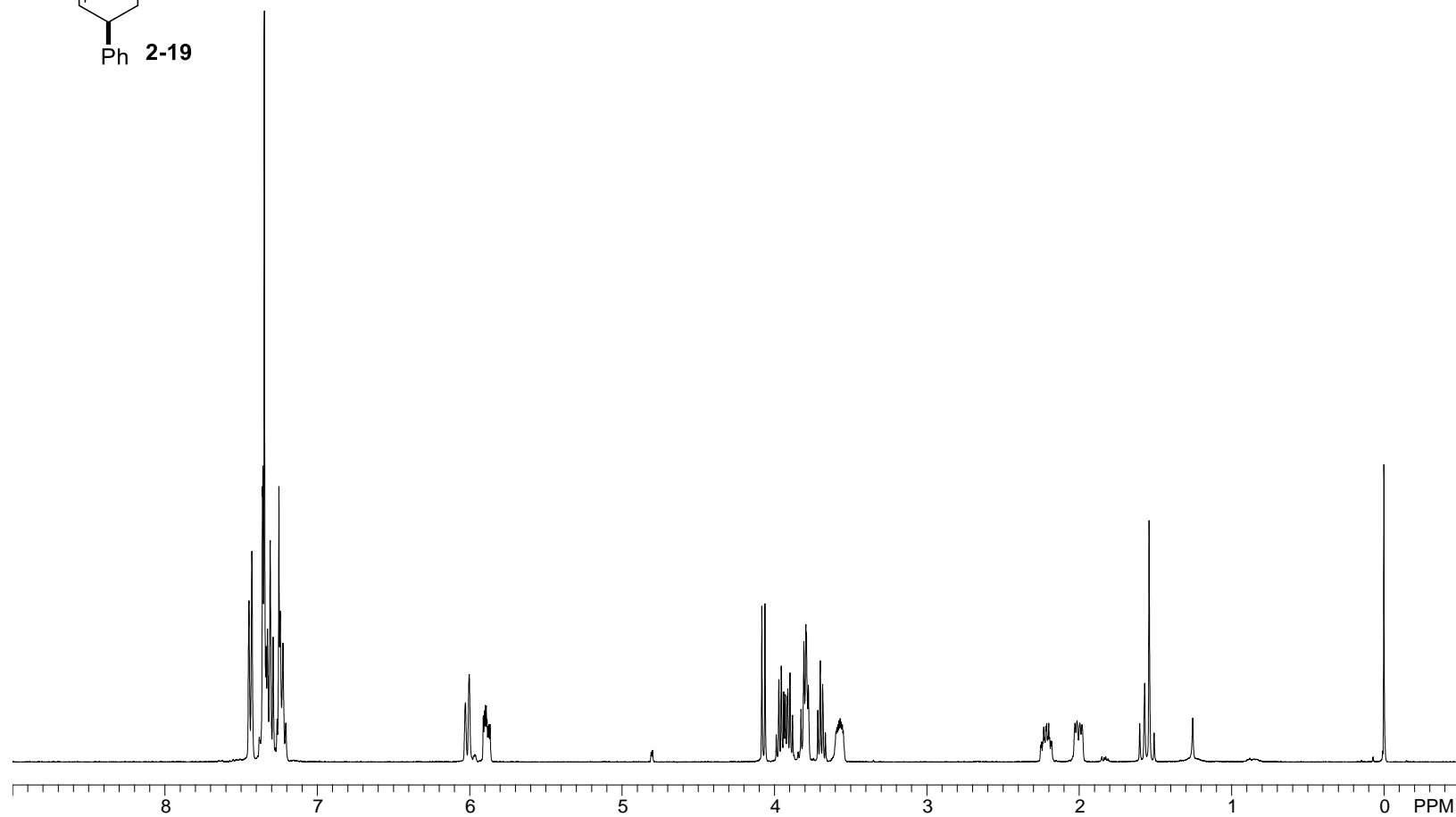
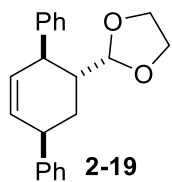
^{31}P NMR, 283 MHz



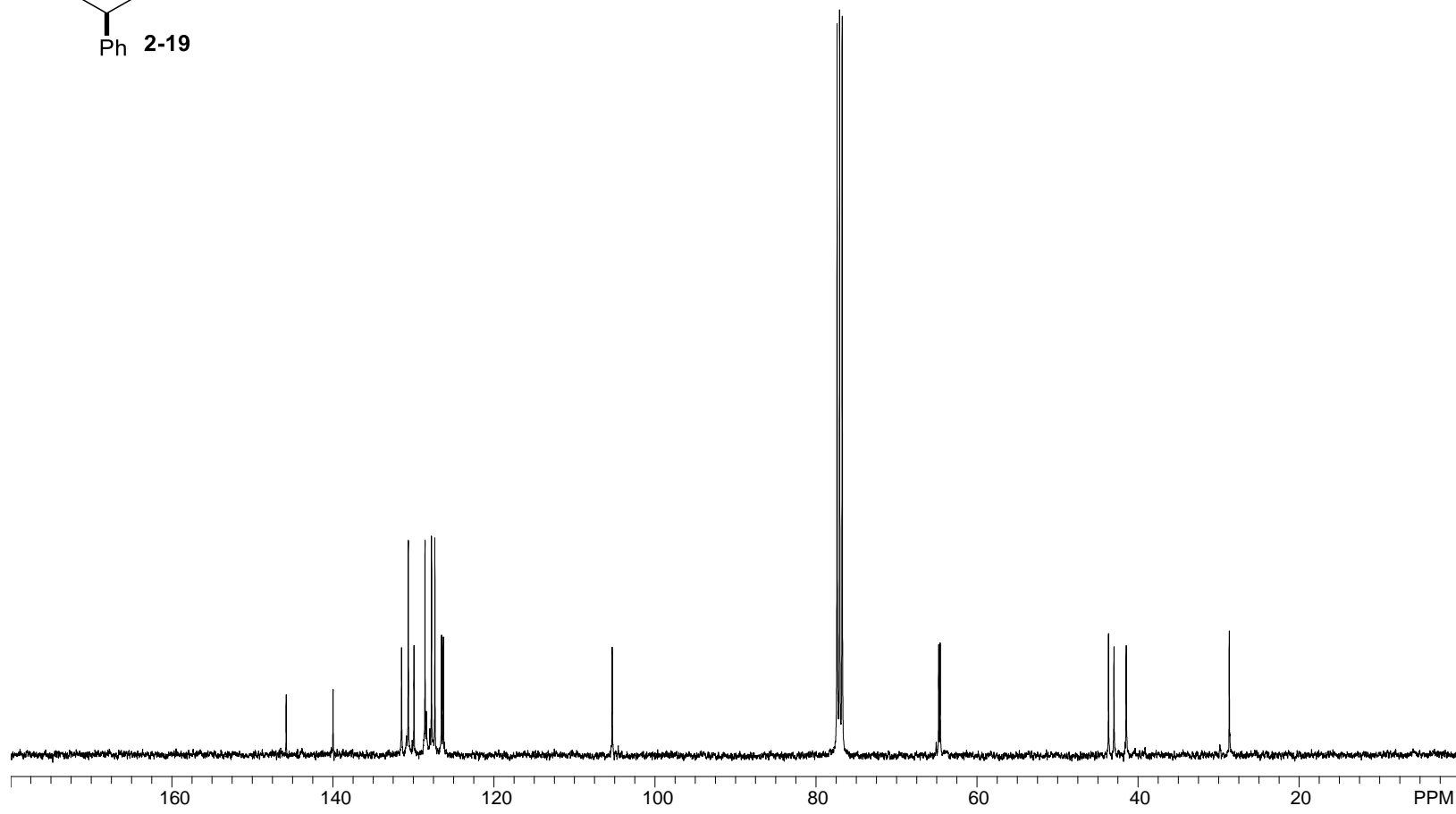
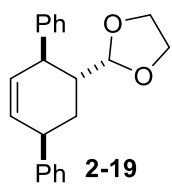
^{19}F NMR, 376 MHz



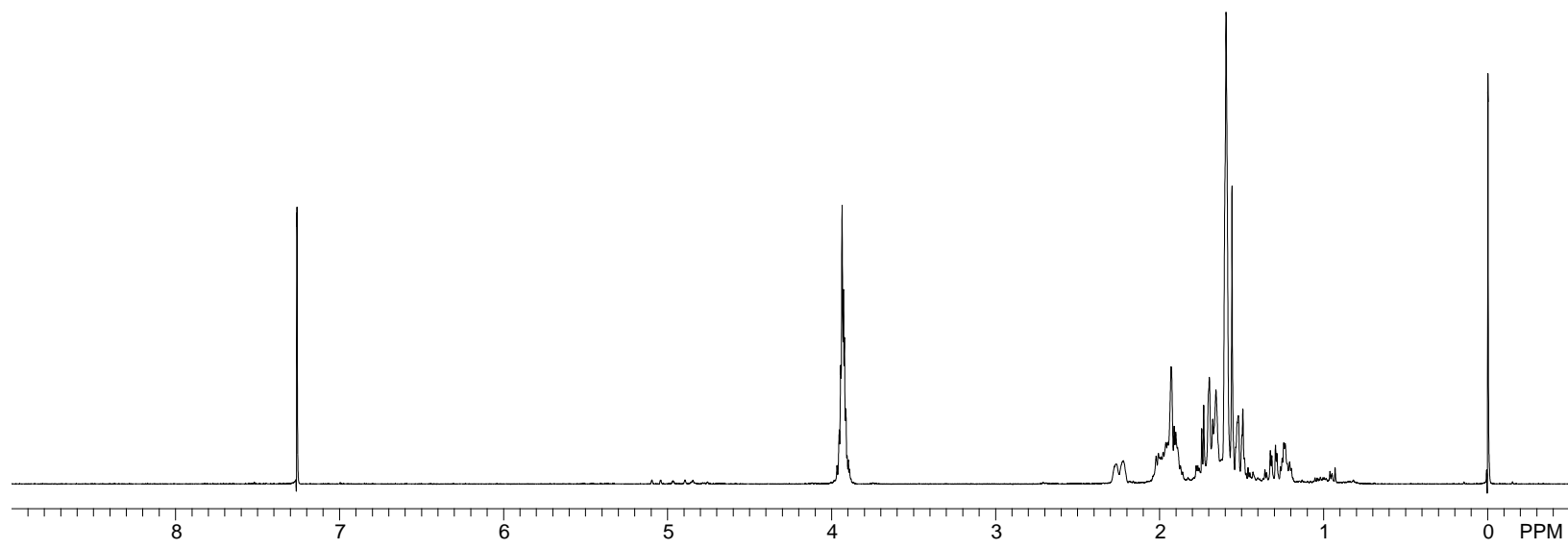
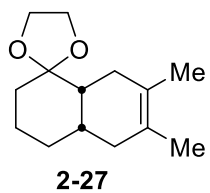
^1H NMR, 400 MHz



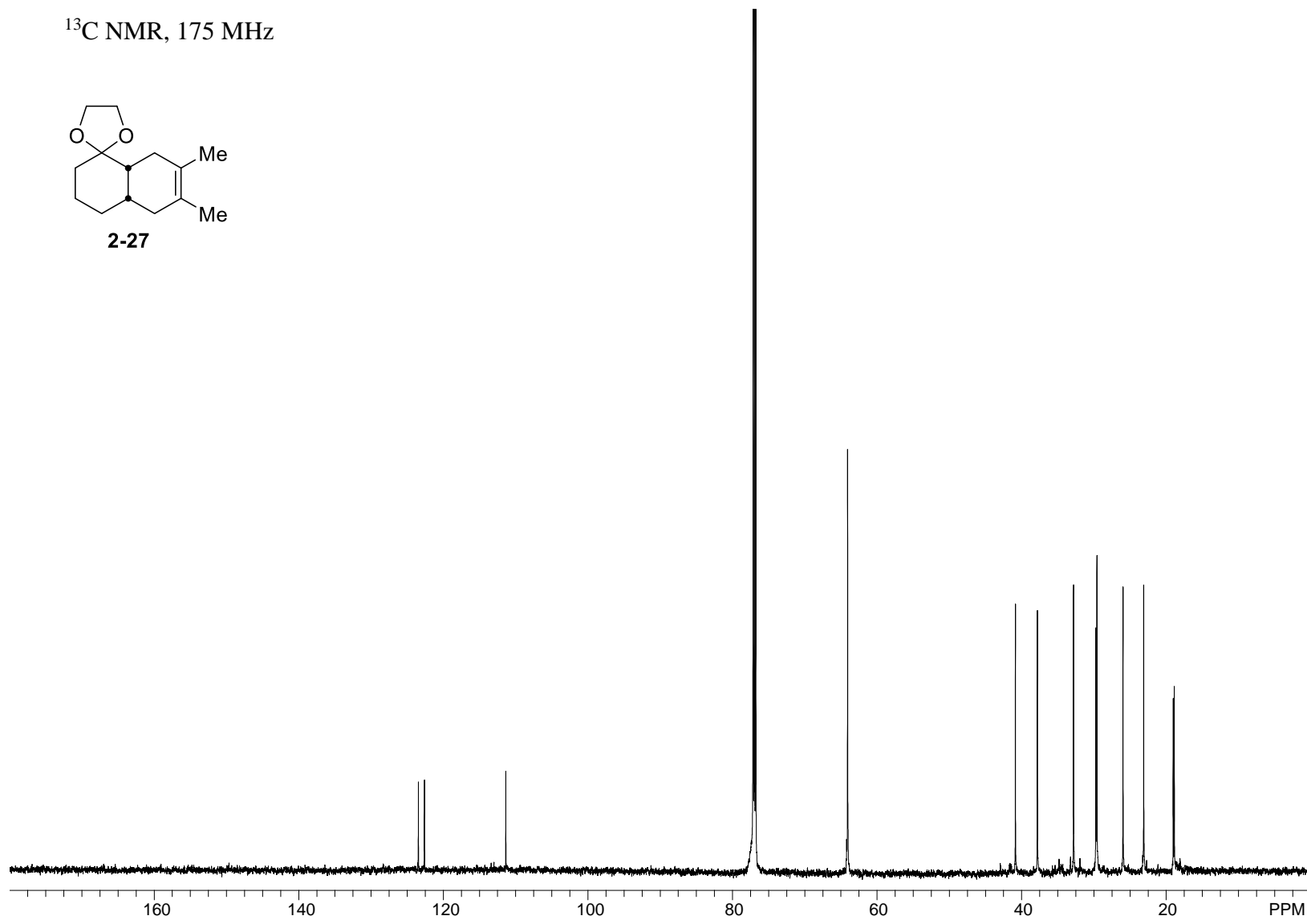
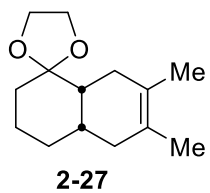
^{13}C NMR, 101 MHz



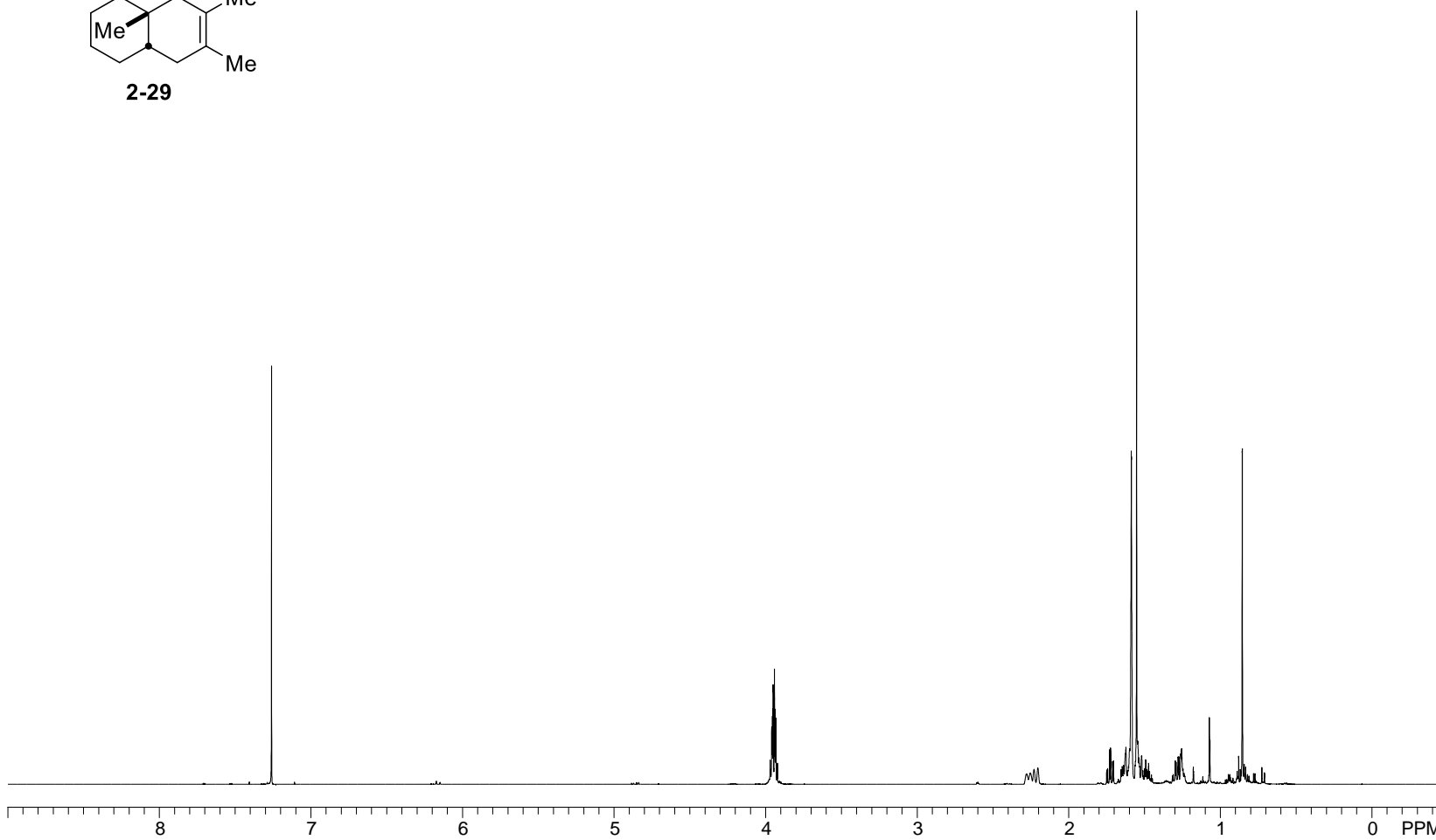
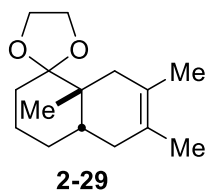
^1H NMR, 400 MHz



^{13}C NMR, 175 MHz

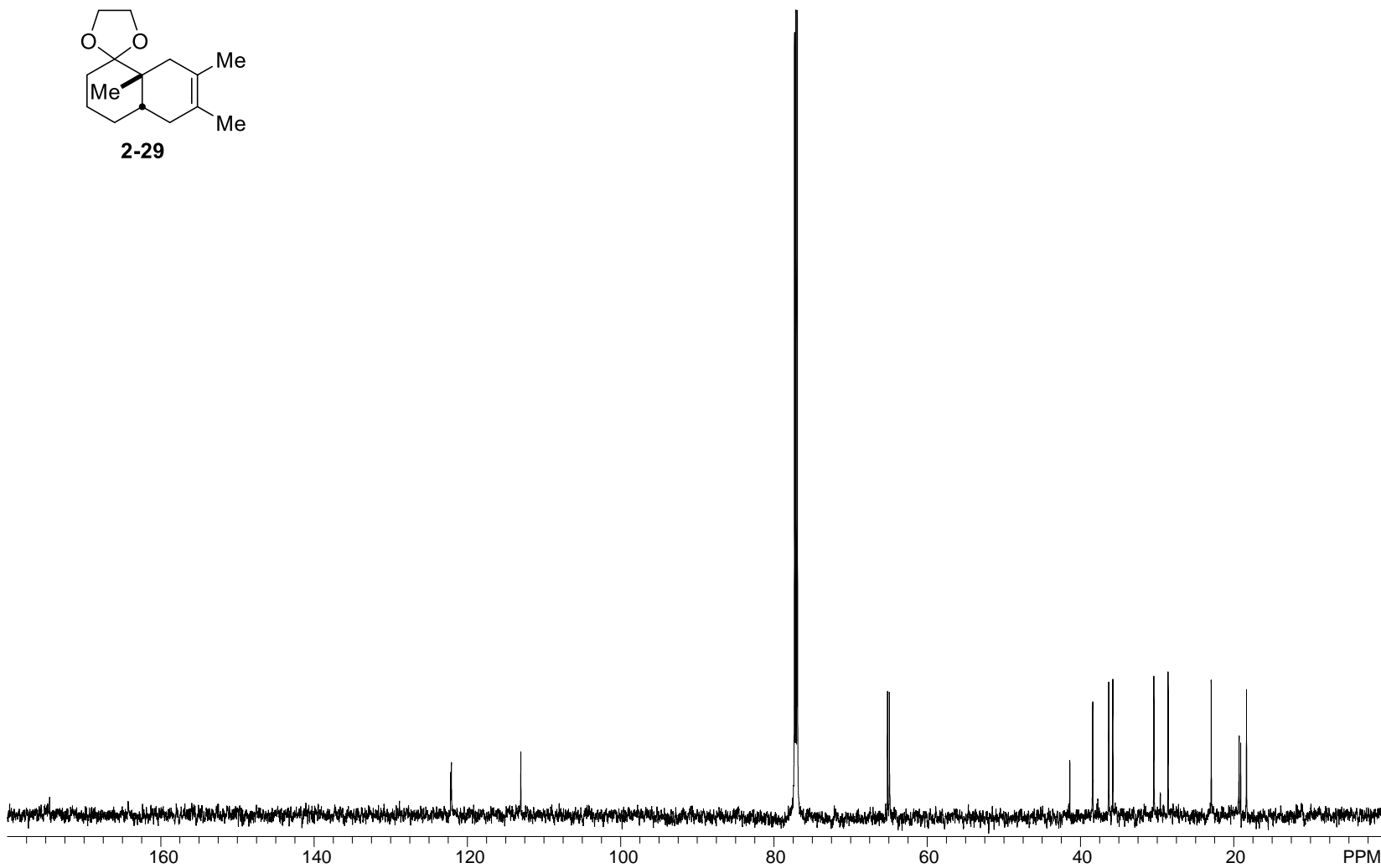
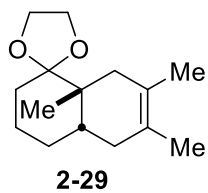


^1H NMR, 700 MHz



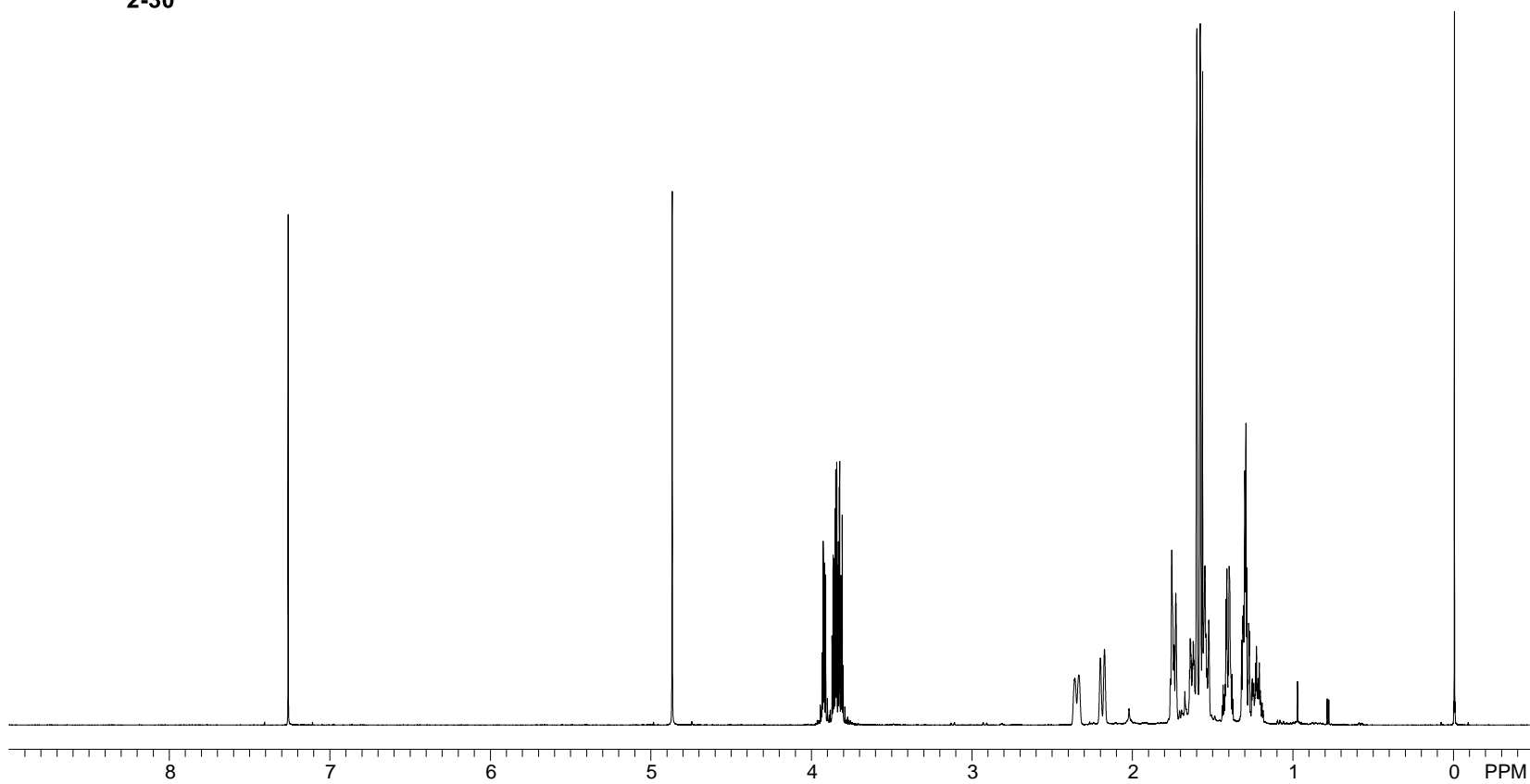
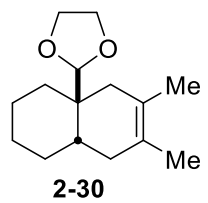
160

^{13}C NMR, 175 MHz

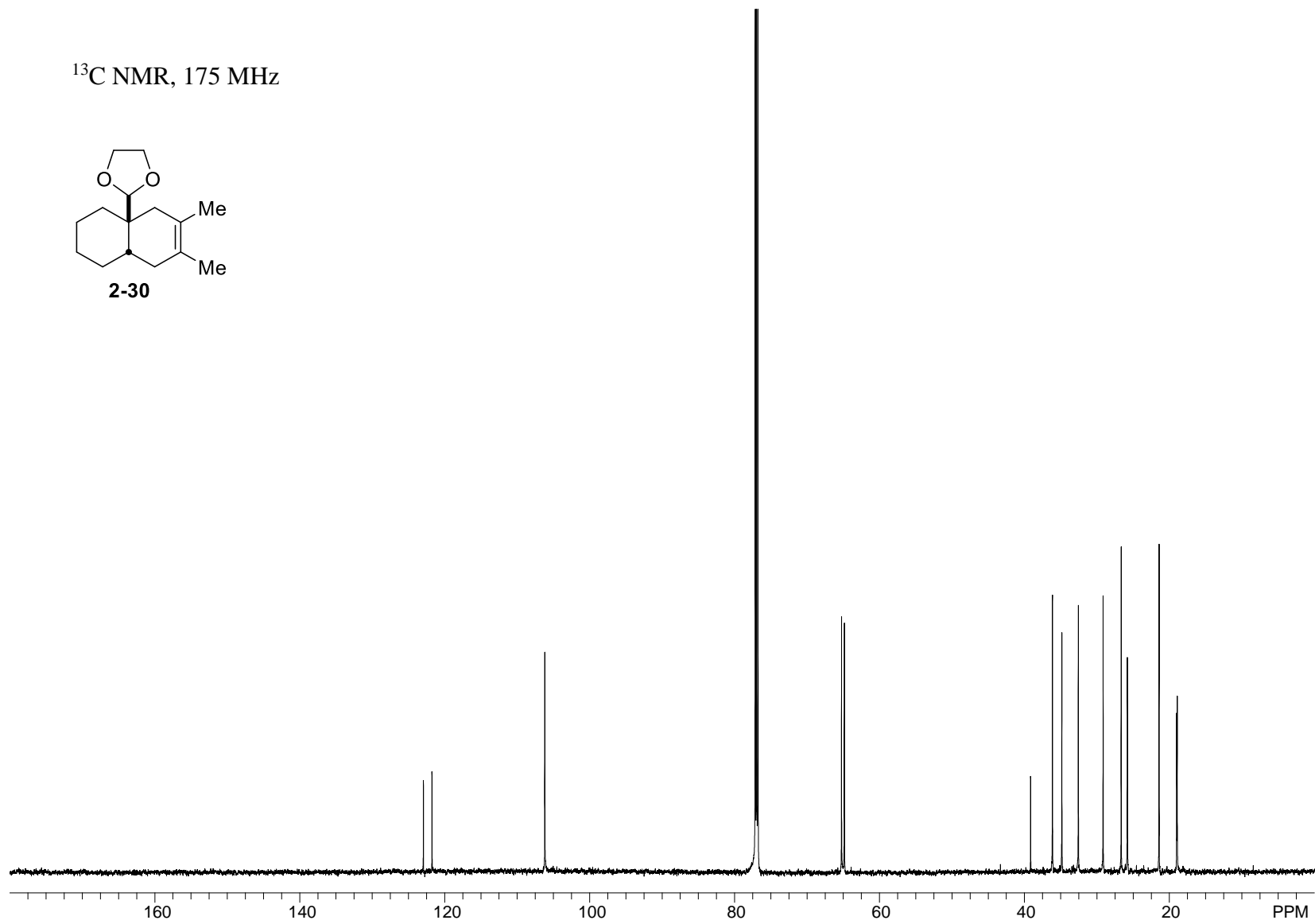
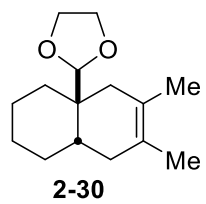


161

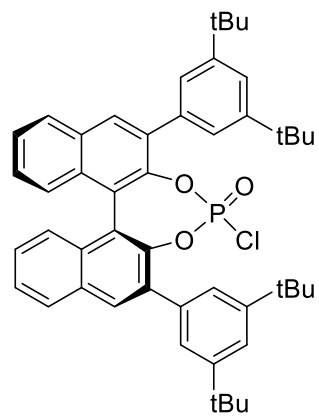
^1H NMR, 700 MHz



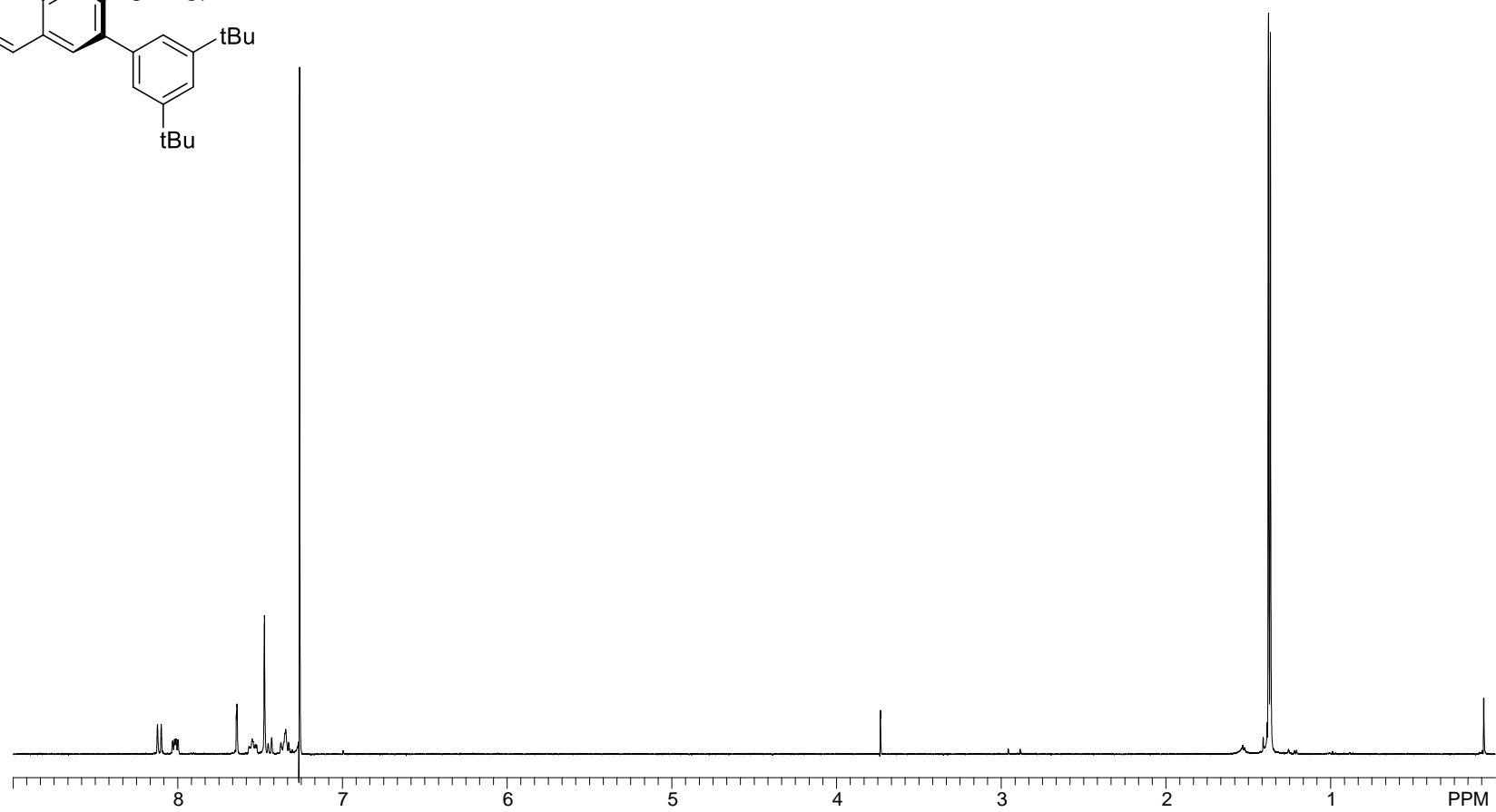
^{13}C NMR, 175 MHz

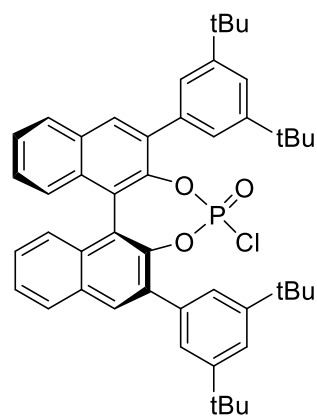


163

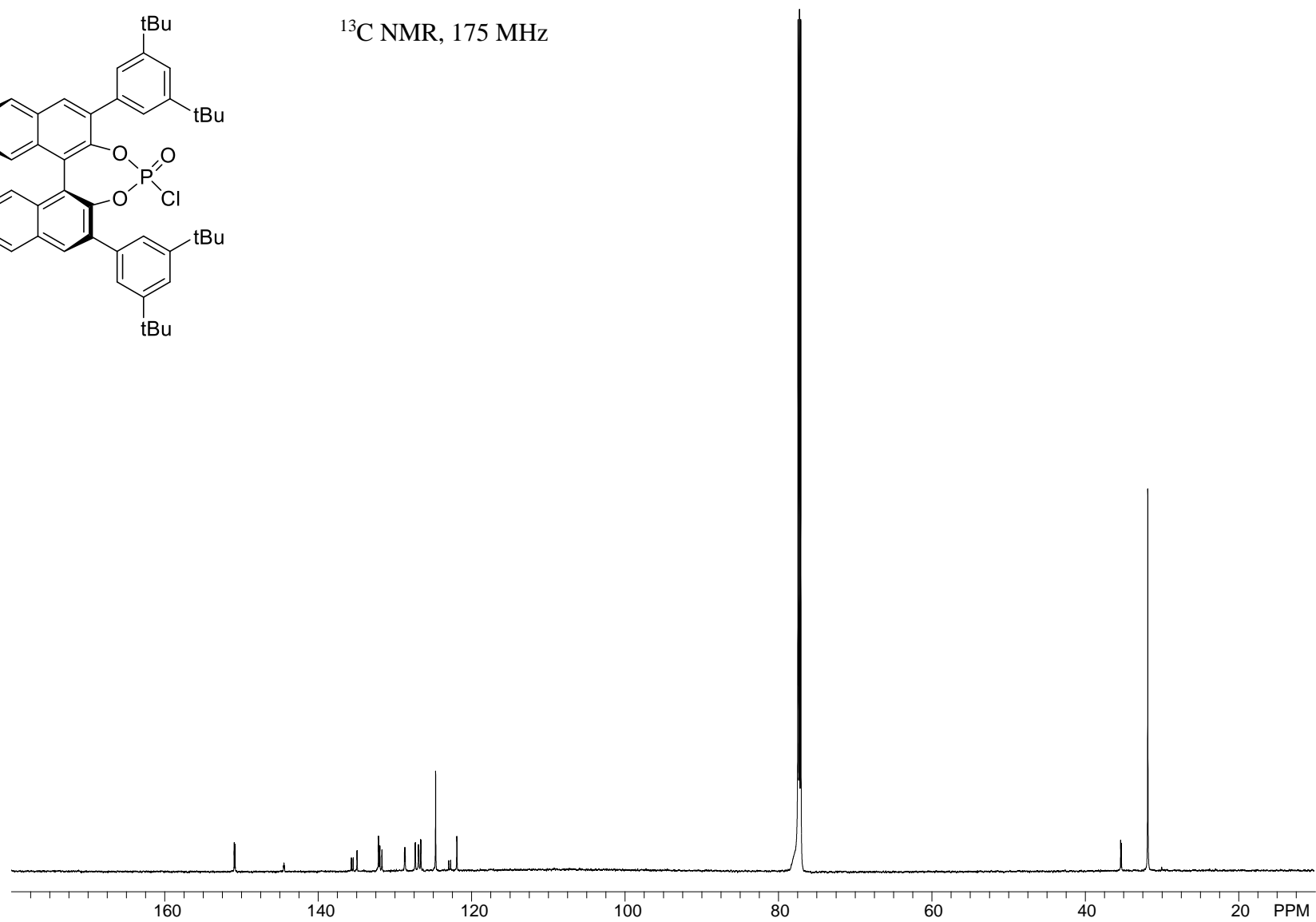


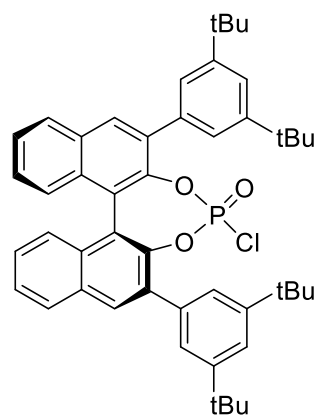
^1H NMR, 400 MHz



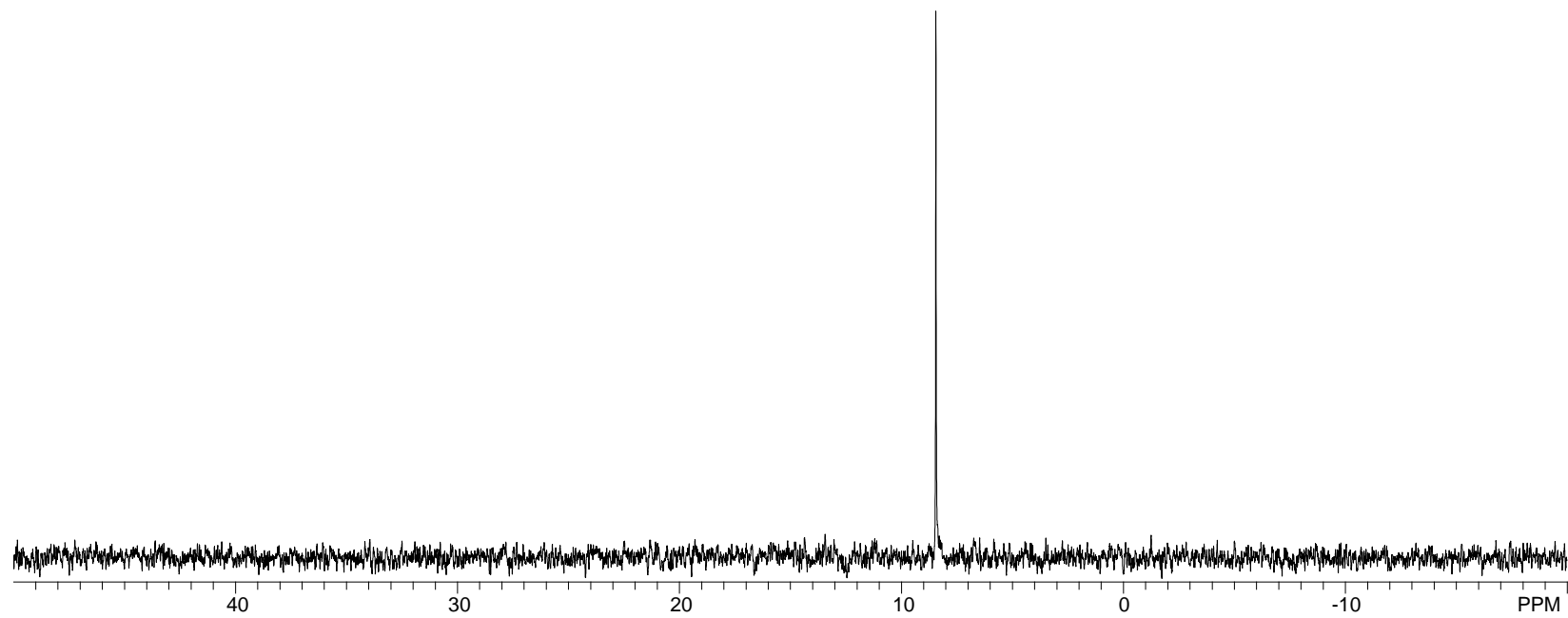


^{13}C NMR, 175 MHz

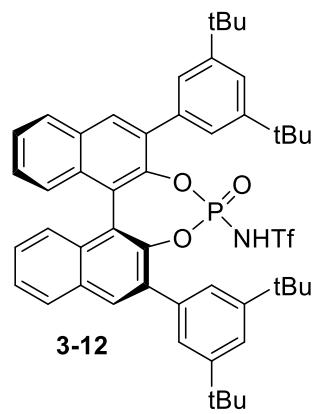




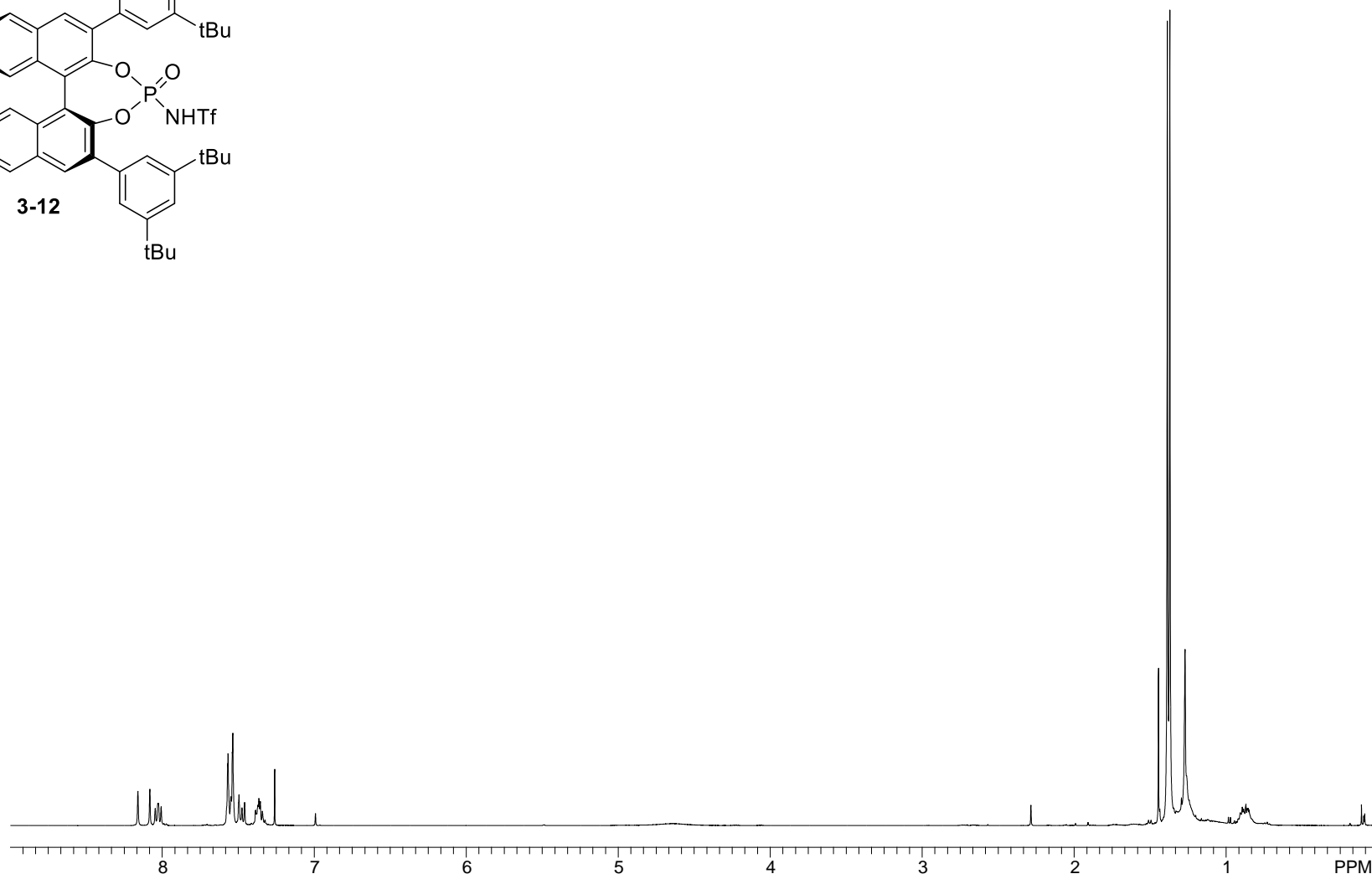
^{31}P NMR, 202 MHz

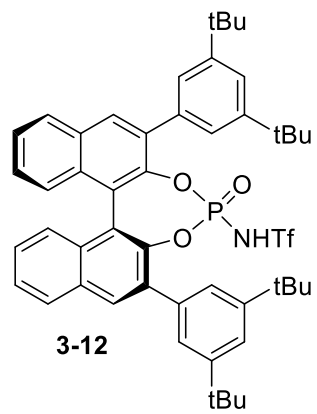


166

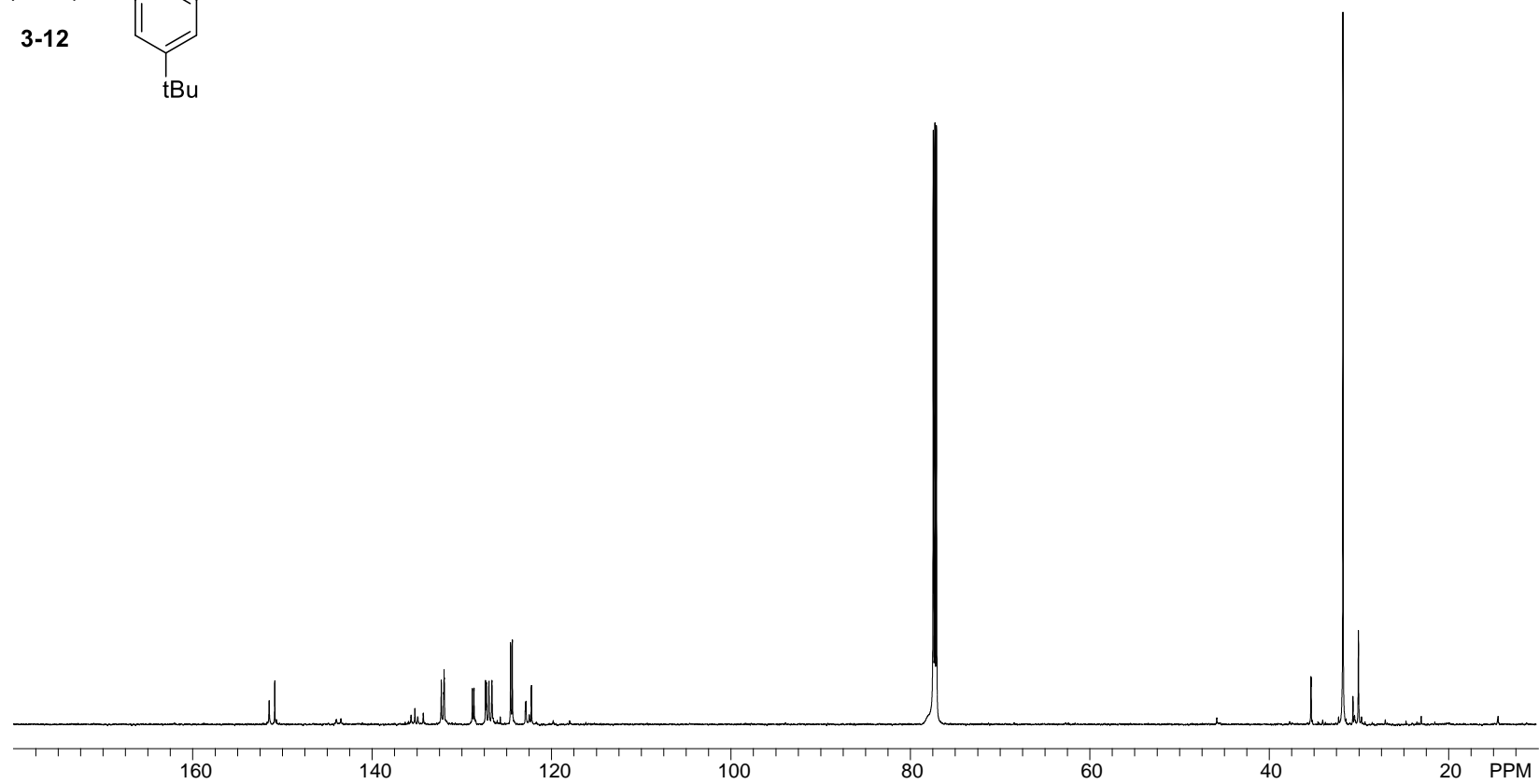


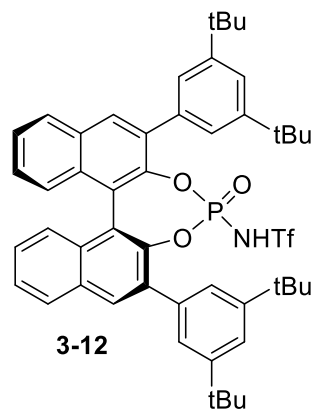
^1H NMR, 500 MHz



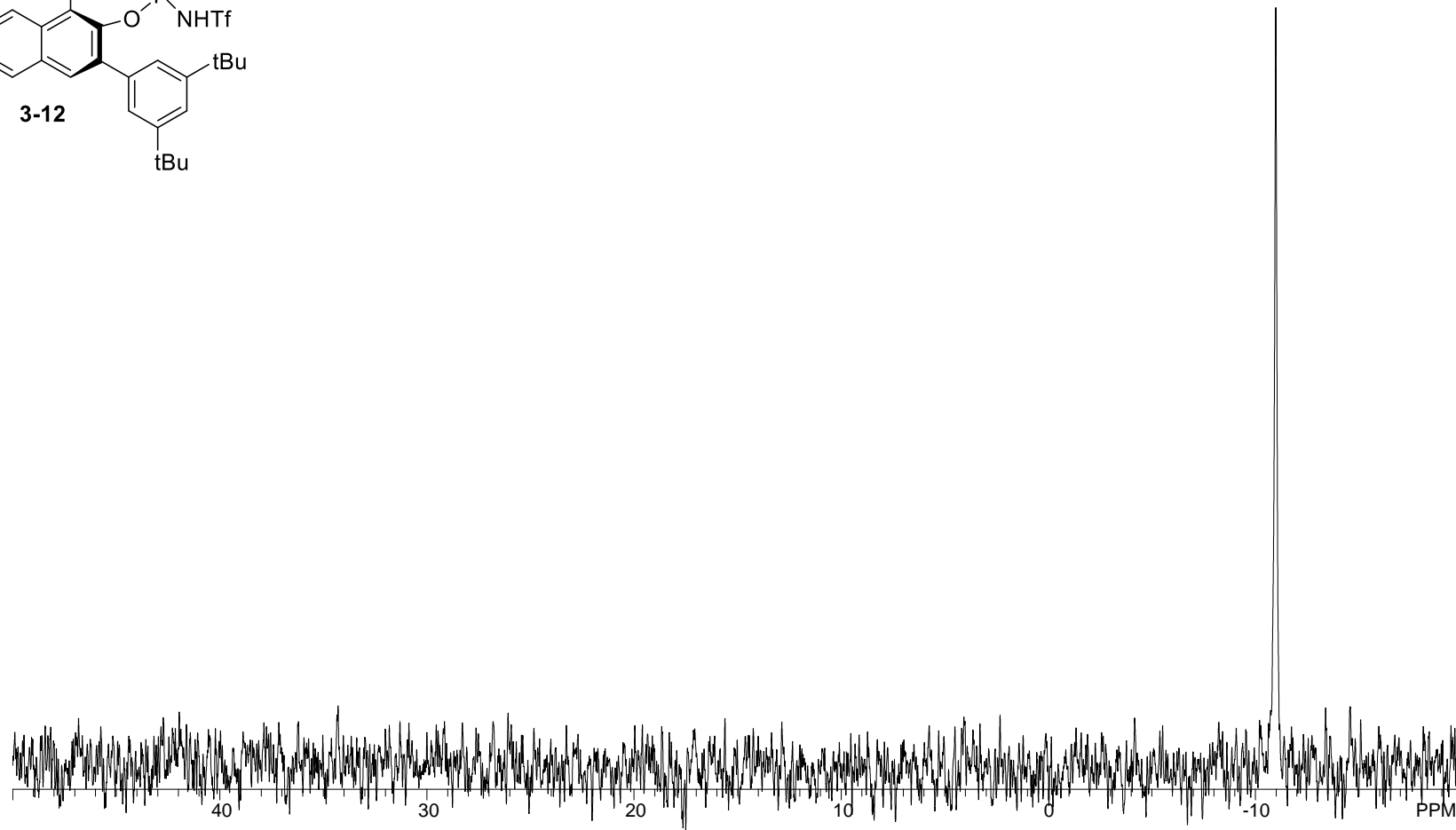


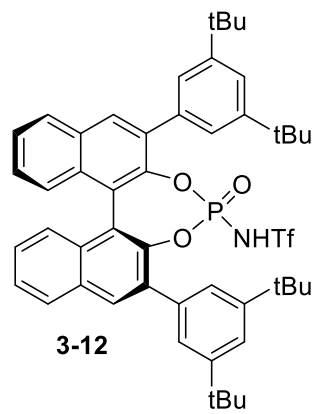
^{13}C NMR, 175



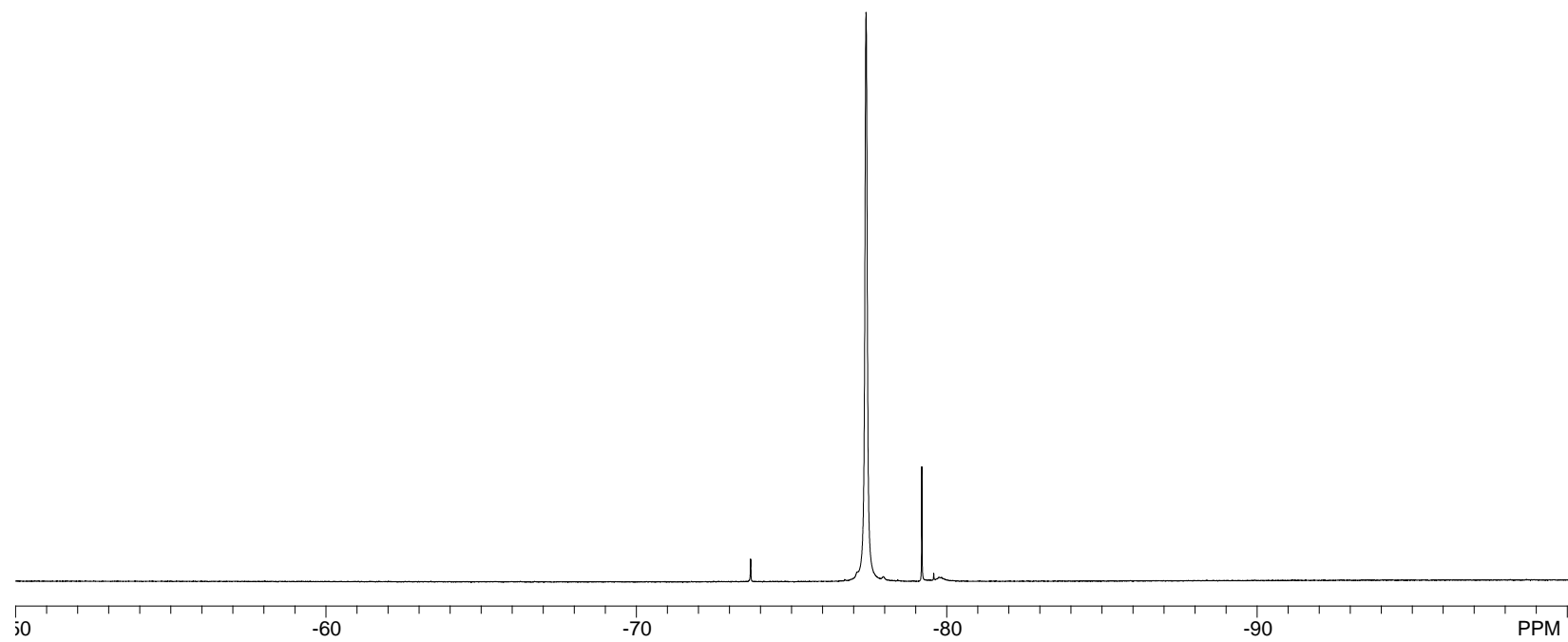


^{31}P NMR, 283 MHz

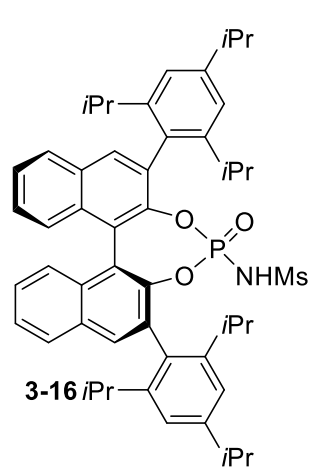




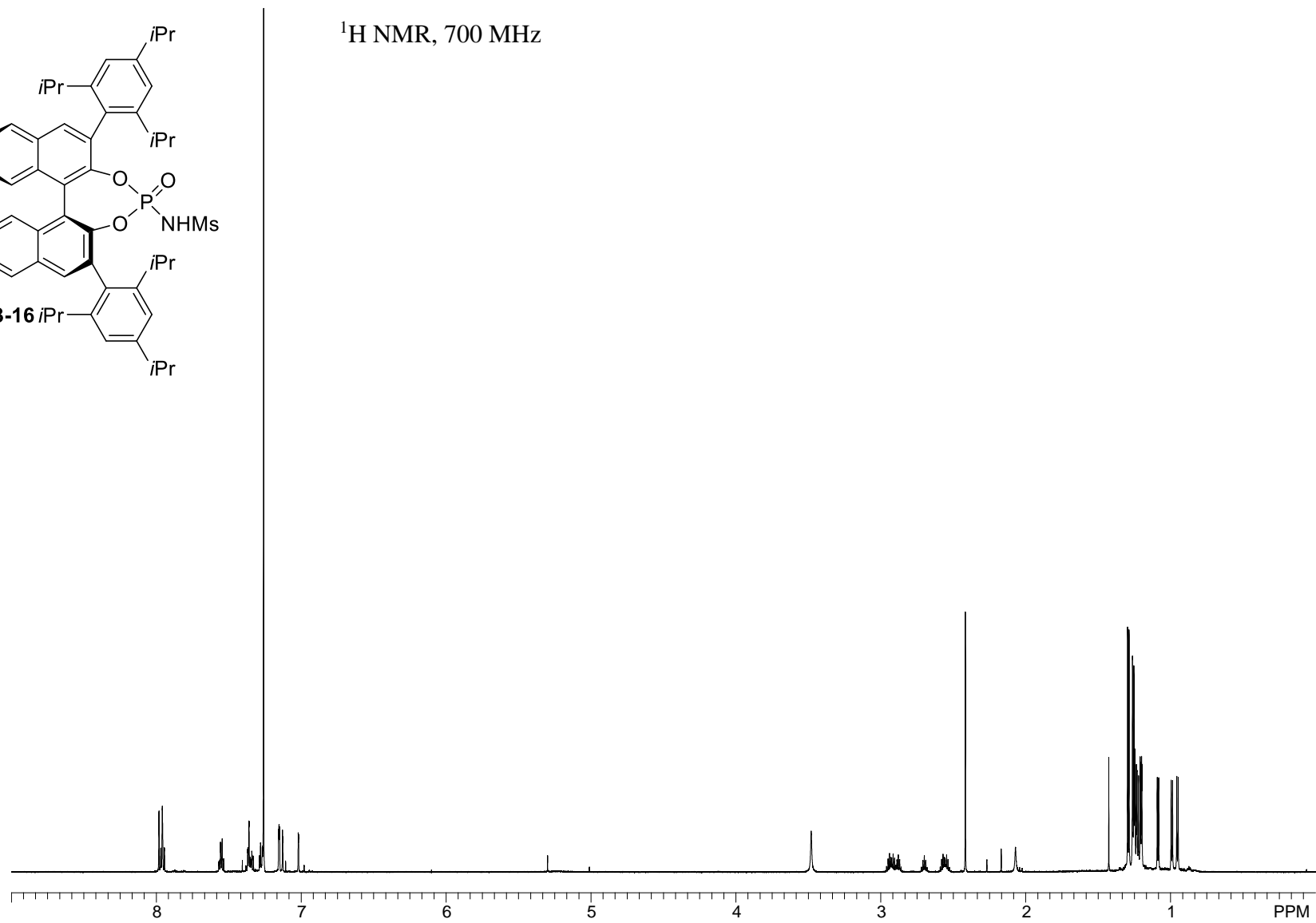
^{19}F NMR, 376 MHz

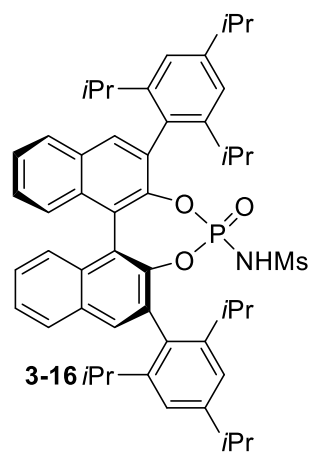


170

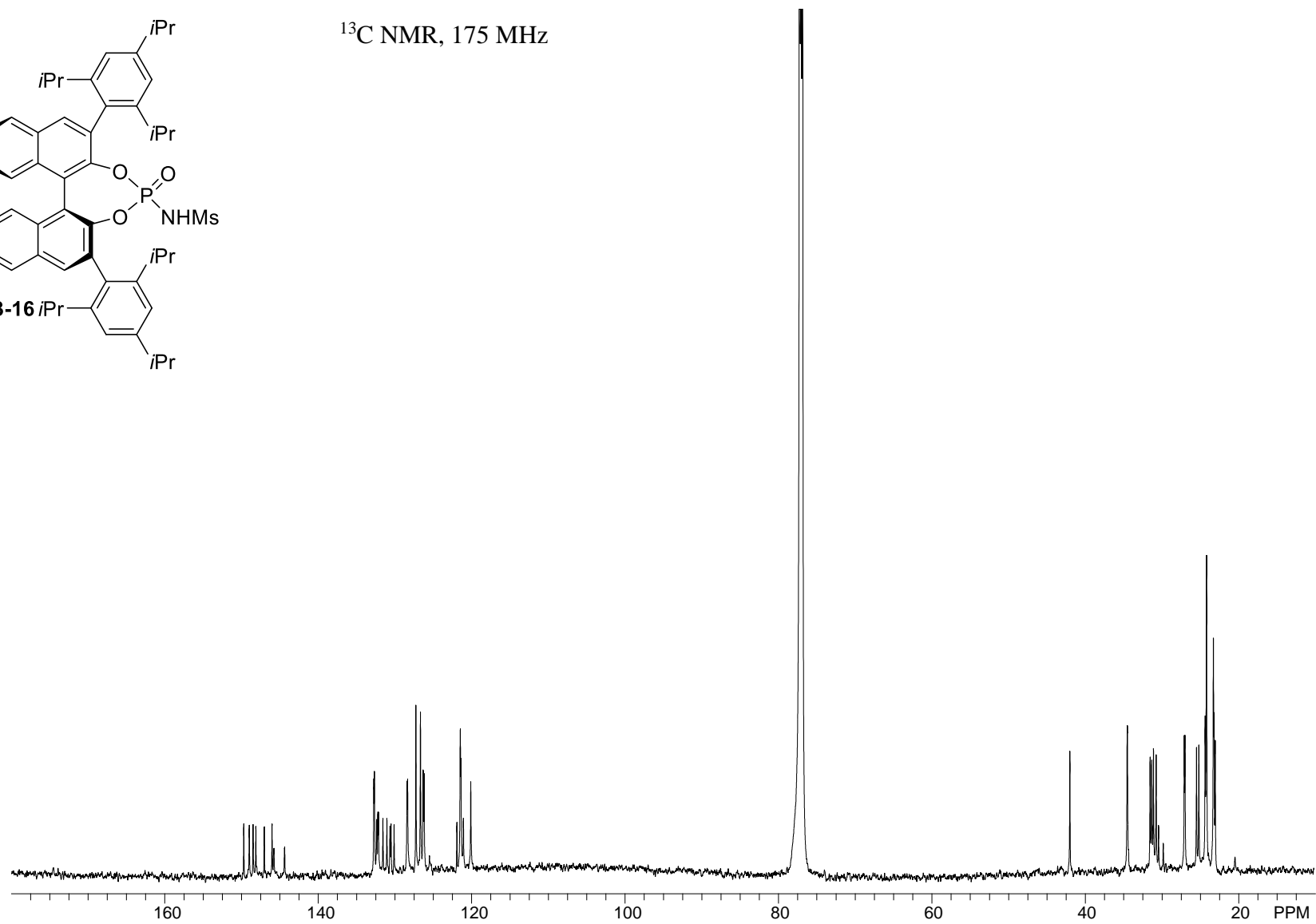


^1H NMR, 700 MHz

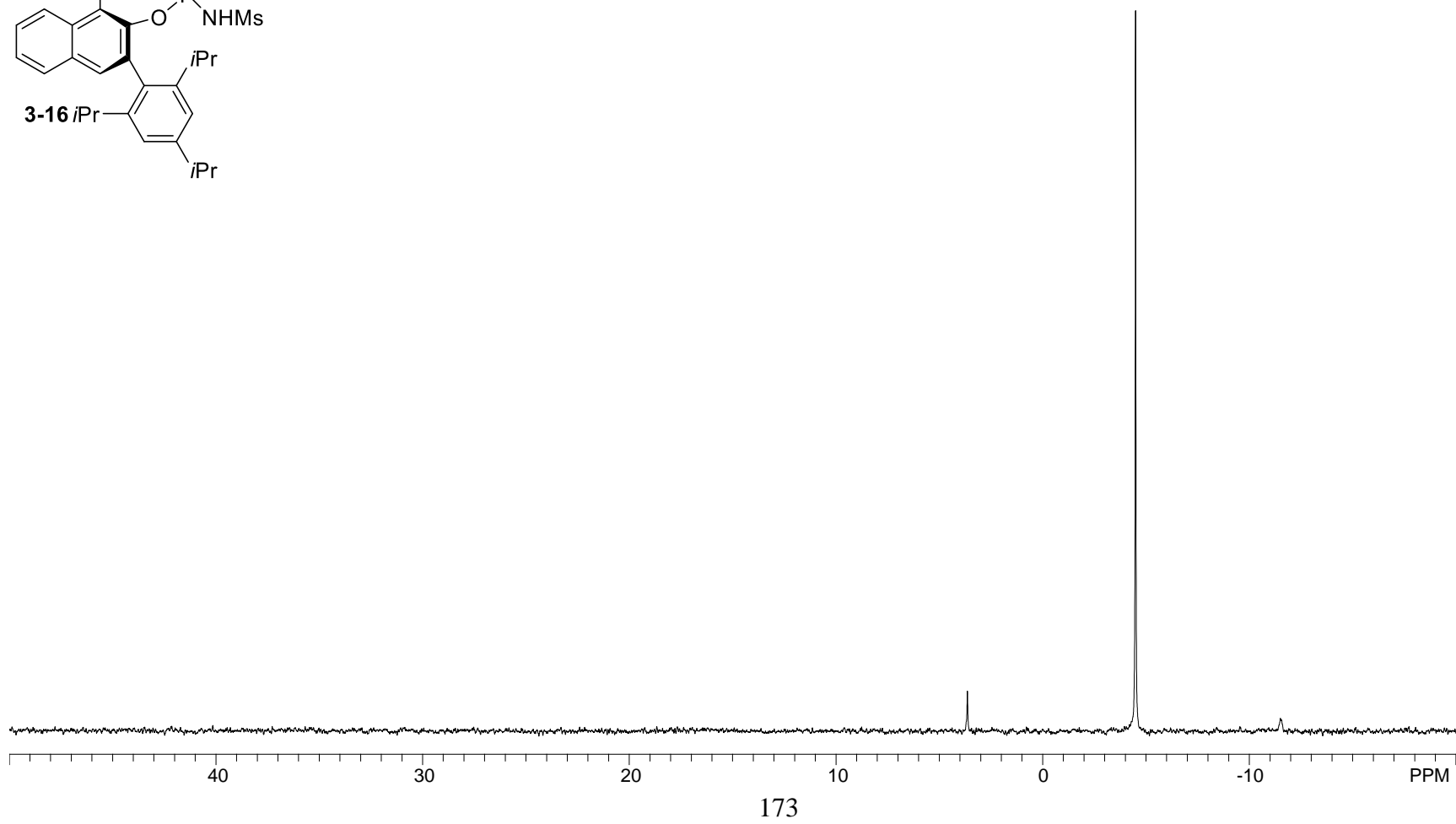
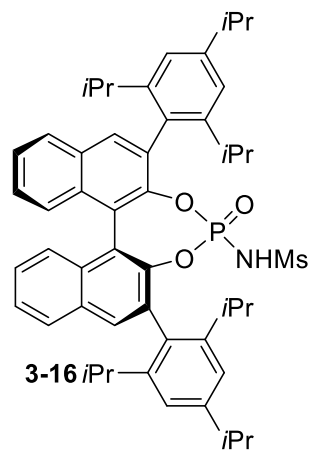




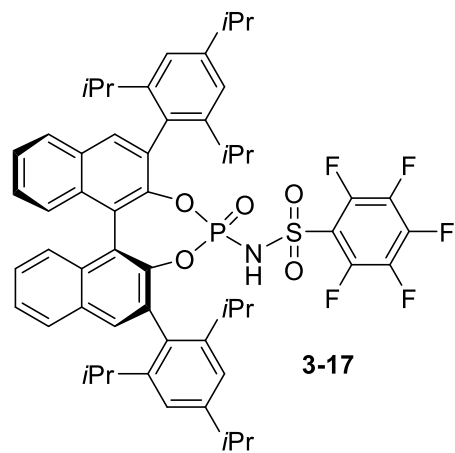
^{13}C NMR, 175 MHz



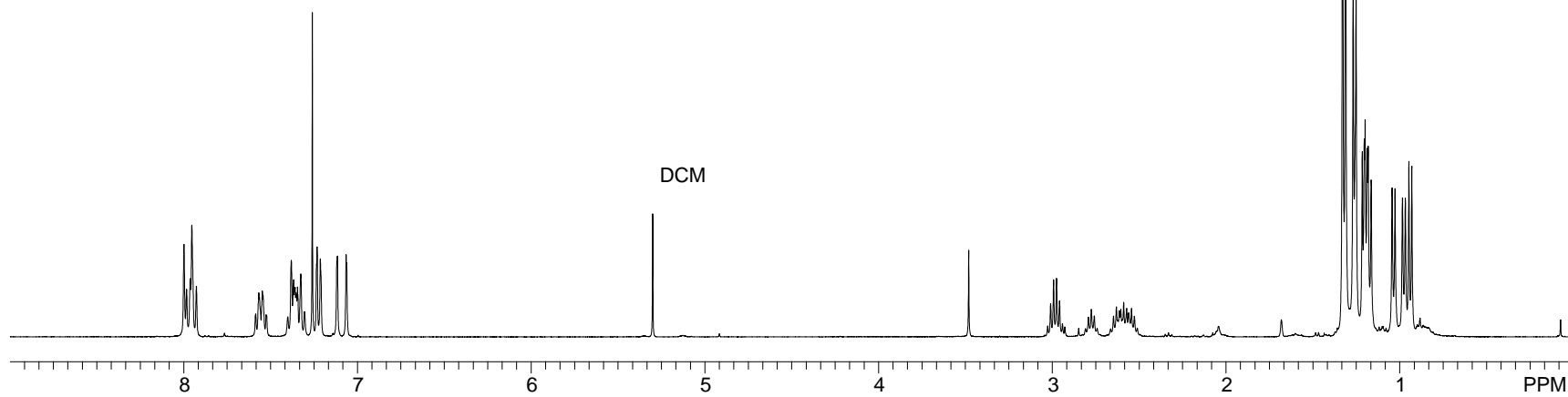
^{31}P NMR, 202 MHz

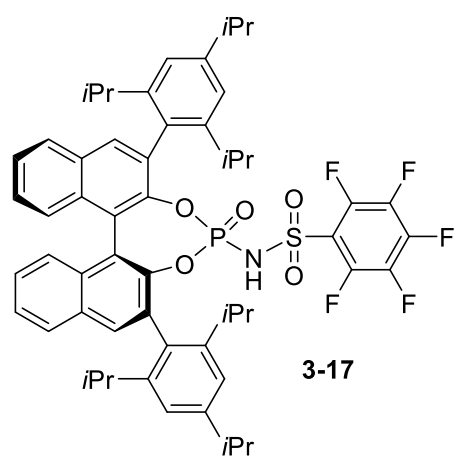


^1H NMR, 700 MHz

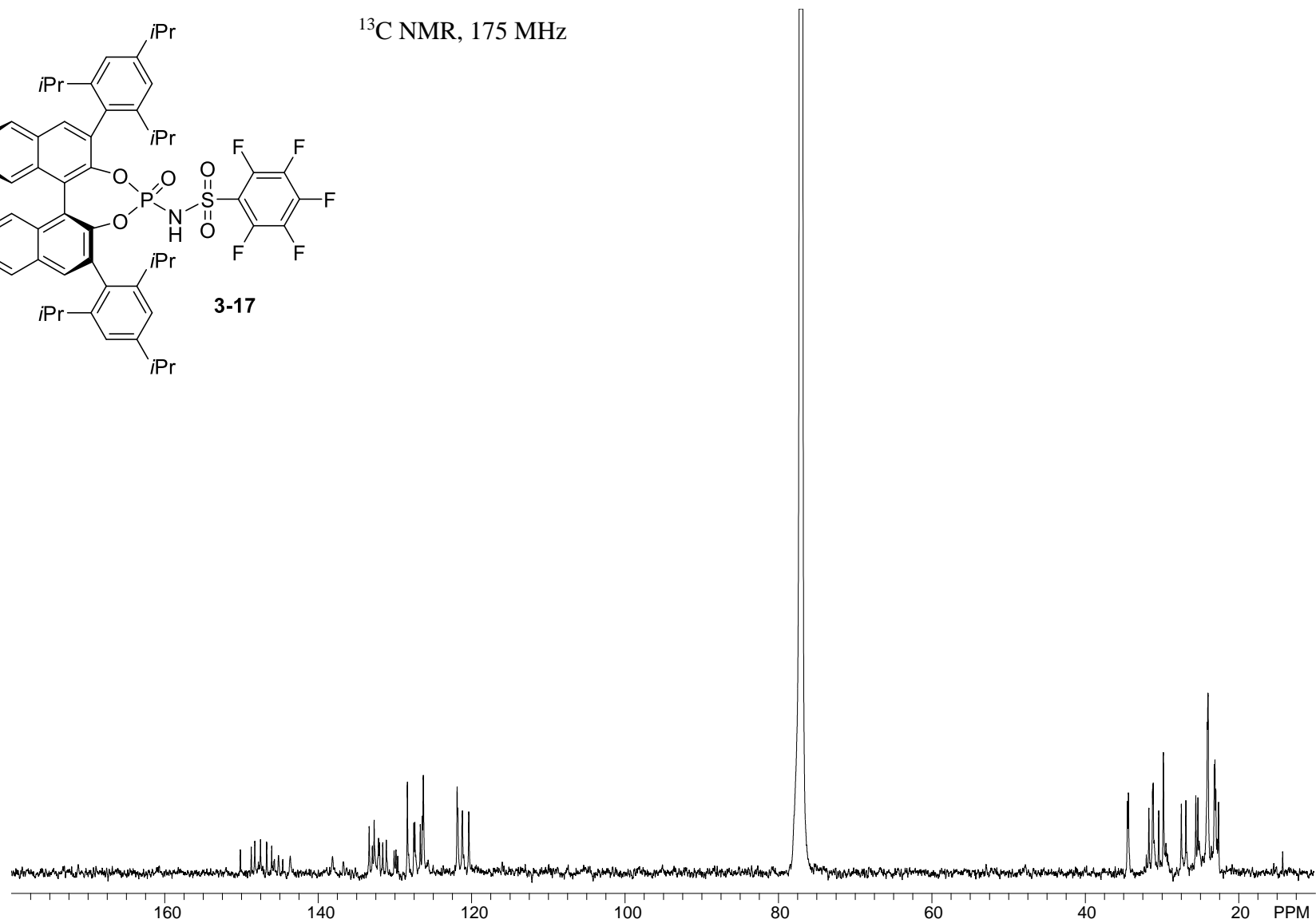


3-17



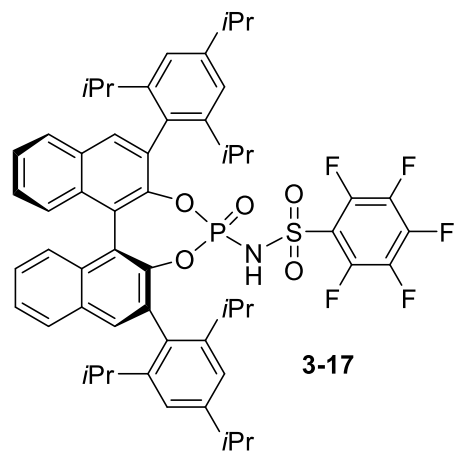


^{13}C NMR, 175 MHz

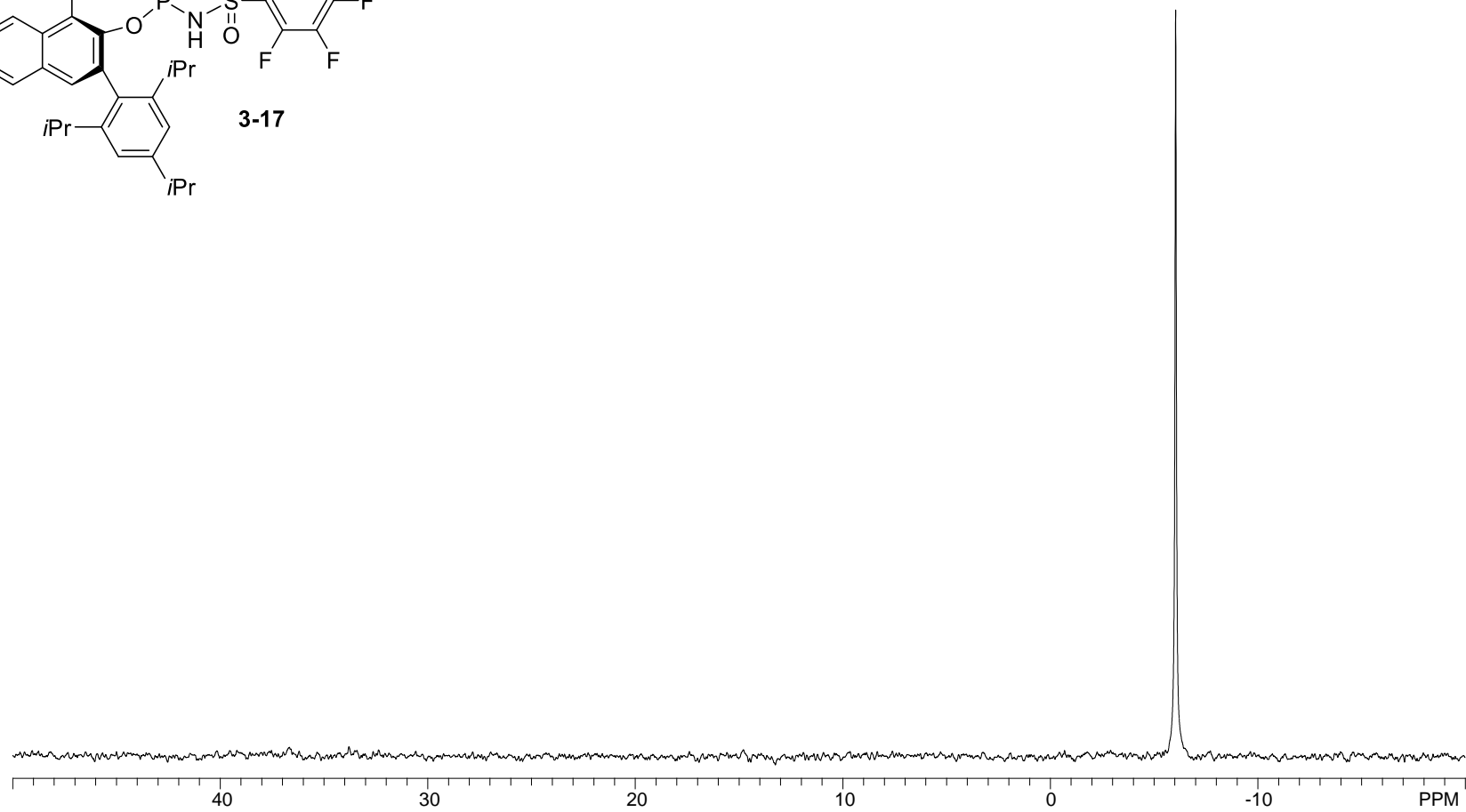


175

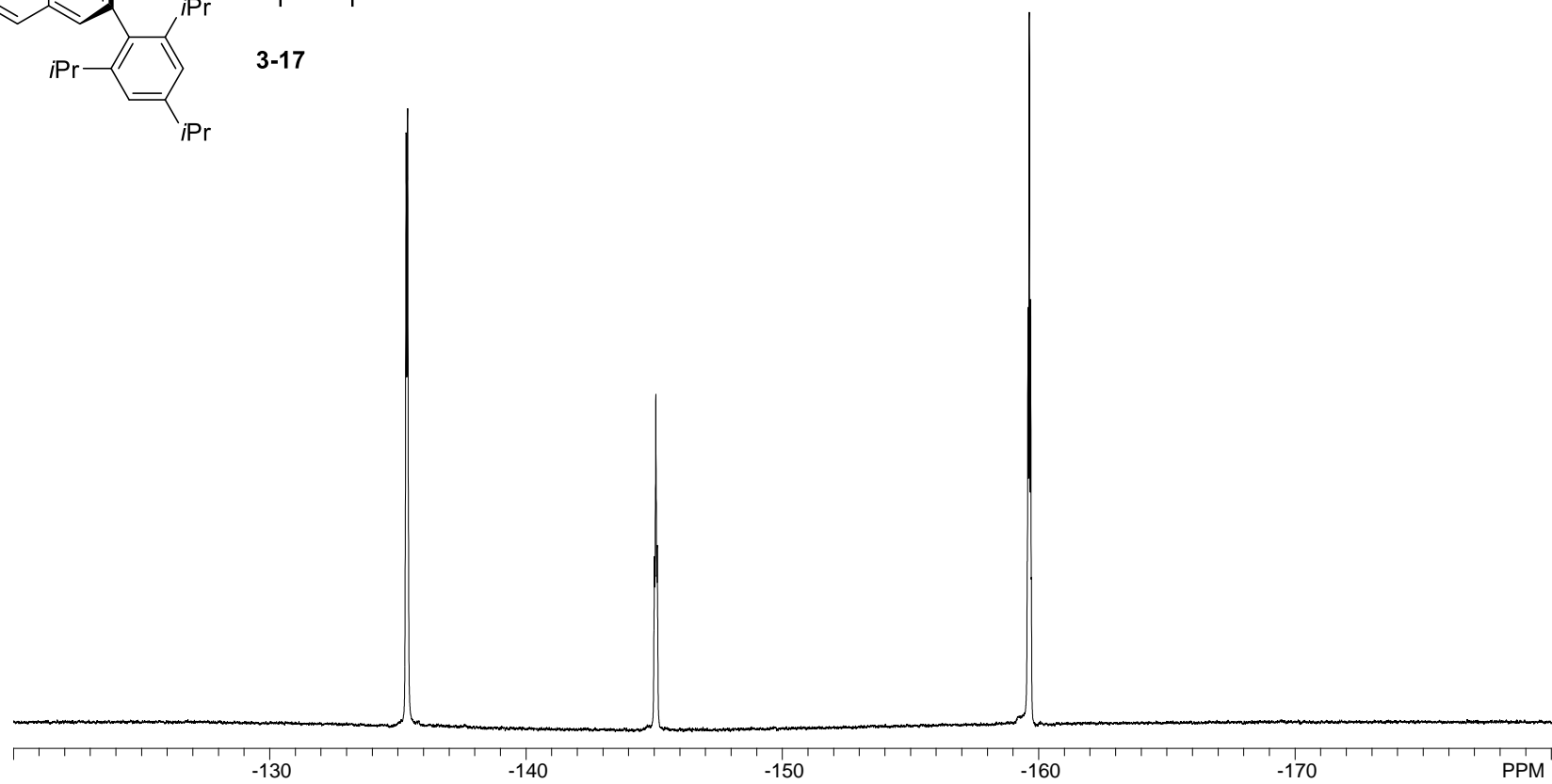
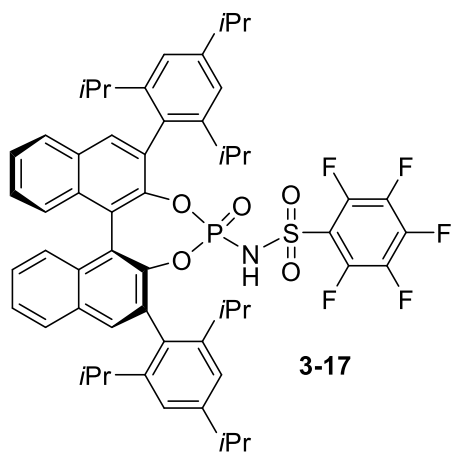
^{31}P NMR, 202 MHz



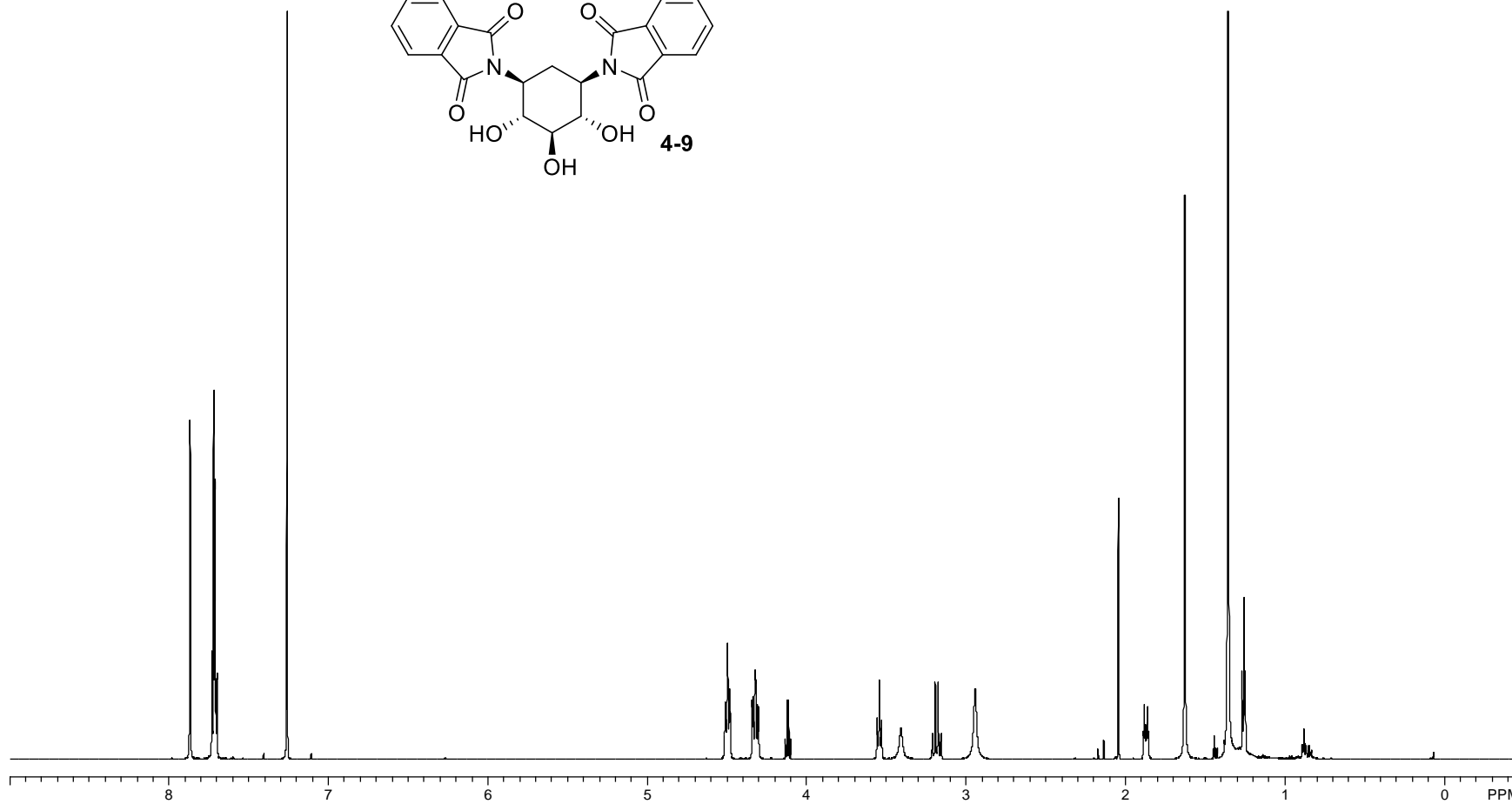
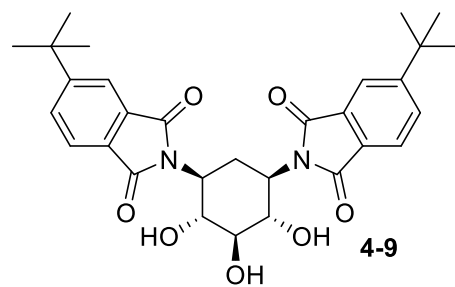
3-17



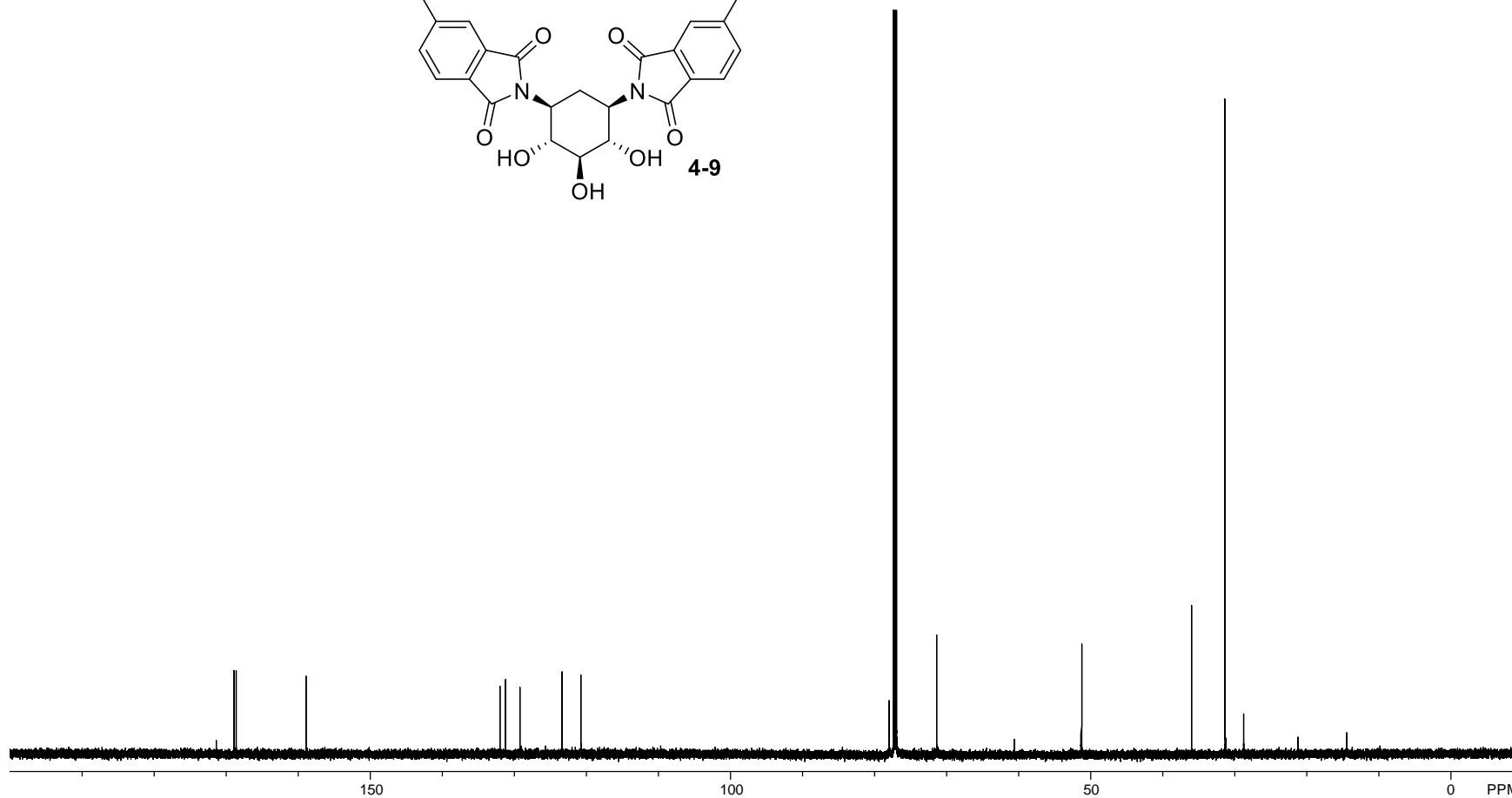
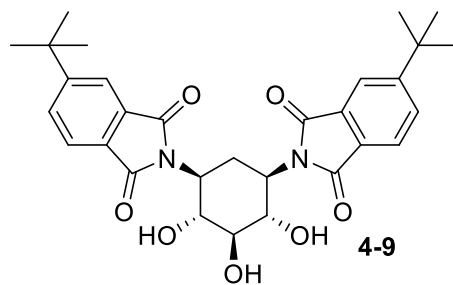
^{19}F NMR, 376 MHz



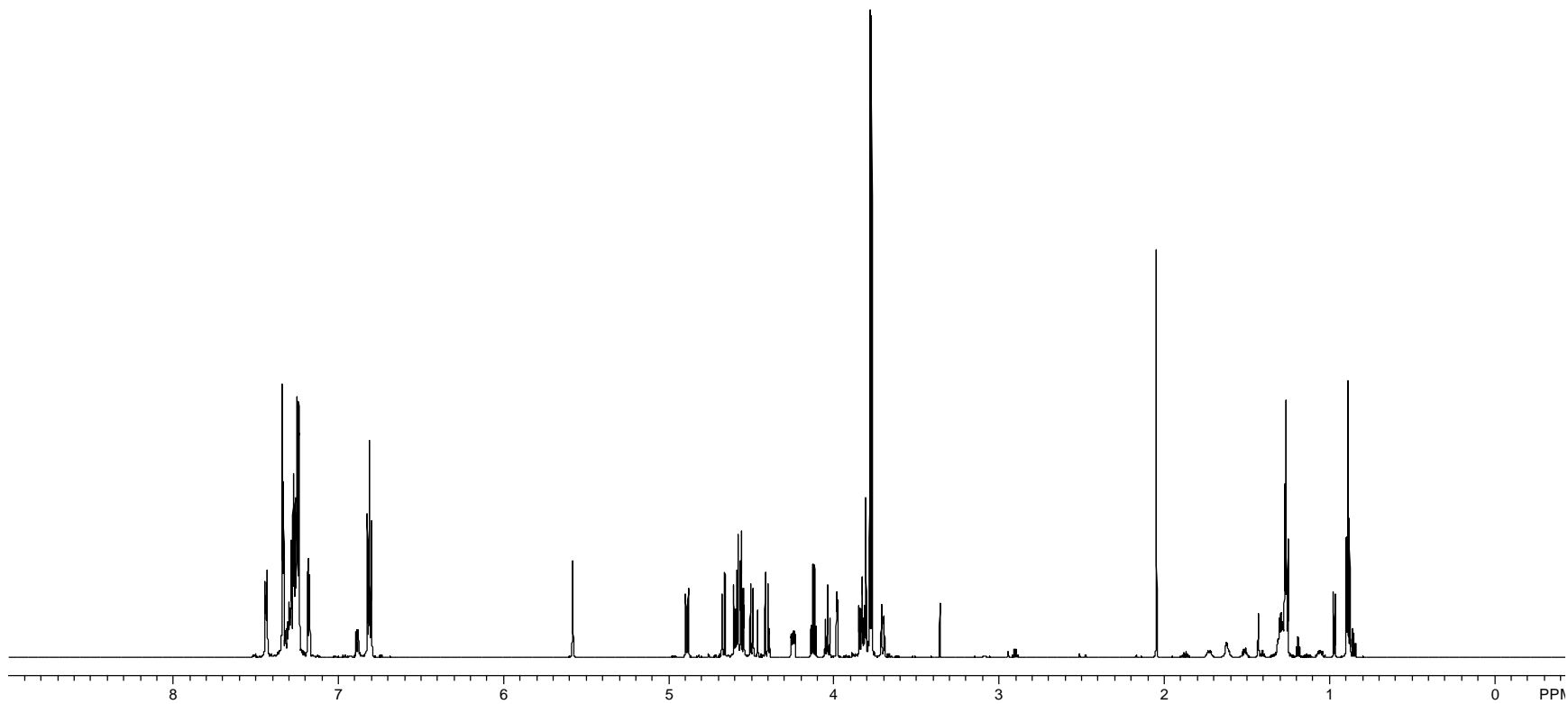
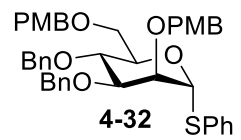
^1H NMR, 700 MHz



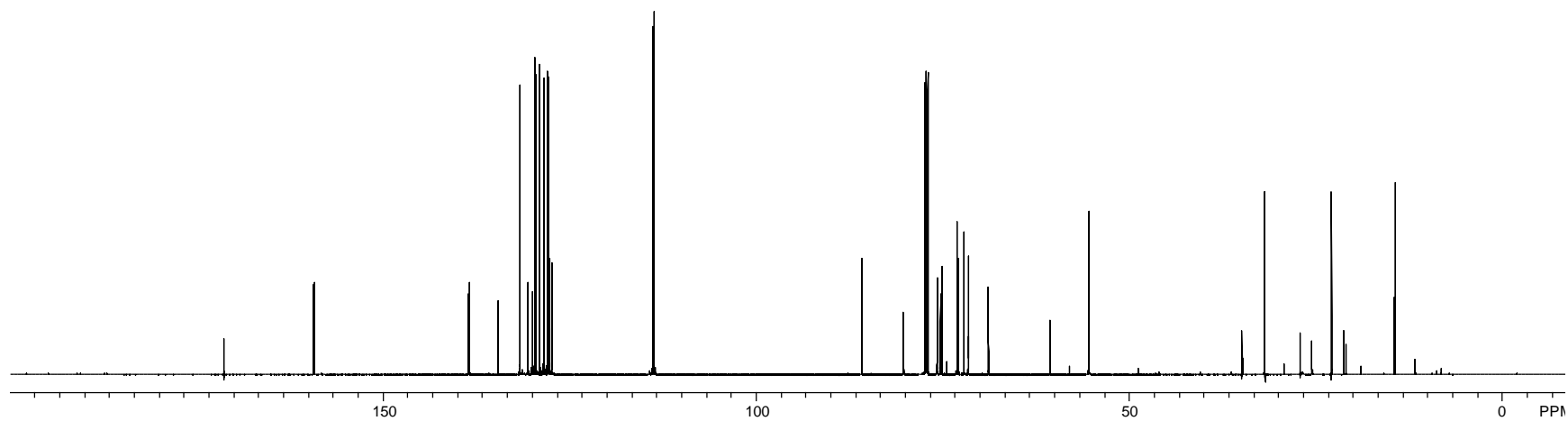
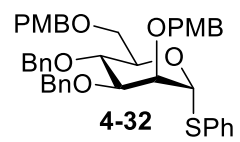
^{13}C NMR, 175 MHz



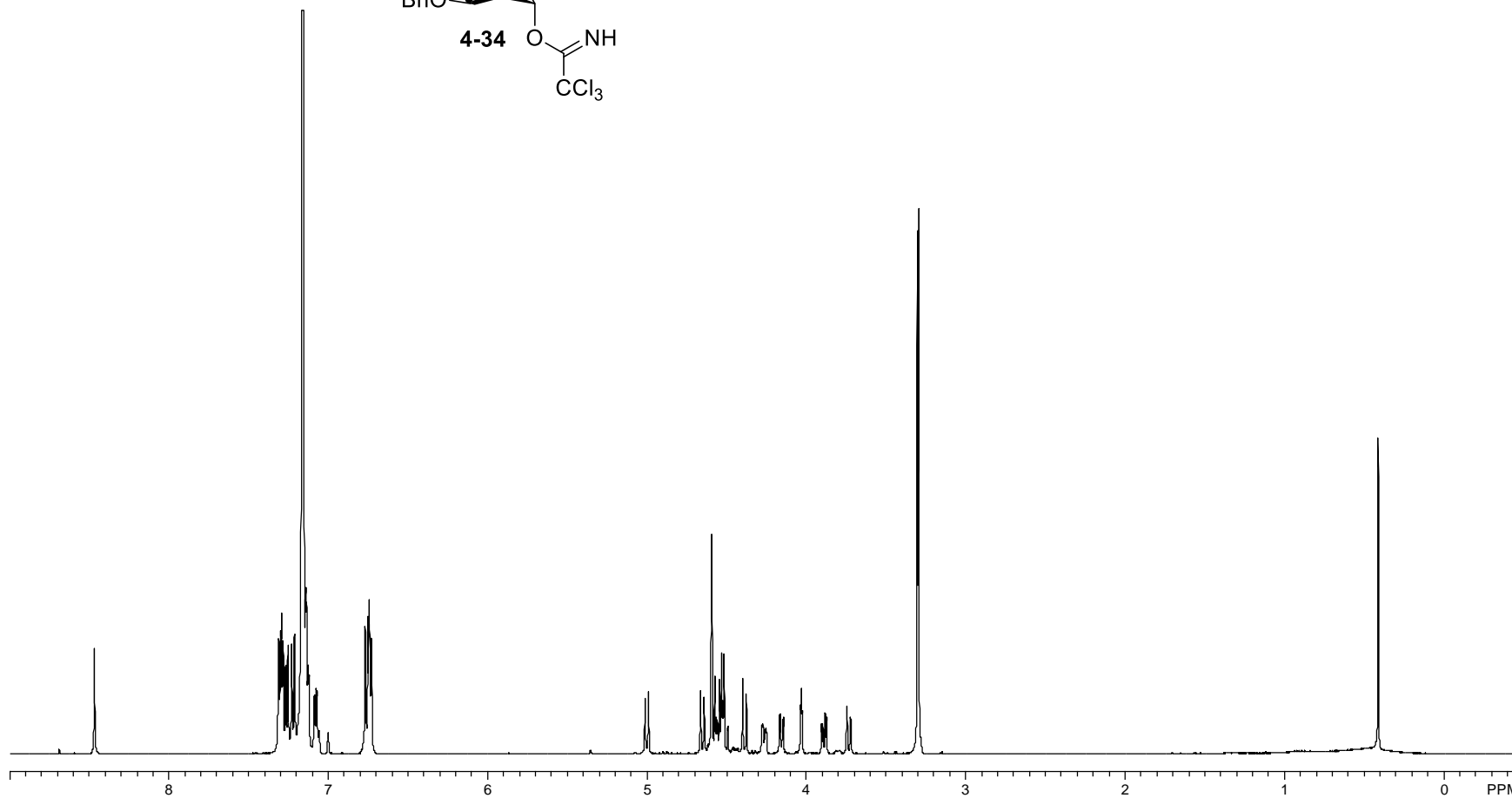
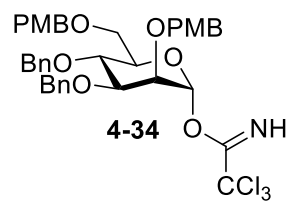
^1H NMR, 700 MHz



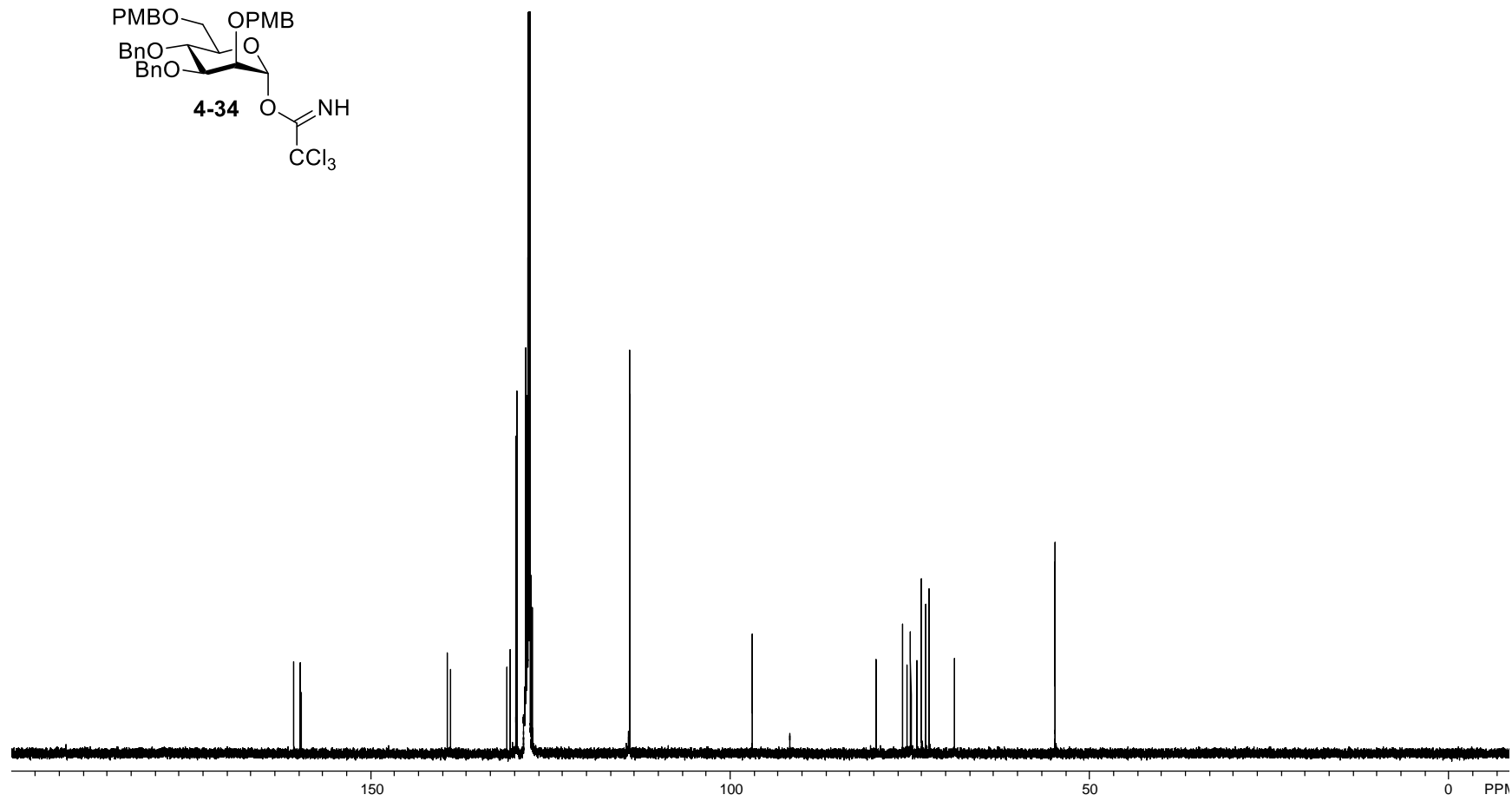
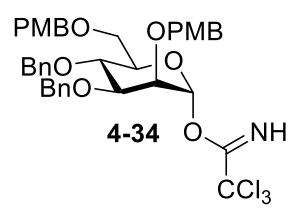
^{13}C NMR, 175 MHz



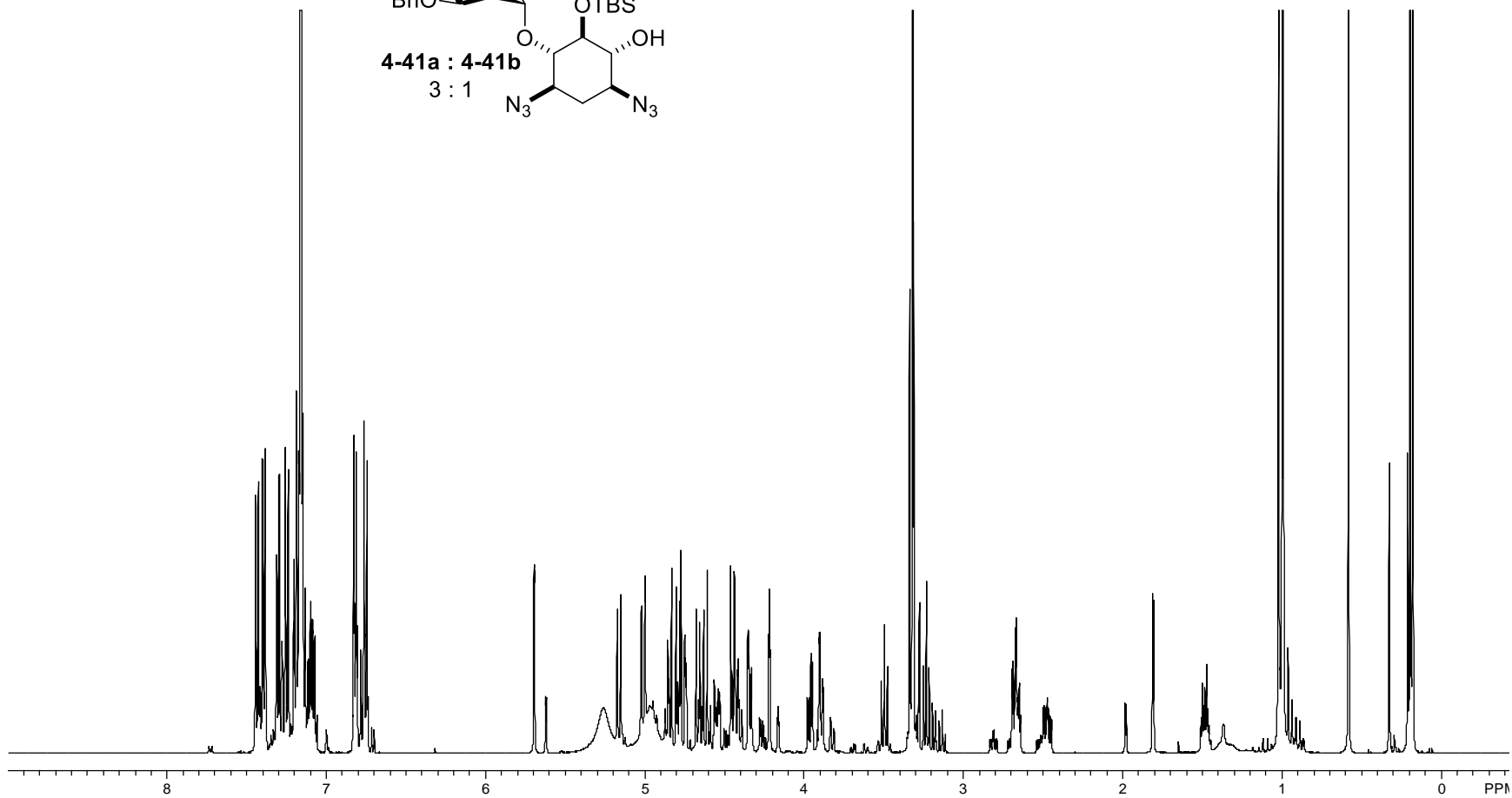
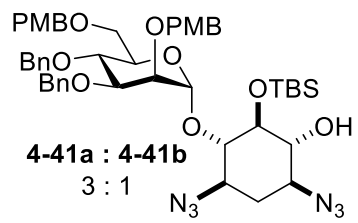
^1H NMR, 500 MHz



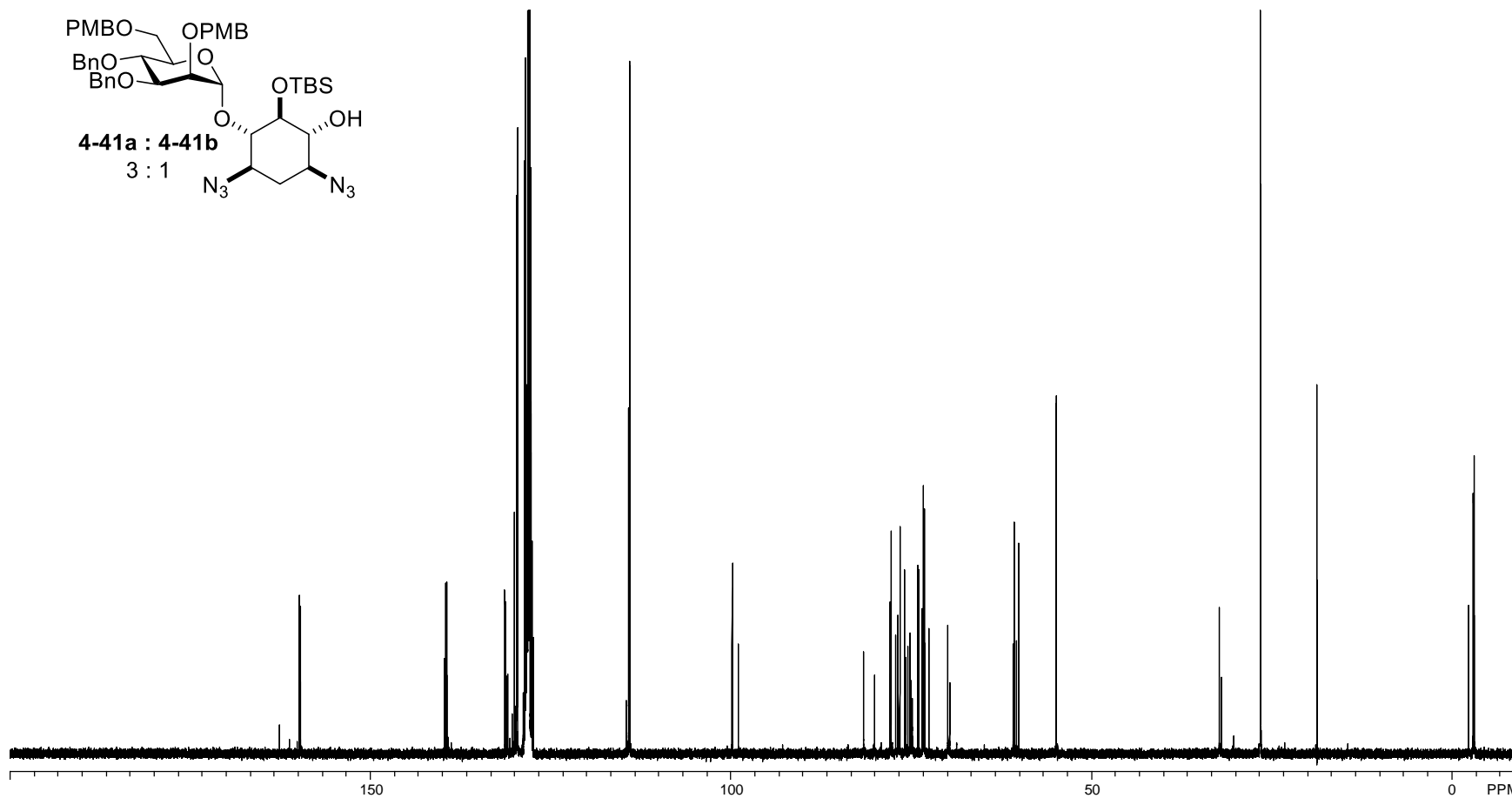
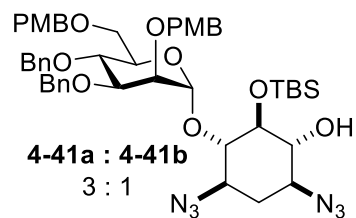
^{13}C NMR, 175 MHz



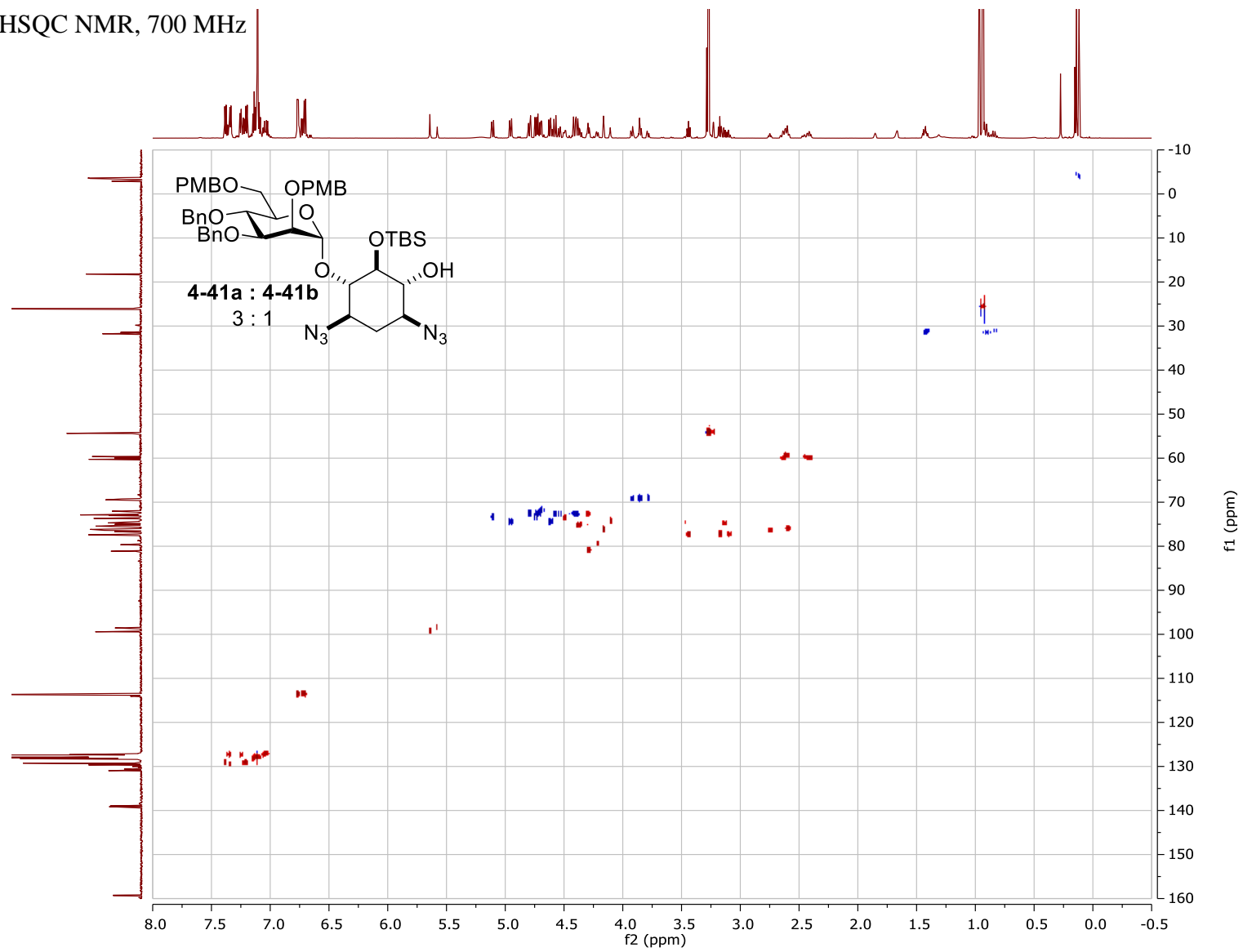
^1H NMR, 500 MHz



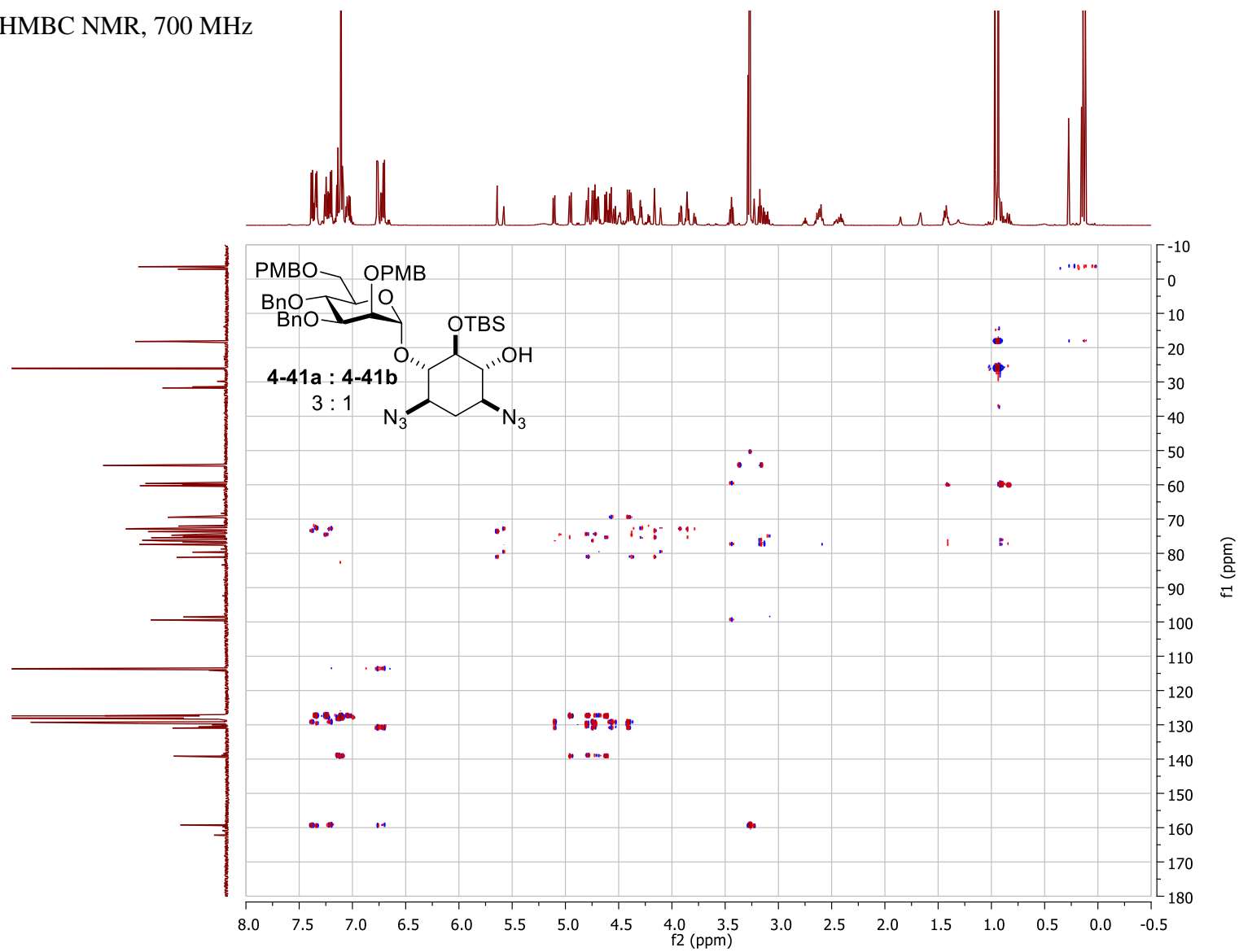
^{13}C NMR, 175 MHz



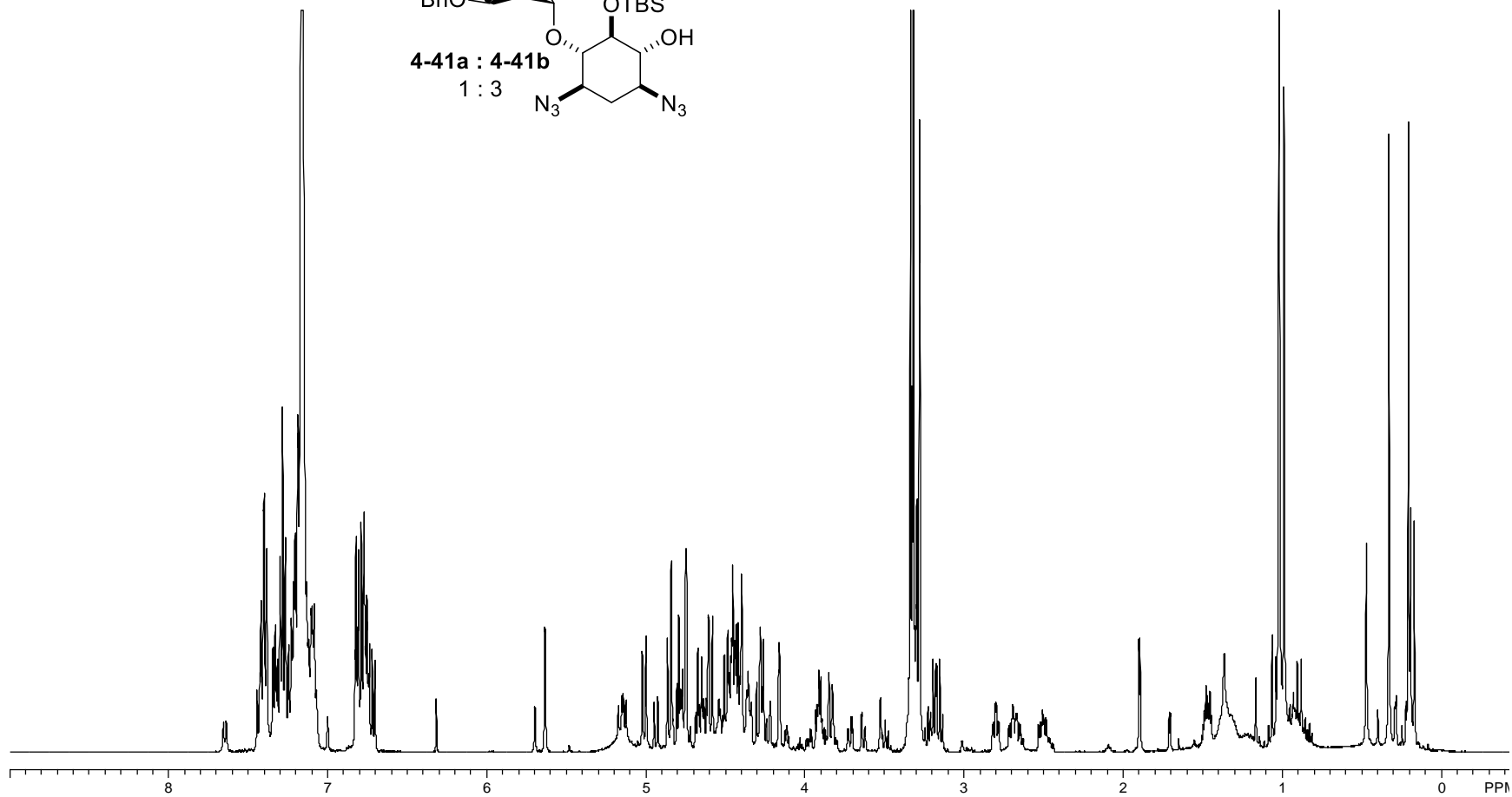
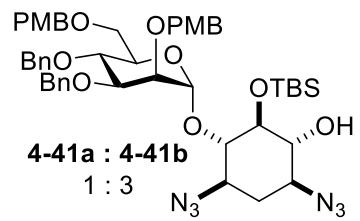
HSQC NMR, 700 MHz



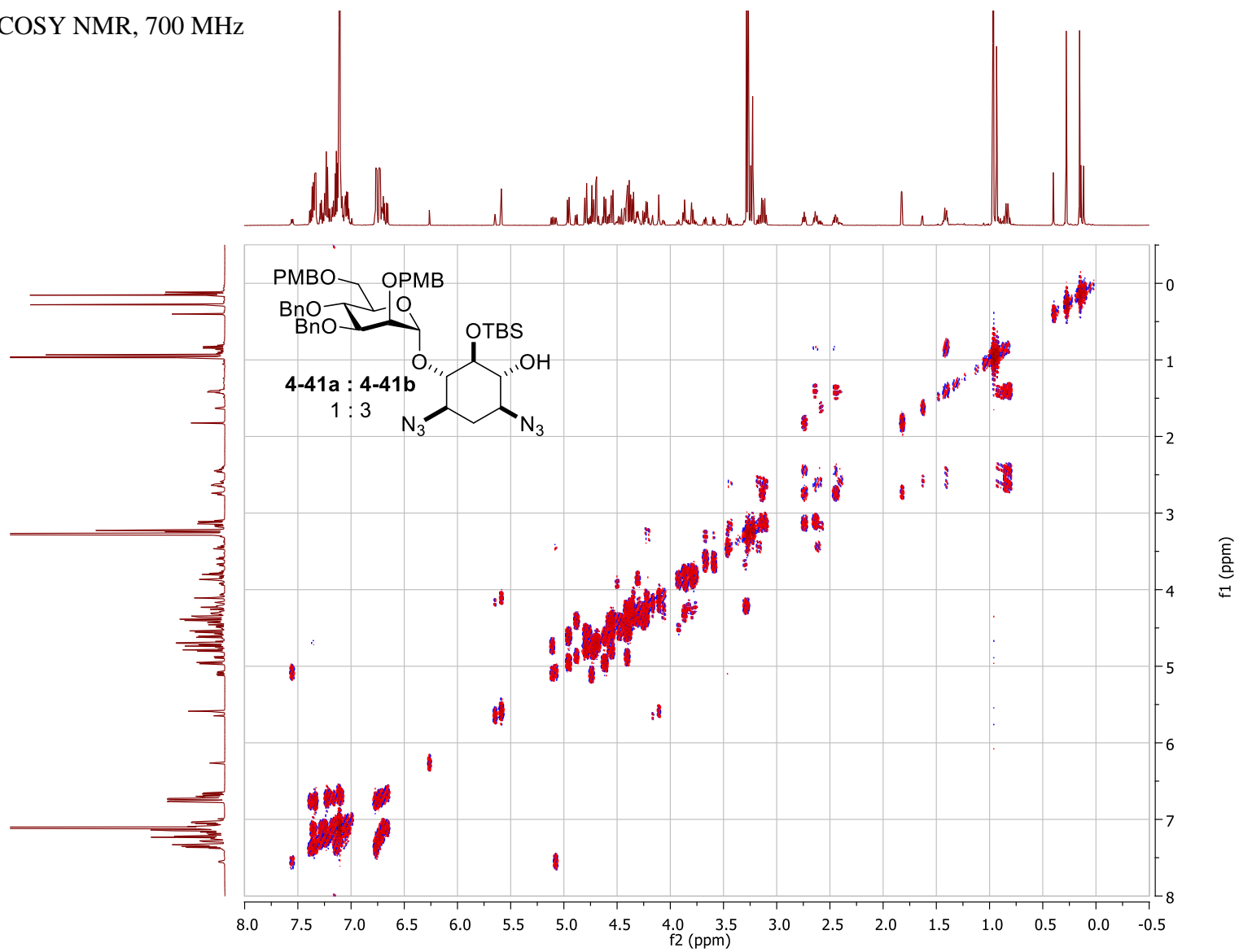
HMBC NMR, 700 MHz

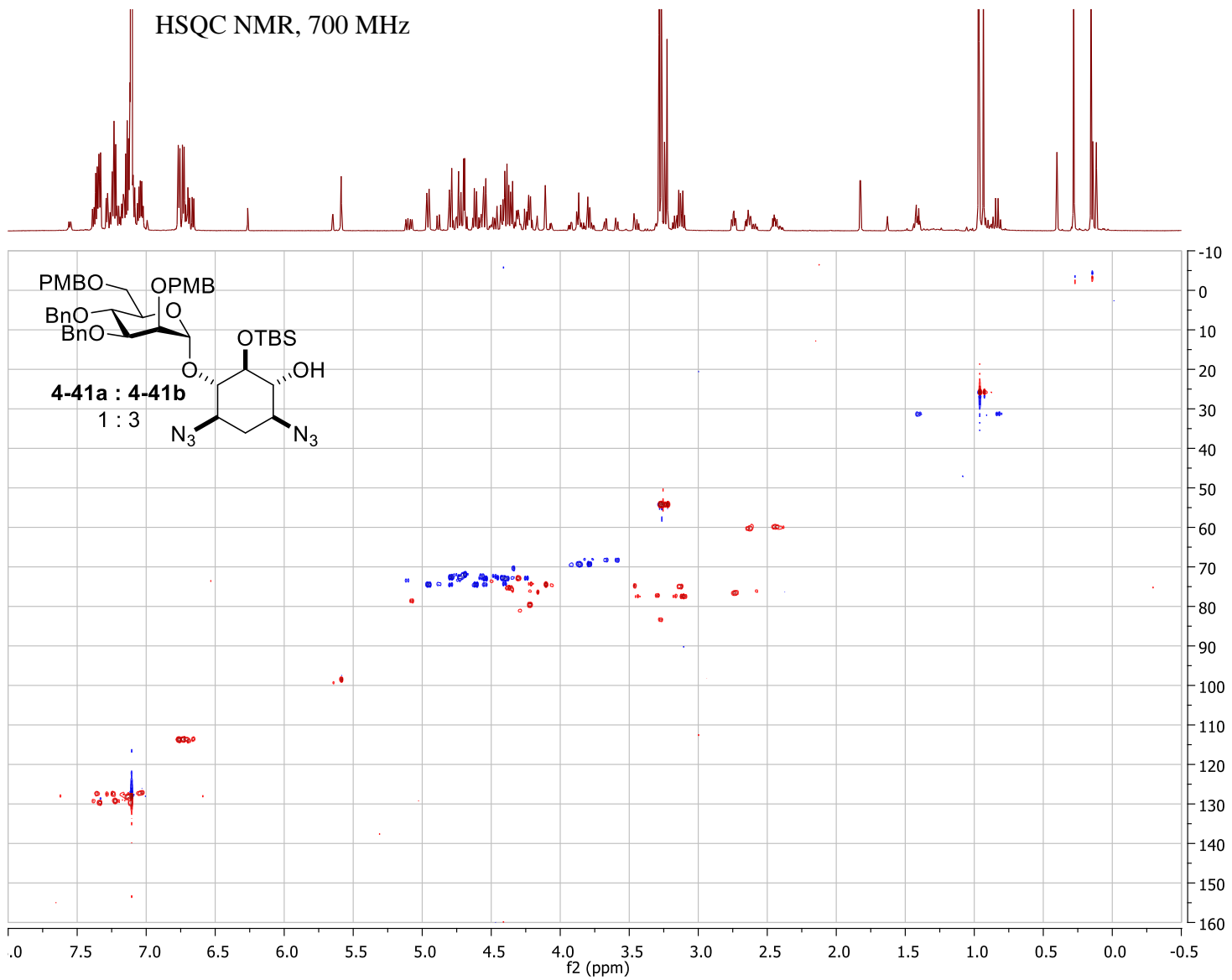


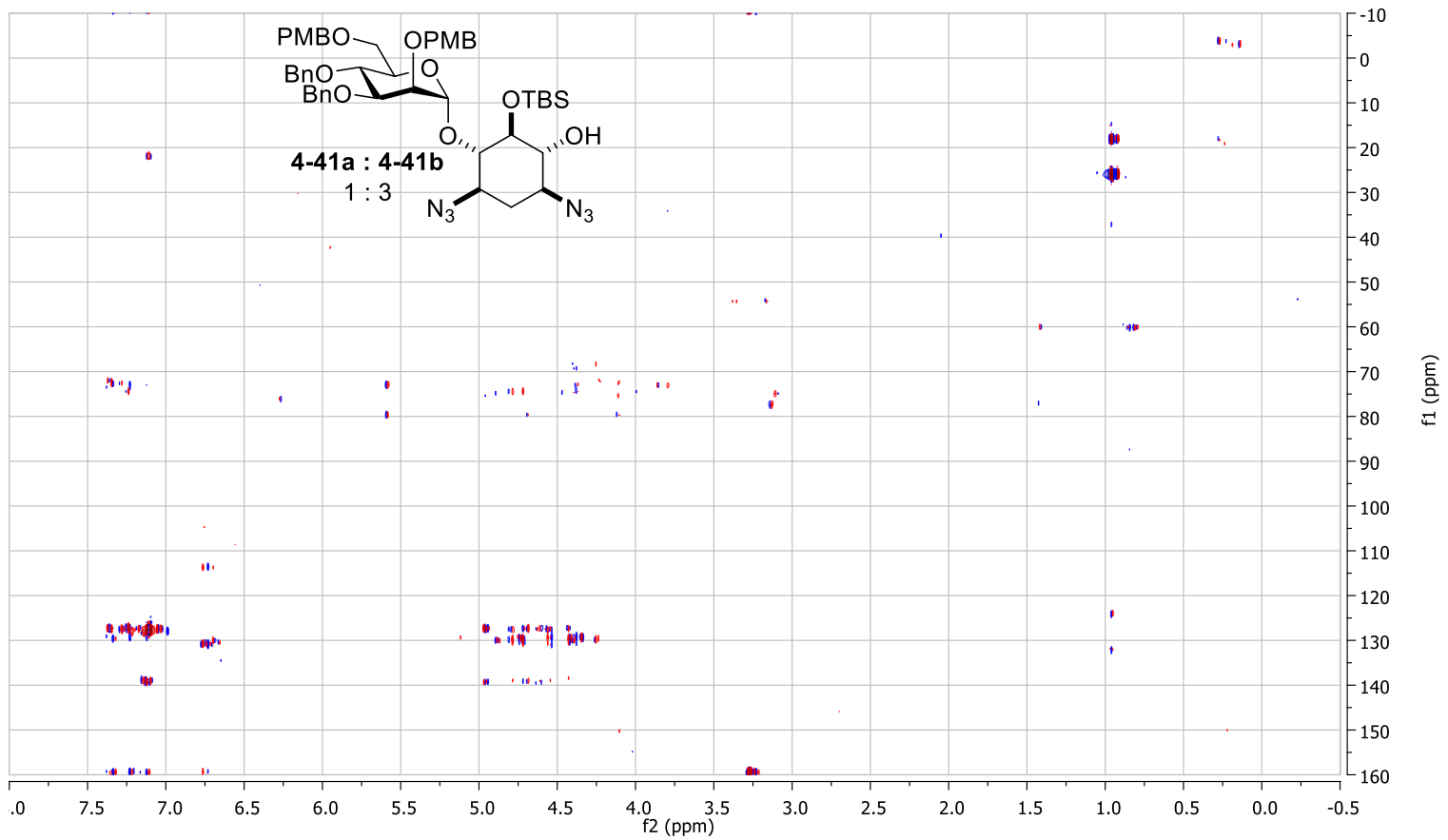
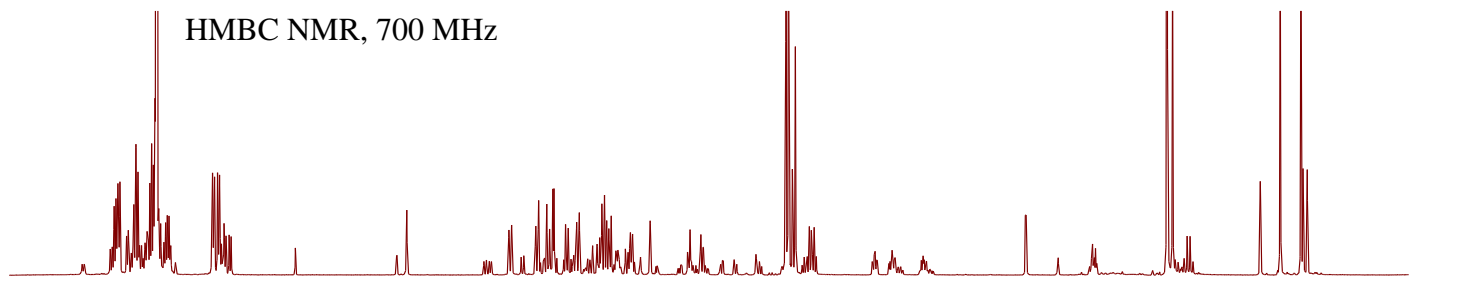
^1H NMR, 700 MHz



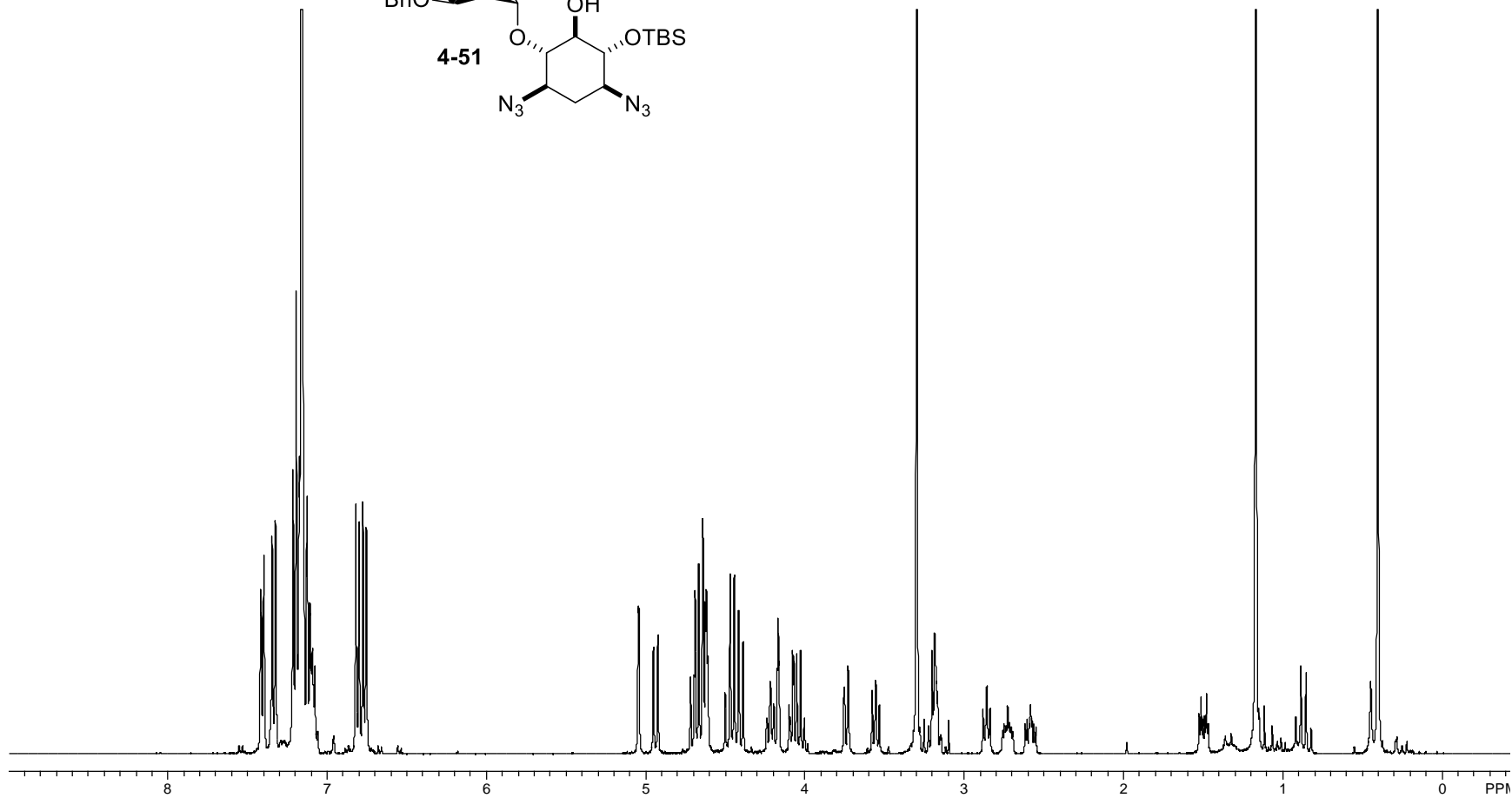
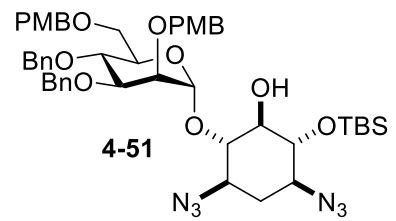
COSY NMR, 700 MHz



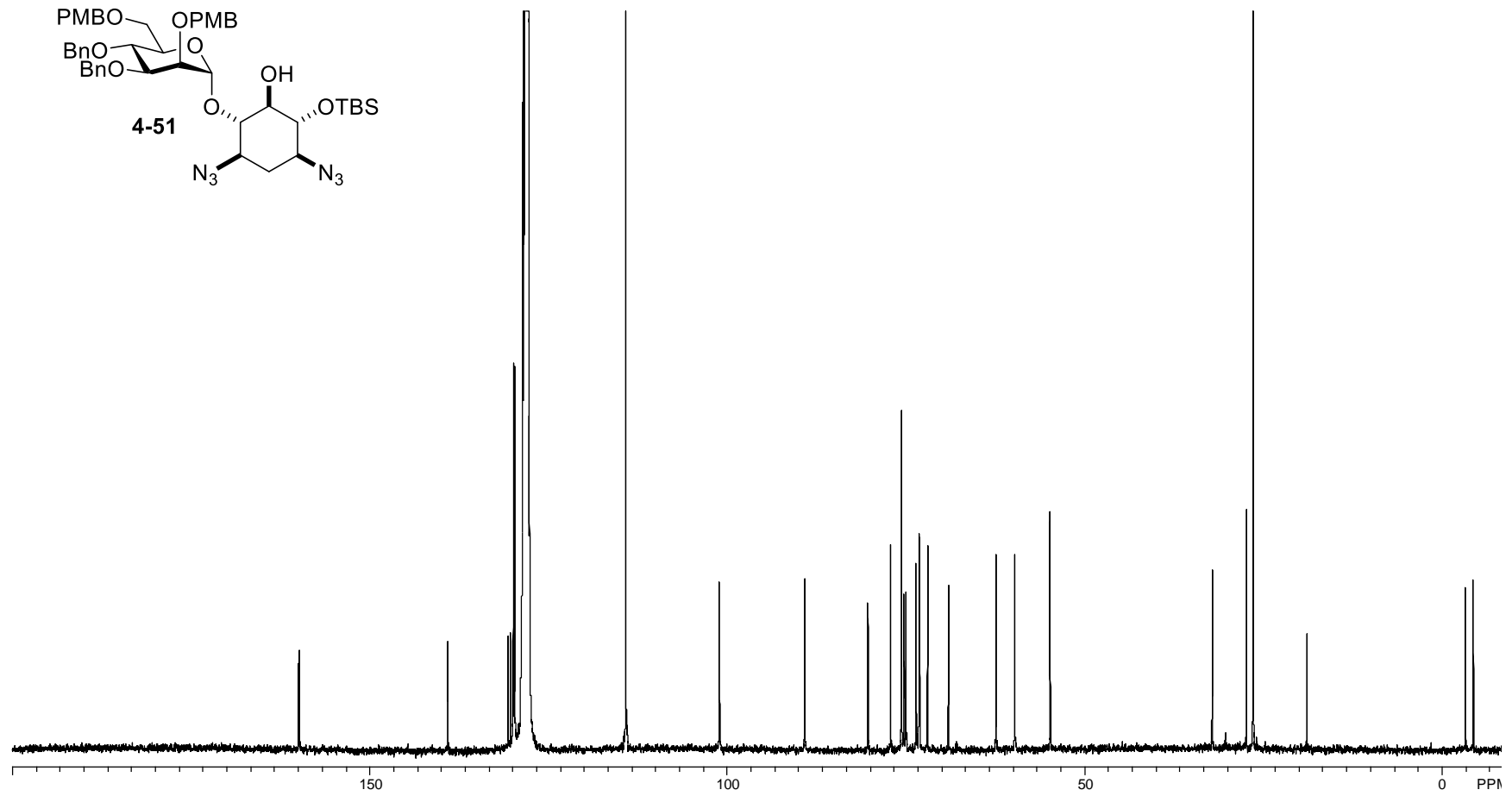
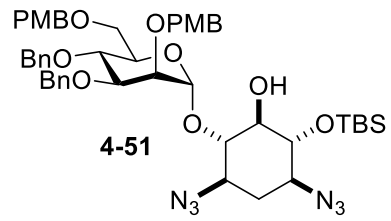




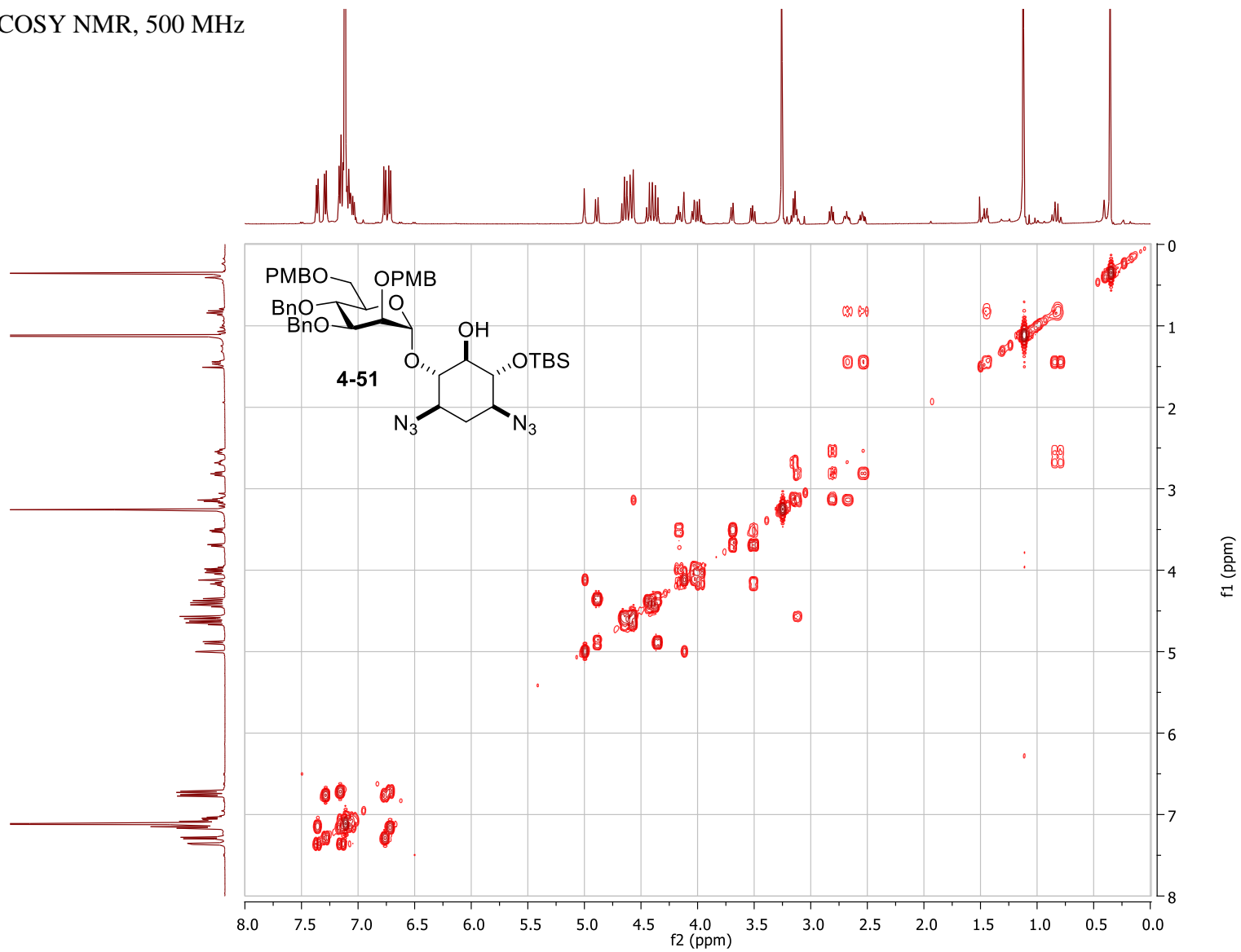
^1H NMR, 500 MHz



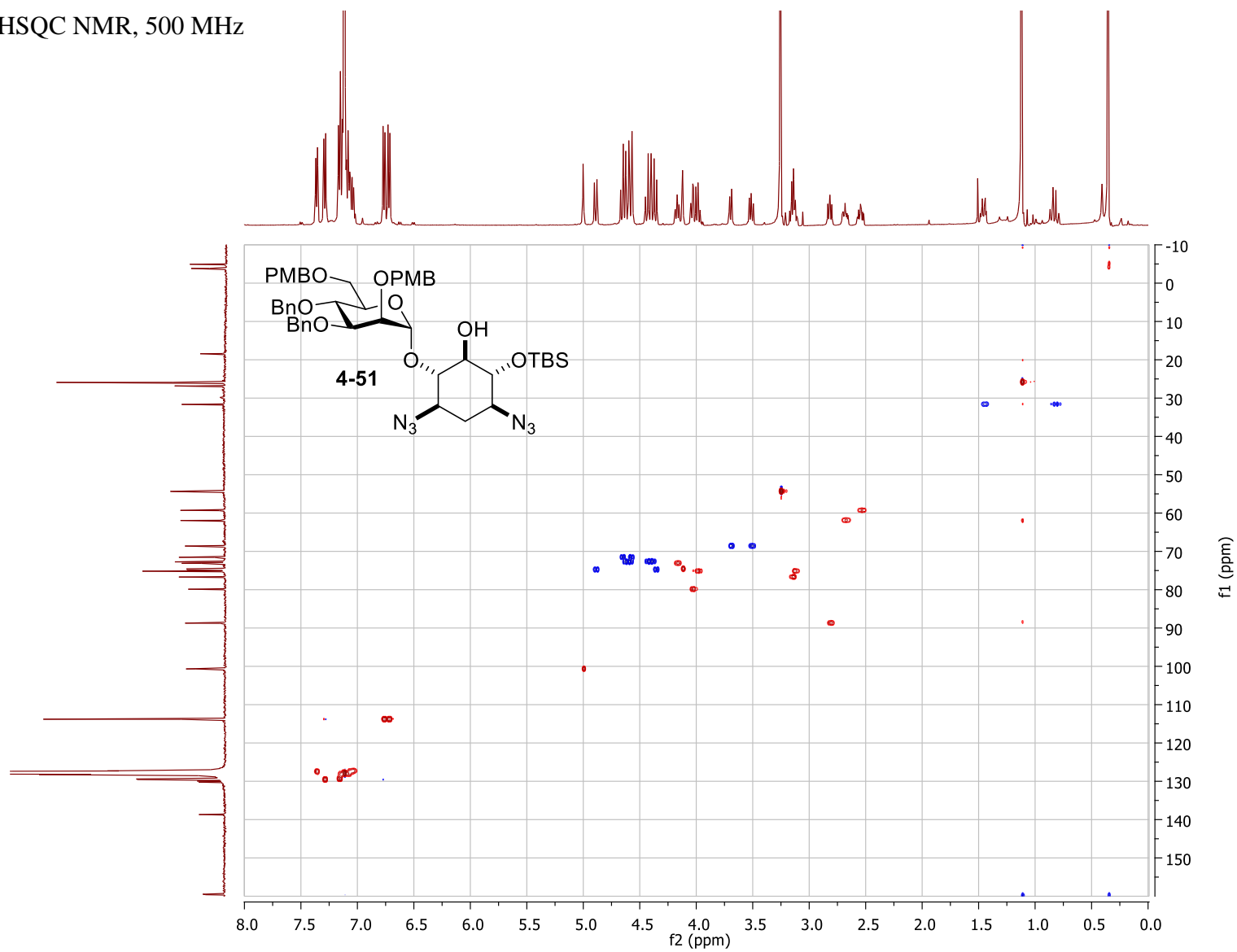
^{13}C NMR, 175 MHz



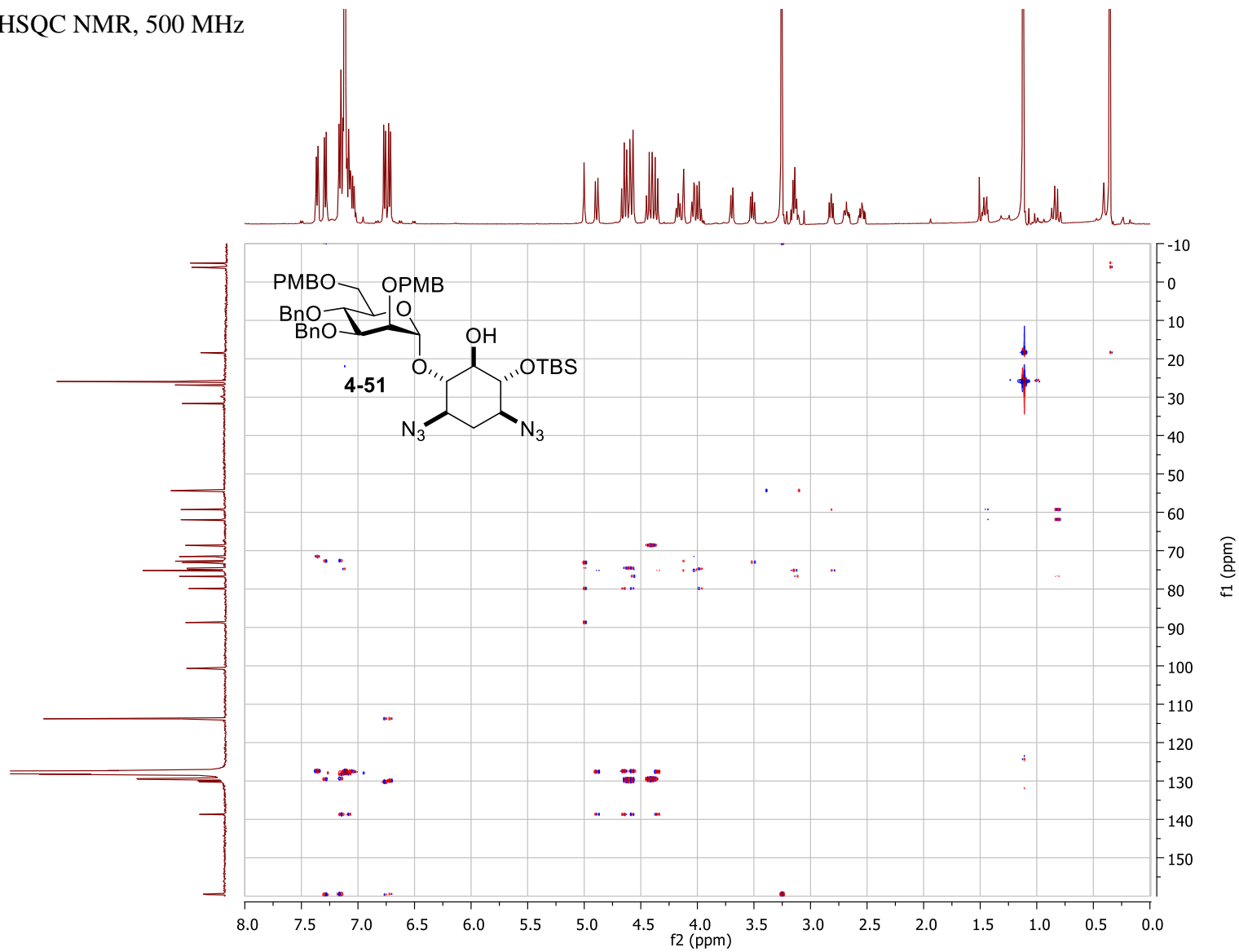
COSY NMR, 500 MHz



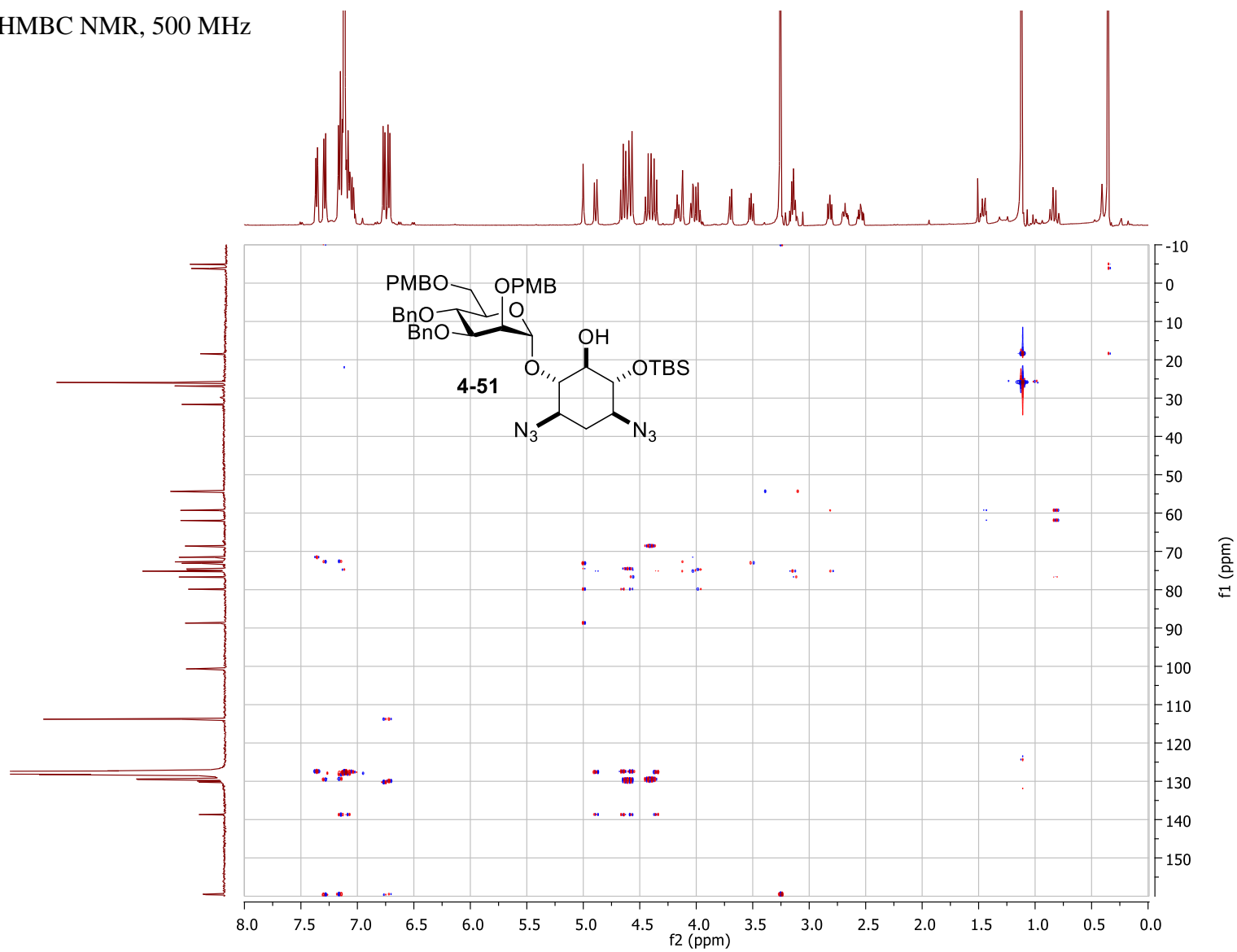
HSQC NMR, 500 MHz



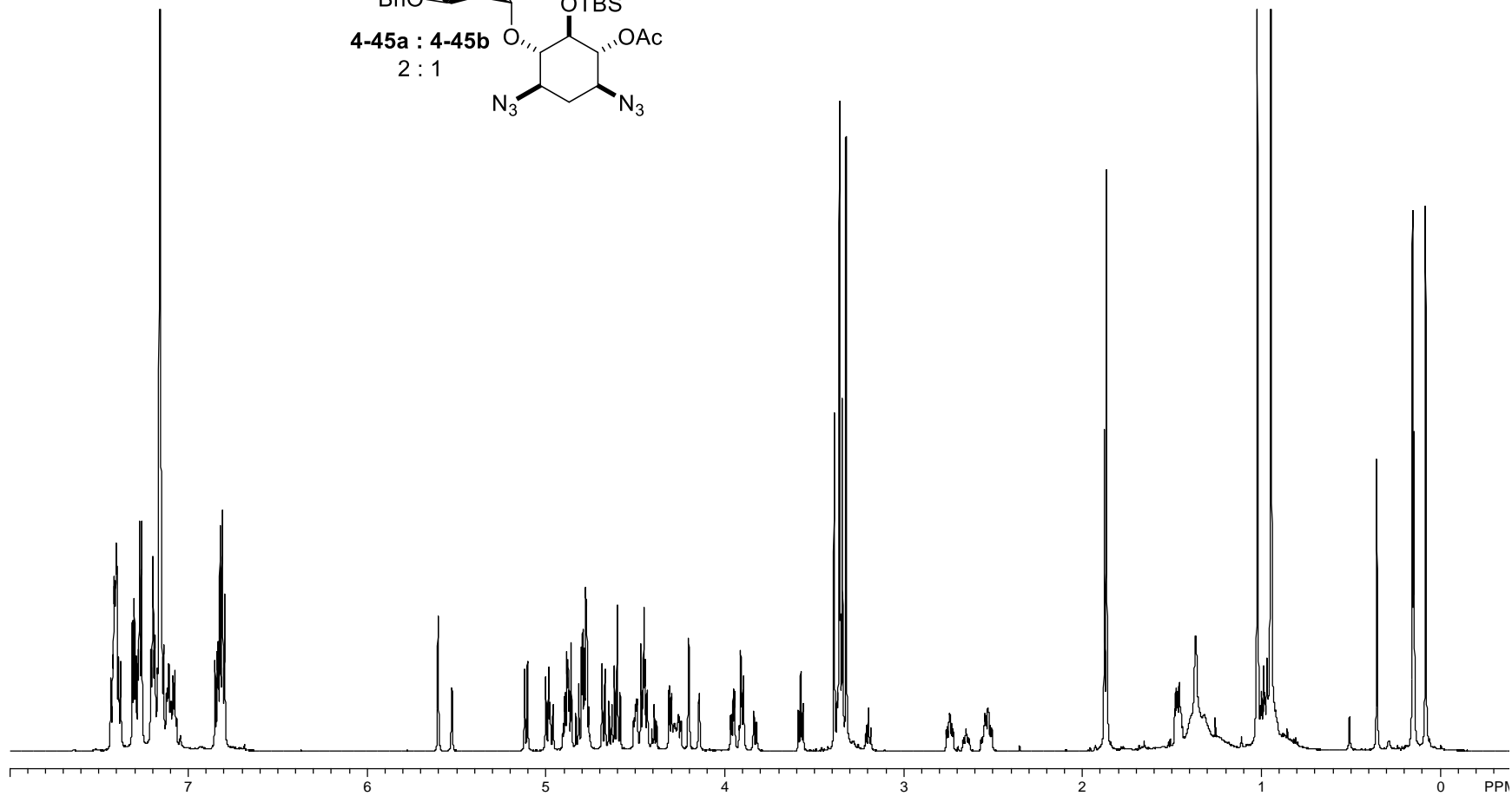
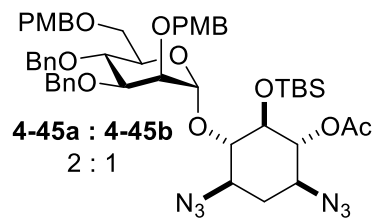
HSQC NMR, 500 MHz



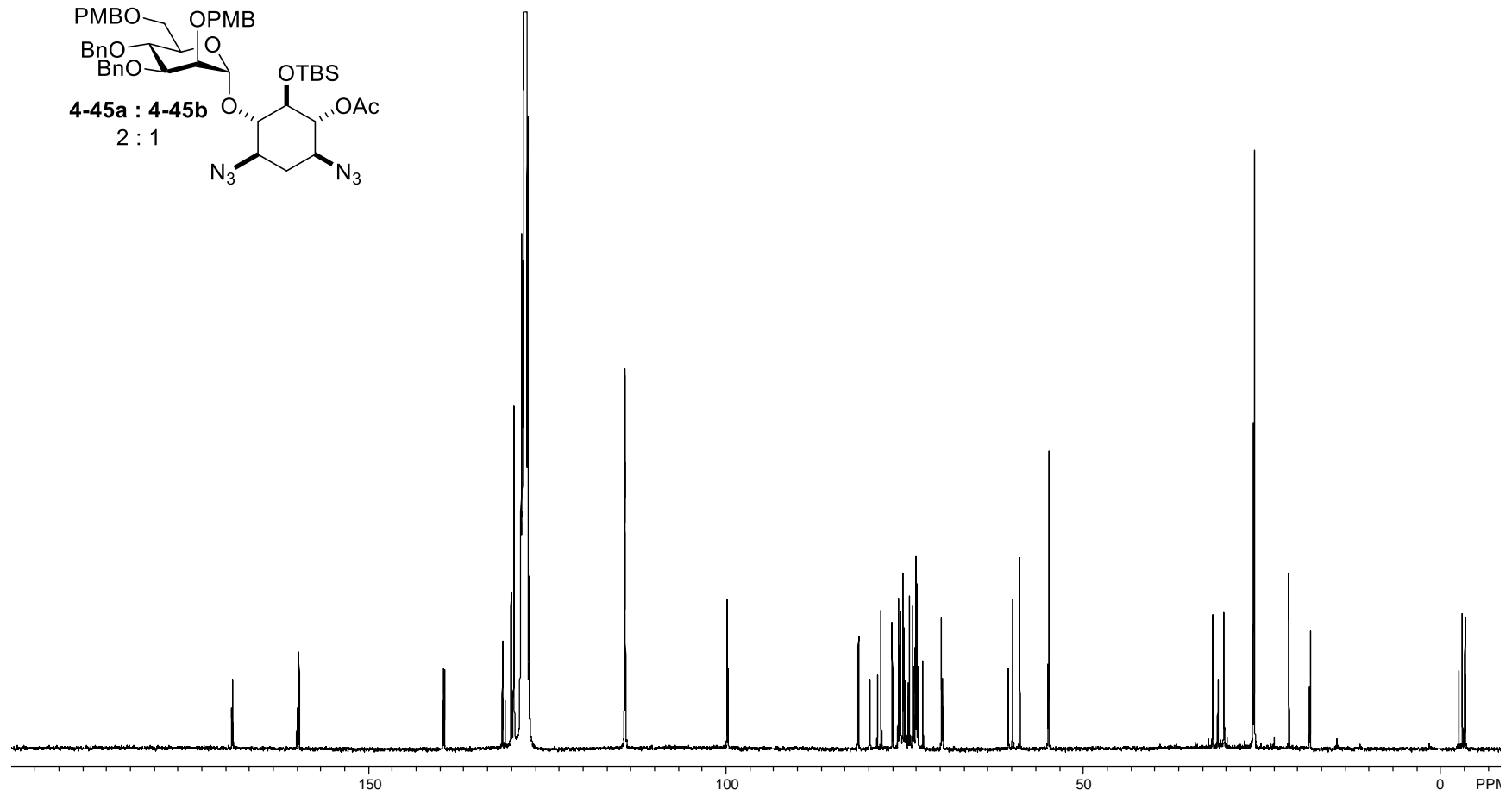
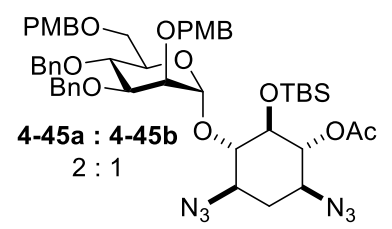
HMBC NMR, 500 MHz



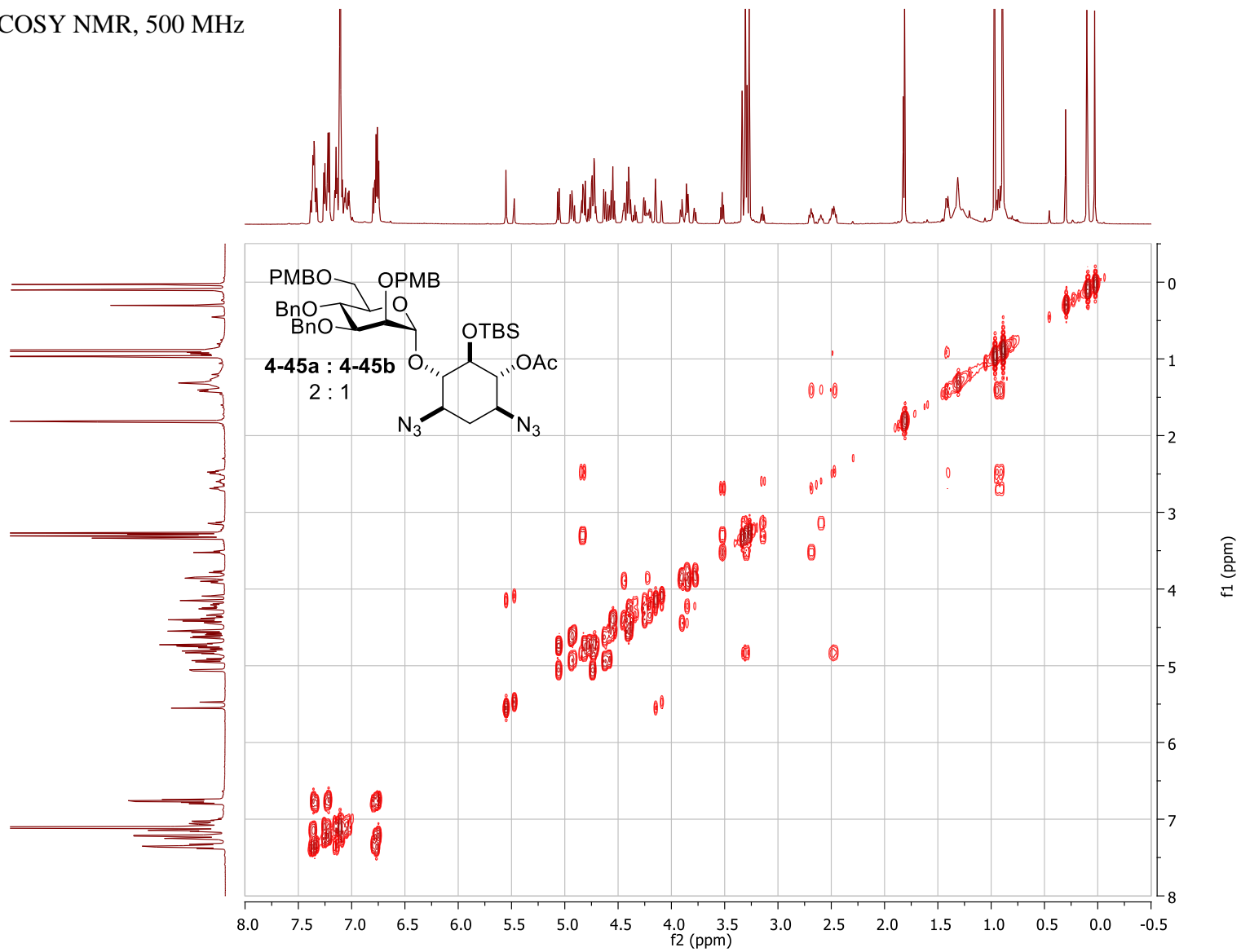
^1H NMR, 700 MHz



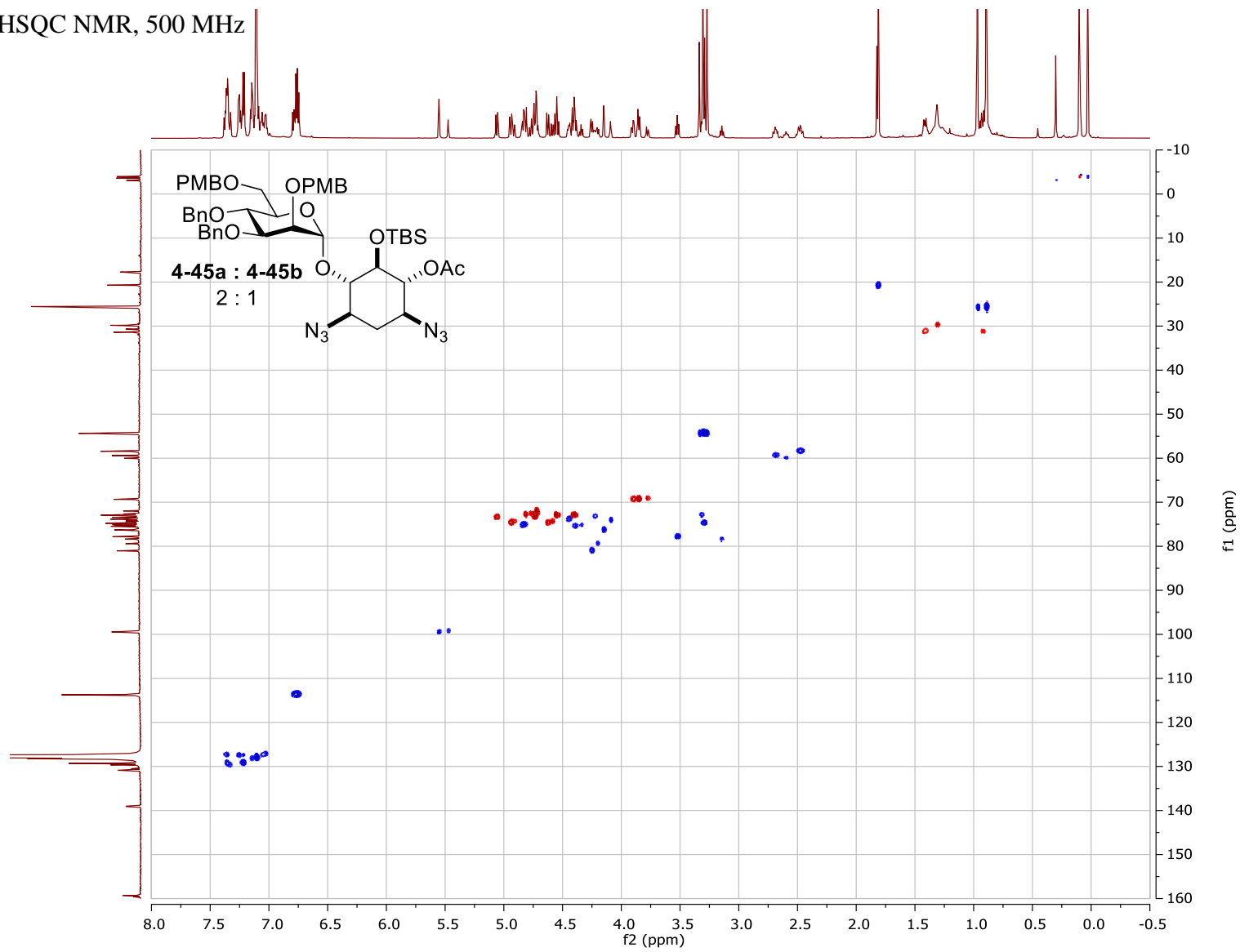
¹³C NMR, 175 MHz



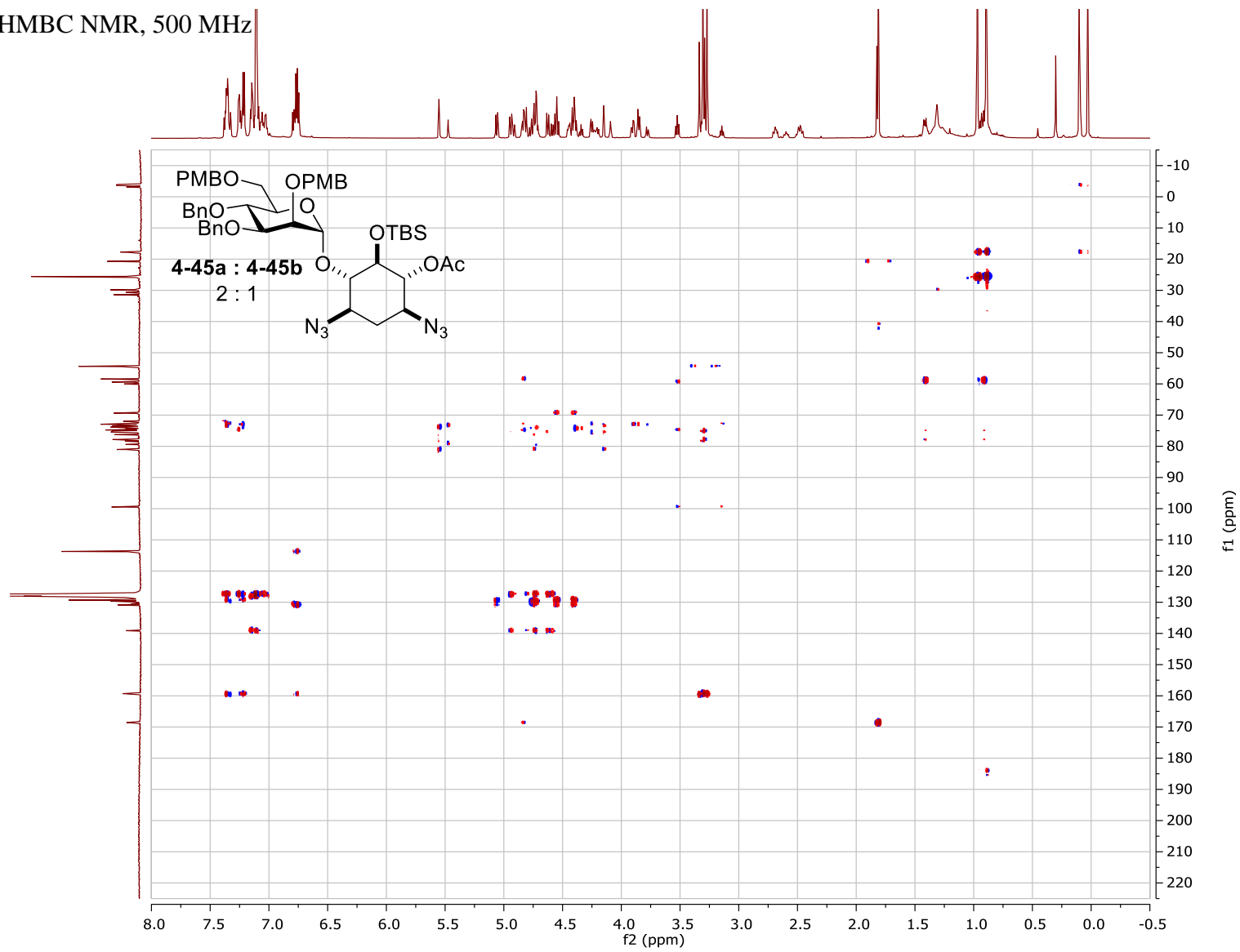
COSY NMR, 500 MHz



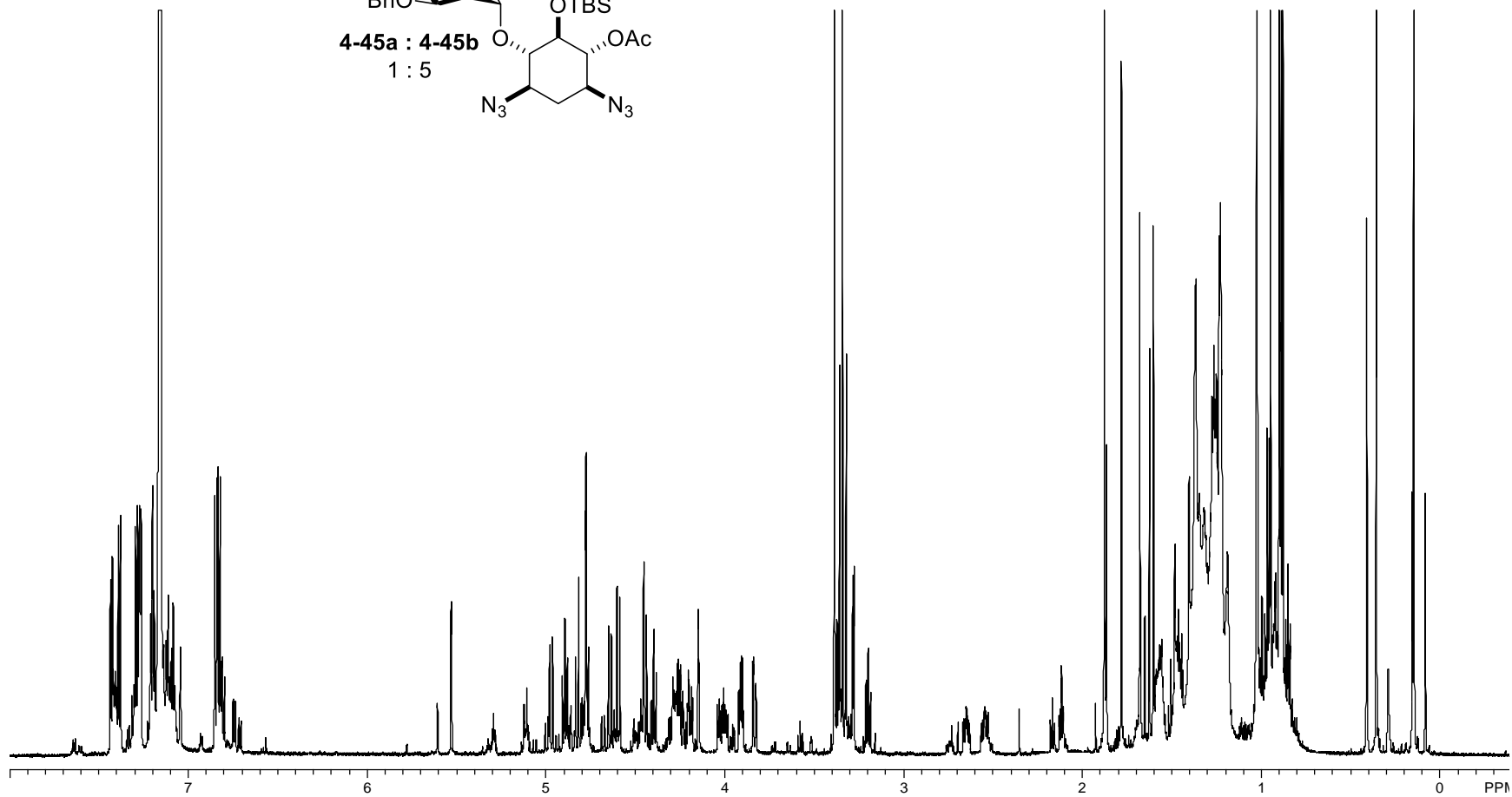
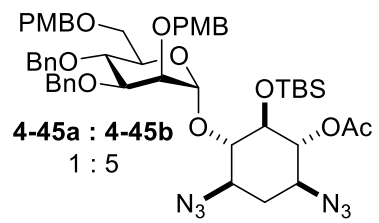
HSQC NMR, 500 MHz



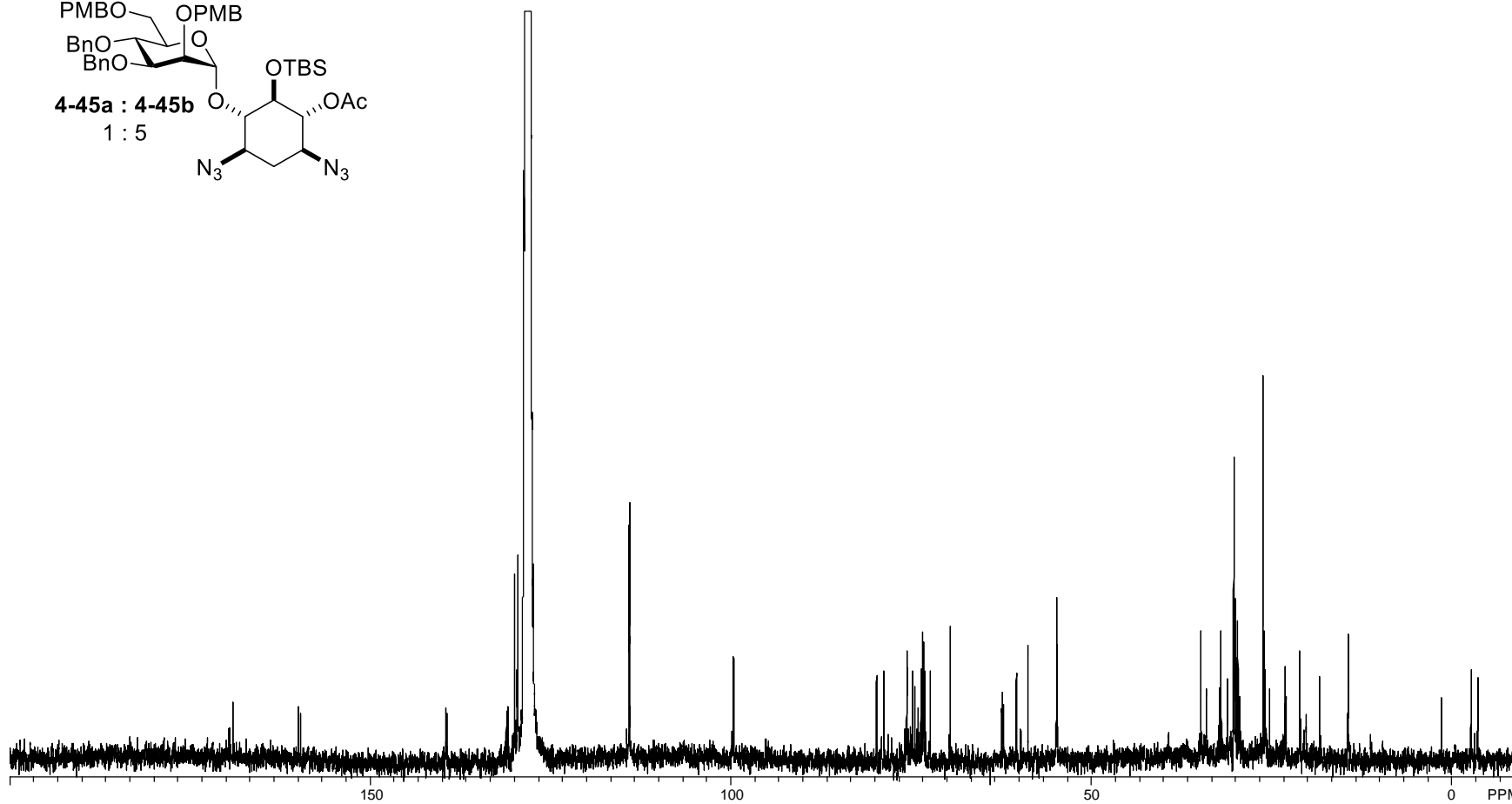
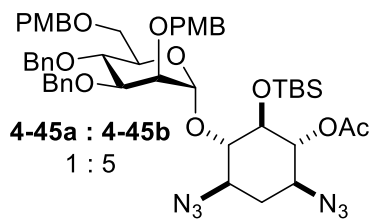
HMBC NMR, 500 MHz



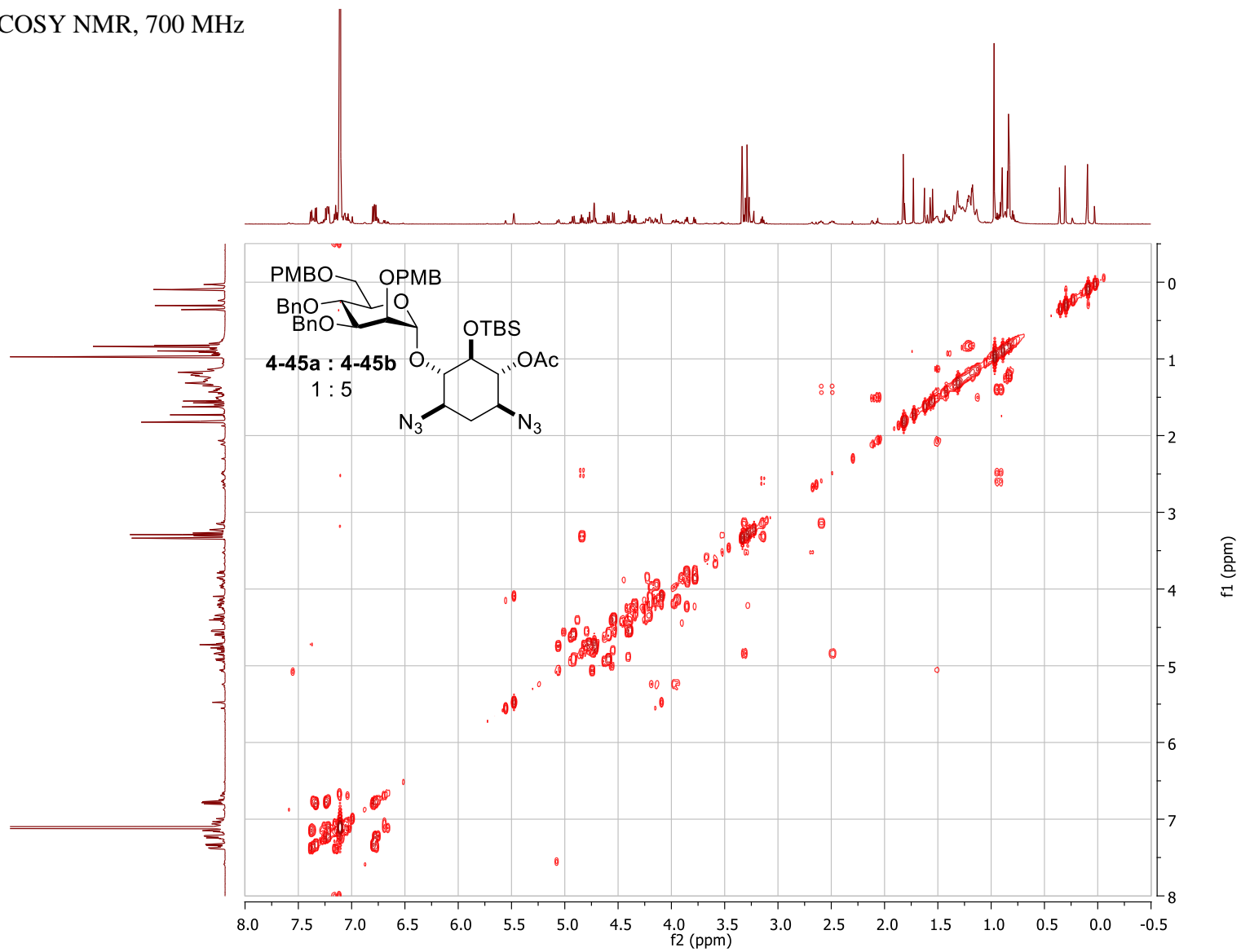
^1H NMR, 700 MHz



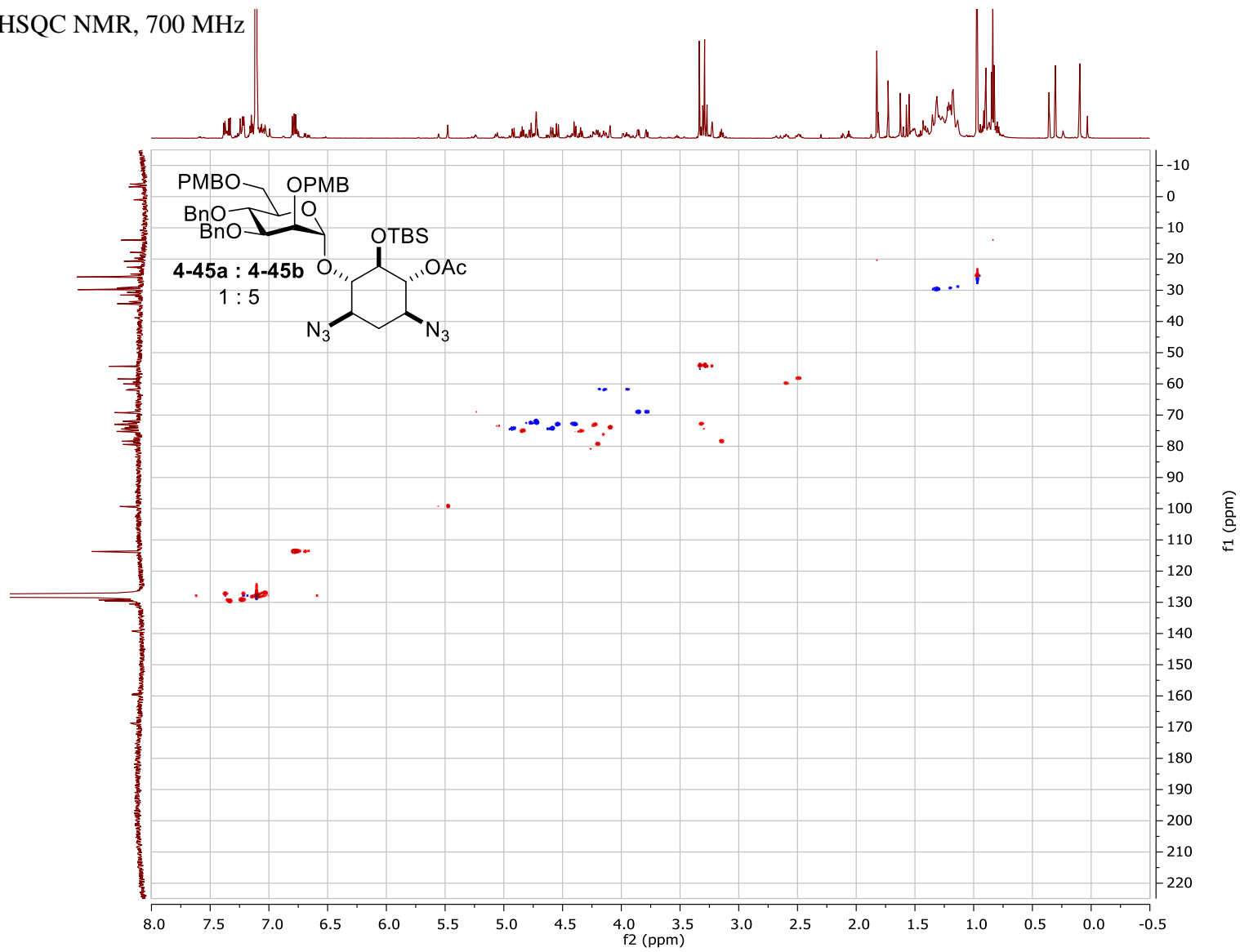
^{13}C NMR, 175 Hz



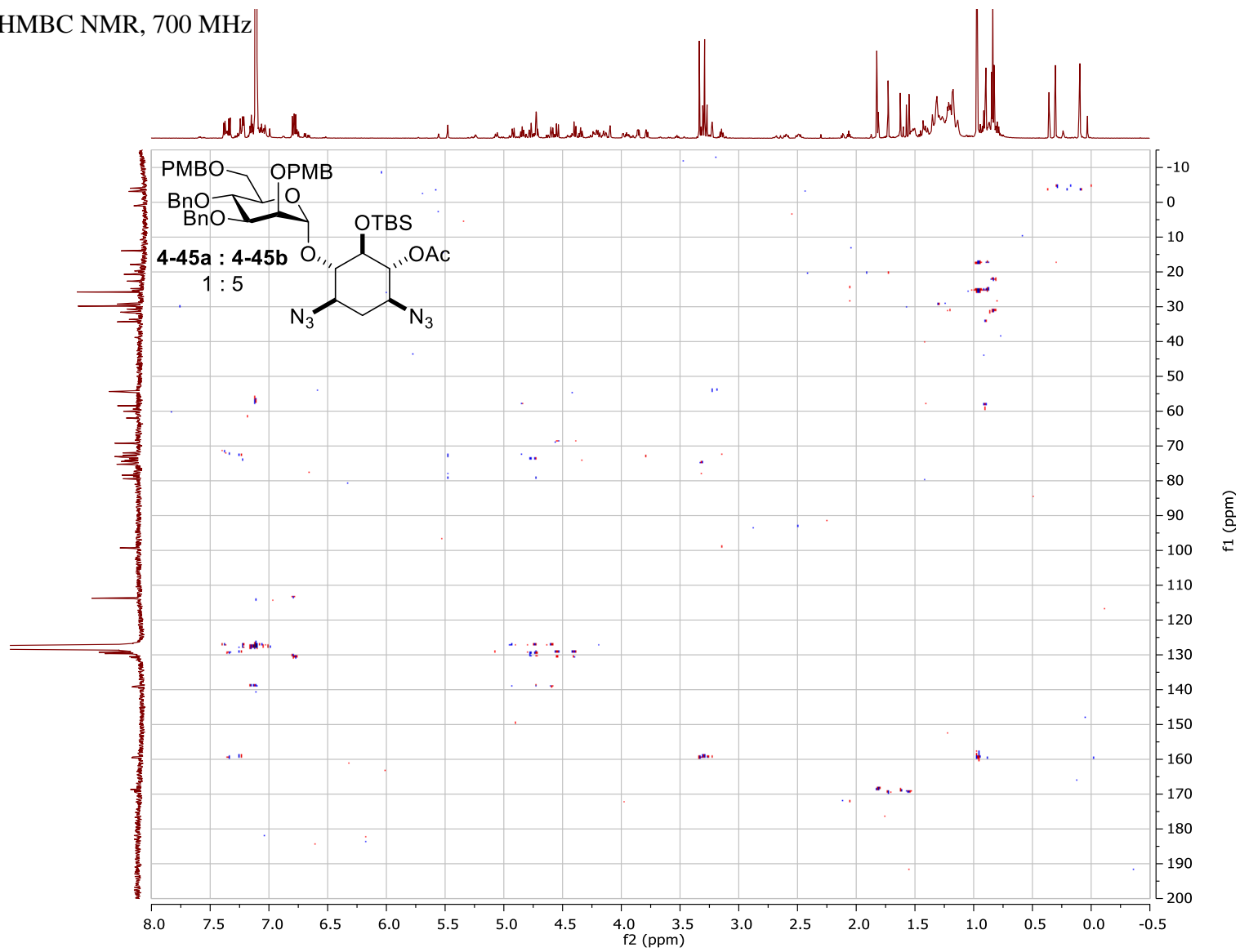
COSY NMR, 700 MHz



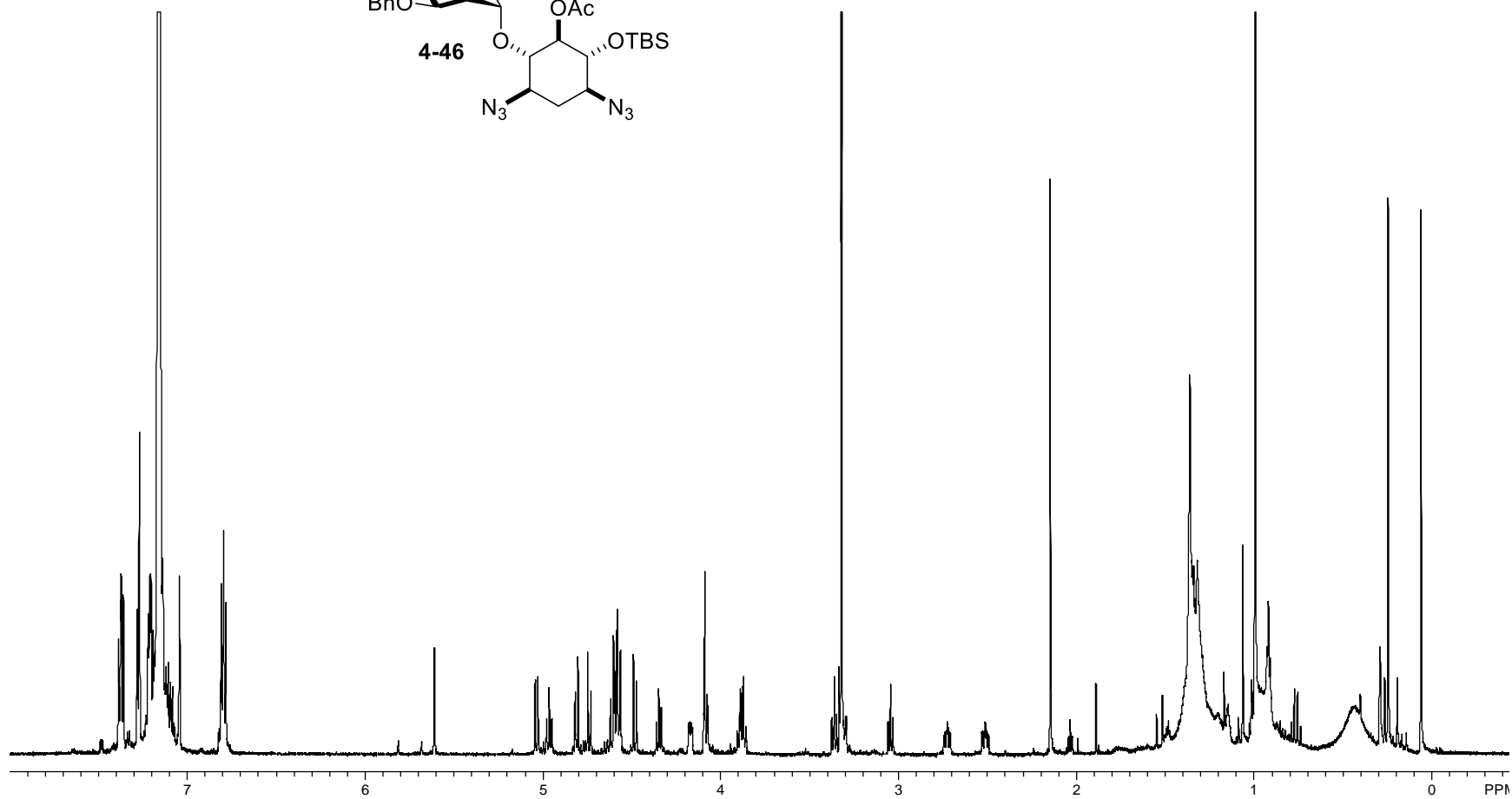
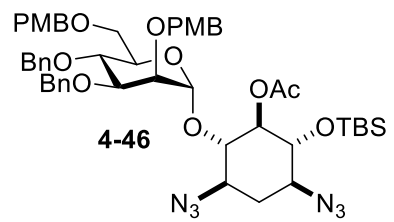
HSQC NMR, 700 MHz



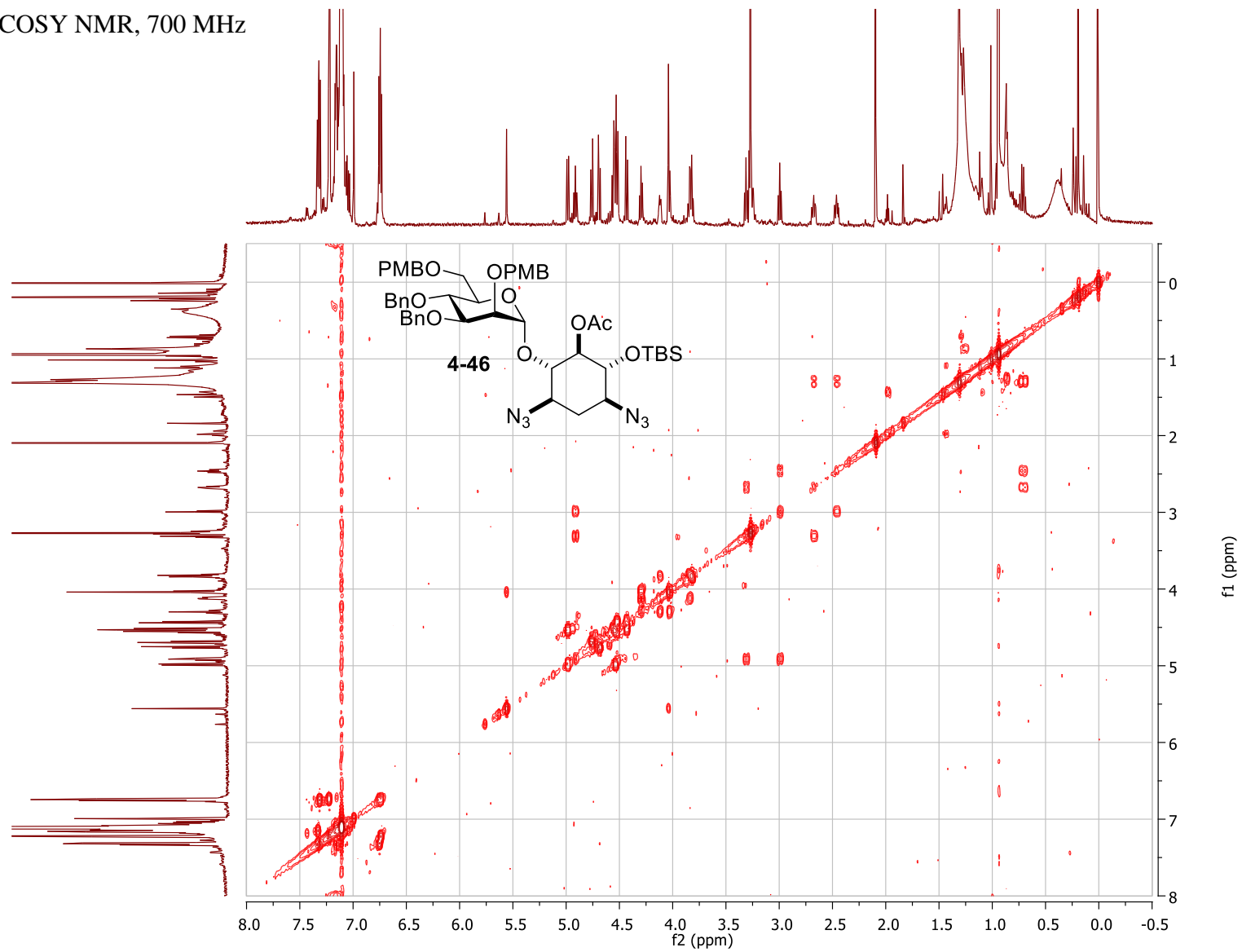
HMBC NMR, 700 MHz

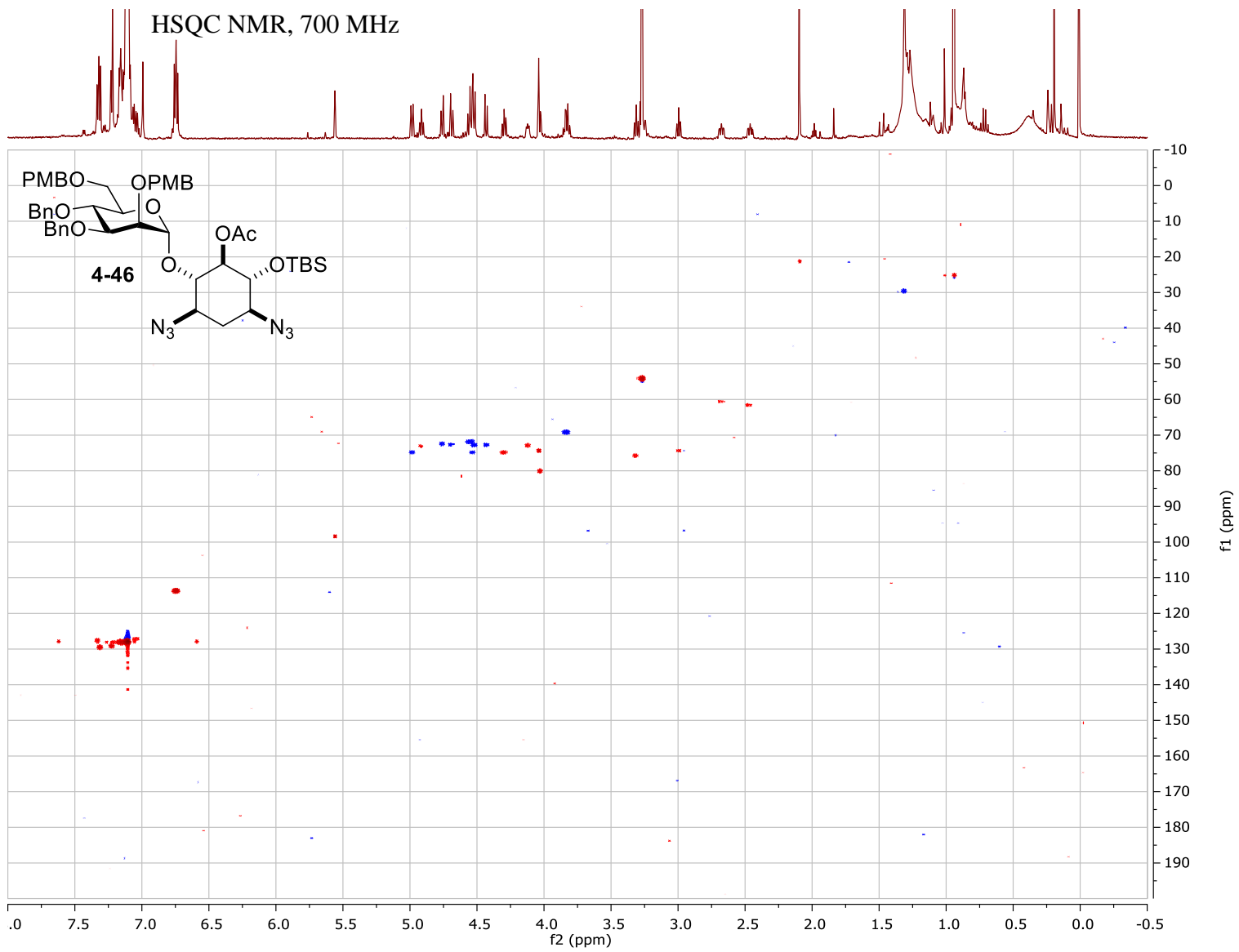


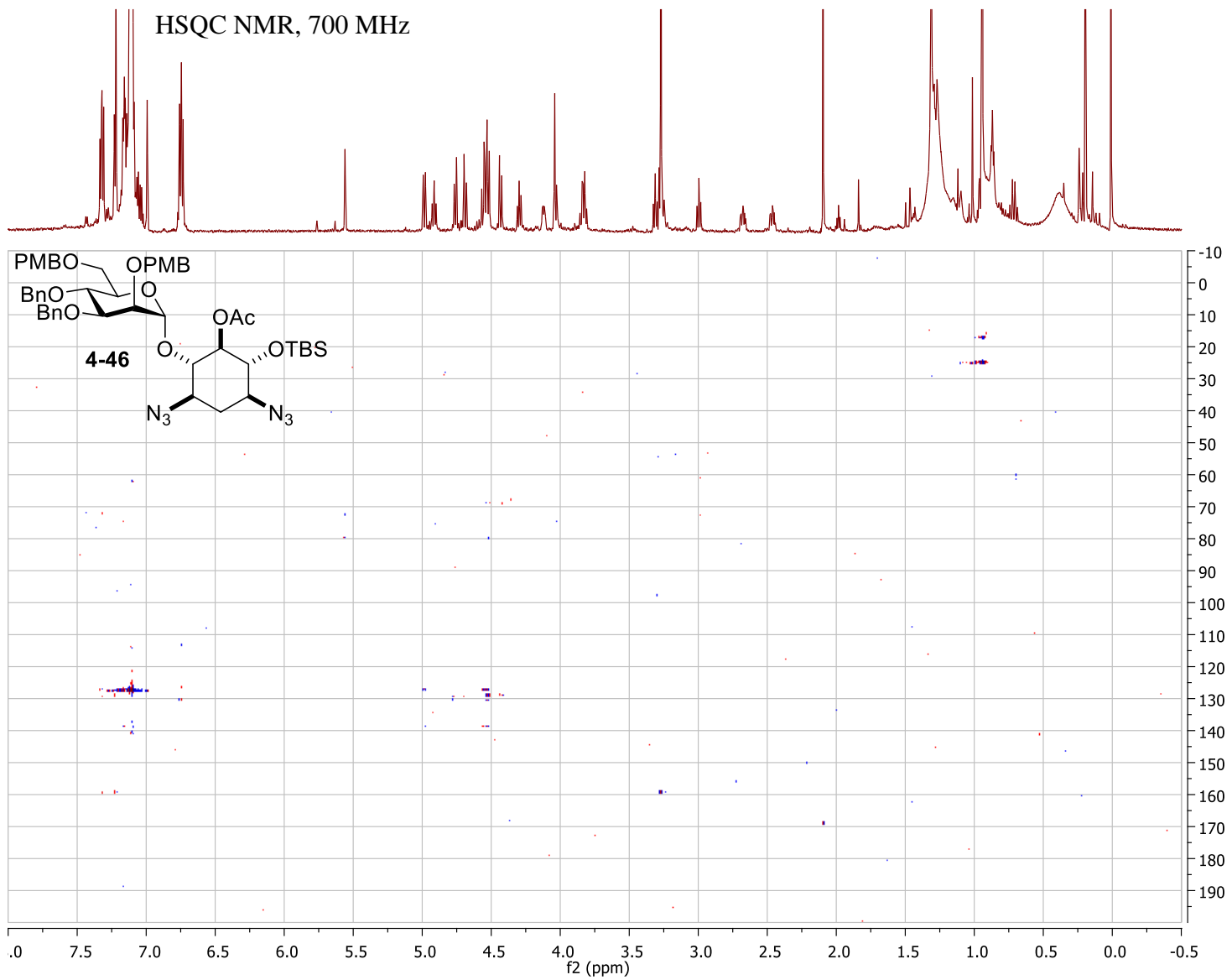
^1H NMR, 700MHz



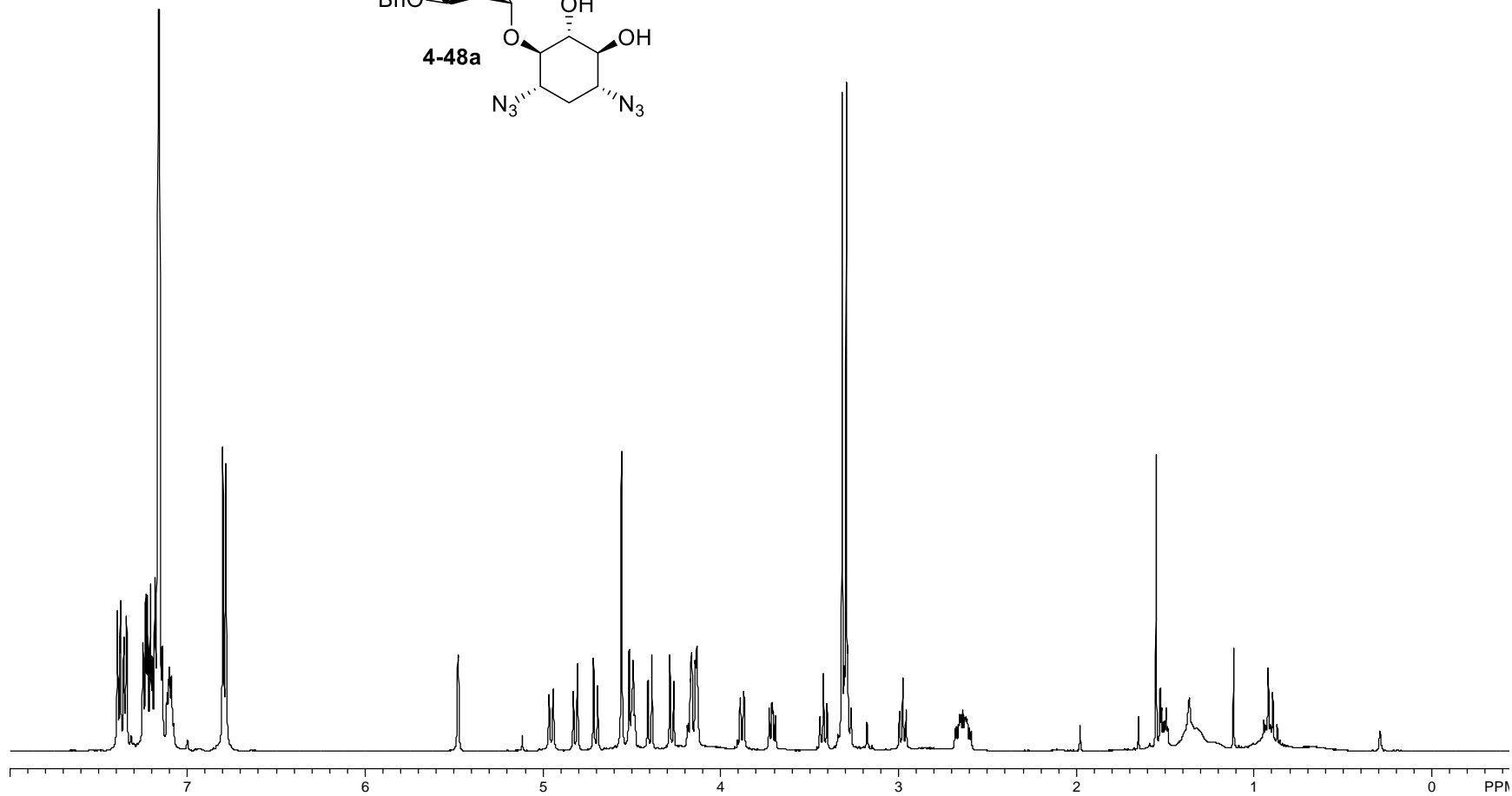
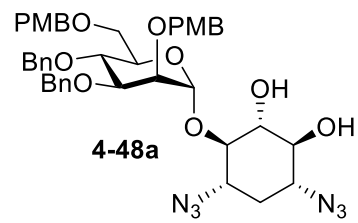
COSY NMR, 700 MHz



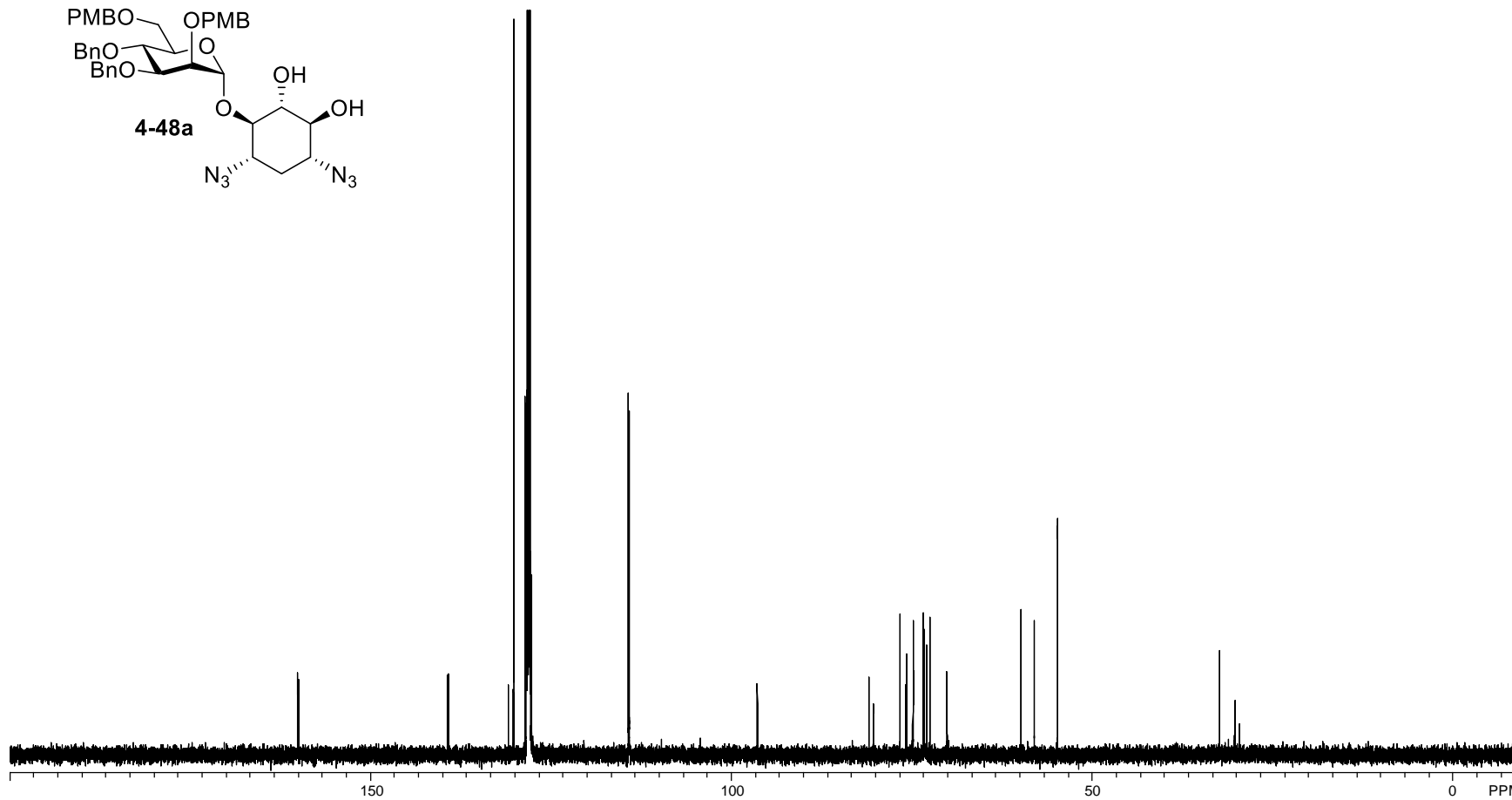
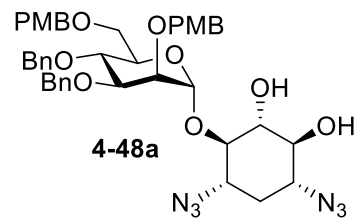




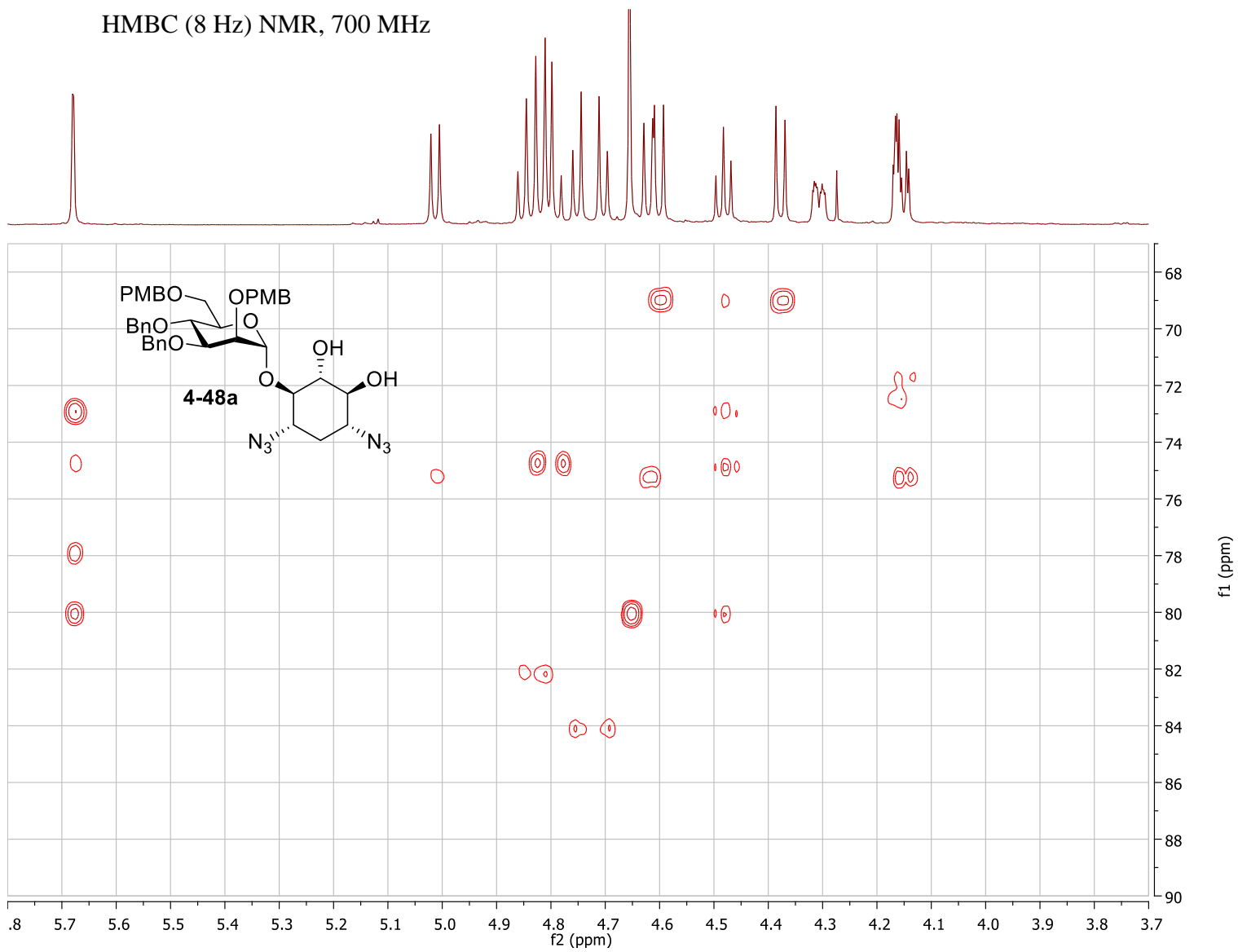
^1H NMR, 500MHz



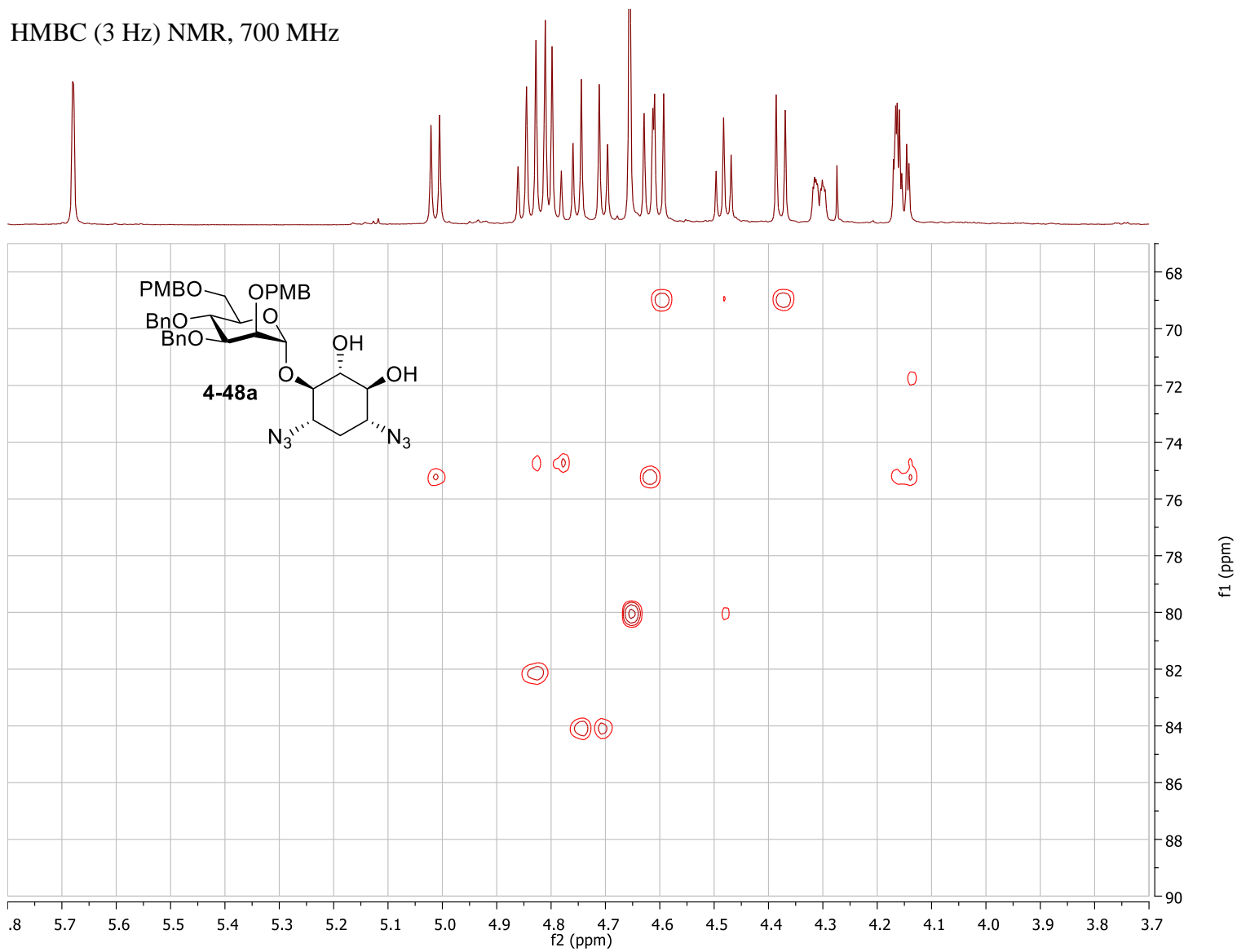
^{13}C NMR, 125 MHz



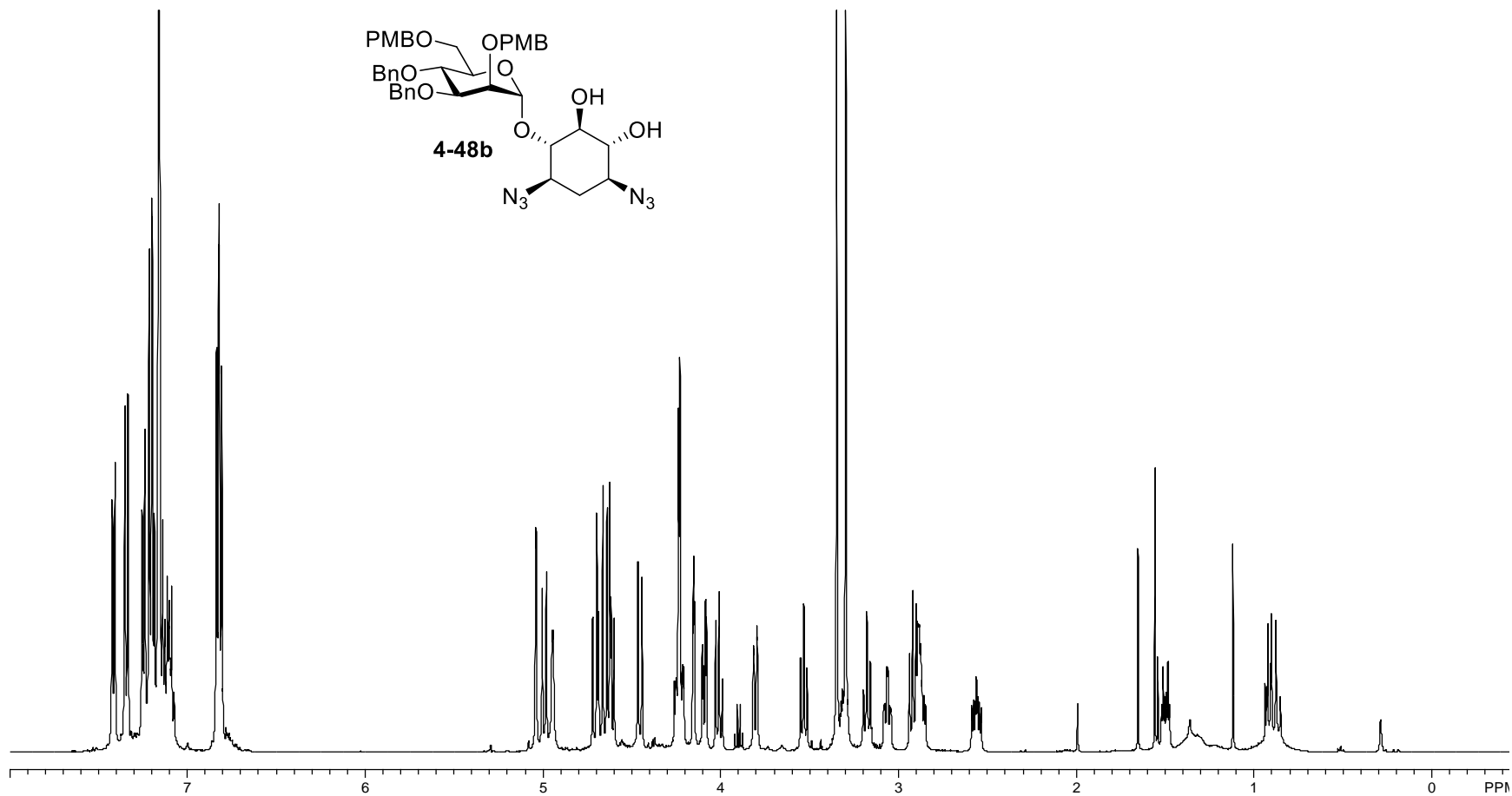
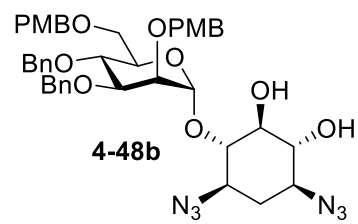
HMBC (8 Hz) NMR, 700 MHz



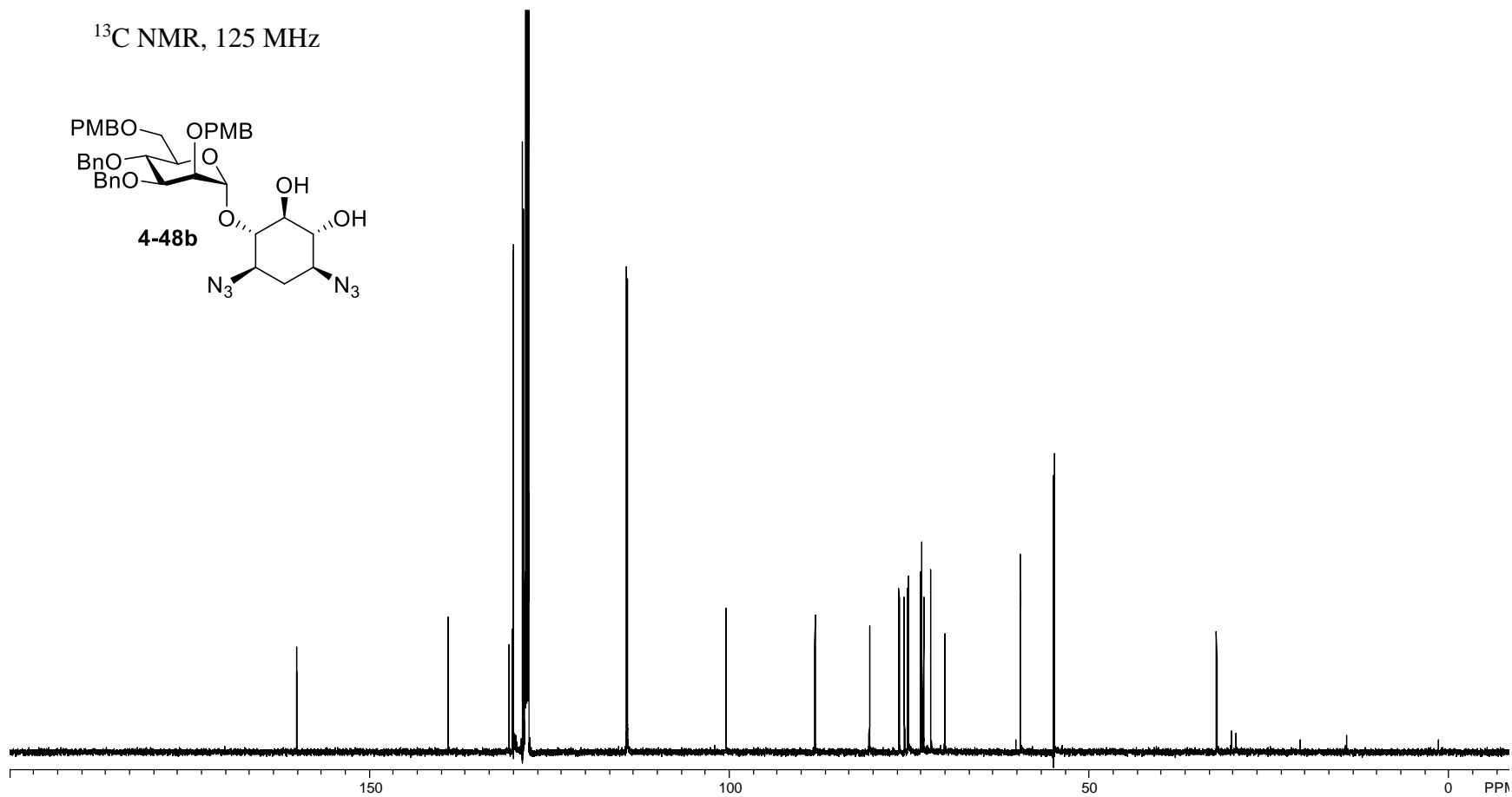
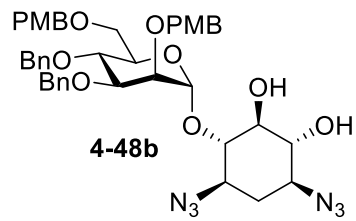
HMBC (3 Hz) NMR, 700 MHz



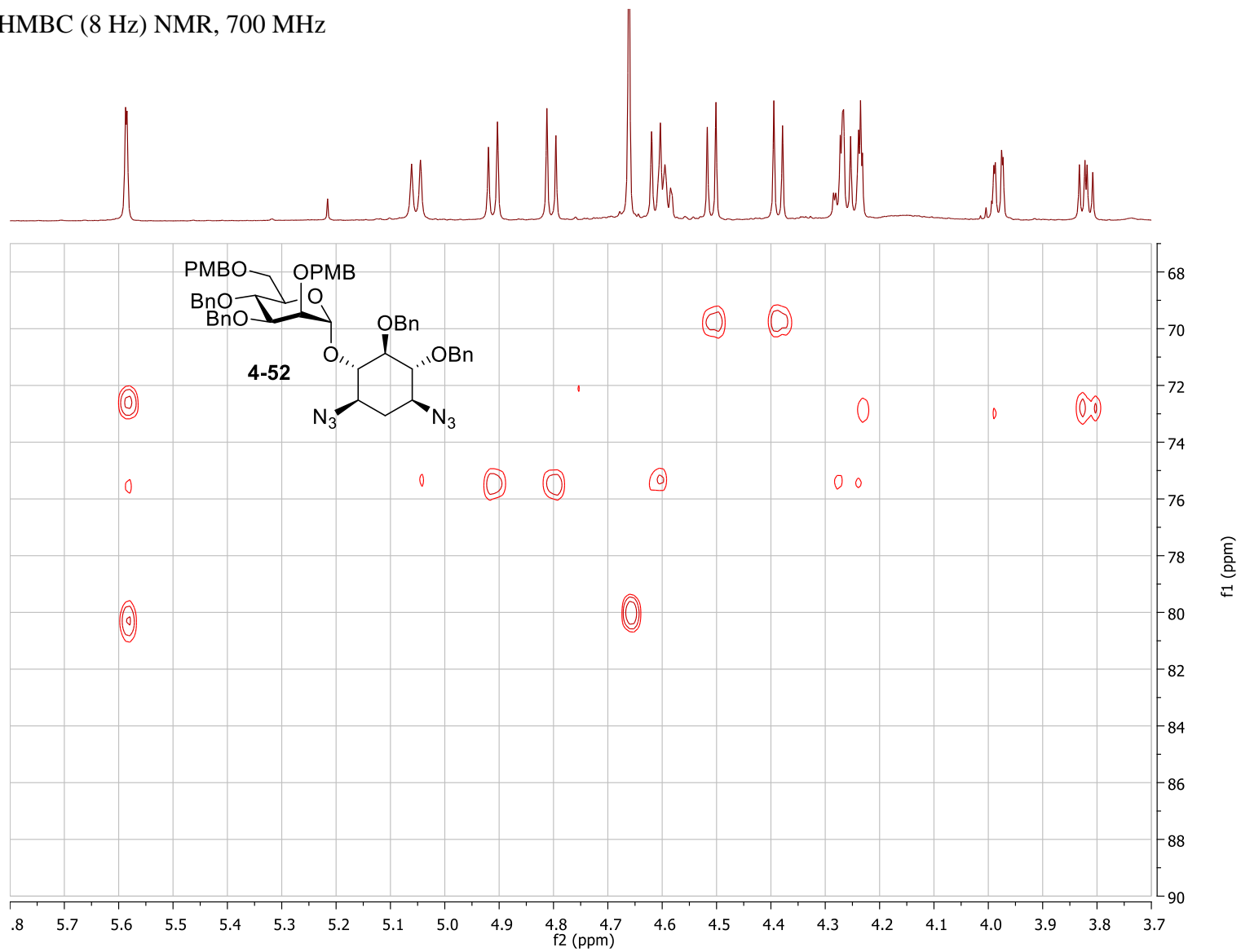
^1H NMR, 500 MHz



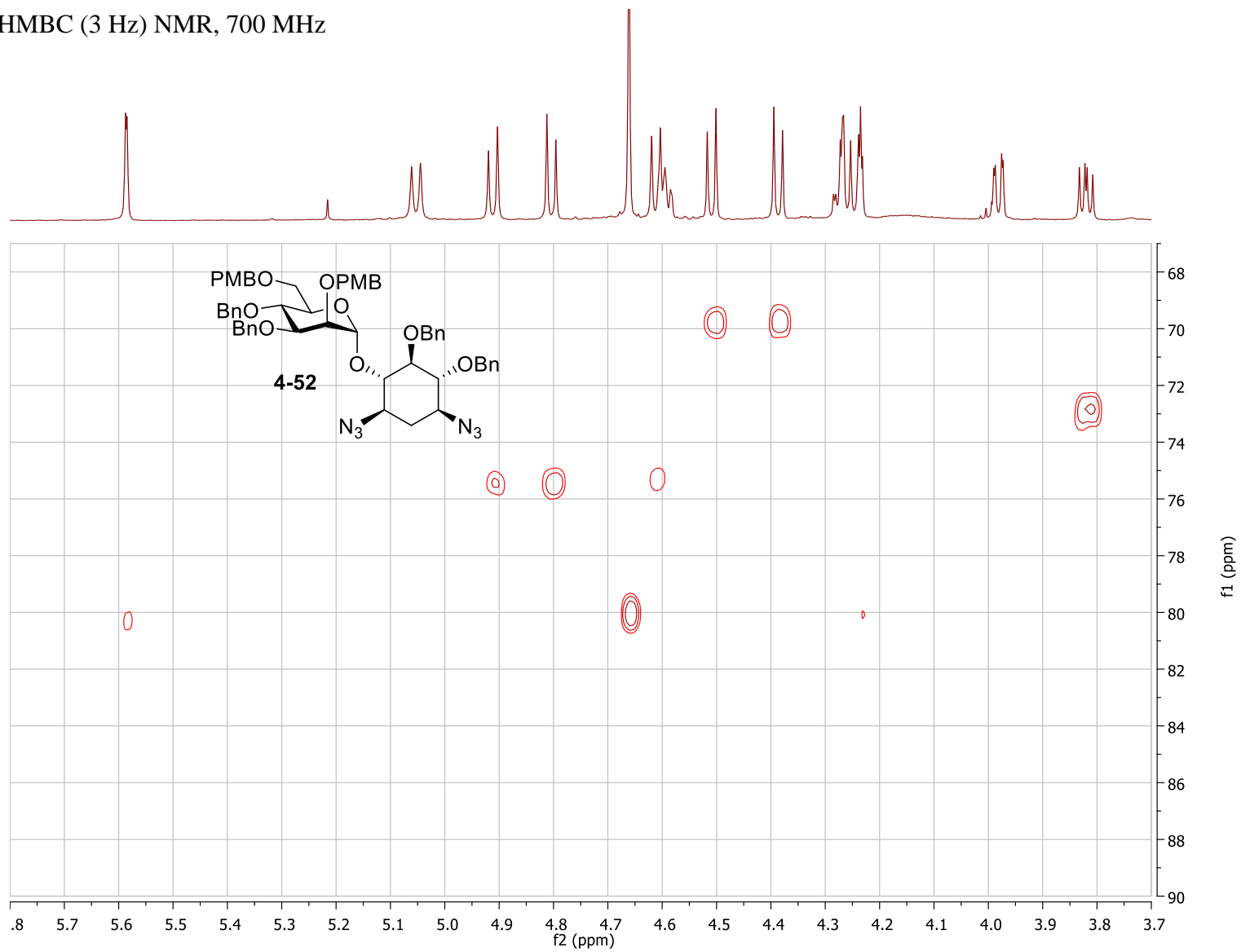
^{13}C NMR, 125 MHz



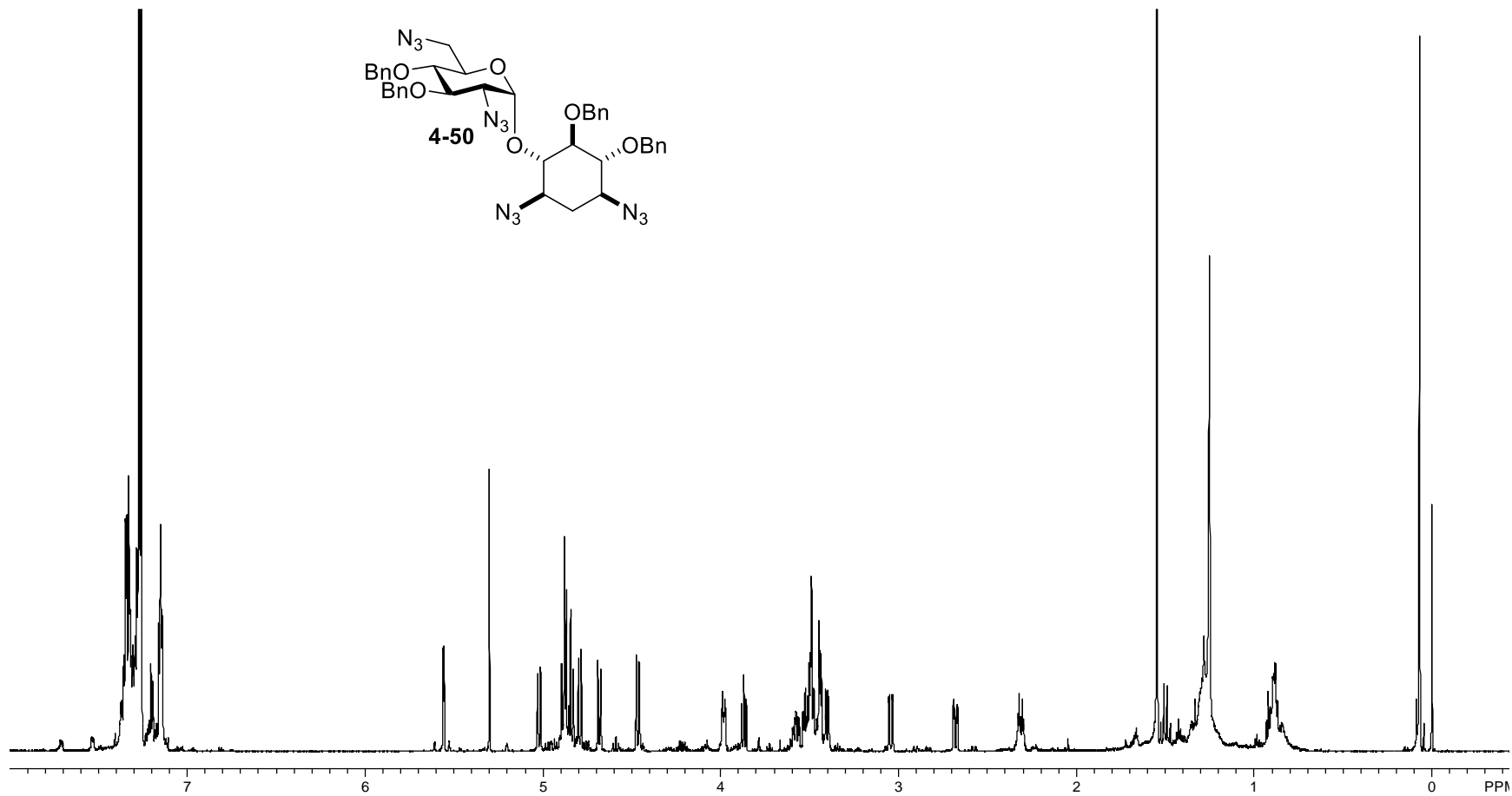
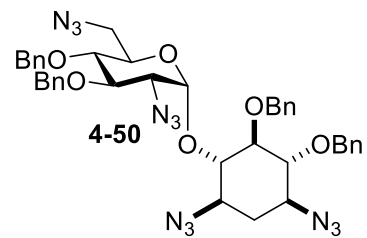
HMBC (8 Hz) NMR, 700 MHz



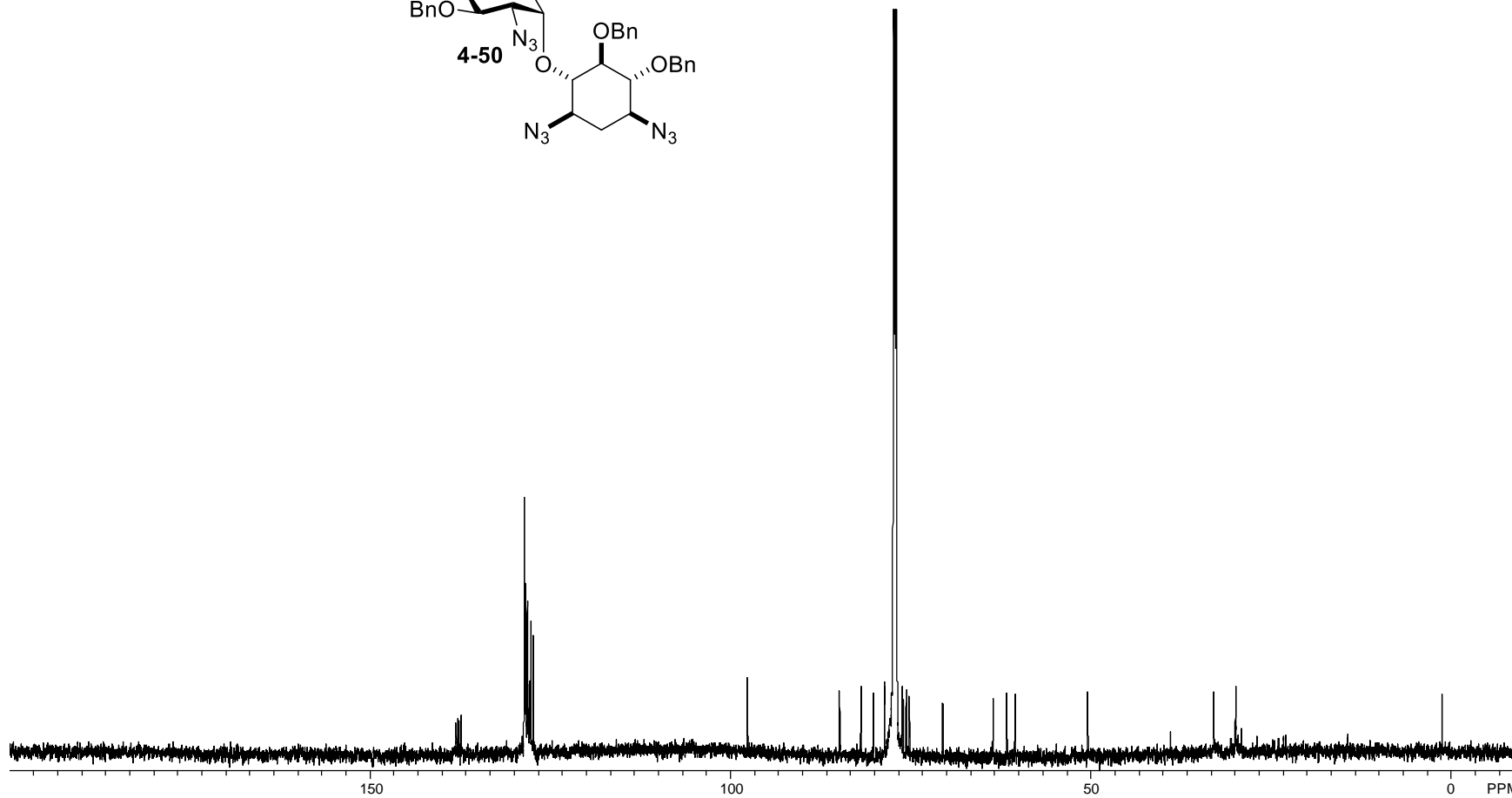
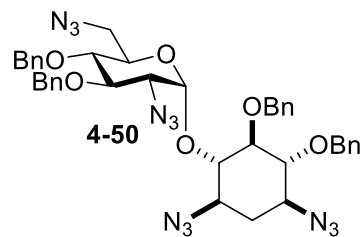
HMBC (3 Hz) NMR, 700 MHz



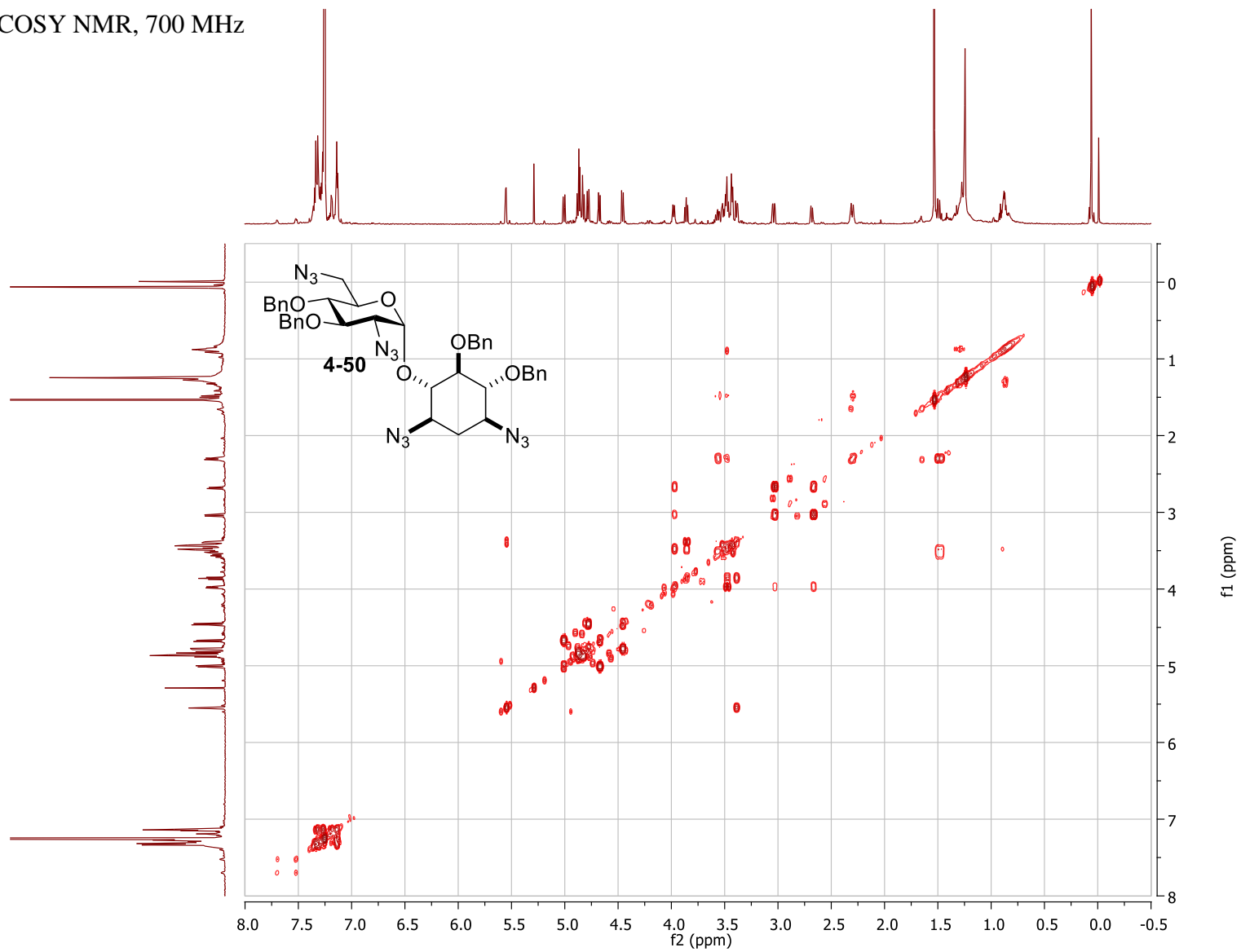
^1H NMR, 700 MHz



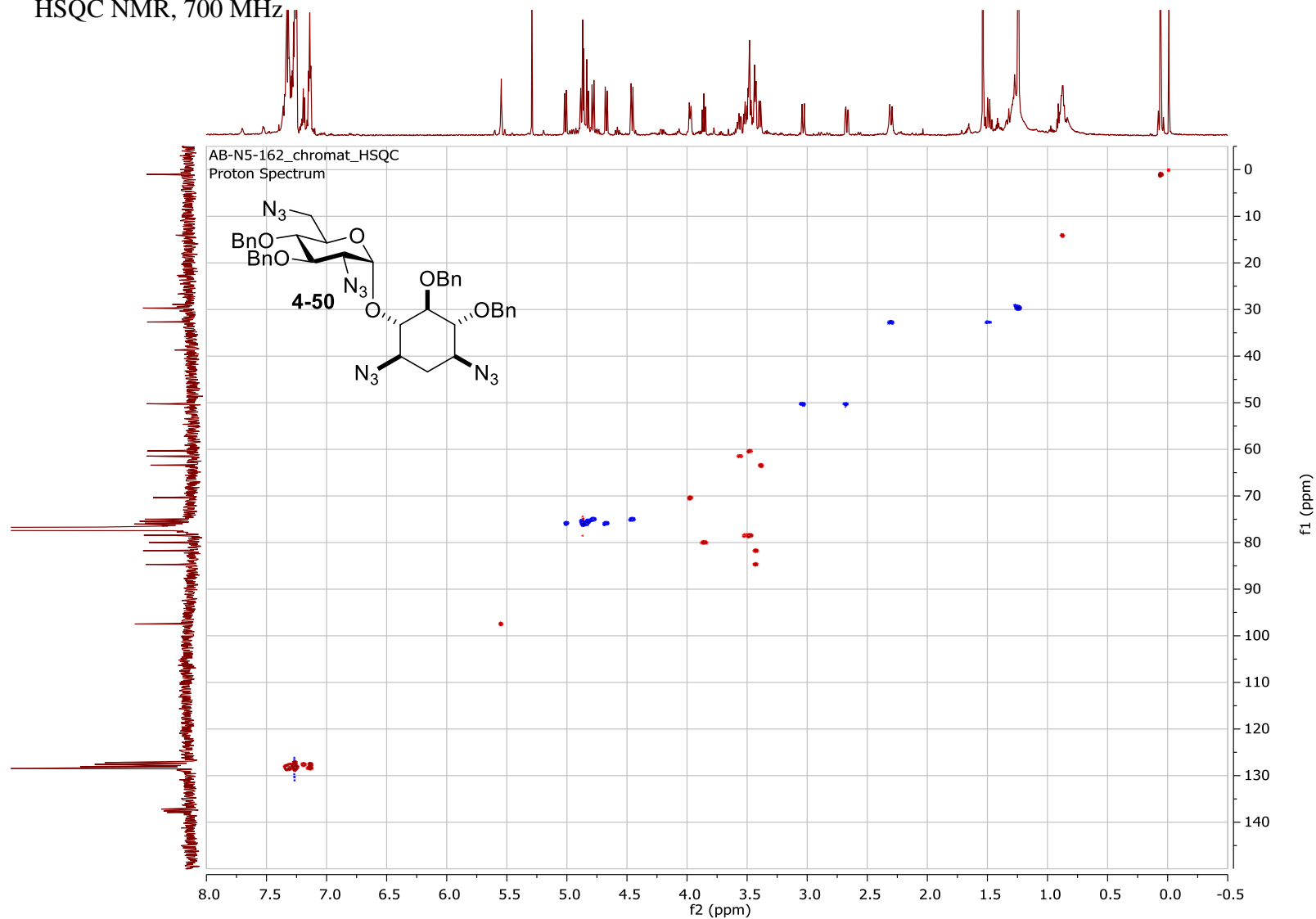
^{13}C NMR, 175 MHz



COSY NMR, 700 MHz



HSQC NMR, 700 MHz



HMBC NMR, 700 MHz

